Technische Universität München
TUM School of Engineering and Design

Integrated Intersection Control for Connected Automated Vehicles, Pedestrians, and Bicyclists

Tanja Niels

Vollständiger Abdruck der von der TUM School of Engineering and Design der Technischen Universität München zur Erlangung des akademischen Grades einer *Doktorin der Ingenieurwissenschaften (Dr.-Ing.)* genehmigten Dissertation

Vorsitz: Prof. Dr.-Ing. Rolf Moeckel

Prüfer der Dissertation:

1. Prof. Dr.-Ing. Klaus Bogenberger
2. Prof. Dr.-Ing. Markos Papageorgiou
3. Prof. Dr. Constantinos Antoniou

Die Dissertation wurde am 29.06.2022 bei der Technischen Universität München eingereicht und durch die *TUM School of Engineering and Design* am 25.10.2022 angenommen.

Acknowledgment

First and foremost, I would like to sincerely thank my supervisor Professor Klaus Bogenberger for his continuous guidance and immense support. I appreciate his scientific advice and encouraging words during countless meetings, which have helped me move forward. His profound knowledge, his enthusiasm, and his positive attitude are truly inspiring to me.

Next, I wish to thank Professor Markos Papageorgiou for serving as a second supervisor. During the fruitful discussions at conferences and in numerous zoom meetings, he has shared his vast knowledge and given valuable feedback which has significantly shaped the optimization-based part of the thesis. I would also like to extend my appreciation to Professor Ioannis Papamichail for sharing the detailed discussions on the optimization problem and Professor Constantinos Antoniou for taking the time to evaluate this thesis.

During the work on this research, I had the privilege to visit the University of South Florida and the Florida Atlantic University. The research stays were a great personal experience and significantly helped me move forward with my dissertation. I want to thank Professor Robert Bertini and Professor Aleksandar Stevanovic for their great hospitality and support. Thank you to their entire teams as well, especially to Professor Nikhil Menon, Dr. Nikola Mitrovic, and Dr. Nemanja Dobrota for the academic collaborations and for making the stays so enjoyable.

I have always enjoyed the very positive working atmosphere at UniBw and TUM. Thank you to all the colleagues, current and former, for sharing professional discussions and fun moments. It is a pleasure to work in such a great and supportive team! I would especially like to thank Professor Heather Kaths for taking on the mentorship for this thesis, Patrick Malcolm, Dr. Majid Rostami, and Dr. Simone Weikl for carefully reading through the thesis and providing valuable feedback, Mustafa Erciyas for helping me with all my questions on traffic signal control, Dr. Lisa Kessler for always being available to support me even with last-minute queries, and Dr. Florian Dandl for being an awesome roommate and giving me such a good start into working with aimsun and Python. Furthermore, I would like to thank all the colleagues at AAU in Klagenfurt for their warm welcome and the relaxing lunch and coffee breaks together.

I am extremely grateful for the love, support, and encouragement of my family, especially my parents and my brother. They helped me a lot, not only during the work on this thesis but throughout my whole life. I also want to thank my friends for their moral support and for helping me get distracted from work when I needed it. Special thanks to Lisa and Saskia for always providing me with a home in Munich. Most of all, I would like to thank my partner Felix for his love, his belief in me, and his incredible patience in this process. I am very much looking forward to having more free time and exploring our current home region with you!

Executive Summary

Traffic at larger or busier urban intersections is currently coordinated using traffic signals to prevent dangerous traffic situations and to regulate the flow of traffic. In future scenarios with 100 % connected automated vehicles (CAVs), conventional traffic signals could be replaced, and vehicles at intersections could be seamlessly coordinated via vehicle-to-vehicle and vehicle-to-infrastructure communication. This thesis presents and evaluates novel intersection control strategies for such future urban traffic scenarios. The main focus lies on the safe, efficient, and understandable integration of pedestrians and bicyclists into the control. All presented strategies are explained in detail, implemented, and evaluated using a microsimulation platform.

A comprehensive literature review on existing intersection control concepts forms the basis for this research. It comprises a brief introduction on the basic concepts and evaluation criteria of traffic signal control (TSC) and a detailed discussion of studies on so-called autonomous intersection management (AIM). While advanced AIM concepts are very promising and able to significantly outperform TSC with respect to vehicle delays, for example, research gaps are identified when it comes to the applicability in a realistic multimodal urban environment. To fill those gaps, new control schemes are developed. They can be assigned to two broader categories: the *slot-based* control strategies work with a discretization of space and time. Discrete zones of the intersection are reserved for specific road user movements during discrete time slots. They are assigned on a first come, first served basis that is appended by a set of rules to integrate pedestrians and bicyclists in such a way that defined maximum waiting times are not exceeded. The *optimization-based* strategies work with a scheduling optimization problem that resolves conflicts and assigns crossing times by applying a rolling-horizon scheme. The objective function minimizes the sum of weighted delays and offers the possibility to balance delays and prioritize road users to achieve policy objectives.

In addition to the simulation-based evaluation of all presented strategies for a set of generic scenarios, the most promising control setup is implemented within a simulation framework of a realistic intersection in Munich with measured heterogeneous demand. The presented scheme is able to reduce average vehicle and bus delays by up to 72 % and 86 %, respectively, while keeping pedestrian and bicycle delays on approximately the same level as with the state-of-the-art TSC. Furthermore, vehicle energy consumption caused by accelerating and decelerating at the intersection as well as maximum applied acceleration and deceleration values can be significantly reduced. To summarize, the key contributions of the thesis are the integration of pedestrians and bicyclists into AIM strategies, the balanced consideration of all road users and the integration of policy objectives into multimodal AIM. The main features are demonstrated via a simulation-based evaluation assuming a real intersection zone with realistic demand.

Contents

Chapter 1

Introduction

Transportation plays a major role in peoples' everyday lives. Ever-increasing vehicle miles traveled coincide with a growing awareness regarding the negative impacts of motorized traffic – especially in urban areas, where rising traffic congestion and emissions are increasingly recognized as a major issue. The need to fulfill peoples' mobility needs while at the same time providing a high quality of life will remain one of the main challenges for municipalities in the next decades. This is particularly important in view of the expected growth of population residing in cities worldwide [UN, 2019]. According to the TomTom Traffic Index, more than 200 cities worldwide have an average congestion index of more than 25%, which means that an average vehicle trip lasts 25% longer than in free-flow conditions [TomTom, 2019]. Additionally, many cities have to cope with high levels of air pollution, and motorized traffic in cities imposes a risk on pedestrians and bicyclists. Within the European Union (EU), around 20 people per 1 million inhabitants died on urban roads in 2018 and more than 50 % of them were pedestrians and bicyclists [European Commission, 2020]. Conflicts predominantly occur at intersection zones, which are the bottlenecks of urban transportation networks.

At the same time, new and fast advancing technologies offer several potential solutions that can be combined to mitigate these problems. Automated vehicles (AVs) will be capable of sensing their environments and navigating different traffic conditions with little or no input from the passenger. Connected automated vehicles (CAVs) will additionally be able to communicate with other vehicles and the infrastructure, which makes it possible to coordinate their movements more efficiently. CAVs are thus expected to have positive effects on fuel efficiency, congestion reduction, and road safety. This especially applies for intersection zones, where vehicle movements could be orchestrated in order to improve both safety and efficiency. This thesis develops and evaluates new integrated intersection control strategies for multimodal urban traffic with CAVs, pedestrians, and bicyclists.

1.1 Research Context

Traffic at larger or busier urban intersections is currently coordinated using traffic signals to prevent dangerous traffic situations and to regulate the flow of traffic. Traffic signals help mitigate conflicts by providing clear instructions, possibly supplemented by additional warning lights, for example when oncoming traffic must be given priority. Additionally, pedestrian and bicycle signal systems are used for allowing pedestrians and bicyclists to cross busy roads or intersections safely. The principle of traffic signals is older than the automobile: the first

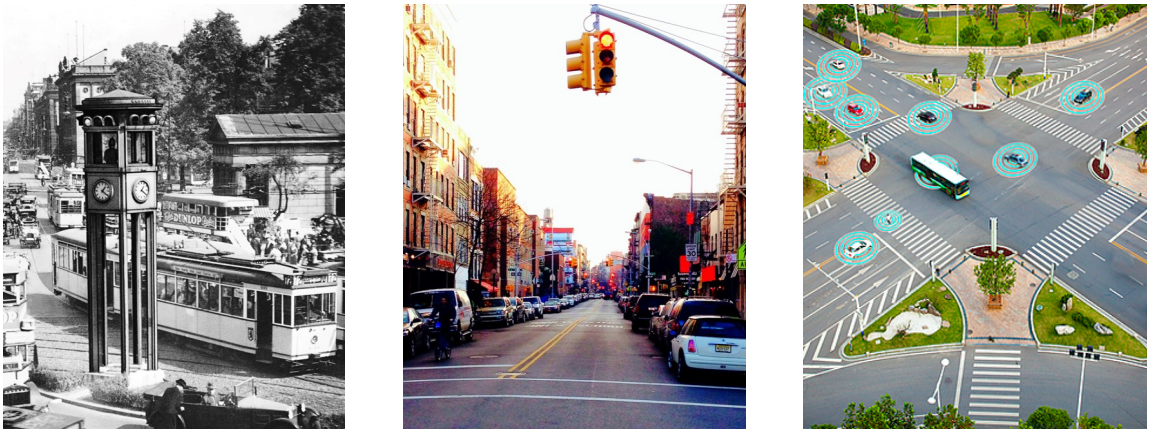

Figure 1.1: Intersection control in the past – today – and in the future?[1]

signal for controlling road traffic with horse carriages and pedestrians was installed in London in 1868, operated by gas light [Mueller, 1970]. However, it was only after the turn of the century, with growing vehicle traffic and the spread of electric light in large cities, that more traffic signals were installed to control road traffic. Those first traffic signals were controlled manually, i.e., police officers gave the right of way to a certain direction of traffic, overseeing the approaches to the intersection from a tower located close to the intersection itself. An example of such a signal tower can be seen in Figure 1.1 on the left. It shows the first traffic signal in Germany which was installed at Berlin's Potsdamer Platz in 1924 [Siemens, 2017].

Today, traffic signals follow a universal color code and are widely implemented around the world. The photo in the middle of Figure 1.1 shows an example in New York City. Traffic in Munich, Germany, is controlled by approximately 1,100 traffic signals [Lutz, 2018], and around 68,000 are assumed to be active throughout all of Germany [Schaar et al., 2013]. Many of these are fixed-time traffic signals with green phase durations usually based on traffic demand measured on an average day or estimated through models. With the measurement of real-time data close to the intersection (usually obtained from loop detectors), the control schemes can be improved as will be explained in Section 2.1. Additionally, modern traffic signals are capable of communicating information to properly equipped vehicles. This enhanced information helps vehicles to approach the intersection with an optimized trajectory and avoid having to come to a complete stop in front of the traffic signal. On the other hand, the information received from approaching vehicles can be used by the signal control to improve phase durations.

If all vehicles are connected and automated, costly implementation of physical traffic signals might no longer be necessary to coordinate vehicle traffic. In fact, with increasing progress in communication technologies and vehicle automation, first concepts of signal-free intersections have already been analyzed. The idea has been presented as a possible future vision of intersection zones in several newspapers and tech magazines, e.g., [Shah, 2018; Tonguz, 2018; Business Insider, 2016; Mattke, 2016]. In these concepts, vehicles communicate with

[1] Figure sources – Left: [Siemens, 2017], Middle: [Bark, 2014], Right: [EENews Europe, 2019]

each other or with infrastructure that is installed at the intersection zone, and reserve a specific time slot or trajectory for crossing the intersection zone safely. They promise both safety and efficiency benefits that go beyond traditional traffic signal control (TSC) optimization [Fajardo et al., 2011]. The picture in Figure 1.1 on the right illustrates such a concept, where the typical blue circles visualize the equipment with communication and sensor technology. In the following, current and expected future developments of the necessary technologies are presented, and implications on pedestrians and bicyclists are discussed.

Technological Development and Deployment of Vehicular Communication and Automated Driving Functions

The development of CAVs follows two dimensions: (i) the development of communication technologies which allow for fast and reliable communication between vehicles and infrastructure, and (ii) the development of automated driving functions that monitor the environment and take over the dynamic driving tasks. Both technologies are relevant for the implementation of the innovative intersection control schemes mentioned above, since (i) vehicles need to broadcast basic messages such as their current position, speed and intention (i.e., desired maneuver) and receive the virtual traffic signal information, and (ii) need to be able to reliably adjust their speed and follow pre-defined trajectories. While the exact technical implementation of these functionalities is not the focus of this thesis, the background description on the following pages helps to understand the key technology concepts, and when they are expected to be available.

Communication technologies for intelligent transportation systems (ITS) have been significantly improved in the past decades. The resulting links, e.g., Vehicle-to-Vehicle (V2V) and Vehicle-to-Infrastructure (V2I), or more generally Vehicle-to-Everything (V2X), allow for a variety of applications including safety-critical functions, traffic efficiency improvements, and infotainment services. Two different system concepts for V2X exist: wireless local area network (WLAN) technology on the one hand and cellular networks on the other hand. In the United States (U.S.), the most common set of communication standards for V2X applications based on the WLAN technology is named Dedicated short-range communications (DSRC) and relies on the WiFi standard IEEE 802.11p defined by the Institute of Electrical and Electronics Engineers (IEEE) [Festag, 2015]. DSRC has been studied in the context of collision avoidance (e.g., through blind spot warning, forward collision warning, and do-not-pass warning messages), but can be used for many other applications as well, e.g., to make electronic toll payments, to assist navigation, and to disseminate traffic updates [Kenney, 2011]. Low transmission latency and packet drop rate (PDR) are perceived as the most safety-relevant criteria for vehicular communication systems, and both criteria are very promising for DSRC [Liu et al., 2018]. In the EU, communication standards are defined by the European Telecommunications Standards Institute (ETSI). The EU has defined a different yet similar and largely compatible stack of protocols: DSRC is referred to as Cooperative ITS (C-ITS), and the standard IEEE 802.11p is functionally identical to ETSI ITS-G5 [Festag, 2015]. In addition to the communication protocols, standard messages have also been defined by SAE International (formerly named Society of Automotive Engineers) and ETSI. They include basic safety messages (BSMs) (named cooperative awareness messages (CAMs) in the EU), that are broadcast

by vehicles in regular intervals and comprise information on position, speed, acceleration, and driving direction of the sender. Specific standards are defined for messages broadcast from traffic signals, e.g., signal phase and timing (SPaT) that include information on the current signal state and the (expected) time for the next phase switch, and a message type called MAP that includes information on the intersection geometry. In order to communicate via DSRC, vehicles need to be equipped with On-Board Units (OBUs), and infrastructure needs to be equipped with Road Side Units (RSUs) that can broadcast and receive messages. While the technology is mature and ready for deployment, only relatively few vehicles are factory-equipped with OBUs to date [ADAC, 2020].

In contrast to WLAN technology, cellular networks based on the long term evolution (LTE) standards work with base stations that coordinate transmissions. This allows for minimizing interference and providing high data rates [Festag, 2015]. Additionally, they benefit from existing mobile communication infrastructure, and necessary devices for equipping vehicles are cheaper and feature over-the-air updates [Hainen et al., 2019]. On the other hand, data packets always need to make the detour via the cellular base station, leading to larger latency. Additionally, communication is not possible where vehicles are not connected to the cellular network, e.g., in tunnels [Festag, 2015]. To overcome these disadvantages, the newer Cellular V2X (C-V2X) standard defined by the 3rd Generation Partnership Project (3GPP), an international cooperation of standardization institutes from the EU, the U.S., China, Japan, Korea, and India, is designed to operate in two modes: (i) device-to-network, which uses the traditional cellular links to enable cloud services and communication over larger distances, and (ii) device-to-device, which allows devices that are close to each other to use a sidelink without the base station detour [Papathanassiou and Khoryaev, 2017]. Current disadvantages of C-V2X as compared to WLAN (such as slower protocols) might be overcome using the new cellular network standard 5G, which promises significant improvements in terms of throughput, reliability, latency, and support for a large number of devices. A global group of telecommunications and automotive industry (named 5G Automotive Association) promotes the deployment of C-V2X with 5G [Wevers and Lu, 2017]. Whether C-V2X or WLAN technology will prevail, is most likely going to be determined by regulation. While China is primarily relying on C-V2X and the U.S. is now also tending toward this technology, Europe is still undecided as to whether vehicular communication should be realized using WLAN or C-V2X [Köllner, 2020].

Vehicle automation is usually defined along a set of operational functions for different levels. The most generally accepted definitions are the “SAE Automation Levels" which describe six levels of automation as shown in Figure 1.2 [SAE International, 2014]. The first three levels (Level 0 to Level 2) assume that the driver is in control of the vehicle and monitoring the environment at all times. In Level 1 and Level 2, the driver is additionally supported by automated features, called advanced driving assistance systems (ADAS). Such functionalities (e.g., adaptive cruise control (ACC) or lane keeping assist systems) are already implemented in vehicles by several manufacturers. In Level 3, the driving task is assumed to be automated under limited conditions such that, in specified situations, the driver does not need to monitor the environment. However, a driver does need to be ready to take control of the vehicle at all times. The leap from Level 2 to Level 3 automation is significant and, so far, only Honda's

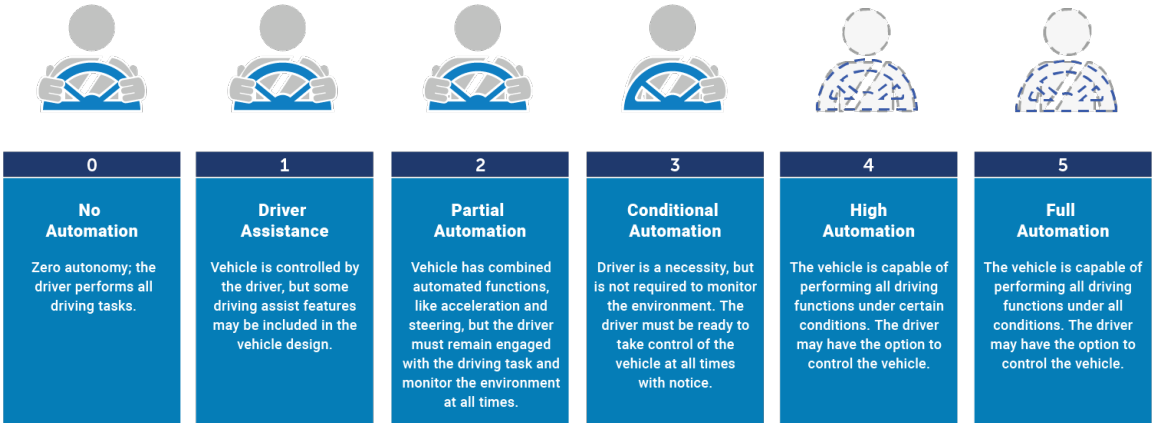

Figure 1.2: Levels of vehicle driving automation. Source: [NHTSA, 2020].

"Traffic Jam Assistant" is authorized as a Level 3 technology [Automotive News, 2021]. Level 4 and Level 5 describe "high" and "full" automation, where no human driver is expected to be available. Level 4 AVs are assumed to work automatically in limited conditions, e.g., in a certain local area, whereas Level 5 AVs are expected to be able to drive everywhere without a driver.

Advances in technology by automotive and tech companies have accelerated the development, testing, and deployment of AVs. Level 4 and 5 automated driving is still a future technology that is not yet available on the market, but tests on public roads are already running or are planned for the near future. Cruise, the self-driving subsidiary of General Motors, operates driverless vehicles (in a test phase) in San Francisco [Bellan, 2021]; Mobileye is attempting to test their automated shuttle in Munich and Tel Aviv this year [Schmidt, 2021]. The German Automotive Industry Federation (Verband der Automobilindustrie (VDA)) has predicted a few years ago that Level 4 automated driving in cities might be commercially available as early as 2030 – given that the required legislation is applied [VDA, 2015]. The actual timeline of large-scale deployment depends on multiple factors and aspects including technologies, legal frameworks, validated safety, and public acceptance. Due to the unpredictability of these factors, studies on the temporal development and market forecast usually work with a set of scenarios. Milakis et al. [2017] expect full automation to be commercially available between 2025 and 2045. Kaltenhäuser et al. [2020] developed a discrete system dynamics model for estimating future market penetration rates of private AVs and autonomous taxis in Germany. According to their model, 23 % of people will regularly use autonomous taxis and a 31.5 % share of Level 4 AVs can be reached among private vehicles in 2040, but people are hesitant about completely giving up on the driving task, i.e., actually buying vehicles without a steering wheel. Bansal and Kockelman [2017] used a simulation framework that was calibrated with data obtained from a survey with more than 2,000 American respondents to forecast the long-term penetration rate of AVs among light-duty vehicles in the U.S.. They conclude that Level 4 AV penetration among privately held light-duty vehicles will most likely range between approximately 25 % and 87 % by 2045, depending mainly on prices and willingness to pay. While these results are widely dispersed, they show that fully automated

vehicle traffic, i.e., a penetration rate of 100 % CAVs, seems to be a long way down the line. Forecasts by consultancies believe that (nearly) full penetration is possible after 2050 [Dorrier, 2014] or 2055 [Shanker et al., 2013]. However, it is conceivable that manually driven vehicles will be banned from at least parts of the street network once CAVs have been proven to be significantly safer than human drivers [J. F. Müller and Gogoll, 2020].

In summary, vehicular communication technologies are already quite mature and are increasingly implemented in vehicles on the global market. Further improvements and larger penetration rates are expected with increasing 5G coverage. Level 4 and 5 automated driving is still in the testing phase and not yet commercially available. The reported technological progress, however, has given rise to the analysis of new services and control strategies. For the control schemes presented in this thesis, it is assumed that all vehicles are connected and able to cross the considered intersection zone without human interference.

Impacts of CAVs on Pedestrians and Bicyclists

Walking and cycling benefit mental and physical health, and are environmentally, socially, and economically sustainable urban transport modes. Therefore, they are increasingly investigated by researchers and supported by policy-makers around the world [Buehler et al., 2020]. Bicycle traffic is especially of interest, since it allows for covering longer trips and carrying parcels at an acceptable average speed in cities. This is further facilitated by electric bicycles. The modal split of bicycling in urban areas in Germany increased from 9% in 2002 to 15% in 2017. Overall, non-motorized traffic has a share of 33% among all transportation modes considering trips, and a share of 6% considering traveled person kilometers in Germany [Nobis and Kuhnimhof, 2018]. In the U.S., walking and bicycle trips account for 11.5% of all undertaken trips [FHWA, 2017].

On average, the estimated health benefits of cycling outweigh the risks of cycling relative to car driving, especially if suitable safety measures are implemented [De Hartog et al., 2010]. On the other hand, pedestrians and cyclists lack the protecting "metal shell" that car occupants have and are thus often referred to as vulnerable road users (VRUs). According to the ITS directive by the EU, the term VRU comprises "non-motorised road users, such as pedestrians and cyclists as well as motor-cyclists [sic] and persons with disabilities or reduced mobility and orientation" [EU, 2010]. In fact, within urban areas in the EU, almost 40% of traffic fatalities in 2018 were pedestrians, 12% were cyclists and 18% were users of powered two-wheelers [European Commission, 2020]. This means that 70% of the approximately 9,000 fatalities on urban roads were VRUs. Approximately five times more were injured severely. While total road fatalities in the EU decreased by 23% as compared to 2010, pedestrian fatalities did not fall at the same pace and the number of cyclist fatalities even increased [European Commission, 2020]. According to the U.S. National Highway Transportation Safety Administration (NHTSA), more than 90 % of car accidents are caused by human error (including inattention, driving too fast, making false assumptions about others road users' actions, among others) [NHTSA, 2018]. Even though it is difficult to quantify the percentage of VRU accidents that are actually caused by human error on the part of the vehicle driver, it is a major goal that CAVs improve VRU safety.

A study on the perception of CAVs by VRUs based on a survey among Pittsburgh residents (as Pittsburgh has been a proving ground for Uber's AVs) indicates that people having interacted with AVs have higher expectations regarding safety implications [Penmetsa et al., 2019]. Botello et al. [2019] interviewed experts from academia and the public and private sectors in the United States. In general, their interview partners were positive about long-term safety impacts of CAVs. However, there are concerns about whether CAVs will be able to precisely detect and predict pedestrian and cyclist movements in the technology transition phase. In fact, AVs still struggle to detect bicyclists [Fairley, 2017]. Safety concerns could be mitigated by an even stricter separation of space for vehicles and VRUs. However, this could impede the freedom and comfort of pedestrians and bicyclists. Overall, the consequences of CAVs on urban street design and pedestrian and bicycle friendliness are not clear yet. Meeder et al. [2017] discuss this question under the topic "Autonomous vehicles: Pedestrian heaven or pedestrian hell?". Similarly to Botello et al. [2019], they conclude that the answer depends a lot on whether CAVs have to adapt to pedestrians' behaviour – or the other way round. These discussions demonstrate the importance of considering pedestrians and bicyclists when planning a future with CAVs. This is currently not the case when innovative automated intersection control strategies are investigated, which leads to the first research question in this dissertation:

Research Question 1 *How can pedestrians and bicyclists be integrated into automated intersection control in a safe and efficient way?*

As will be discussed in the literature review in Chapter 2, most studies on automated intersection control assume a situation with perfect information and communication, i.e., all vehicles crossing the intersection are automated and equipped with communication devices. The control entity knows their positions, speeds, etc. at all times. One of the major difficulties when considering pedestrians and bicyclists in such systems is the fact that they are currently not connected to each other, other road users, or the infrastructure, and hence their presence, desired destination, and speed are not easily predictable. Answering the research question above thus requires the discussion of a set of preceding questions: Do pedestrians and bicyclists need to connect to the infrastructure? How can they be sure that they are given the right of way?

Potential of Automated Control Strategies for Multimodal Urban Intersections

In German regulations, the road network is divided into several categories according to the roads' functionality, e.g., residential streets, arterial roads, and highways [Eisenkopf et al., 2017]. This definition applies for intersections as well, which means that at some intersections a high throughput of cars may be the most important, whereas at other intersections other road users may be given priority, which raises the second research question:

Research Question 2 *How can policy objectives be integrated into automated intersection control?*

Such policy objectives could include the prioritization of VRUs or public transport (PT) vehicles. It needs to be analyzed whether such a prioritization is possible in a balanced manner, i.e., without excessive delays for other road users.

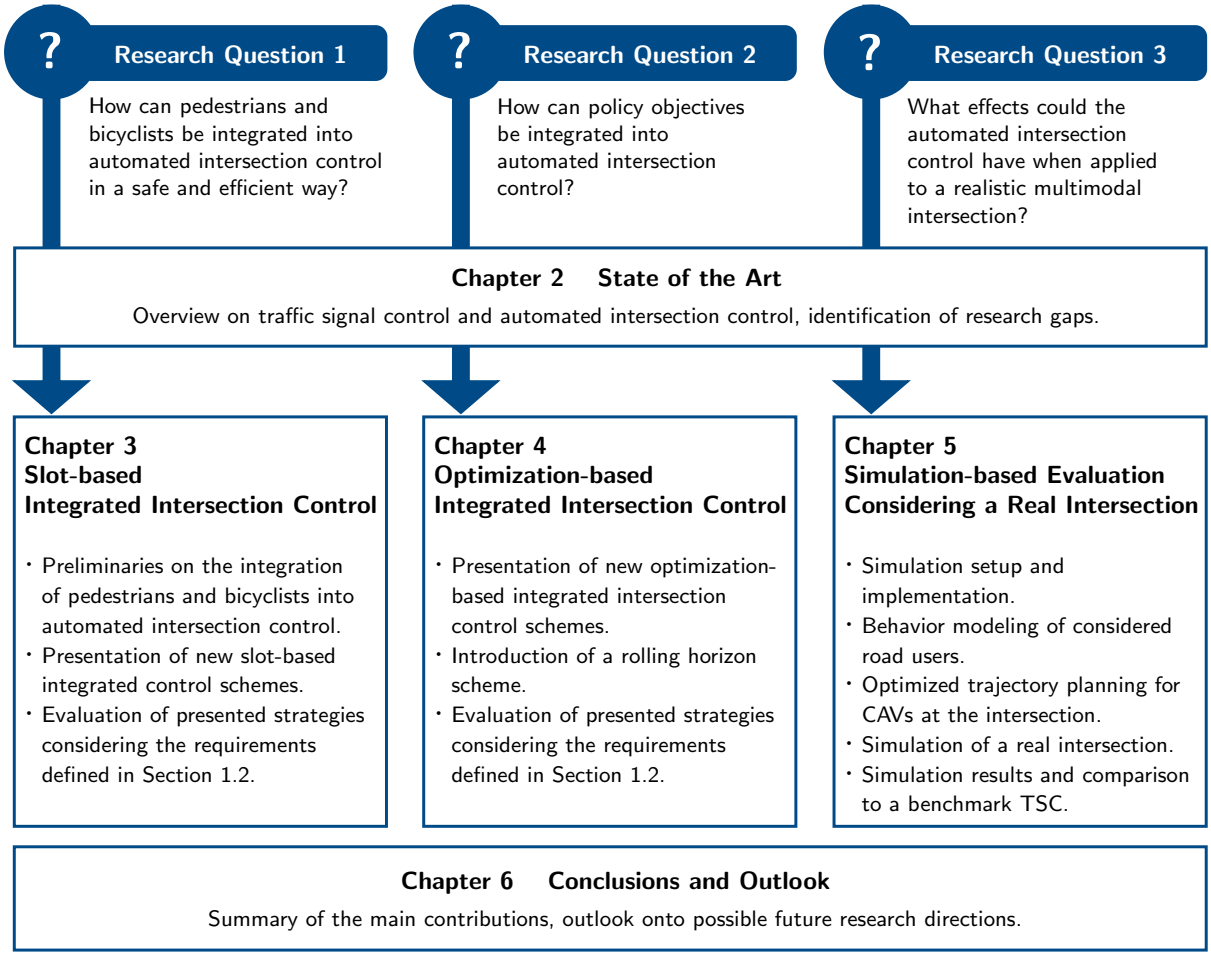

Figure 1.3: Research design and structure of the dissertation.

Finally, new intersection control schemes will only prevail if they offer significant benefits as compared to state-of-the-art TSC. This leads to the third research question:

Research Question 3 *What effects could automated intersection control have when applied to a realistic multimodal intersection?*

As will be described below, answering this research question requires the development of multimodal control strategies, and a simulation study considering a realistic intersection zone.

1.2 Research Objectives and Design

Following the research questions defined above, the overall objective of this thesis is to explore applicability and potential of new automated intersection control strategies for multimodal urban traffic. Answering the research questions requires a sound methodology that will be described below. As displayed in Figure 1.3, the scope of this research includes the following:

Literature Review A comprehensive literature review on existing intersection control concepts forms the basis for this research. First of all, basic concepts of TSC and their evaluation criteria are introduced. They provide the basis for understanding and evaluating new intersection control strategies. Afterwards, the vast literature on automated intersection control is categorized along a set of attributes. Research gaps are identified where existing concepts do not meet the requirements defined by the research questions.

Development of New Integrated Intersection Control Strategies In order to bridge the identified research gaps, new integrated intersection control strategies for CAVs, pedestrians, and bicyclists are developed and evaluated in this thesis. The research questions defined above imply certain requirements on these control strategies that will be explained in the following. ***Research Question 1*** concerns the integration of pedestrians and bicyclists in a safe and efficient way. Clearly, accessibility of public space should not be infringed by the new control schemes. This calls for a control design that is understandable for VRUs and does not require them to use connected devices, for example. These considerations will be summarized as "low-tech" and will be further substantiated in Section 3.1. All in all, answering Research Question 1 implies the following requirements:

Multimodality The control should integrate all modes of transportation that are common at urban intersections, especially vehicles, pedestrians, and bicyclists.

Safety by Design The control should ensure safe crossing of the intersection zone for all considered road users by resolving conflicting movements and implementing safe time gaps.

Efficiency The control should reduce the overall delay for road users at the intersection zone. The evaluation will follow the concept that is commonly used for signalized intersections and will be explained in Section 2.1.

Low-Tech The control should be easy to understand, especially for pedestrians and bicyclists, and not force them to have to adapt their current behavior in the futuristic setup.

In order to answer ***Research Question 2***, the control strategies shall be able to integrate policy objectives in a balanced and demand-responsive way. This implies the following requirements:

Policy Integration Different road users compete for space-time in the intersection, and very short delays can often not be entirely achieved for everyone at the same time. The control should allow for dynamically prioritizing certain road users (e.g., public transport vehicles or emergency vehicles), depending on applied policies and the current traffic situation.

Balance The control should be able to balance the delays of all considered road users at the intersection zone. The prioritization of a road user group or movement should not lead to excessive delays for others.

Demand Responsiveness The control should be able to react to the current demand and integrate all road users in a demand-responsive way if necessary data are available. VRU detection possibilities will be discussed in Section 3.1.

Answering ***Research Question 3*** requires the control strategy to be implementable at a realistic intersection with realistic demand. This includes the consideration of possibly heterogeneous road users and diverse geometries.

Heterogeneity The control should be able to integrate heterogeneous road users, e.g., vehicles with different dimensions and kinematic limitations. This is rather effortless in phase-based TSC, but needs to be considered explicitly in control schemes with individual consideration of each vehicle.

Transferability The control should be easily applicable to diverse intersection layouts (as encountered in the field) with little adaptation. This comprises non-symmetric geometries or different numbers of incoming lanes, for example.

The simulation-based evaluation will discuss to which extent each of these requirements is fulfilled by the proposed control strategies.

Simulation-based Evaluation A realistic intersection zone in Munich is simulated in order to demonstrate feasibility of the approach assuming a realistic intersection layout and measured demand. Special attention is put on the modeling of road user behavior, the simulation of a realistic benchmark control, and the evaluation of the resulting energy consumption by vehicles following optimized trajectories.

1.3 Outline of the Dissertation

The structure of this dissertation is shown in Figure 1.3 and outlined in the following. *Chapter 2* provides a brief introduction on state of the art TSC before presenting a comprehensive literature review on automated intersection control. The numerous studies are categorized based on a set of attributes that describe how vehicle arrivals are scheduled, for example, and research gaps are elaborated. The core of this thesis is the presentation and evaluation of new integrated intersection control strategies for CAVs, pedestrians, and bicyclists in Chapters 3 and 4. Two different control schemes are introduced which differ with regard to several attributes. *Chapter 3* focuses on general considerations about integrating pedestrians and bicyclists into automated intersection control. It presents slot-based integrated intersection control strategies and evaluates how different levels of available information on pedestrian and bicycle arrivals affect resulting delays for all road users. *Chapter 4* builds on the concepts developed in Chapter 3 and presents optimization-based strategies that feature improved flexibility, efficiency, and options to integrate policy objectives. In both chapters, the respective strategies are explained in detail and simulation results are discussed. In *Chapter 5*, the implementation of the new strategies into a simulation framework is explained, and results of a simulation study assuming a realistic intersection with realistic demand are presented. The chapter explains the behavior modeling of considered road users and the implementation of an optimized trajectory planning approach. The proposed control scheme is then compared against the currently implemented TSC considering delays of all road users and overall energy consumption assuming a fleet of electric vehicles. Finally, *Chapter 6* concludes the thesis by summarizing the main contributions of this work and providing an outlook onto possible future research directions.

Chapter 2

State of the Art

The rapid development of CAV technologies offers the possibility to rethink the way intersection zones are controlled. However, the concept, algorithms, and evaluation criteria are built on a long history of intersection control via traffic signals. Therefore, a brief introduction to TSC is given in Section 2.1 before literature about the new concepts is presented in Section 2.2 and research gaps are identified in Section 2.3.

2.1 Traffic Signal Control

This section first describes the basic operational principles of traffic signals and how prevailing traffic conditions and signal timing affect the capacity of an intersection in Section 2.1.1. In Section 2.1.2, evaluation criteria for signalized intersections are discussed. These evaluation criteria have evolved and proved their worth over many years and thus build the basis for evaluating new intersection control strategies later in this thesis. The increasing availability of traffic information from sources ranging from stationary detectors to floating car data allows state of the art TSC to be dynamically optimized with quasi real-time information about approaching vehicles. A brief introduction on advanced signal control systems is given in Section 2.1.3, and potentials of the integration of CAVs are briefly described in Section 2.1.4. The section is concluded with a summary in Section 2.1.5.

2.1.1 Preliminaries on Signal Timing

The development of safe and efficient signal timings is an important part of urban traffic control. The following preliminary descriptions are based on the American Signal Timing Manual (STM) [Koonce and Rodegerdts, 2008; Urbanik et al., 2015]. Similar manuals exist in other countries, e.g., the "Richtlinien für Lichtsignalanlagen" (RiLSA) in Germany [FGSV, 2015b]. The primary purpose of a traffic signal is to separate conflicting movements with the aim of ensuring that all road users are served safely and without excessive delay. Here, the term 'movement' describes any road user action at an intersection, e.g., southbound vehicular right turn or pedestrians using the north crosswalk. Signal timing is the process of selecting appropriate values for timing parameters that are implemented in the signal controller which indicates via signal heads if the respective movements are currently allowed to cross the intersection. Movements which are given the right of way can be protected (i.e., no conflicting movements are allowed in the intersection at the same time) or permitted (i.e., conflicting movements are allowed in the intersection at the same time and traffic rules apply). Common

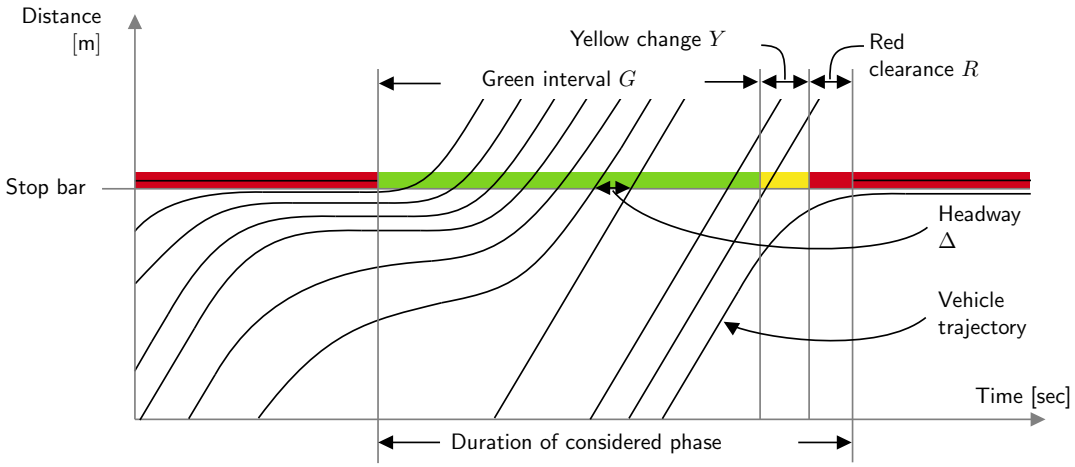

(a) Example trajectories at a signalized movement.

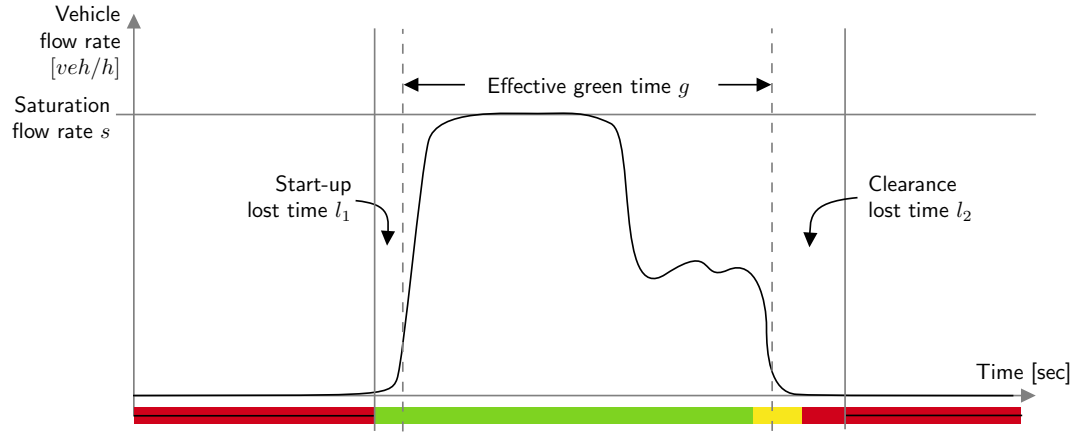

(b) Example flow rates at a signalized movement. Own figure based on [Koonce and Rodegerdts, 2008]

Figure 2.1: Visualization of trajectories and flow rates at a signalized movement.

permitted movements include left-turning movements which are served at the same time as adjacent through movements, or turning movements which are served concurrent to pedestrian movements. A signal phase is defined as the "right of way, yellow change and red clearance intervals in a cycle that are assigned to an independent traffic movement or a combination of movements" [FHWA, 2012]. The red clearance intervals at the end of a signal phase are needed to ensure that road users of the previous phase have left the critical conflict points before the road users of the new phase get there. A cycle is defined as the total time to complete one sequence of signalization for all movements at an intersection. The simplest signal control strategy is a pre-timed strategy which implements a fixed sequence of phases, each with a fixed green time. Let T be the cycle time and $p_1, \ldots, p_n$ be the phases that are run successively with green times $G_1, \ldots, G_n$. The ratios $G_1/T, \ldots, G_n/T$ are determined based on historical data and do not have to be fixed throughout the day. Often, different programs are run during peak hours or during the night time. The different parameters are established through time-of-day plans.

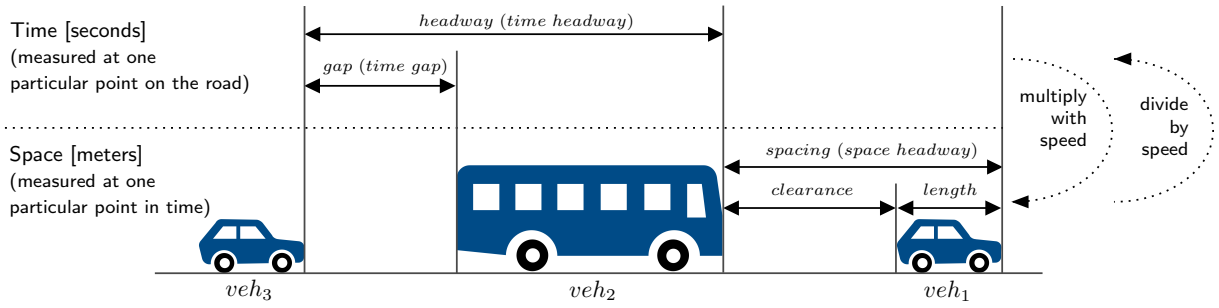

Figure 2.2: Gaps and headways between vehicles.

Every phase switch leads to lost times in which no or significantly fewer vehicles pass through the intersection. These lost times are caused by the startup time in the beginning of a green interval and by the clearance time at the end of a phase, which can best be explained with the help of Figure 2.1. Figure 2.1a shows trajectories of vehicles crossing the signalized intersection zone with the timeline on the x-axis and covered distance on the y-axis. Figure 2.1b shows the same timeline on the x-axis, but the y-axis shows the vehicle flow rate, i.e., the number of vehicles per hour that cross the stop bar. While the signal is red, vehicles stop at the traffic signal and form a queue. The vehicle flow rate hence equals zero. When the signal turns green, vehicles idling at the red signal need some time to react and accelerate, and the first few vehicles cross the intersection at a relatively low speed. This leads to the start-up lost time. Afterwards, the flow stabilizes at the saturation flow rate until the queue waiting at the traffic signal has passed and the flow decreases due to fewer vehicles arriving at the signal. After the end of the green interval, a yellow change interval is implemented to call the drivers' attention to the upcoming signal switch. Some vehicles still pass during the yellow change interval. Finally, a red-clearance interval is implemented before the start of the next phase and it is clear that no vehicle can (or at least should) pass the intersection during that interval. The lost times play an important role when calculating a movement's capacity as described below.

The capacity C_m for a particular vehicular movement m can be calculated as $C_m = s_m \times \frac{g_m}{T}$, where g_m is the effective green time of movement m, T is the cycle time, and s_m is the movement's saturation flow rate. As can be seen in Figure 2.1, the effective green time g for any vehicular movement is given as $g = G + Y + R - (l_1 + l_2)$, where G, Y, and R are the durations of the green (G), yellow change (Y), and red clearance (R) intervals, and l_1 and l_2 are the lost times. The lost times occur at every phase switch and are independent of the phase duration. Therefore, longer green intervals G and fewer phase switches per hour, i.e., a longer cycle time T, can increase vehicle capacity C at the intersection zone. The other important input value for calculating C_m is the saturation flow rate s_m. It depends on the number of lanes available for movement m and on geometric properties as well as traffic characteristics.

For the sake of simplicity, let us assume that vehicle movement m is assigned to one lane and is fully protected. The decisive input parameter for the evaluation of the saturation flow is the time headway Δ between vehicles entering the intersection from this lane. It can be

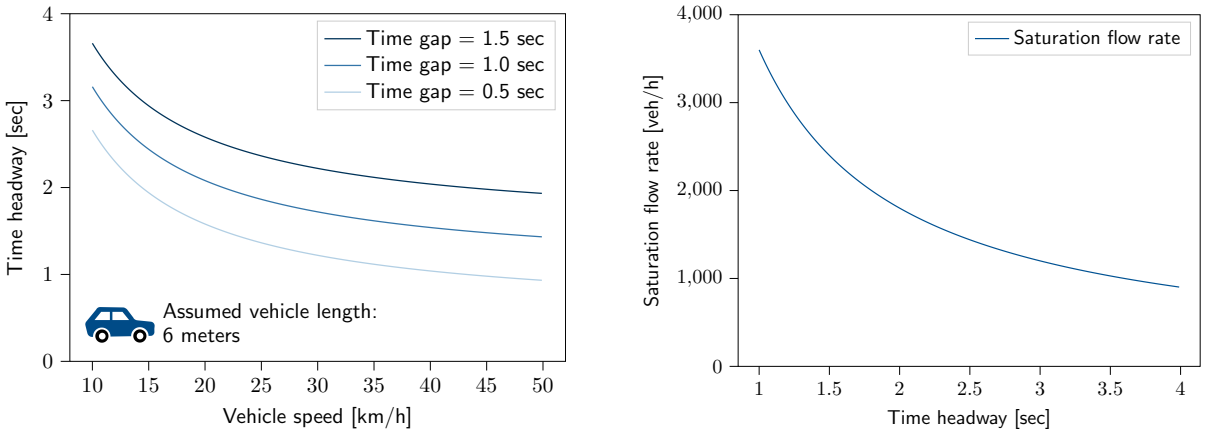

(a) Time headway depending on vehicle speed and time gap.

(b) Saturation flow depending on time headway.

Figure 2.3: Effect of different input parameters on headway and, ultimately, saturation flow rate.

described as the time difference between two successive vehicles arriving at a certain location as indicated in Figure 2.1a. Let Δ be given in seconds per vehicle. The saturation flow rate in vehicles per second can then be calculated as $\frac{1}{\Delta}$. Since vehicle flow rates are usually expressed in the unit 'vehicles per hour' (compare Figure 2.1b), the following formula is used: $s = \frac{1}{\Delta}[\frac{veh}{sec}] \times 3600[\frac{sec}{h}]$. The time headway of two vehicles depends on the length of the front vehicle, the gap between the two vehicles, and their speed. The relationship between these fundamental values is shown in Figure 2.2. Let us assume that the time difference between two successive vehicles arriving at one particular location is measured. First of all, the first vehicle needs to pass entirely. The time needed depends on the length of the vehicle and its speed: clearly, fast and small vehicles pass faster than slow and large vehicles. The second vehicle then arrives after a certain time gap has passed, which is necessary for safety reasons and incorporates the reaction time of drivers. Human drivers should respect a time gap to the front vehicle of at least 0.9 seconds, and most official sources recommend a gap of around 2 seconds when driving at larger speeds [Wagner, 2016]. However, gaps are often shorter, especially in urban traffic and during peak hours. Figure 2.3a shows how the time headway changes depending on the vehicle speed. Vehicle length is assumed to be fixed, and the curves for three different values of time gaps are shown. Resulting time headways in this simple example range between 1 and 4 seconds. These headways are now used to calculate the saturation flow rate and, as can be seen in Figure 2.3b, results differ significantly. The calculated saturation flow rates and, ultimately, the intersection capacity thus significantly depend on assumed input parameters, which are, at this stage, completely independent of the chosen signal timing. This illustrates the importance of explaining assumptions being made and comparing evaluation results with field measurements. Input parameters can be influenced by time, location, movement, and weather conditions, among others. According to the American Highway Capacity Manual (HCM), saturation flow rates commonly range from 1,500 to 2,000 passenger cars per hour per lane [TRB, 2000].

It is clear that the intersection capacity should be large enough to be able to accommodate the estimated traffic demand at the intersection, since long queues occur otherwise. As stated above, longer cycle times T can increase vehicle capacity C at the intersection zone. On the other hand, long cycle times lead to longer average waiting times if the intersection is not operating close to the capacity limit, and to long VRU waiting times. Furthermore, signal timing parameters should be coordinated with surrounding traffic signals to harmonize traffic flow on arterials. This already gives us a first impression on the necessary balancing of the different road users' interests at signalized intersections. In Section 2.1.2, objectives of signal control and the most important evaluation criteria are explained.

2.1.2 Evaluation Criteria of Signal Control Schemes

Objectives of signal control are manifold, including safety, mobility, and accessibility for all different road users as well as vehicle queue length management and environmental impact mitigation [Urbanik et al., 2015]. By nature, different travel modes and directions compete for the limited space-time, and the stated objectives can often not be entirely fulfilled for all road users at the same time. Therefore, a good balance needs to be found that is in line with the overall traffic management concept of a city or region, and additionally depends on the setting of the considered intersection. The evaluation criteria that are used to assess the performance of proposed signal timings need to be meaningful to road users and quantifiable through field measurement [Bonneson et al., 2011].

First of all, safety is aspired by providing sufficient clearance times in between two phases and including appropriate yellow change intervals that allow drivers to appropriately react to the phase switch [Retting et al., 2002]. When developing signal control schemes, safety is hence a requirement that sets constraints on the definition of timing parameters. Nevertheless, some considerations represent a trade-off between increased safety and efficiency, such as the decision whether permitted turning movements are allowed or a fully protected setup is implemented. The safe operation of the proposed signal control scheme needs to be carefully assessed and ensured in the field [FGSV, 2015b].

Assuming safety to be satisfactory, the decisive parameter to evaluate the level of service (LOS) at signalized intersection zones according to both the American HCM [TRB, 2000] and the German counterpart, the Handbuch zur Bemessung von Straßenverkehrsanlagen (HBS) [FGSV, 2015a] is the control delay per vehicle or VRU, respectively. This user-centric performance indicator can serve as "a measure of driver discomfort, frustration, fuel consumption, and increased travel time" [TRB, 2000]. The two manuals HCM and HBS describe six different LOS which are denoted by (American) school grades A to F. Average and maximum delays that are used as criteria for the definition of LOS for different road users are shown in Table 2.1. When developing a signal timing plan, the LOS is evaluated for each movement separately. As explained above, not all of the movements will receive excellent grades. Instead, a good trade-off needs to be found such that no movement experiences excessive delays. In addition, prioritization depends on policy and setting. Generalized strategies as presented by Koonce and Rodegerdts [2008] include the focus on pedestrians and bicyclists in down-

LOS	Vehicle delay [sec]		PT delay [sec]		VRU wait time [sec]	
	Mean (HCM)	Mean (HBS)	Mean[1] (HCM)	Mean[2] (HBS)	Mean (HCM)	Max (HBS)
A	≤ 10	≤ 20	—	≤ 5	≤ 10	≤ 30
B	$10 - 20$	$20 - 35$	—	$5 - 15$	$10 - 20$	$30 - 40$
C	$20 - 35$	$35 - 50$	—	$15 - 25$	$20 - 30$	$40 - 55$
D	$35 - 55$	$50 - 70$	—	$25 - 40$	$30 - 40$	$55 - 70$
E	$55 - 80$	> 70	—	$40 - 60$	$40 - 60$	$70 - 85$
F	> 80	—[3]	—	> 60	> 60	> 85

[1] Not defined. Values for vehicle delay apply.
[2] Values for PT vehicles on separate lanes or at intersection with PT prioritization only.
[3] Movement is evaluated by LOS F if demand exceeds capacity.

Table 2.1: Definitions of LOS at signalized intersection zones according to the American HCM and the German HBS [TRB, 2000; FGSV, 2015a]

town areas, or near schools, universities or parks; the focus on PT along transit corridors or near PT stations, or the focus on vehicle traffic in locations with high vehicle traffic or along freight corridors. Further evaluation criteria include queue lengths, emissions, and number of stops. Additionally, vehicle LOS is often measured (and optimized) for a corridor of intersections instead of an individual one, which better reflects the experience of travelers and resulting emissions. The following Section 2.1.3 describes how traffic-responsive (instead of the above presented pre-timed) TSC can help achieve efficiency objectives or prioritization of certain user groups.

2.1.3 Dynamic Traffic Signal Control

Pre-determined phase sequences and durations as described in Section 2.1.1 can be inefficient in situations with fluctuating demand. Additionally, specific vehicles with preferential treatment (e.g., PT and emergency vehicles) cannot be considered with priority if the timing plan is fixed. Therefore, advanced signal timing programs have been developed that dynamically react to changes in demand and incorporate priority requests. Changes in demand are usually recognized via loop detectors or cameras that are placed at different locations, e.g., at the stop bar, at the entrance of right- or left-turn storage bays, midblock on the approach to the intersection, or at the upstream intersection. PT vehicles such as busses and trams can be detected via radio frequency transponders mounted on the vehicles or via Global Positioning System (GPS) detection [Smith et al., 2005]. Emergency vehicles can request signal preemption via radio transmission as well, or use the light-based, infrared-based or sound-based detector/emitter systems available today [Paniati and Amoni, 2006]. Communication via V2I and V2V technologies is promising for all of these applications, too. A brief overview on past, present, and future research trends with respect to dynamic TSC in the light of changing technologies and community interests is given by the Standing Committee on Traffic Signal Systems of the Transportation Research Board (TRB) [Day et al., 2019].

Dynamic signal control can be classified as traffic actuated or adaptive. Preferential treatment for specific vehicles can be integrated into both of them and is thus described separately below. The following brief introduction is again based on the STM [Koonce and Rodegerdts, 2008; Urbanik et al., 2015].

Actuated Traffic Signal Control

Actuated signal control schemes react to measured demand changes based on pre-defined rules. If all incoming lanes are equipped with detectors, the system is considered to be fully actuated – if only a subset of lanes detects incoming traffic, the system is called semi-actuated. Actuated traffic control programs can include some or all of the following features:

Dynamic phase duration. Instead of a fixed green interval, a minimum and maximum green time is defined in actuated traffic signals. If the traffic flow falls below a certain threshold, the phase can be ended earlier. This is usually recognized through measuring time headways on the approach to the intersection: if a gap in detector occupancy is greater than a predefined passage time, this indicates that the respective flow rate is no longer efficient and the green time is ended. Recalling Figure 2.1, the traffic flow significantly decreases after approximately two thirds of the assigned green time. Therefore, depending on threshold and demand situation on the other movements, the green interval could be ended at that point.

Phase skipping. Phases can be integrated on demand and thus be skipped if no demand is detected for the movements assigned to a specific phase. Examples are protected left-turn phases, pedestrian phases that are skipped if the pedestrian button has not been activated, or special PT phases that need to be requested by PT vehicles.

Phase combination. Compatible phases without conflict can be given the right of way at the same time. These phases can thus be combined dynamically. One well-known example that makes use of this property is the ring-and-barrier signal design which is explained in the STM [Urbanik et al., 2015].

Adaptive Traffic Signal Control

Instead of using the measured data to reactively implement signal actions following a rule-based flowchart, adaptive signal control strategies use more complex models for predicting future traffic states and choosing suitable actions. The conceptual basics can be described as iteratively repeating the following three steps [Koonce and Rodegerdts, 2008]:

1. Real-time data from detectors and sensor systems are used to estimate the current traffic conditions.

2. A model is used to evaluate the effects of alternative signal timing strategies on the traffic flow. The best strategy is identified based on some performance metric.

3. The strategy identified in Step 2 is implemented.

Especially the optimization involved in Step 2 of the concept can be computationally expensive. Therefore, the optimization search process is often limited by time or boundary conditions, or heuristic methods and artificial intelligence are used instead of actual optimization. Additionally, to avoid high fluctuations of signal timings, the search domain can be limited, too [A. Stevanovic, 2010]. The evaluation of effects in Step 2 often has a longer time horizon than the actual implementation in Step 3. This allows for dynamically revising the decisions when new data are obtained. This concept is called a rolling horizon scheme and is commonly used in dynamic control. It will be introduced in Chapter 4.

Over the past years, many different adaptive signal control models and approaches have been presented. These strategies are complex and require significantly more description and discussion to be understood, which is out of the scope of this thesis. A good overview on concepts, requirements, and deployment is given by A. Stevanovic [2010].

Preferential Treatment for Specific Vehicle Groups

Preferential treatment at signalized intersections can be implemented to give specific vehicles the right of way with limited delays. Two different levels of preferential treatment can be distinguished:

Signal preemption can be translated as "absolute priority", i.e., an immediate green interval is requested. In the Manual on Uniform Traffic Control Devices, signal preemption is defined as "the transfer of normal operation of a traffic control signal to a special control mode of operation" [FHWA, 2012]. This is usually applied for emergency vehicles which should experience no delay and would have trouble maneuvering through traffic fast and safely without the signal preemption.

Signal priority can be understood as the request to consider a specific vehicle with preference, but this request is integrated in such a way that limited impacts on other road users and the signal operation overall can be ensured. Signal priority is commonly implemented for PT vehicles such as busses and trams to reduce their delays and improve the overall travel time and reliability of PT systems. In contrast to preemption, the priority request may or may not be granted. Priority is usually applied via green time extension or red truncation. If the PT vehicle approaches a green signal, the controller can extend the current green time to allow the PT vehicle to proceed on an extended green signal. If the PT vehicle approaches a red signal, the controller can end the current phase earlier to allow the PT vehicle to proceed on an early green signal.

Summary on Dynamic Traffic Signal Control

Dynamic TSC can significantly improve capacity and LOS at intersections, since the green times are efficiently allocated on a cycle-by-cycle basis. Additionally, the preferential treatment of specific vehicle groups allows for the integration of policy objectives. On the other hand, detector implementation and maintenance are costly [Koonce and Rodegerdts, 2008]. Furthermore, the complexity of the advanced systems presents an additional challenge for

agencies, and requires the employment and proper training of experts [A. Stevanovic, 2010].

2.1.4 Potentials of the Integration of Connected Automated Vehicles

It has been discussed by several researchers that CAVs can lead to improvements regarding average delay, fuel consumption, and emissions at intersection zones. Improvements can be achieved on several levels: first of all, if vehicle headways can be reduced via uniform driving behavior and shorter reaction times, the saturation flow can be increased which ultimately increases the number of vehicles that can pass the intersection within a given time interval. This can be seen in Figures 2.2 and 2.3 and is explained for example by Friedrich [2016]. Secondly, if vehicles can receive information from surrounding vehicles and the signal controller and can thus be informed about phase switches and queues on the approach to the intersection, they can adjust their trajectories in order to arrive at the intersection zone with the optimal speed. This can reduce start-up and clearance lost times at the intersection zone [Stebbins et al., 2017]. Additionally, optimized acceleration profiles and a decreased number of stops can reduce emissions and increase user comfort [Typaldos et al., 2020; Rostami-Shahrbabaki, Niels, et al., 2020]. One important issue considering these applications is the prediction of phase switches. As described in Section 2.1.3, the start and end of a signal phase is triggered using real-time data that is fed into flowcharts or optimization schemes. Therefore, it is difficult to predict when green intervals will start and end, an information that is needed for green light optimal speed advisory (GLOSA) [A. Stevanovic, J. Stevanovic, et al., 2013]. Furthermore, the success of traffic responsive signal control systems depends on detection coverage. The information that is needed for the signal timing optimization in adaptive traffic signals can be enhanced by the information received from vehicles via V2I-communication which contains more detailed data, e.g., vehicle positions and speeds on an individual level [Priemer and Friedrich, 2009; J. Kaths et al., 2015]. Finally, real-time information about signal timings and queues can be used to improve route guidance [Guo et al., 2019].

2.1.5 Summary

This section has provided a very brief introduction into the wide domain of TSC. Understanding the basic concepts and evaluation criteria will be helpful when developing and evaluating new intersection control strategies in this thesis. As described above, modern actuated and adaptive signal control strategies are complex systems that need further description and discussion to be fully understood, what goes beyond the scope of this thesis. However, even though modern traffic signal operations use many degrees of freedom and advanced optimization techniques in the timing process, the basic concept remains: groups of road users, e.g., vehicles on one particular movement, are given the right of way in an alternating fashion. If all vehicles are connected and automated, they could instead be considered at an individual level and conflicts could be resolved in a seamless manner. Such new concepts will be described in the following section.

2.2 Intersection Control for Connected Automated Vehicles

If a large percentage of vehicles are connected and automated, they can share information with other vehicles and the infrastructure in order to plan collision-free trajectories and increase the safety and efficiency on roads and intersection zones. In recent years, many intersection management schemes for a 100% CAV penetration rate have been proposed which could replace traditional traffic rules, signs, and signals. Most studies focus on classic intersection zones, i.e., junctions where two roads cross at the same level. Nevertheless, the presented concepts can be adapted for other locations where the paths of different road users intersect, such as roundabouts, construction sites, and pedestrian crossings, among others. The so-called intersection control or intersection management schemes that can be found in the literature are referred to by different names. Examples include the terms autonomous, automated, or cooperative intersection management. In order to improve readability, the consistent and probably most common term and abbreviation autonomous intersection management (AIM) is going to be used in the following.

The first notable work on AIM was presented by Kurt Dresner and Peter Stone [Dresner and Stone, 2004; Dresner and Stone, 2006]. They presented a multi-agent approach where vehicle agents communicate with an intersection agent in order to exclusively reserve discrete areas of the respective intersection zone. The implementation requires the intersection to be divided into a grid of "tiles". Each of the tiles can be used by one car in each time step. Approaching vehicles send messages to the so-called intersection manager, a central entity that coordinates the requests. The messages sent by the vehicle contain information on the arrival time of the vehicle at the intersection, the velocity at which the vehicle will arrive, the turning information, as well as vehicle dimensions and kinematic limitations. With the given information, the intersection manager simulates the trajectory of the vehicle through the intersection and determines the sequence of cells and exact time slots that need to be reserved for the vehicle. If no conflict has been detected, i.e., all cells are available at the requested times, then the reservation is accepted and the tiles are blocked for the respective vehicle. Otherwise, the reservation is rejected. The vehicle then decelerates and sends a new request with a later arrival time at the intersection. The authors simulated the new reservation-based control approach in a custom simulator and reported significant delay reductions compared to a simple traffic signal. Motivated by the promising results and driven by the continuous development in communication and automation technology, many studies by scholars from all over the world followed: The authors of a recent survey found more than 120 conference and journal papers concerning the topic [Khayatian et al., 2020], and more than 60 papers have been published since 2015 alone [Namazi et al., 2019]. AIM attracts researchers from various fields of research, including traffic engineers, computer scientists, and mathematicians. Consequently, presented concepts focus on different aspects, e.g., mathematical optimization techniques or necessary communication protocols. A number of attributes can be distinguished, as described in the most important surveys [L. Chen and Englund, 2016; Qian et al., 2017; Khayatian et al., 2020; Zhong et al., 2021]. A selection of these attributes and their specifications are shown in Figure 2.4.

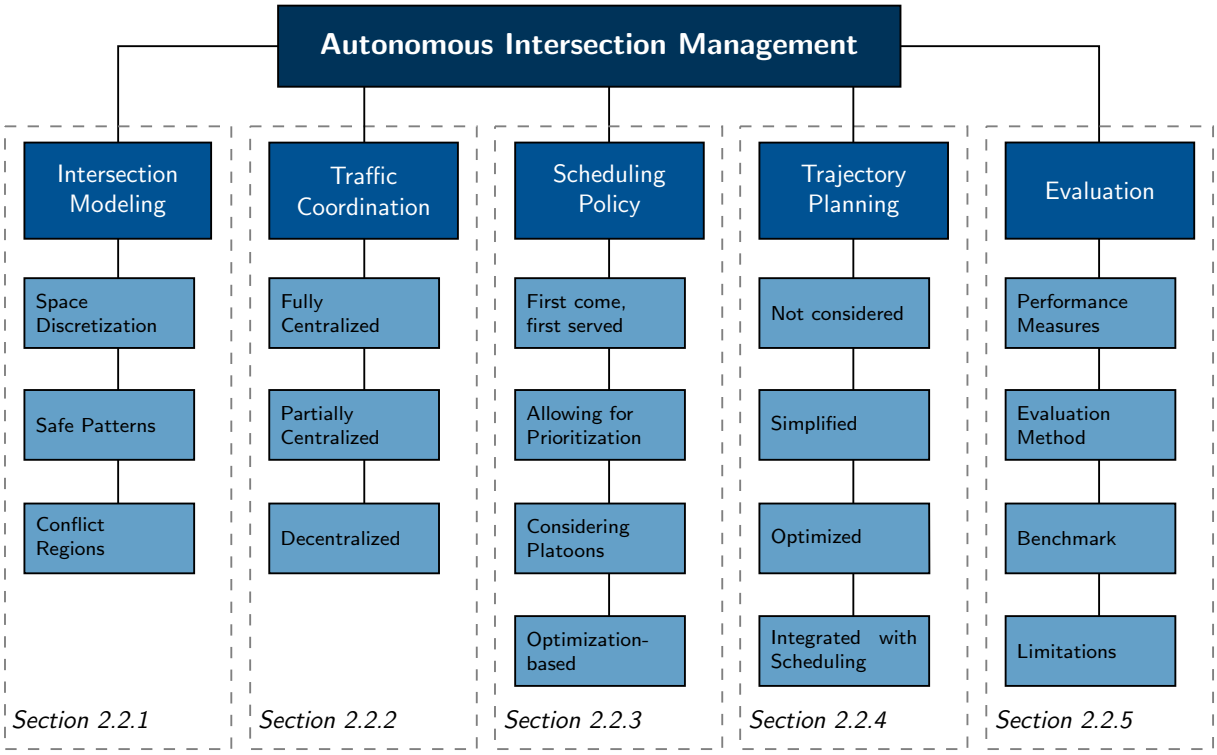

Figure 2.4: A selection of attributes and respective characteristics that can be used to characterize AIM approaches.

The figure also shows the structure of this literature review which follows the most important steps of the process of designing an AIM concept from intersection modeling to approach evaluation. First of all, different approaches for the detection of conflicting trajectories are described in Section 2.2.1. Traffic coordination describes whether the most important tasks, i.e., conflict-free scheduling and trajectory planning, are organized by a central control unit or by the approaching vehicles themselves, different concepts of which are explained in Section 2.2.2. A main focus is put on presenting the evolution of scheduling policies in Section 2.2.3. Section 2.2.4 provides a brief introduction on how trajectories are planned, and Section 2.2.5 discusses how concepts are evaluated in the presented studies. Each of the sections is concluded with a short discussion on benefits and limitations of the presented concepts and current research trends. Section 2.2.6 provides a summary of the literature review on AIM. In addition to the description of literature in the following subsections, a tabular overview of reviewed studies and the main attributes of the concepts presented therein is provided in Appendix A.

2.2.1 Intersection Modeling

One of the most important tasks for the AIM approach is to identify conflicting trajectories and adjust vehicle movements such that conflicts are resolved. With the exception of very few recent studies (e.g., [B. Li et al., 2018]), two general assumptions are being made in current literature: (i) both entrance and exit lane are decided before the vehicle enters the intersection, and (ii) for each combination of entrance and exit lane there exists a predefined path that

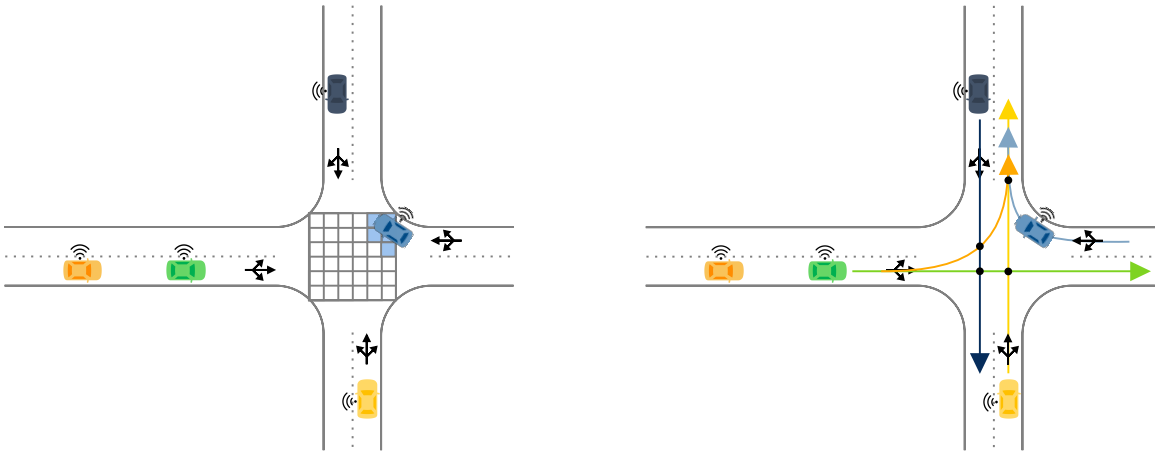

(a) Space discretization. (b) Conflict points.

Figure 2.5: Intersection modeling.

the respective vehicle is going to follow. Therefore, the intersection zone is not considered a continuous two-dimensional space, but a set of "pipes" that connect entering and exiting lanes of the intersection zone. The AIM thus needs to detect vehicle paths that overlap or cross each other and, since vehicles cannot alter the physical path through the intersection, obtain the conflict resolution by ensuring sufficient time gaps between each two vehicles.

There exist two major approaches for completing these two steps that will be presented in the following. The first one is the concept of space discretization, shown in Figure 2.5a, the second one is the concept of conflict region modeling by intersecting the prescribed vehicle paths, shown in Figure 2.5b.

Discretization of Space

A common approach when modeling AIM is to first discretize the space of the intersection zone, i.e., to divide it into a set of pairwise disjoint cells as shown in Figure 2.5a. Each vehicle path defined by entrance and exit lane passes a predefined set of these discrete zones in a given order. In order to determine the time that a vehicle needs to cross each of the zones, the vehicle trajectory is either simulated [Dresner and Stone, 2004], or the vehicle speed is assumed to be fixed throughout the trajectory [Y. Wu et al., 2019]. In this case, the time a vehicle needs to cross one of the cells depends on the vehicle size, speed, and on the size of the cell. Now, conflicts can be avoided by limiting the occupancy of each cell to one vehicle at a time. This discretization was first used in the work by Dresner and Stone [2004], where the intersection zone was divided into a grid of $n \cdot n$ cells with n being denoted as the granularity. A granularity of $n = 1$ leads to high delays, since only one vehicle is allowed in the intersection zone at the same time. This means that even non-conflicting vehicle movements running on parallel lanes compete with each other. Therefore, it is recommended that n corresponds to at least the number of incoming and outgoing lanes. In general, a higher granularity increases the accuracy of considered gaps and the efficiency of the control. However, it also increases the complexity of the calculation [Dresner and Stone, 2008]. The discretization of space

is often combined with the fragmenting of time (e.g., in time slots of a fraction of a second), such that the problem of intersection zone coordination becomes, from the mathematical perspective, a discrete problem that can be approximated or solved with discrete optimization methods.

Conflict Region Modeling

Instead of discretizing the whole intersection zone into a number of cells, the predefined vehicle paths can be used to generate a binary matrix that indicates whether two paths intersect, and so-called safe patterns, i.e., sets of vehicle movements that can be allowed at the same time. This approach is often used for simplified intersections with through movement only. For example, in the studies presented by Fayazi and Vahidi [2018] and Yao et al. [2020], vehicles traveling eastbound and vehicles traveling westbound are allowed in the intersection at the same time, while respecting a sufficient time gap for the car following behaviour of vehicles coming from the same direction. Vehicles traveling north- or southbound are then only allowed to enter the intersection if all previously assigned vehicles on the east-west movement have left the intersection zone entirely. This definition of safe patterns allows for the intuitive consideration of platoons. It is possible that, if turning movements were included, the approach could become inefficient: a left-turning vehicle, for example, would block the entire intersection for the majority of other movements.

Zhu and Ukkusuri [2015] improved on this approach by extending the simple binary conflict matrix and including the exact distances between two conflict points. Then, two vehicles with conflicting movements are allowed in the intersection zone at the same time if sufficient spacing between these two vehicles at their conflict point can be guaranteed. Consider the blue and the yellow vehicle in Figure 2.5b, for example. If a sufficient time gap at their common conflict point is respected, then their movement does not conflict anywhere else in the intersection, either. Levin, Fritz, et al. [2016] describe that, for smaller intersection zones, modeling the intersection zone with a conflict-point based formulation requires less computational complexity than a tile-based modeling with high granularity. In particular, they draw a comparison with the implementation presented by Fajardo et al. [2011] who divide the considered intersection into tiles with a width of only 0.25 meters. Assuming lane widths of 3 meters, the intersection in Figure 2.5a would be divided into $24 \cdot 24 = 676$ tiles. On the other hand, with four incoming lanes and three turning movements per lane there are a total of 12 paths through the intersection. Even if all of the paths had conflict points with all other paths, which is not the case, this would lead to only $\binom{12}{2} = 66$ conflict points. It needs to be noted that the number of conflict points may scale worse than the number of tiles with a growing number of lanes [Levin, Fritz, et al., 2016]. However, the scaling effect can be questioned, as the number of lanes going into an intersection is fairly limited.

Discussion

This introduction serves the purpose of better understanding how conflicts are detected and resolved in the AIM approaches that will be presented in the following. The definition of conflict points as described above is based on the logical connection between paths, whereas

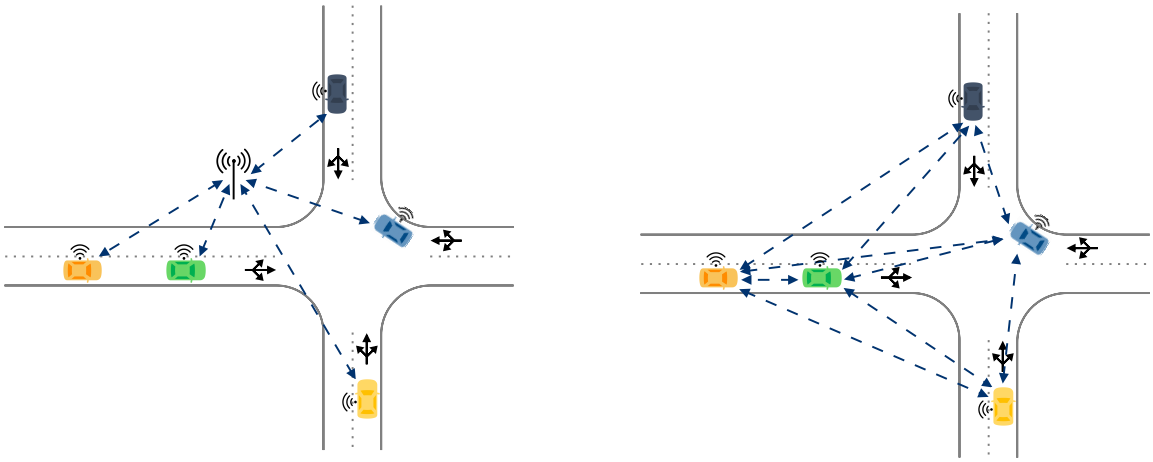

(a) Centralized traffic coordination. (b) Decentralized traffic coordination.

Figure 2.6: Traffic coordination.

the cells deal more with dividing the intersection space. However, in practice there is no clear boundary between the two presented concepts. In fact, cells can be transformed into conflict regions by omitting redundant tiles, and conflict points can be framed with spacial gaps and thus be transformed into discrete cells. Both concepts can, but do not have to, be combined with a discretization of time.

2.2.2 Traffic Coordination

Conflicting vehicle paths can be identified using suitable intersection models as described above. Now, vehicle movements have to be changed in such a way that conflicts are in fact resolved. This is done through traffic coordination. The coordination consists of several steps:

1. *Scheduling*
   (i) Identify the sequence in which vehicles (with conflicting paths) enter the intersection zone.
   (ii) Assign the exact arrival time at the intersection zone and the respective speed for each vehicle.
2. *Trajectory planning*
   Plan the trajectory of each vehicle from the current time until it leaves the intersection zone.

The traffic coordination at an intersection zone can either be organized with the help of a central control, or in a cooperative manner, where vehicles communicate with each other and follow a protocol without the need for a central coordination unit. These two approaches are schematically displayed in Figure 2.6. Approaches that involve a central controller will be called centralized in the following, even if the central controller does not perform all of the coordination steps above. In some approaches, only parts of the coordination process (usually

the scheduling of vehicles) are performed by a central controller, but others (usually the trajectory planning) are handled individually or cooperatively. The arrival sequence and exact arrival times of vehicles are typically determined in one joint step: based on the arrival sequence, the earliest possible conflict-free arrival time is set for each vehicle, or vice versa. One exception is the study by Bian et al. [2019]: the authors first decide on the sequence of vehicles to arrive at the intersection zone, the exact arrival times are then determined by evaluating a trade-off between delay minimization and driver comfort, where staying at a constant speed is considered to be more comfortable than accelerating to the maximum allowed speed.

In the following, the main ideas behind centralized and decentralized approaches are described.

Centralized Approaches

Centralized strategies assume that a coordination unit collects information and gives instructions to vehicles on when and how to pass the intersection zone – somewhat similarly to a traffic signal. Centralized approaches have the advantage of lower communication requirements (each vehicle only communicates with the central unit), and the computation of a feasible solution can be done centrally with all available information [L. Chen and Englund, 2016]. On the other hand, centralized approaches heavily rely on the intersection control entity. If this central controller fails, the whole intersection management system does not work anymore. In such a situation, a fallback option is needed. This could work similarly to situations in which a conventional TSC fail and, instead, traffic rules and negotiation apply. Two different types of protocol for centralized approaches can be seen in literature [Khayatian et al., 2020]:

Query-based approaches. In query-based approaches, vehicles request a certain trajectory, and the intersection manager either *accepts* or *rejects* the trajectory that the vehicle proposed. If the vehicle's trajectory is rejected, the vehicle slows down and requests a new one [Dresner and Stone, 2004]. It is clear that the vehicle can only enter the intersection zone with an existing reservation. Therefore, if it is not successful with the first requests, it can come to a full stop at the entrance of the protection zone around the intersection. The approach can lead to a lot of communication overhead, because vehicles might have to request the reservation of space-time over and over again. Furthermore, the limited response possibilities of either accepting or rejecting requests does not allow for including advanced scheduling strategies. On the other hand, the complexity of the controller task is rather low compared to assignment-based approaches [Khayatian et al., 2020].

Assignment-based approaches. In assignment-based approaches, the intersection manager receives the requests and, for each approaching vehicle, decides on a specific time of arrival and speed for crossing the intersection which the controller sends back to the vehicles (see e.g., [E. R. Müller et al., 2016a; Fayazi and Vahidi, 2018]). Assignment-based approaches are much more common in literature. They allow for collecting several requests and applying sophisticated strategies for finding suitable time slots for each vehicle. This makes the scheduling task more complex but can improve throughput significantly as will be discussed in Section 2.2.3.

Fully and Partially Centralized Approaches

In fully centralized approaches, the AIM develops a full trajectory for each vehicle (either in advance or via acceleration and deceleration commands in every time step). Vehicles need to exactly follow this trajectory or hand over the complete control to the intersection control unit. Main concerns about fully centralized approaches include the question of whether full take-over of control will be feasible in practice and whether the system is scalable for larger intersection zones [Qian et al., 2017; Khayatian et al., 2020]. Partially centralized approaches instead involve a centralized scheduling process, but with vehicles individually or collectively planning their trajectories (see e.g., [Jin et al., 2012]). Vehicles need to confirm that they can in fact meet the proposed arrival time and speed or cancel their reservation in case they experience delays. In some studies, the centralized controller does not directly communicate with all vehicles, but only with leading vehicles that request time slots on behalf of a platoon as in Bashiri and Fleming [2017]. Vehicles within a platoon then communicate with each other in order to approach the intersection together. Partially centralized approaches are discussed as a feasible option regarding vehicle control autonomy and scalability [Qian et al., 2017]. The discussion raises many issues including technological feasibility, data privacy, security, and liability, which will certainly become more relevant in the future. However, at the current stage, the majority of papers focus on other aspects, and presented approaches do not allow for a clear categorization as being fully or partially centralized.

Decentralized Approaches

Decentralized approaches do not require support from the infrastructure. Instead, vehicles communicate directly with each other and negotiate the right of way following given protocols. As there is no single point of failure, decentralized AIM are considered to be more robust. On the other hand, it also requires more communication effort to ensure information consistency, and reaching a global objective is more difficult [L. Chen and Englund, 2016; Qian et al., 2017]. One strategy of decentralized AIM is that the approaching vehicle which is closest to the intersection zone temporarily takes the role of the leader, assigns crossing times to individual vehicles and then hands over to the next leader (see e.g., [L. Li and F.-Y. Wang, 2006; Ferreira et al., 2010]). Another approach is the strategy of "token reservation". Each conflict zone has a certain token and only the vehicle holding the token is allowed to pass the respective zone. Vehicles constantly communicate to know which vehicle is currently holding which token [Naumann et al., 1998]. Vehicles can claim the token for a certain amount of time and, if no vehicle has claimed it yet, can reserve it. Claims can also dominate each other, meaning that a new claim can overrule and thus cancel existing claims if the new vehicle has a higher priority [VanMiddlesworth et al., 2008]. In cooperative approaches, it is a challenge to ensure information consistency for all approaching vehicles.

Discussion

While both approaches have their advantages and disadvantages, the majority of studies use centralized concepts [L. Chen and Englund, 2016; Khayatian et al., 2020]. The decision of which concept to apply is mainly based on the use case, i.e., on whether the approach focuses on trajectory optimization at a small intersection with low traffic volume or on the

orchestration of a large number of vehicles at a major intersection. The two concepts can thus roughly be transferred to today's unsignalized and signalized intersections. If a small intersection with low demand is considered, vehicles could negotiate the right of way directly, thus saving the money for dedicated infrastructure equipment. If the intersection currently requires a traffic signal, the communication overhead of cooperative approaches might be too large. If human drivers, pedestrians, or bicyclists are considered as well, then a central controller might be needed, since there is no clear communication protocol with human road users. Therefore, the central intersection control could be combined with a signalization for pedestrians, bicyclists, and human drivers.

In the following Sections 2.2.3 and 2.2.4, the two main tasks of intersection coordination are described in more detail: vehicle scheduling and trajectory planning.

2.2.3 Scheduling Policy

The scheduling policy describes how the order and arrival times of vehicles entering the intersection zone are determined. In this section, selected scheduling policies are explained along the classifications (i) first come, first served strategies, (ii) other rule-based approaches, e.g., including prioritization or platoon-consideration, and (iii) optimization-based strategies.

First Come, First Served Policy

One of the most widely used concepts is the first come, first served (FCFS) strategy, also known as first in, first out (FIFO) derived from warehousing. As the name suggests, it processes requests of approaching vehicles in the order of their receipt. It works for both centralized and distributed systems, is easy to implement, and can provide an immediate response for the vehicle that has requested passage, thus making it easy to plan trajectories accordingly. Fajardo et al. [2011] test the FCFS approach against optimized pre-timed two- and three-phase traffic signals and show that vehicle delays can be reduced significantly in every considered scenario. However, the presented test scenarios do not cover very high demands. Levin, Boyles, and Patel [2016] found several situations in which traditional traffic signals outperformed the FCFS approach. In fact, FCFS schemes can be inefficient, as they do not take advantage of the knowledge the system has about arriving vehicles. Usually, the gaps for following vehicles are smaller than the gaps for vehicles whose paths intersect. Therefore, it is beneficial for vehicles coming from the same direction to form platoons that cross together [Lioris et al., 2016]. This idea is displayed in Figure 2.7: It is assumed that the minimum headway for vehicles on the same approach (Δ^{same}) is 2 seconds and the minimum headway at the conflict point p for crossing vehicles (Δ^{cross}) is 3 seconds. The FCFS strategy lets the orange and blue vehicles depicted in Figure 2.7a cross in an alternating order as shown in Figure 2.7b. Here, the dotted lines show the fastest possible trajectories of the vehicles, and the continuous lines show the actual trajectories in a simplified way. The delay of each individual vehicle is calculated as the difference between the earliest possible arrival time at the conflict point p and the actual arrival time: veh_1 does not experience delay, veh_2 experiences 2 seconds of delay, and so on. The total delay resulting from the FCFS schedule is 20 seconds. A more sophisticated approach could take advantage of the knowledge that there are more orange

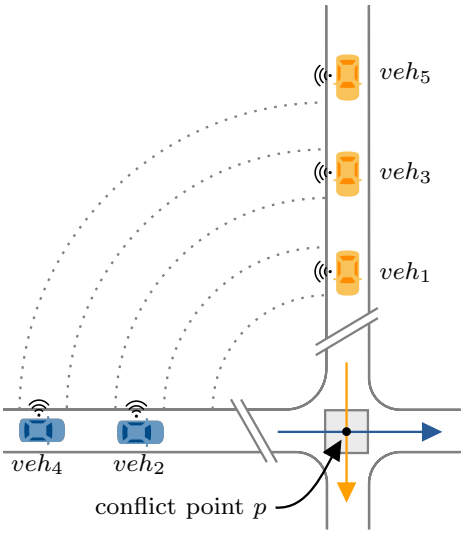

(a) Example of a simple intersection zone with five approaching vehicles.

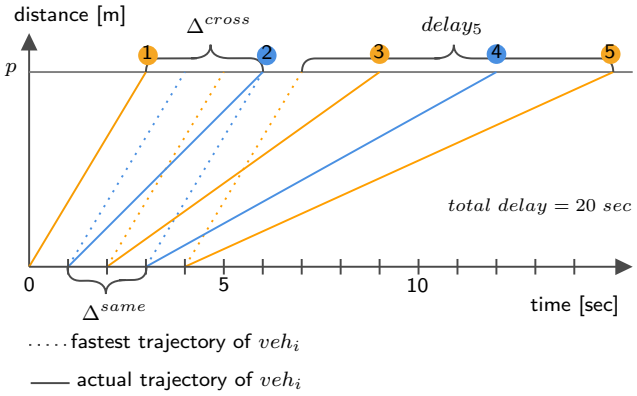

(b) Schedule resulting from FCFS strategy.

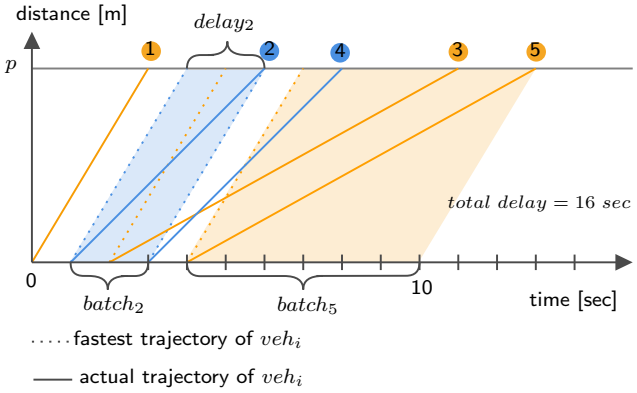

(c) Schedule resulting from *BATCH* strategy.

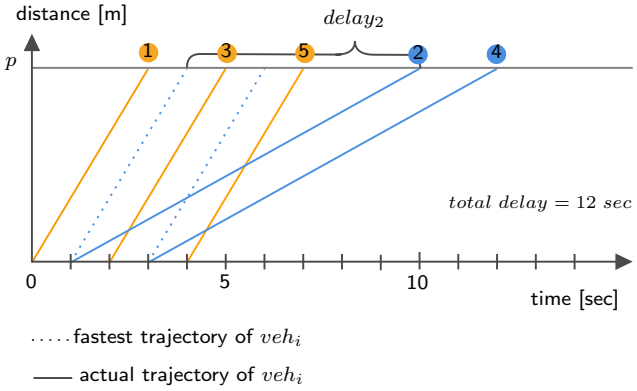

(d) Schedule resulting from optimization-based strategy.

Figure 2.7: Comparison of FCFS, *BATCH*, and an optimization-based control strategy.

vehicles to come directly behind the first one. Additionally, the strict paradigm of classic FCFS does not allow for prioritization of vehicles. The fairness of FCFS is considered a benefit of the control that also becomes apparent in Figure 2.7. However, that does not mean that each vehicle experiences roughly the same delay. If demand is not symmetric and a queue is formed on one of the approaches, then there might be vehicles at the back of the queue that cannot yet communicate with the intersection manager. Vehicles on other approaches with less demand can approach the intersection zone quickly and start communicating with the controller. This means that less delay is experienced on the approaches with less demand. A traffic signal would work the other way around and assign a higher share of green time to the approaches with high demand, usually leading to less delay on the major roads [Levin, Boyles, and Patel, 2016].

Other Rule-Based Scheduling Policies

In order to overcome the shortcomings described above, several researchers have proposed combinations of the FCFS scheme with prioritization strategies or have developed other rule-based scheduling policies.

Prioritization of Vehicles
In Dresner and Stone [2006], the authors extend their previously presented approach and include emergency vehicles. Emergency vehicles send reservation requests with a special priority level. The intersection manager keeps track of all incoming lanes and if there is an approaching emergency vehicle on one of the lanes, only requests from this same lane are accepted by the intersection manager. Thus, emergency vehicles and the vehicles driving in front of them are strictly prioritized. As a consequence, delays of emergency vehicles are significantly lower than delays of other vehicles, especially in high traffic demand scenarios.

Even if prioritization is not as critical as in the emergency vehicle case, different vehicles and road users might have different values of time or might be prioritized for policy reasons. Several approaches use trading or bidding strategies to incorporate such prioritization: the vehicle agents either negotiate directly with the intersection controller or they trade in order to exchange reserved time slots. Schepperle, Böhm, and Forster [2007] propose a time slot exchange (TSE) approach: vehicles request time slots for crossing the intersection zone and are accepted following an FCFS scheme. At the same time, every vehicle has a certain value of time, i.e., a price that the passenger would be willing to pay for a delay reduction of 1 second. If drivers are unsatisfied with the assigned time slot they can try and exchange their time slot with another vehicle. The time slot exchange is organized by the central controller, that collects the TSE request. It first looks for feasible exchange candidates and asks them one by one if they would be willing to exchange their time slot. If the exchange can be conducted, the requesting vehicle pays the price derived from its delay reduction and value of time directly to the vehicle that agreed to exchange the time slot. The presented mechanism is rather restrictive, since it does not allow other vehicles that have a fixed time-slot but are not involved in the TSE (e.g., a vehicle driving behind a vehicle that is willing to negotiate) to be delayed due to the deal. Therefore, less than 10% of vehicles initialized a successful TSE and average delays only changed slightly.

In order to overcome this limitation, Schepperle and Böhm [2007] describe an initial time slot auction (ITSA) scheme: the intersection controller leads auctions, where time slots for crossing the intersection are offered. Those vehicles that are eligible for requesting a time slot, i.e., vehicles that are the first vehicle in their queue and do not yet have a reserved time slot, send their bids to the controller. The intersection controller assigns the time slot to the vehicle with the highest bid. In an extension of their algorithm, vehicles can additionally subsidize vehicles in front of them to advance faster. The two presented ITSA schemes slightly increase average delay as compared to the FCFS scheme, but reduce average weighted delay, where the delay of each vehicle is multiplied by its value of time as defined in the previous paragraph. Carlino et al. [2013] use a similar approach, but additionally include system bids with the goal of improving fairness, increasing throughput or reducing queue lengths. They test their approach on four different street networks. Results differ in each scenario – system bids sometimes reduce and sometime increase overall performance. The presented approaches thus allow for prioritizing vehicles, but the overall efficiency is not significantly increased, and it is difficult to incorporate "system goals."

Platoon-based Scheduling Policies
Some researchers present FCFS-like scheduling concepts with the adaptation that vehicles form platoons on the approach to the intersection zone and only the platoon leader communicates with the intersection controller. Bashiri and Fleming [2017] show a significant decrease in vehicle delay and communication overhead for increasing platoon sizes. Additionally, they implement an optimization approach that enumerates all platoon schedules and chooses the one with minimum average delay or minimum delay variance which further improves the performance. However, in each time step, the algorithm considers only those four platoons which are closest to the intersection on their approach, which leads to 24 possible schedules. Additionally, safe patterns are not considered, i.e., vehicles without conflicting movements are not allowed to pass at the same time [Bashiri, Jafarzadeh, et al., 2018].

One of the most famous platoon-based control strategies is the approach presented by Tachet et al. [2016]. The authors model a simple intersection zone such as the one in Figure 2.7a and apply queuing theory: vehicles arrive according to stochastic processes in both approaches. Their service time Δ, i.e., the time the conflict zone is blocked for them, depends on whether they follow a vehicle on the same approach (Δ^{same}) or a vehicle on the conflicting approach (Δ^{cross}). Both Δ^{same} and Δ^{cross} are fixed, as is the case in Figure 2.7 where Δ^{same} is 2 seconds and Δ^{cross} is 3 seconds. Based on the observation that $\Delta^{same} < \Delta^{cross}$, they develop an algorithm called *BATCH* with the goal of processing requests in batches and thus forming platoons. As long as vehicles are able to pass the intersection zone without delays, no batches with more than one vehicle are formed. Let t_i^{min} be the earliest possible arrival time of vehicle veh_i at the intersection and t_i be the actual arrival time following the schedule proposed by the intersection manager. Once a vehicle which requests passing experiences delays following the FCFS-scheme, i.e., $delay_i = t_i - t_i^{min} > 0$, then the algorithm collects requests with earliest possible arrival times in the time window $[t_i^{min}, t_i^{min} + delay_i]$. These vehicles are reordered in such a way that the vehicles coming from the same direction as vehicle veh_i pass first, and the other vehicles afterwards. Considering the situation in Figure 2.7, vehicle

veh_2 experiences a delay of 2 seconds as shown in Figure 2.7c. Two other vehicles have their earliest arrival time in the time window displayed by the blue shadow: veh_3 and veh_4. Those two vehicles are reordered such that the vehicle coming from the same approach as vehicle veh_2 (that started the batch) crosses first, and the vehicle on the other approach crosses afterwards. Vehicle veh_5 is not considered in the batch since it arrives later, but it would start off with a new batch-forming step, since it experiences delay as well. The look-ahead time defined by the delay is small in the case of veh_2, for veh_5 it is already significantly larger, i.e., $delay_5 = t_5 - t_5^{min} = 6\,\text{seconds}$. If delays grow further, the look-ahead time can potentially grow to infinity. In order to ensure fairness, the batch sizes are limited. The $BATCH$ approach performs significantly better than FCFS and theoretical capacity of the intersection increases with an increased maximum batch size. On the other hand, prioritization cannot easily be included into the control.

Optimization-based Scheduling Policies

The strategies presented above offer many further options, e.g., a combination of bidding strategies and platoon-forming. However, it can be seen, e.g., from Carlino et al. [2013], that system objectives are not easily integrated and the rule-based character of the approaches does not necessarily lead to optimal solutions. Therefore, there has also been significant effort to develop optimization-based scheduling policies. Optimization-based scheduling problems are usually formulated as mixed-integer linear programs (MILPs). A more general introduction on MILPs is given in Chapter 4.

The first notable MILP formulation of the scheduling program for intersection control was published by E. R. Müller et al. [2016a]. The authors consider a similar intersection as the one shown in Figure 2.7a. Instead of deciding based on rules which vehicles to serve first, they formulate an optimization problem, where the objective is to minimize the total time vehicles spend to arrive at the intersection. The speed for crossing the intersection is fixed beforehand and each vehicle needs to arrive at the intersection with the same speed. The authors divide the set of vehicles considered in the scheduling process into two disjoint sets depending on the approach the vehicles use. In order to minimize the total time spent by vehicles on the approach to the intersection, the objective function is defined as follows:

$$\min \left(\sum_{veh_i \in \mathcal{V}^E} t_i + \sum_{veh_j \in \mathcal{V}^S} t_j \right)$$

where t_i is the arrival time of vehicle veh_i at the intersection zone and $\mathcal{V}^E$ and $\mathcal{V}^S$ are the sets of vehicles traveling eastbound and southbound, respectively. The set of constraints includes physical limitations and safety gaps. Depending on the current position and speed, and on kinematic limitations of each vehicle veh, the arrival time of veh at the intersection is bounded by t_{veh}^{min} and t_{veh}^{max}. The time window defined by the lower and upper bounds narrows with veh getting closer to the intersection. In the beginning, t_{veh}^{max} is potentially infinitely large, as veh could stop and wait for an indefinite amount of time. If veh is already very close to the intersection, it might not be possible for it to stop and accelerate to the required speed any more, due to physical limitations. The authors also consider two different parameters Δ^{same}

and Δ^{cross} as described above and shown in Figure 2.7. Since the intersection considered by the authors looks similar to the one depicted in Figure 2.7a, it is clear that vehicles cannot overtake on the approach to the intersection. Therefore, FCFS applies for vehicles on the same approach, and a gap of Δ^{same} needs to be respected between them. Vehicles coming from two different approaches need to cross the conflict point with a time gap of Δ^{cross}, while either one of the two vehicles $veh_i \in V^E$ and $veh_j \in V^S$ can pass first. In the considered study, vehicles start communicating with the central intersection controller at a distance of 150 meters to the intersection zone. They directly adapt their speed depending on the proposed arrival time and update their minimum and maximum arriving time for the next optimization run accordingly. From the paper it is unclear in which time interval the optimization is run or if it is triggered by new vehicle arrivals. In contrast to assumptions made in other papers, the gaps considered by the authors are such that $\Delta^{same} > \Delta^{cross}$, which leads to alternating right of way [E. R. Müller et al., 2016a]. For better comparison to the other approaches presented in this thesis, we consider the same values as in the previously explained policies for our small example. Even though E. R. Müller et al. [2016a] implemented their approach to minimize the total time spent on the approach to the intersection, the resulting schedule is equivalent to a schedule that minimizes total delay. This is due to delay being obtained by subtracting the (pre-determined) earliest possible arrival time from the assigned arrival time of each vehicle. The solution to this optimization problem is shown in Figure 2.7d. It can be seen that the three orange vehicles are served first, before the two blue vehicles are allowed to pass. The resulting total delay of all vehicles is 12 seconds. This is less than the total delay of 16 seconds in the *BATCH* scenario and 20 seconds in the FCFS scenario.

In a second paper, the authors extend their approach for a T-intersection with allowed turning movements [E. R. Müller et al., 2016b]. In order to do so, they model the intersection zone with conflict regions (similar to Figure 2.5b) and consider the gaps Δ^{same} and Δ^{cross} at each conflict point.

A similar MILP approach is used by Fayazi and Vahidi [2018] and later Yao et al. [2020]. In both studies, a four-leg intersection with through movement from all directions is modeled as one conflict space, where vehicles in safe patterns are allowed to move together while respecting a sufficient gap Δ^{same} for car-following behavior, and crossing movements are only allowed after a sufficient time gap Δ^{cross}.

Levin and Rey [2017] use a similar approach to the one presented by E. R. Müller et al. [2016b]. They assume constant, but not uniform speeds within the intersection. Vehicle speeds are defined as decision variables in their approach, limited by defined minimum and maximum speeds. Vehicle movement within the intersection zone is described in more detail: in particular, the amount of time that the vehicle spends at a certain conflict point is determined depending on vehicle length and speed and on the curve radius of the vehicle path. Therefore, minimum gaps are defined for each pair of vehicles with conflicting movement individually. The authors run a number of Monte Carlo simulations with vehicle earliest arrival times based on a Poisson distribution with a demand of 800 vehicles per hour per lane. Since the problem can only be solved in real-time for up to 30 vehicles, they introduce a rolling

horizon approach with promising results. The concept will be introduced and discussed in more detail in Chapter 4.

Yu et al. [2019] implement a similar approach to the one presented by Levin and Rey [2017], but use tile-based conflict detection, i.e., the sequence of tiles and the time needed to travel between them is known and instead of separating vehicle movements at conflict points, the necessary gaps are considered at each tile. They compare the approach with an FCFS strategy and the *BATCH* strategy presented by Tachet et al. [2016]. Their results confirm the significant improvements of *BATCH* over FCFS and show additional significant improvements of their optimization-based control, especially for larger vehicle demand. One major limitation is that the optimization problem cannot be solved in real time. However, no detailed computation times are presented and the number of vehicles and number of tiles considered in the optimization process are not given. It can thus not be determined whether the seemingly suboptimal problem setup with a large number of tiles leads to these issues. New custom optimization algorithms and good initial solutions or bounds could improve the runtime.

The MILP-formulation could additionally be combined with prioritization by multiplying parts of the objective function with weighting factors. This has been described by Levin and Rey [2017], but has not been fully explored yet. R. Chen et al. [2020] use weighting factors in their max-pressure control for a network of intersections with vehicle and pedestrian movement. Max-pressure control, originally applied to wireless networks, maximizes throughput and is able to stabilize queue lengths under certain circumstances [Varaiya, 2013]. The control presented by R. Chen et al. [2020] is based on the conflict point-based AIM scheme presented by Levin and Rey [2017]. In the objective function, the weighting factors of vehicles and pedestrians are defined depending on queue lengths on incoming and downstream links and walkways, respectively. The approach is evaluated using numerical simulation with time steps of 15 seconds. The authors show that an increase in pedestrian demand results in an increase in average vehicle delay, presumably since large pedestrian demand results in a higher priority for pedestrians. An increase in vehicle demand has more of a mixed effect on average vehicle delay: on the one hand, larger vehicle queues lead to larger delay, on the other hand, larger vehicle queues lead to larger weighting factors for vehicles. While it can be seen that the weighting factors seem to work, the effect and potential of prioritization has not been evaluated in detail. Prioritization in MILP formulation will be further explored in Chapter 4.

Other Scheduling Policies

The presented assets can be used to categorize the majority of current approaches, but it is clear that the broad spectrum is not classified in its entirety and many other strategies exist. For example, heuristics and metaheuristics including genetic algorithms [Zhuofei Li et al., 2018], ant colony systems [J. Wu et al., 2012] and particle swarm optimization [Guney and Raptis, 2020] are applied to tackle the problem. Additionally, some papers do not consider a separate scheduling policy, but seamlessly resolve conflicts by planning suitable trajectories as will be described in Section 2.2.4.

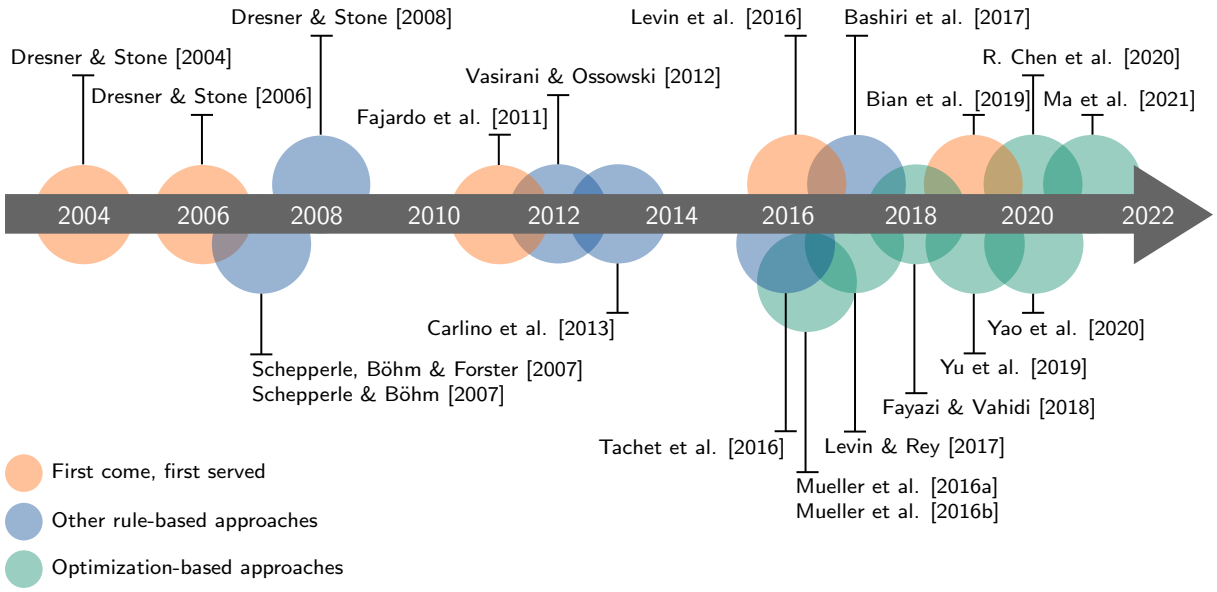

Figure 2.8: Timeline of the development of AIM scheduling policies with selected publications.

Discussion

In contrast to the previous aspects of AIM, a clear evolution can be observed regarding scheduling policies. The timeline of when selected approaches were first presented is shown in Figure 2.8. Starting from simple FCFS approaches, several adaptations have been made to improve overall efficiency until optimization approaches which can further reduce delay were introduced. A simple comparison of the three most recognized approaches is shown in Figure 2.7. It shows that significant improvements can be obtained with advanced strategies. Nevertheless, the "optimal" strategy depends on numerous aspects. One of the major drawbacks of optimization-based approaches is the computation time, which can be an issue if a larger intersection zone is considered. Additionally, fairness and transparency can be infringed. As can be seen in Figure 2.7d, delay could be considered as unfairly distributed among the orange and blue vehicles. On the other hand, the definition of weighting factors can be used to balance the delays of different road users or to integrate policy considerations which has not been fully explored yet. In general, it is difficult to directly compare different approaches, because so far no clear evaluation protocol has been established and restrictive assumptions often limit the comparability of results as will be discussed in Section 2.2.5.

2.2.4 Trajectory Planning

In most of the reviewed papers, the workflow of letting one particular vehicle veh cross the intersection is structured as shown in Figure 2.9: first of all, kinematic limitations and speed limits set constraints on the possible arrival times of vehicle veh at the intersection (Step 1 in Figure 2.9). Usually, an earliest possible arrival time t_{veh}^{min} is obtained assuming that the vehicle drives at the maximum allowed speed until reaching the intersection. If the vehicle is already very close to the intersection or is required to enter at a specified speed, the current speed and kinematic limitations can additionally imply an upper bound on feasible arrival times

STEP (1) Obtain physical limitations on the arrival time of veh.

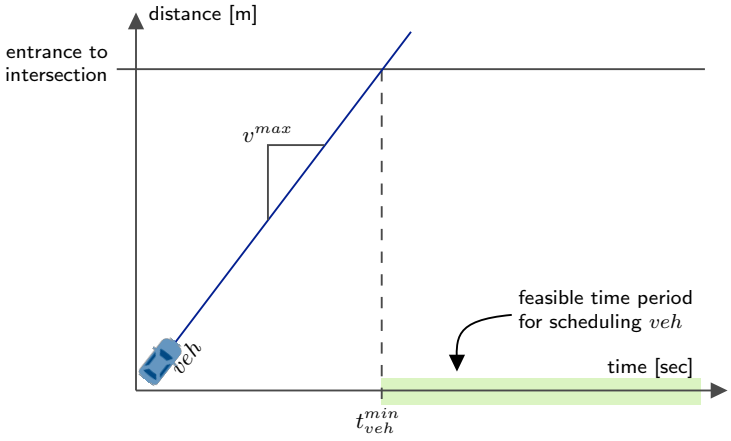

STEP (2) Schedule the arrival time (and possibly speed) of veh.

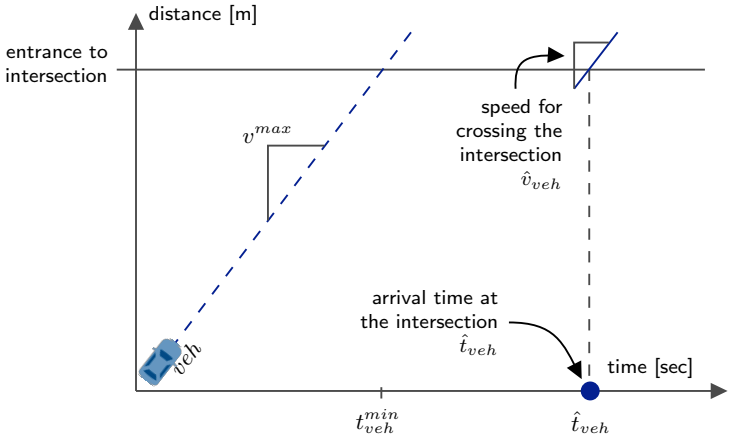

STEP (3) Generate a trajectory for veh to meet the schedule.

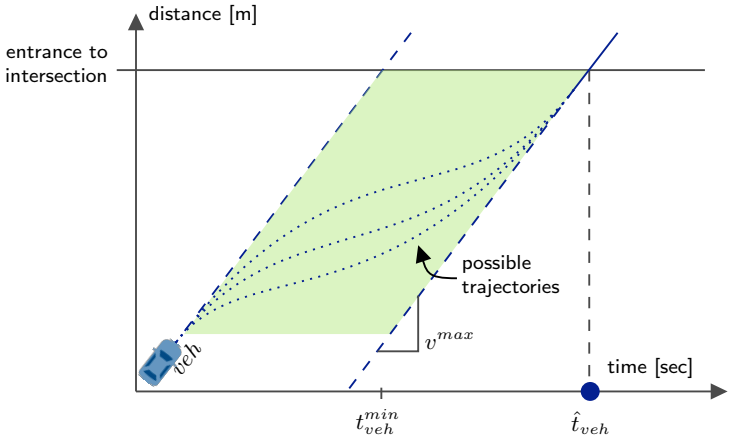

Figure 2.9: Trajectory planning is usually the third step of the process of organizing how a vehicle crosses the intersection.

[E. R. Müller et al., 2016a]. The boundary conditions are considered as constraints in the scheduling policy, Step 2 of the process. As described in Section 2.2.3, an arrival time $\hat{t}_{veh}$ and, in some of the studies, a specified speed $\hat{v}_{veh}$ for crossing the intersection is assigned. The specified speed helps to determine how long intersection cells or conflict points need to be blocked for veh. Additionally, larger speeds reduce the amount of time that the intersection space is blocked for particular vehicles. Based on the information returned from the scheduling policy, a trajectory for veh needs to be found that meets the boundary conditions of assigned arrival time and speed.

This section briefly describes how the trajectory planning process (Step 3 in Figure 2.9) is described in the considered papers. In general, three different levels of detail and optimization can be distinguished: some papers do not consider trajectory planning at all, whereas others use simplified approaches to obtain a feasible trajectory. Very few AIM studies use optimization-based trajectory planning. Finally, papers that do not follow the workflow shown in Figure 2.9 are described.

No Consideration of Trajectory Generation

Several studies do not consider the trajectory generation of approaching vehicles at all. Papers that mainly focus on advanced algorithms for the scheduling process often evaluate their approaches with discrete models (see e.g., [Tachet et al., 2016; Levin and Rey, 2017; R. Chen et al., 2020]). They use Monte Carlo experiments or Poisson arrival processes to generate earliest possible arrival times t_{veh}^{min} at the intersection, which are used as an input to the scheduling policy. The actual arrival times $\hat{t}_{veh}$ are then obtained using the described scheduling algorithm. This means that both Step 1 and Step 3 in Figure 2.9 are essentially skipped. The evaluation focuses on delays and throughput, but does not consider the microscopic vehicle behavior.

Simplified Trajectory Generation

The trajectory generation needs to consider the current state of a vehicle veh given by the current time t, the position x and the speed v, i.e., $[t, x_{veh}(t), v_{veh}(t)]$, and the planned future state $\left[\hat{t}_{veh}, \hat{x}_{veh}, \hat{v}_{veh}\right]$, where $\hat{x}_{veh}$ is the entrance to the intersection. The trajectory is additionally constrained by kinematic limitations of the vehicle, i.e., maximum acceleration and minimum deceleration. Potentially infinite trajectories exist that fulfill all these conditions [E. R. Müller et al., 2016a]. Many reviewed papers use a simplified rule-based scheme to obtain a feasible trajectory that can then be implemented in a microscopic traffic simulation, for example. He et al. [2018] implement four consecutive phases to accomplish the movement from the initial to the planned final state: (i) constantly decelerating, (ii) constantly moving at minimum speed, (iii) constantly accelerating, and (iv) constantly moving at destination speed phase. The minimum speed at which the vehicle travels in phase (ii) is chosen such that it is as large as possible. Based on the current, minimum and destination speed as well as assumed acceleration and deceleration rates, the time of switching from one phase to the next is calculated beforehand. E. R. Müller et al. [2016a] describe a similar approach, but instead of calculating the time steps of switching from one phase to another beforehand, the

vehicle speed is chosen individually for each time step following a set of rules. Fayazi and Vahidi [2018] define fixed access points before entering the intersection. This simplifies the trajectory generation process in the sense that vehicles do not have to drive at a specific speed when arriving at the access point, but the distance between access and entrance positions can be used to accelerate if necessary. The authors present a trajectory-planning engine with two subroutines: (i) computing a feasible trajectory for the vehicle to reach the access point at its assigned time, and (ii) a car-following subroutine which makes sure that safe gaps to the vehicle in front are respected. How car-following safety gaps are kept is not particularly described in other studies.

Optimized Trajectory Planning

Instead of planning a simplified feasible trajectory, the constraints above can be used as input to an optimization problem. Optimized trajectory planning with the objective of minimizing emissions or improving comfort is rarely considered in literature about AIM. Based on the schedule derived from their MILP policy, Yao et al. [2020] apply a trajectory optimization model that aims at reducing the fuel consumption of vehicles. Their trajectory optimization is modeled as an optimal control problem. It thus follows existing work that does not describe an AIM approach, but focuses specifically on trajectory optimization, e.g., Ntousakis et al. [2016] focusing on passenger comfort, Typaldos et al. [2020] focusing on fuel consumption reduction, and X. Wu et al. [2015] focusing on energy consumption reduction.

Trajectory-based Scheduling

Not all of the reviewed papers follow the steps shown in Figure 2.9. First of all, in query-based approaches such as the one by Dresner and Stone [2004], the central intersection controller receives planned trajectories by vehicles and either accepts or rejects the trajectories as a whole. Furthermore, some studies consider the trajectory planning problem inherently in the scheduling formulation or instead of the scheduling problem itself. In such formulations, acceleration and deceleration of vehicles are integrated into the objective function and the constraints of the overall problem formulation. For example, J. Lee and Park [2012] formulate a nonlinear optimization problem that aims at minimizing trajectory overlaps while respecting acceleration limitations and minimum time gaps in car-following situations. Kamal et al. [2015] formulate an objective function that includes the cost related to velocity deviation from the desired value, acceleration, and risk of collisions. Other papers decide on accelerations and decelerations within learning approaches [Y. Wu et al., 2019] or based on game theoretic considerations [Elhenawy et al., 2015]. Both studies obtain promising results, but the main difficulty is the computational complexity.

Discussion

In the vast majority of considered papers, trajectory planning is not a major topic. Instead, the output of most studies is an assumed-to-be feasible schedule. Some authors propose that their approaches could then be combined with existing trajectory optimization schemes by passing down the assigned arrival times and speeds. One issue that would have to be analyzed further in

the case of optimized trajectory planning is whether the scheduling algorithm forfeits flexibility. Especially optimization-based approaches run the three steps in Figure 2.9 iteratively, taking advantage of all available information each time the scheduling process is run. If a vehicle veh starts decelerating early on, their earliest possible arrival time t_{veh}^{min} increases, thus reducing the degrees of freedom for the scheduling algorithm. Additionally, Figure 2.9 is simplified in the sense that only one vehicle is displayed. An important issue is whether proposed trajectories are compatible with leader and follower vehicles with potentially heterogeneous driving behavior.

2.2.5 Approach Evaluation

Due to the lack of a sufficient number of CAVs, the missing implementation of necessary infrastructure and the safety-criticality, the concepts presented in literature have not been tested in reality so far. Therefore, concepts are evaluated via theoretical considerations, numerical methods, and simulations. The approach evaluation in current studies does not follow a consistent concept which makes it difficult to compare approaches with each other. On the other hand, this is not surprising, since authors are from different fields of research and papers thus provide insights into diverse aspects of intersection control. This section describes evaluation criteria, methods, and benchmarks that are commonly used in existing studies. Additionally, common assumptions of existing studies are discussed which might limit the informative value of evaluation results.

Performance Measures

There are several studies that aim at proving a concept, i.e., feasibility of AIM implementation with available sensors and communication technologies, or the validity of a mathematical model. They evaluate and discuss whether a certain concept would be implementable and under what constraints. These papers do not evaluate any particular performance measure except for the sheer possibility of implementation itself. Most of the other papers consider performance measures that are also common when evaluating traffic signal timing. Since concepts are mostly tested using simulation, the chosen evaluation criteria need to be measurable in simulation as well. Recalling the evaluation criteria for signalized intersections described in Section 2.1.2, the performance indicators that are used predominantly are capacity, average delay (defined as LOS), emissions, numbers of stops, and queue lengths. These criteria are in principle suitable for evaluating AIM approaches as well. The most common one is average delay or average travel time (see e.g., [Dresner and Stone, 2006; E. R. Müller et al., 2016a; Tachet et al., 2016; Levin and Rey, 2017]). Evaluating the average delay does not require detailed trajectories and can instead be calculated as the difference between the earliest possible arrival time and the scheduled arrival time (compare Figure 2.7). Other papers consider queue lengths [Choi et al., 2019], idling times [Kamal et al., 2015] and fuel or energy consumption [Zohdy et al., 2012; Pelosi et al., 2020]. These performance measures require information on vehicle trajectories, which already indicates that the way results are generated varies between different studies. This is going to be described in the following.

Evaluation Method

Most of the approaches presented so far have been tested using simulation. The level of detail ranges from simplified numerical simulations via microscopic traffic simulation to vehicle-in-the-loop (VIL) testing, where a real vehicle is connected to a virtual reality environment in which the intersection is simulated. The evaluation method strongly depends on the background of researchers and the aspired evaluation criteria.

If new scheduling policies are defined, they are often tested using simplified queuing models (e.g., [Tachet et al., 2016]) or numerical simulation (e.g., [Levin and Rey, 2017]). In particular, vehicle arrival times at the intersection zone are generated from a Poisson process and are then altered according to the scheduling policy. These studies are usually not concerned with the ability of vehicles to actually arrive at the intersection zone at the specified time and speed and thus do not consider vehicle trajectories, compare Section 2.2.4. Since one only needs to generate random arrival times, experiments are easily reproducible if all necessary parameters are listed. Unfortunately, this is not always the case.

Other researchers use custom traffic simulation, e.g., the software 'AutoSim', which was invented at Carnegie Mellon University [Aoki and Rajkumar, 2018; Azimi et al., 2014]), or 'FAUSim' developed at Florida Atlantic University [A. Stevanovic and Mitrovic, 2018]. Custom software leaves more freedom to developers, such as lane reversal, which is not easily possible with standard simulation software [A. Stevanovic and Mitrovic, 2018]. If such innovative functionalities are not necessary, standard commercial or open-source simulation platforms can be used such as aimsun.next[1] [E. R. Müller et al., 2016b; Olsson and Levin, 2020], Vissim[2] [J. Lee and Park, 2012; Zhixia Li et al., 2013] or SUMO[3] [Jin et al., 2013; Sayin et al., 2018]. One major benefit of using an established simulation platform is that the underlying models can be assumed to be validated. Since detailed trajectories can be retrieved from these platforms, it is additionally possible to estimate resulting emissions, fuel consumption, idling times, for example. On the other hand, their vehicle dynamics model is simplified and only longitudinal accelerations and speeds are modeled. Some papers integrate detailed vehicle driving dynamics into the trajectory planning by including lateral movement or even aerodynamics and rolling resistance, e.g., Bichiou and Rakha [2018]. Fayazi, Vahidi, and Luckow [2019] connect a VIL-simulator to verify that the required vehicle movement can in fact be realized on the road and to measure the actual resulting fuel consumption.

Independent of the evaluation method, conducted experiments are often not reproducible. Even if well-established models are used, the variety of input parameters needs to be sustained for each individual simulation study. It has been discussed in Section 2.1.1 that simple input parameters such as assumed vehicle lengths, speeds and time gaps can lead to large differences in results. This is arguably not reflected enough in existing literature.

[1] Commercial simulation platform by aimsun: `https://www.aimsun.com/aimsun-next/`

[2] Commercial simulation platform by PTV Group: `https://www.ptvgroup.com/en/solutions/products/ptv-vissim/`

[3] Open-source simulation platform developed at the German Aerospace Center: `https://sumo.dlr.de/`

Benchmark

Since presented results significantly depend on assumptions and parameters, it is very difficult to compare approaches presented in different papers and, consequently, the value of isolated results is limited. Most researchers thus compare their approaches to a benchmark intersection control which can be a four-way stop, a roundabout, a traditional TSC (pre-timed or actuated) or a different AIM approach. Pre-timed TSC and FCFS schemes are the most common benchmarks [Zhong et al., 2021]. The comparison with a commonly known status quo can significantly improve the overall evaluation. However, conclusions are not always that simple.

First of all, in some papers, the vehicle driving behavior differs between the different control schemes that are tested. This usually aims at comparing the status quo with the proposed future scenario as in [E. R. Müller et al., 2016a]. While vehicles in the AIM scenario are fully automated and their speed is controlled by the intersection controller in every time step, vehicles at the traffic signal are modeled with human-like driving behavior. As an example, a reaction time of 1.8 seconds for vehicles stopped at the traffic signal is assumed [E. R. Müller et al., 2016a]. Consequently, the very promising benefits in vehicle delay in the AIM scenario might not only result from the improved control scheme, but – at least partially – from omitted reaction times. Even if vehicles are modeled with the same driving behavior in different scenarios to improve comparability, a sub-optimal benchmark control might still infringe the significance of results. As discussed previously, improved signal timings can significantly enhance LOS at signalized intersections, and traffic-actuated or adaptive control strategies have even more potential [Urbanik et al., 2015].

Furthermore, from the studies by Fajardo et al. [2011] and Levin and Boyles [2016], it can easily be seen that scenario selection also has a big impact on the outcome: both studies evaluate the same FCFS control scheme against optimized signal timing plans but conclusions are different. From their papers as well as the study by Yu et al. [2019], it can be concluded that FCFS outperforms TSC in low-demand scenarios, but is inefficient for high-demand scenarios. The proposed optimization-based policy could instead outperform even actuated TSC in all demand scenarios [Yu et al., 2019].

It is thus necessary to compare the proposed AIM with a valid benchmark under the same assumptions for a set of scenarios. Most importantly, all assumed parameters need to be clearly stated in order to facilitate the reader's understanding of reported evaluation results.

Limitations

In addition to the reported difficulties when comparing the analyzed performance measures of different studies, further limitations need to be considered. Most studies consider a rather simple four-leg intersection similar to the one that is shown in the previous Figures 2.5 to 2.7. Many papers additionally limit possible turning movements and only allow vehicles to go straight, e.g., [Fayazi and Vahidi, 2018]. This drastically limits the number of potential conflicts. Additionally, most test intersections are perfectly symmetric, such that arising conflicts are also symmetric. With the exception of Dresner and Stone [2006] and R. Chen

et al. [2020], pedestrians and bicyclists are not considered at the test intersections. Instead, in most of the presented studies, a penetration rate of 100% CAVs is assumed, and vehicles are additionally assumed to be homogeneous, i.e., they all have the same dimensions and vehicle dynamics.

Discussion

The wide range of research areas involved in developing AIM concepts is reflected in the way approaches are evaluated. The considered performance measures are mostly taken from the evaluation of traditional TSC with average delay being the most prevalent. Since real world implementations are not available so far, concepts are mostly tested using simulations. While it is common practice to evaluate new traffic control strategies using simulation as well, an additional challenge is presented here by the lack of real world data that are normally used to calibrate the simulations. It is clear that the vehicle driving behavior characteristics of CAVs cannot be known since these vehicles are not yet on the market. The considered field of research hence requires many assumptions to be made and reported results cannot easily be compared across different papers. Most studies thus compare their results with a benchmark intersection control, mostly fixed-time TSC or AIM using the FCFS protocol. All in all, the results reported so far seem very promising. However, they can vary a lot depending on the chosen input parameters, and it is thus necessary to make justifiable assumptions and consider realistic scenarios. Additionally, the applicability of presented approaches to real world conditions, e.g., considering multimodal traffic and realistic intersection layouts, needs to be analyzed further.

2.2.6 Summary

This literature review has provided insights into the broad spectrum of AIM. There exist numerous approaches to detect conflicting trajectories and coordinate vehicle movements at futuristic intersection zones, each focusing on different aspects. The studies were categorized along the major steps involved, i.e., (i) intersection modeling, (ii) traffic coordination, (iii) scheduling, (iv) trajectory planning, and (v) approach evaluation. Different strategies exist for each of these steps. The decision on intersection modeling techniques and traffic coordination concepts are mainly based on use cases and on-site conditions, e.g., whether the considered intersection is assumed to be equipped with proper infrastructure or not. Many of the papers reviewed in this thesis put a special focus on the scheduling procedure, and the analysis of published scheduling algorithms clearly shows an evolution from simple FCFS approaches towards optimization-based scheduling (compare Figure 2.8). Especially the latest optimized scheduling policies are very promising and vehicle delays at intersection zones could be significantly decreased in the future. These approaches could also allow for an integration of policy objectives. It can also be expected that energy consumption or emissions can be reduced with a proper proactive trajectory planning. However, there exists no clear protocol for evaluating the strategies, and restrictive assumptions (e.g., assumed vehicle-only traffic) limit the real world applicability. This will be further discussed in Section 2.3. A tabular overview of the presented studies and their characteristics is provided in Appendix A.

2.3 Research Gaps

It is clear that the overall benchmark for the futuristic AIM control strategies is the status quo, i.e., current TSC. The basic concepts and evaluation criteria of TSC were described in Section 2.1. While AIM concepts can significantly outperform traditional traffic signals considering isolated performance measures, it is important not to lose sight of the overall objective of intersection control: providing safety and efficiency *for all road users* at an intersection. Most intersection zones are in urban environments, and many use cases of automated driving (such as on-demand shuttles and automated parcel delivery) shall be applied in urban areas in the future, where pedestrian and bicycle traffic plays a major role. As described in Section 2.1, the objectives of traffic control at an urban intersection need to be identified in collaboration with local and regional agencies. They depend on the environment of the intersection and on urban development plans and the city's overall concept. This context is not yet discussed in AIM studies. The three major research gaps tackled in this thesis are hence:

1. The integration of pedestrians and bicyclists into AIM strategies.
2. The balanced consideration of all road users and the integration of policy objectives.
3. The thorough evaluation considering a realistic multimodal urban intersection.

In the following, these research gaps will be described in more detail, and a summary will be given.

1. Integration of Pedestrians and Bicyclists

While the AIM approaches presented in literature so far could lead to a more efficient use of intersection space in the future, the continuous vehicle movement infringes pedestrian and bicyclist possibilities to cross the intersection. It has to be noted that this is a major difference to traditional TSC which grants the right of way in an alternating fashion. Even though the focus of signal timing often lies very much on vehicle traffic, the phase-based principle of traffic signals allows pedestrians and bicyclists to cross the intersection together with parallel vehicle movements. In contrast, AIM approaches are vehicle-based, i.e., each vehicle is given the right of way individually upon request. Simply speaking, if no space-time is requested by or on behalf of pedestrians and bicyclists, there will be no green phase that they can be appended to. Therefore, they need to be considered explicitly in the reservation process.

Nevertheless, pedestrians and bicyclists have been considered in very few studies on AIM so far. The most famous one is presented by Dresner and Stone [2006]. The authors implement a hybrid intersection control that assumes a pre-timed traffic signal in combination with their previously presented FCFS control [Dresner and Stone, 2004]. The overall idea is that human drivers, pedestrians, and bicyclists can cross the intersection as it is the case in today's traffic, i.e., following the pre-timed signalization. Approaching CAVs communicate with the intersection manager to request a time slot for crossing the intersection. The intersection manager either tells them to arrive when their respective signal is green, or it accommodates their movement along with the movement on another green phase that does not use the same

intersection areas. If, for example, the signal for northbound movement is green, CAVs traveling from west to south can cross the intersection at the same time, because their movement does not conflict with those of the other, possibly human-driven, vehicles. With an increasing share of CAVs, the delay at the intersection is reduced and the control converges towards the 100% FCFS scheme. Even though pedestrians and bicyclists are theoretically considered in a sense that they will be able to cross the intersection safely, they are not integrated in a demand-responsive way, their movement is not simulated, and their delays are not evaluated in the study.

There are only very few studies that integrate pedestrians into AIM in a demand-responsive way. W. Wu et al. [2022] propose that the intersection shall be equipped with so-called "automated pedestrian shuttles", i.e., automated vehicles that carry pedestrians to the other side of the street. They include the routing and scheduling of the shuttles into an MILP formulation and evaluate how the number of available shuttles impacts the pedestrian LOS. To this end, short-term numerical simulations are conducted. M. I.-C. Wang et al. [2021] present an optimization-based AIM scheme that integrates CAVs, pedestrians, and upstream/downstream intersections for spillback handling. They assume pedestrians to be equipped with connected devices and present the integration of individual pedestrian requests into their framework. Their approach is evaluated using the SUMO simulator, but no dedicated simulation results are reported with respect to pedestrian delays or the impact of pedestrian requests on vehicle delays. R. Chen et al. [2020] develop a max-pressure control for a network of intersections with vehicle and pedestrian movement based on the MILP formulation by Levin and Rey [2017] (compare Section 2.2.3). In the objective function, both vehicles and pedestrians are considered. Their delays are multiplied by weighting factors that are defined depending on queue lengths on incoming and downstream links and walkways, respectively. Pedestrians indicate their presence via a push button in order to be considered in the optimization. They are assumed to cross the street only when their respective crosswalk is activated and the conflict points between vehicles and pedestrians are then considered in the constraint matrix. The approach is evaluated using numerical simulation with time steps of 15 seconds. In each simulation step, a pedestrian crosswalk is reserved for either vehicle or pedestrian movement. The authors conduct simulations to test the effects of pedestrian demand on intersection efficiency and show that delays of pedestrians and vehicles are negatively correlated. While this correlation is expected, since all road users compete for the same intersection space-time, the results demonstrate the importance of evaluating control strategies including the entire (multimodal) demand at an intersection zone. However, pedestrian LOS is not evaluated in detail, their movement is not simulated microscopically, and many simplifying assumptions are made. Overall, there remain open questions regarding safety, practicability, and user-friendliness that need further evaluation, and the integration of bicyclists is not discussed in the mentioned papers.

2. Balanced Consideration of Road Users and Integration of Policy Objectives

The STM proposes an outcome-based approach to signal timing that allows practitioners to "develop signal timing based on the operating environment, users, user priorities by movement, and local operational objectives." [Urbanik et al., 2015] The first steps of the approach in-

clude (i) defining the operating environment including physical location characteristics as well as the local operating agency's goals, (ii) identifying primary users at the intersection, and (iii) establishing user and movement priorities. There are many examples where certain road users or movements are prioritized, e.g., PT vehicles (compare Section 2.1.2). Reasons for prioritization are various, including environmental considerations, reduction of people delay instead of vehicle delay, or a general political agenda that aims at promoting certain modes of transport. All in all, prioritization should reflect the municipality's goals for its mobility system without undermining the fair balance of all road users' interests. Which objectives prevail is ultimately a political decision. Therefore, new intersection control schemes should be able to allow transportation planners to flexibly adjust priorities depending on the political agenda, location, time of day, etc. [Schmöcker et al., 2008].

These considerations are not yet integrated into AIM approaches. The auction-based scheduling policies described in Section 2.2.3 consider prioritization [Carlino et al., 2013; Schepperle, Böhm, and Forster, 2007; Schepperle and Böhm, 2007]. However, the integration of policy objectives is reported to be difficult and interventions of the auction by including 'system bids' show mixed outcomes [Carlino et al., 2013]. The possibility of including prioritization into the MILP formulation via weighting factors is described, but not fully explored yet [Levin and Rey, 2017; R. Chen et al., 2020; Sayin et al., 2018].

3. Evaluation Considering a Real Intersection Zone

The evaluation considering a real intersection zone with realistic multimodal traffic offers the possibility to actually compare a new scheme to the status quo which has not been done so far. Such a comparison could give answers regarding applicability and potential improvements assuming availability of CAVs. As described in Section 2.2.5, the intersection zones considered in existing studies are usually very restrictive and some approaches might not easily be applicable to intersection zones with turning movements, non-symmetric layouts, and heterogeneous road users. Rare exceptions considering real world intersection geometries are the studies by Carlino et al. [2013] and E. R. Müller et al. [2016b]. In the first study, four different American cities are simulated, including San Francisco, California and Austin, Texas. The implemented simulation model is built based on Open Street Map (OSM) data and covers the entire city for each of their simulations, including minor and major intersections. However, the study lacks a detailed description of the actual intersection zones where their control scheme is applied, since the majority of intersections in their study are controlled in a "traditional" way, i.e., via four-way-stops and traffic signals. Additionally, considered demand and driving behavior are not described. E. R. Müller et al. [2016b] simulate a real intersection in Brazil using the simulation platform aimsun.next. Their study shows the applicability of their MILP algorithm to a non-symmetric intersection layout with several turning movements. However, their study does not consider demand measured on site, and vehicle dimensions and kinematic limitations are not listed. In particular, neither study considers the multimodal traffic usually encountered at urban intersections, including pedestrians, bicyclists, passenger cars, busses, and trucks.

Summary

Based on the identified research gaps, the following chapters present and evaluate new integrated intersection control strategies for urban intersections with CAVs, pedestrians, and bicyclists. Two different control families are developed, each containing a set of strategies for multimodal intersection control:

- The slot-based integrated intersection control strategies described in Chapter 3 follow a rule-based approach. They are implemented in order to explore the possibilities of integrating pedestrians and bicyclists into AIM scenarios in a comprehensive way. As such, they form the basis for developing advanced control strategies in Chapter 4.
- The optimization-based integrated intersection control approaches described in Chapter 4 build on the ideas developed in Chapter 3 and take the approaches to the next level by using more sophisticated scheduling algorithms and including prioritization.

In Chapter 5, the most promising strategies are evaluated using a microsimulation platform assuming a real intersection zone in Munich with realistic demand.

Chapter 3

Slot-based Integrated Intersection Control Strategies

The slot-based integrated intersection control (SlotIIC) schemes presented in this chapter are developed and implemented in order to achieve the overarching goal of a multimodal integrated intersection control. They work with a discretization of space and time. To this end, considered intersection zones are divided into several mutually exclusive conflict areas, and the timeline is divided into time slots of fixed duration. In this dissertation, not only the conflicting movements of vehicles are considered, but also the conflicts between vehicles, bicyclists, and pedestrians. This means that all road users reserve the cells of the intersection zone that they want to pass, and only a single vehicle or a group of pedestrians or bicyclists is allowed to occupy a single conflict area during any particular time interval.

This chapter describes the development of the SlotIIC strategies step by step. Section 3.1 discusses how pedestrians and bicyclists can generally be integrated into AIM. Section 3.2 presents the overall control architecture and communication protocol. The intersection modeling and identification of conflicting movements is described in Section 3.3. The core of the control strategy, the multimodal scheduling algorithm, is explained in detail in Sections 3.4 to 3.6. Results are presented in Section 3.7. Section 3.8 describes how the presented control strategies can be extended to intersection zones with several vehicle lanes on each approach. The chapter is concluded with a summary on the presented control schemes and an overview on benefits and limitations in Section 3.9. The concepts show that it is possible to integrate pedestrians and bicyclists into AIM (both with fixed cycles and on demand) and set the basis for developing more sophisticated optimization-based control schemes in Chapter 4.

3.1 Preliminaries to the Integration of Pedestrians and Bicyclists into AIM

As described in Section 2.3, so far there are no AIM schemes that feature the integration of pedestrians and bicyclists in a comprehensive way. AIM schemes usually work on two premises: (i) the arrival times and desired movements of all vehicles can be known in advance, and (ii) the arrival times and speeds for crossing the intersection can be reliably influenced. Neither premise is usually true for pedestrians and bicyclists. Therefore, several questions arise, for example: Does the intersection controller know about the arrival and presence of

pedestrians and bicyclists, and if so, how? How can pedestrians and bicyclists be reliably informed that they are being given the right of way? Before discussing such conceptual questions in Section 3.1.2, a brief background on pedestrians and bicyclists at signalized intersection zones is given in Section 3.1.1.

3.1.1 Pedestrians and Bicyclists at Signalized Intersection Zones

The overall objective of signal control, as explained in Section 2.1, is to provide safe and efficient mobility for *all* road users. Nevertheless, traditional signal timing objectives often focus on minimizing vehicle delay and stops which can lead to large waiting times for pedestrians and frequent stops for bicyclists [S. M. Kothuri, 2014; Taylor and Mahmassani, 2000]. In recent years, non-motorized road users and their needs have been increasingly investigated, and new ideas to improve their safety and LOS have been proposed and implemented. In the following, the consideration of pedestrians and bicyclists in traffic signal control will briefly be described.

VRU Safety at Signalized Intersections

Naturally, intersections impose a special risk on VRUs, since they are the locations where vehicles', cyclists', and pedestrians' paths cross each other. According to Isaksson-Hellman [2012], more than 75% of the analyzed bicycle-vehicle crashes in Sweden occur in intersection situations. At signalized intersections, conflicts between different road users' movements are resolved by assigning them to different phases that are not allowed in the intersection at the same time. However, turning vehicle movements and VRUs are usually permitted which means that they are given the right of way at the same time, and turning vehicles are expected to yield to bikes and pedestrians during their green phase. In order to improve safety for bicyclists, bicycle coordinators in the Netherlands, Denmark, and Germany plead for a physical separation of vehicle and bicycle movements and recommend brightly colored bike lanes within intersections [Pucher and Buehler, 2008]. Vehicle turning movements also represent a considerable safety problem to pedestrians. Approximately one out of five accidents at signalized intersections involve a turning vehicle hitting a pedestrian [Lord et al., 1998]. According to Robertson and Carter [1984], around 60% of turning accidents are left-turning and approximately 40% are right-turning accidents. A more recent simulator study additionally found that "when drivers are making a permissive left-turn some drivers fail to search areas where pedestrians are likely to be present" [Marnell et al., 2013]. It is thus recommended to separate vehicle and VRU movement as much as possible. This is sometimes realized via a separate phase during which the intersection is completely blocked for all vehicle movements.

The simultaneous movement of pedestrians from different directions during such an all-pedestrian phase is generally assumed to be non-problematic, and the concurrent movement of bicyclists is also increasingly implemented. Firstly, Right-Turn-on-Red (RToR) is already allowed for bicyclists in several European cities [Freyer et al., 2019]. Furthermore, in the Netherlands, an "all-directions-green" phase for bicyclists has been implemented at several signalized intersections [Van der Zee and Te Brömmelstroet, 2018]. In this phase, bicyclists cross the intersection zone completely separated from vehicles. Since bicyclists coming

from all directions as well as pedestrians on the legs of the intersection are allowed to cross at the same time, the control requires VRUs to be considerate and give way to each other (as also indicated on a supplementary sign). Despite the seemingly chaotic VRU phase, the separation of vehicle and VRU movements has significantly increased safety, and the setup works so well that the Dutch city of Groningen has expanded the implementations to 28 intersections some years ago [Groningen Cycling City, 2016].

Nevertheless, the strict separation of vehicle and VRU movements is difficult to broadly implement in conventional signal control. Three drawbacks of a separate VRU phase as described above are reported [Furth et al., 2014]. First of all, they often significantly reduce vehicle capacity at the intersection. Secondly, the integration of an additional phase leads to long cycle times which cause long waiting times for all road users. Finally, the long waiting times can reduce pedestrian and bicyclist compliance with the signal. This was, for example, reported by Zhang et al. [2015], who compared pedestrian safety at intersections with concurrent and exclusive pedestrian phasing. Furth et al. [2014] propose a scheme in which pedestrians and bicyclists are given the right of way along with parallel vehicle through movements, while right-turning vehicle movements are protected and allowed together with non-conflicting left-turning vehicles. However, this only makes sense if all vehicle movements have separate lanes, which is often not the case.

VRU Level of Service at Signalized Intersections

The study cited above by Zhang et al. [2015] and other papers show that limited waiting times for pedestrians are not only a convenience feature, but can also be a safety criterion. While compliance with pedestrian signalization depends on many different factors, longer maximum waiting times do lead to a higher share of red-light violations [Brosseau et al., 2013; Van Houten et al., 2007]. In the current version of the German HBS, the maximum waiting time, which is determined by the maximum red-light duration of the respective signal, also defines the LOS for both pedestrians and bicyclists [FGSV, 2015a]. In the American HCM (as well as the previous version of HBS), LOS for VRUs is determined by the mean waiting time [TRB, 2000; FGSV, 2001]. This evaluation criterion seems more natural, since it represents what the average pedestrian and bicyclist at the intersection perceives. All in all, it can be concluded that both mean and maximum waiting times should be considered – the lower the better for VRUs. For fixed-time traffic signals, average VRU waiting times can be calculated analytically via the cycle time and respective green phase durations. The calculation is based on the assumption that the arrival times of VRUs are equally distributed throughout the cycle time. While this is generally a good approach for pedestrians, the assumption can be questioned for bicyclists. Since they usually cross several consecutive signalized intersections on their route, they often arrive at the next intersection in groups.

In contrast to the consideration of motorized traffic, the mentioned guidelines (HBS and HCM) do not yet discuss signal coordination for bicyclists. It is reasonable to assume that bicyclists, just like vehicle drivers, prefer trips with few stops and limited overall delay. Additionally, stopping (or rather, accelerating after a stop) requires additional physical effort for bicyclists, and bicyclists stopped at the intersection could be exposed to a larger dose of local

air pollution. Signal coordination for bicyclists has been proposed in the literature and has already been implemented in several European cities with a large share of bicycle traffic [Taylor and Mahmassani, 2000; Beyer, 2009; Grigoropoulos et al., 2021]. In a detailed evaluation and comparison of different traffic management techniques for bicyclists provided by Knight et al. [2011], it is rated as one of the most favorable measures for bicyclists and recommended to be considered for use in more cities. Difficulties regarding the implementation include the comparatively heterogeneous bicycle progression speed as compared to vehicles. This issue can be mitigated by providing information on the assumed progression speed to bicyclists as will be described below [Beyer, 2009].

Similarly to with signal coordination, literature on signal timing optimization for isolated intersections often focuses on vehicle traffic. Many studies do not analyze and report impacts on VRUs. Reasons are manifold, but likely include the circumstances that intersection capacity is limited more strictly with regard to vehicle movements, and that more predictive knowledge about vehicle arrivals is available. This information gap might be decreased with a variety of ITS applications for VRUs.

ITS Applications for VRUs at Intersection Zones

In recent years, several studies and market-ready products related to ITS applications for VRUs have been introduced which could help increase their safety and LOS at intersection zones. A good overview on pedestrian support is provided by El Hamdani et al. [2020]; MacArthur et al. [2019] present technologies for bicyclists. Given the prevailing safety issue of VRUs at intersections, many of the proposed applications include functionalities such as detection and warning. Infrastructure-based detection technologies have already been evaluated a few decades ago, e.g., via infrared or microwave detectors. These technologies can, for example, capture pedestrian movements on the street, and improve safety by extending the crossing times if necessary [Hughes et al., 2001]. A good introduction on possible infrastructure-based installations for VRU detection can be found in [S. Kothuri et al., 2017; Larson et al., 2020; NACTO, 2014; Alta, 2021]. More recent papers often focus on applications that make use of connected devices for pedestrians and bicyclists. Examples include smartphone applications that broadcast awareness messages and alert distracted VRUs and drivers in order to prevent collisions [Sewalkar and Seitz, 2019]. Connected devices are expected to improve safety implementations, because no additional sensors need to be installed, and enhanced information about detected road users is available (such as turning intentions). Additionally, they provide more sophisticated and precise options to inform or warn VRUs, for example via visual, acoustic, or tactile signals applied directly to the respective bicycle or smartphone. Nevertheless, approaches that require VRUs to carry connected devices are not without controversy. Alongside data privacy concerns, there are worries that accident liability will be shifted from vehicles towards VRUs [McLeod, 2014].

ITS technologies can be used not only to improve safety, but also to improve efficiency at intersections. This can be achieved by planning on-demand VRU signal phases and dynamically shortening or extending their green phase durations. For example, Liang et al. [2020] present a pedestrian-friendly dynamic signal control optimization scheme that uses real-time

(a) Green wave indicated by colored lamps on the street. Source: [Cardwell, 2014]

(b) GLOSA for bicyclists using a smartphone application. Source: [TAVF, 2020]

Figure 3.1: Different waves to indicate a green wave for bicyclists.

pedestrian information and minimizes a weighted average of vehicle and pedestrian delays, and Grigoropoulos et al. [2021] show that the extension of green times for bicyclists using loop detector-based actuation can reduce bicycle delays. Additionally, different technologies can be used for informing VRUs, especially bicyclists, about upcoming signal changes. Nygårdhs [2021] conducted a before-after study and found out that countdown timers help cyclists to cross the signal without stopping and reduce start-up delays of stopped cyclists but, at the same time, lead to more red light violations at the beginning or the end of the bicycle red phase. A study by H. Kaths, Grigoropoulos, et al. [2019] found mixed results with respect to red light violations and concluded that results depend on the geometry, traffic flow, and other intersection-specific characteristics. De Angelis et al. [2019] present a comparison of different ways to indicate a green wave to cyclists: survey participants preferred numeric-based countdown at the traffic signal, and light-emitting diode (LED) lines or bands on the street. The LED lines or LED road surfaces guide bicyclists by showing a green band that moves with the speed of the green wave. Staying within the green area thus helps bicyclists to cross the next signal without stopping. A similar feature with several LED lights, shown in Figure 3.1a, is installed in Copenhagen and other cities. Most of the infrastructure-based solutions were preferred over on-bike devices such as the one shown in Figure 3.1b by survey participants [De Angelis et al., 2019].

3.1.2 Discussion on Control Design

In the following, the conceptual questions raised in the beginning of this section are discussed based on the background given above, and decisions on the control design for the strategies presented in this thesis are explained.

Do pedestrians and bicyclists need to connect to the infrastructure? As described above, connected devices can help to improve safety and LOS for both pedestrians and bicyclists, for example through collision warnings or GLOSA. Considering the great popularity of smartphones and connected devices in other parts of everyday life, it is likely that more VRUs will be using connected devices for ITS services in the future. However, it should arguably not

Figure 3.2: Images of a pedestrian crosswalk at a traffic signal with light concrete technology. Source: [LCT GesmbH, 2018].

Figure 3.3: Image of an "intelligent pedestrian crosswalk." If someone stands in the red area (left picture) and it is safe to cross, a pedestrian crossing appears (right picture). Source: [Ayoubi, 2017].

be assumed for everybody on the road to be connected to the infrastructure and surrounding road users at all times. Reasons for this opinion include privacy concerns and an unacceptable shift of responsibility from cars and drivers to VRUs. These concerns are also shared by others, for example the interview partners in the study by Buehler et al. [2020] or respondents of a survey by the American League of Bicyclists [McLeod, 2014]. The consideration of VRUs in future transportation systems should not happen at the expense of privacy and accessibility of public space. Therefore, it is assumed in this thesis that (at least some) pedestrians and bicyclists are not connected to the infrastructure.

How can pedestrians and bicyclists be sure that they are given the right of way? Pedestrians and bicyclists need to be notified when they are given the right of way. While there are several approaches on how automated vehicles could communicate with pedestrians and display the right of way to them in the future [Rasouli and Tsotsos, 2020], it is assumed here that busier intersections will be equipped with a proper signal infrastructure for pedestrians and bicyclists. This could be realized by traditional signal heads or by more futuristic displays that function as human machine interfaces (HMIs). Examples of such modern interfaces are shown in Figures 3.2 and 3.3. Figure 3.2 shows how traffic signals could be

Technology	Examples of Captured Information	
Push buttons	✓	Pedestrian detection
		- Pedestrian presence at crosswalk (number of pedestrians is not available)
		- Desired destination, if different buttons exist
	(✓)	Bicycle detection
		- Not recommended, because bicyclists need to stop to activate the button
Loop detectors	✗	Pedestrian detection
	✓	Bicycle detection
		- Information on arriving bicyclists
		- Turning intention, if bicyclists enter via dedicated turning lanes
Video, thermal camera,	✓	Pedestrian detection
or radar sensors		- Pedestrian presence at crosswalk (number of pedestrians depending on setup)
		- Desired destination, if different waiting areas exist
	✓	Bicycle detection
		- Information on arriving bicyclists
		- Turning intention, if sensors are able to detect and interpret hand gestures

Table 3.1: Examples of detection technologies for VRUs at the intersection zone. Detection technologies taken from [Alta, 2021; S. Kothuri et al., 2017]

supplemented with illuminated signs on the street surface. Figure 3.3 shows an example of an "intelligent pedestrian crosswalk:" if someone stands on the sensor shown in the left picture and it is safe to cross, a pedestrian crosswalk is projected onto the street.

Does the intersection controller know about the arrival of pedestrians and bicyclists, and if so, how? In principle, VRU signal phases can be integrated into intersection control in fixed cycles as presented by Dresner and Stone [2006]. If suitable sensors are installed at the intersection zone, pedestrians and bicyclists can be integrated into the intersection control in a demand-responsive way. For pedestrians, this is already the case with pedestrian buttons – in the future, pedestrian buttons could be replaced by other sensors or cameras as described in the previous subsection. An overview on possibly suitable detection technologies listed in the literature and what information they could provide to the controller is shown in Table 3.1. In general, the captured information about pedestrians and bicyclists is similar, but pedestrian movement is more difficult to predict. Therefore, it is assumed to be beneficial that bicyclists are captured ahead of time, whereas pedestrians are detected when they are already at the crosswalk.

How can safety for VRUs be guaranteed? In order to ensure the safety of the AIM scheme, VRU movement is strictly separated from vehicle movement within the intersection. This means that vehicle movements (including turning movements) are only allowed, if all bicycle lanes and pedestrian crosswalks that need to be passed by the vehicle are clear. After VRU green phases, a sufficient clearance time is implemented. Accidents of turning vehicles and VRUs can hence be omitted. Additionally, this policy allows vehicles to cross the inter-

section zone with a pre-defined speed and without stopping (except for emergency situations). Conflicts between pedestrians and bicyclists can in principle be resolved similarly to the conflicts between VRUs and motorized vehicles. However, these conflicts do not necessarily have to be resolved by the scheduling program. Instead, VRUs are expected to give way to each other and resolve conflicts by negotiation, hand gestures, and social rules. While this requires VRUs to be prudent, it is in line with current efforts to develop street space into more of an open space for pedestrians and bicyclist. Additionally, as described earlier, it has been proven to be safe at real intersections already. As with any new signal control setup, traffic safety needs to be carefully monitored when implemented, and it will be important to check whether the possibly simultaneous VRU green phases lead to confusing or dangerous situations.

3.1.3 Summary

The decisions justified above form the basis for the integration of pedestrians and bicyclists into the control strategies presented in this thesis. All in all, they aim at not forcing VRUs to have to adapt their current behavior in the futuristic setup. Additionally, safety for all road users is assumed to be improved, because conflicts involving motorized vehicles are resolved by the controller. The following premises can be summarized:

- VRUs are assigned to signal phases and cross the intersection roughly at the same time. Conflicting movements of VRUs without the involvement of vehicles are not resolved by the control.
- Space-time must be used exclusively by individual vehicles or groups of VRUs. Accidents involving motorized vehicles can hence be omitted.
- Depending on the available information on VRU arrivals and turning intentions, their green phases can be integrated in a demand-responsive way.

In the following sections, the control architecture and the intersection modeling concept will be explained before introducing the scheduling approach and presenting results.

3.2 Traffic Coordination

This section describes the traffic coordination concept of the presented control schemes. Recapitulating the attributes and classifications introduced in Chapter 2, the control strategies developed in this thesis can be considered as partially centralized. As displayed in Figure 3.4, they consist of a central controller that schedules all arriving road users while trajectories are planned by vehicles. Pedestrians and bicyclists are assumed to behave "naturally," i.e., no trajectories are planned for them, but they react to the information provided for them by the control infrastructure that serves as a human-machine interface. In order to simplify the presented approach, an isolated intersection zone wihtout surrounding intersections will be considered.

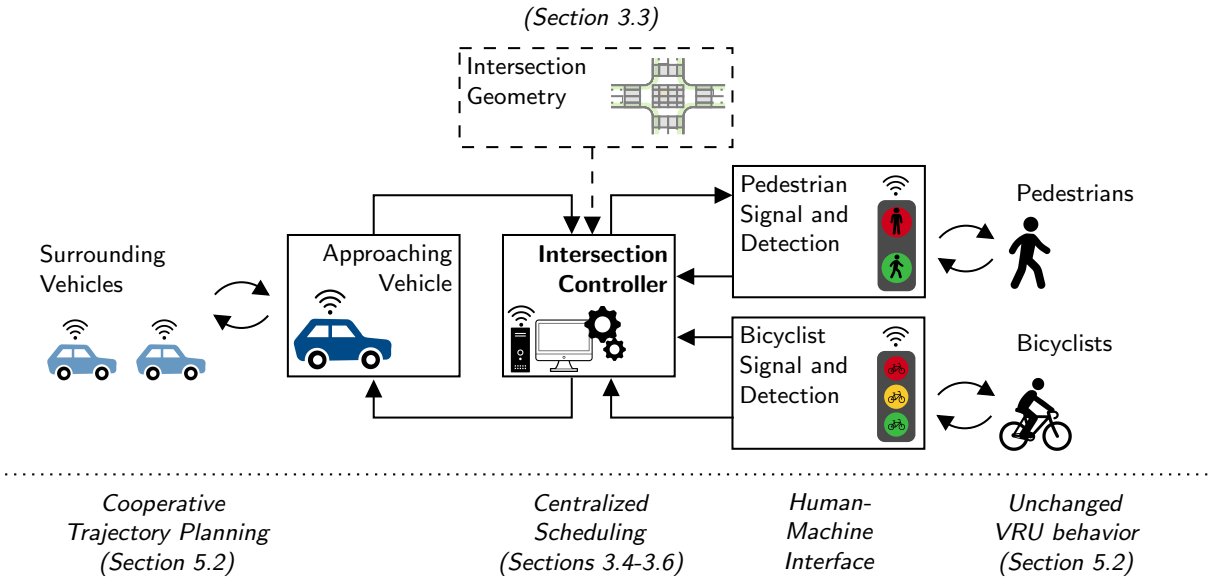

Figure 3.4: Traffic Coordination Scheme.

3.2.1 Coordination of Approaching Vehicles

It is assumed that all vehicles at the considered intersection are connected and automated, and that all vehicles have the same dimensions and kinematic limitations. Approaching vehicles start communicating to the intersection controller as soon as possible, i.e., upon entering the link to the intersection or getting into the communication range of the controller. The communication between approaching vehicles and the intersection controller is displayed in Figure 3.5. Vehicles send their current position and speed as well as their desired turning movement to the controller. The intersection controller combines the received information with its background model of the intersection geometry and its database with existing reservations. It schedules the vehicle's arrival time according to an FCFS approach which will be described in Section 3.4, and informs the vehicle about its assigned arrival time at the intersection. It is assumed that all vehicles cross the intersection zone at exactly the same speed which remains constant until they have left the intersection. The vehicle adjusts its speed in order to reach the intersection at exactly the scheduled time. In contrast to other AIM approaches, the reserved time slots in this control scheme are subject to change. Reasons for rescheduling the arrival time of a vehicle include situations in which priority is given to pedestrians, bicyclists, or other vehicles. In that case, the intersection controller again requests the earliest possible arrival time of the vehicle at the intersection, and schedules a new arrival time. Both the scheduling and the rescheduling procedure are explained in Section 3.4.

3.2.2 Coordination of Pedestrians and Bicyclists at the Intersection

As motivated in Section 3.1, the behavior of pedestrians and bicyclists is assumed to be unchanged in this futuristic scenario, i.e., similar to what can be observed at signalized intersections today. It is assumed that pedestrians and bicyclists are not connected to each other or the infrastructure, but could be detected when they are at the intersection or, in the case of

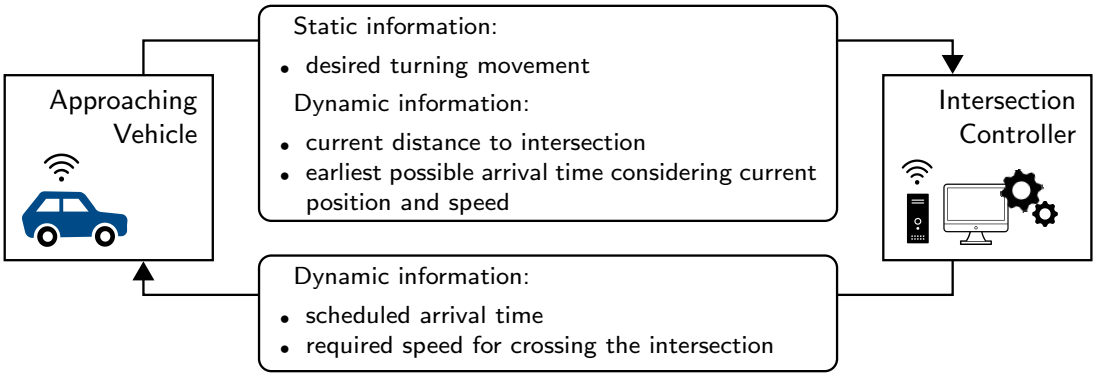

Figure 3.5: Information that is exchanged between approaching vehicles and the intersection controller.

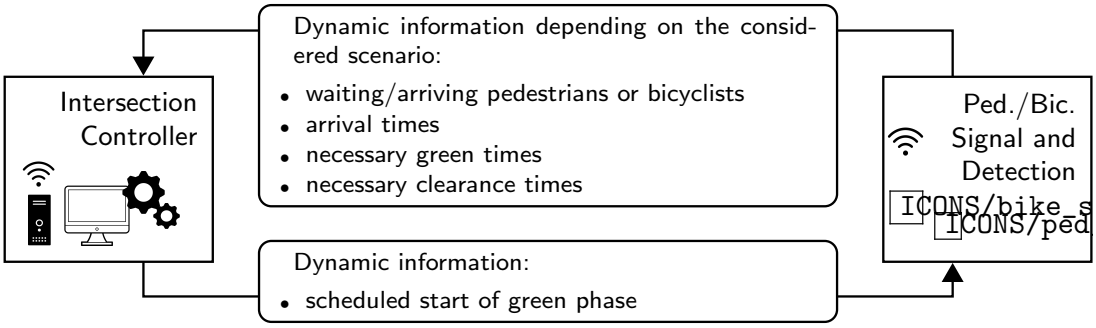

Figure 3.6: Information that is exchanged between the intersection controller and the VRU signalization.

bicyclists, on the approach to it. Assuming different intersection configurations, varying levels of information are considered in the control strategy. In general, the VRU signalization already serves as a human-machine interface today that indicates if road users are given the right of way. The pure signalization can be enhanced by features such as countdown timers or optimal speed advisory as described in Section 3.1. Additional information can be provided for VRUs via smartphones or other connected devices, but, in order to not infringe upon accessibility, it is not assumed that all pedestrians and bicyclists will be equipped with these devices. Instead, the intersection shall be equally accessible for non-connected VRUs and the signalization shall be easily understandable for everyone. Therefore, the control communication loop is implemented between the central control entity and the VRU signalization as displayed in Figure 3.6. The manner in which the VRU green phases are planned depends on the level of information that the controller has about their arrivals and on the implemented control scenario as will be explained in detail in Sections 3.5 and 3.6.

3.3 Intersection Modeling

The intersection geometry that includes the division of space into discrete conflict cells is the first input into the control. It is used by the controller to determine which cells need to be

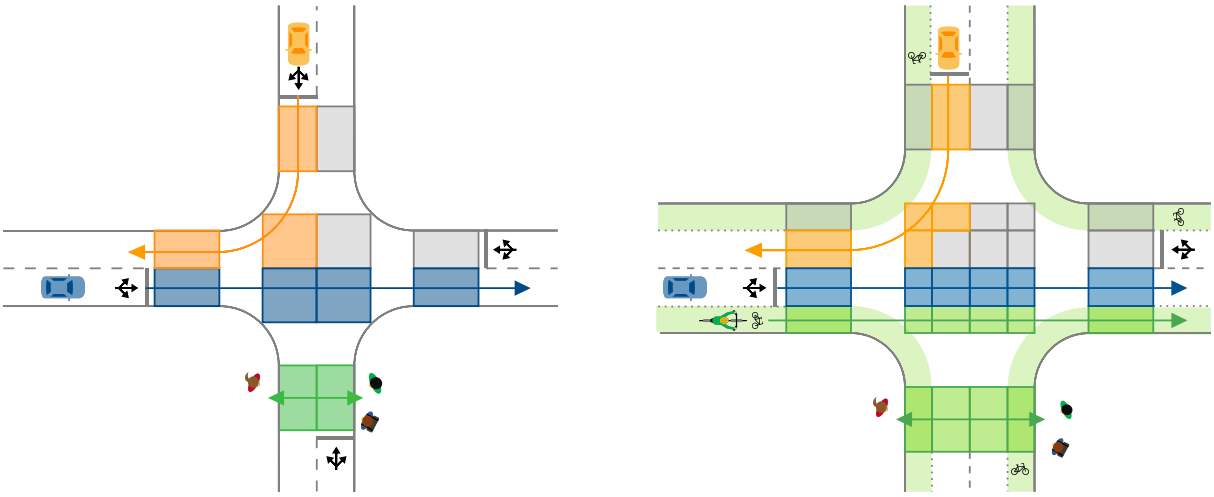

(a) Example intersection with vehicle and pedestrian movement.

(b) Example intersection with vehicle, pedestrian, and bicycle movement.

Figure 3.7: Division of intersection zone into conflict cells.

reserved for certain movements. The setup works with the assumption that all road users roughly travel through the intersection along predefined paths. This is already the case in current traffic: vehicle paths are defined by entrance and exit lanes, bicyclists follow the marked bike lanes through the intersection, and pedestrians cross the legs of the intersection zone at defined crosswalks. These predefined paths allow for determining the sequence of cells that each road user needs to reserve. In this thesis, a cell granularity that equals the number of lanes on each leg is used, i.e., a four-leg intersection zone with one incoming lane and one outgoing lane on each direction is divided into a $2 \cdot 2$ grid of cells. While a higher granularity can lead to more efficiency, it also increases the computation time as explained in Section 2.2.1. According to Dresner and Stone [2008], a granularity of 2 is a good trade-off for a small intersection. In addition to the cells that represent vehicle-vehicle conflicts, cells that represent vehicle-pedestrian, vehicle-bicyclist, bicyclist-pedestrian or bicyclist-bicyclist conflicts are added. This is displayed in Figure 3.7, where the simple intersection with one vehicle lane per approach is divided into 12 conflict cells if pedestrians are included, and 32 cells if, additionally, bicyclists are included with a separate lane on each approach. In Figures 3.7a and 3.7b, the blue cells are the cells that will be crossed by the blue vehicle, the orange cells will be crossed by the orange vehicle, and the green cells are reserved for VRU movement. It is worth noting that not all of the colored cells are reserved for the respective road users during the entire time of them crossing the intersection. The main reason for the discretization into cells in the first place is to occupy only the portion of space that is needed during a particular time interval.

A simplified situation that only features vehicle-vehicle conflicts is shown in Figure 3.8. Figure 3.8a shows snapshots of the intersection during different time slots. In general, only one vehicle is allowed to occupy a conflict zone during a particular time slot. However, this general rule is slightly adapted to account for increased safety gaps and the ability to allow safe patterns in the intersection zone at the same time. In order to increase safety, the conflict

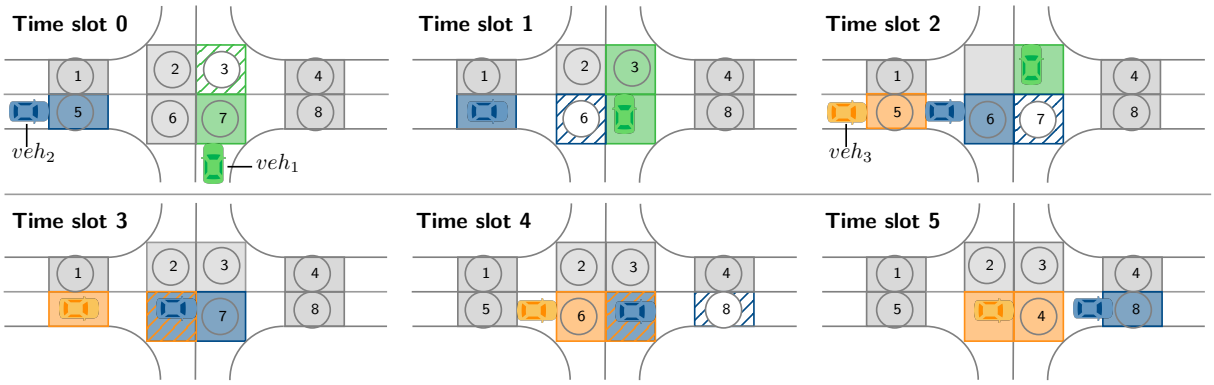

(a) Example of space tile / time slot reservation for three vehicles.

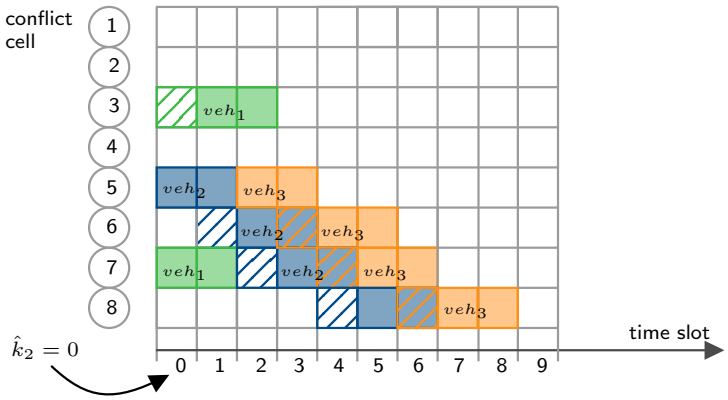

(b) Schedule corresponding to the situation depicted above.

Figure 3.8: Explanation of space tile / time slot reservation.

cells are reserved for an additional time slot if the reserving vehicle follows a vehicle with a crossing movement. In time slot 2, for example, cell 7 is already "pre-reserved" for the blue vehicle. The same happens with the orange vehicle in time slot 4. In this case, however, the blue vehicle holding the reservation is not an issue, since the blue and orange vehicle come from the same direction.

Figure 3.8b shows the list of intersection tiles with the respective reservations. For each newly arriving road user, the intersection controller needs to know the sequence of tiles and corresponding time intervals that need to be reserved for the respective movement. Therefore, possible origin-destination (OD) relations at the intersection are listed, and this list is appended with the set of conflict zones (denoted by C) and respective time slots for each of the movements. Let $\hat{k}_i$ be the time slot that is assigned for vehicle veh_i, i.e., the time that veh_i is supposed to arrive at the entrance to the first conflict zone it needs to pass. In the example shown in Figure 3.8, $\hat{k}_2$ equals 0 and $\hat{k}_3$ equals 2. Vehicle movement from west to east in the situation shown in Figure 3.8 is listed as follows (compare Figure 3.8b):

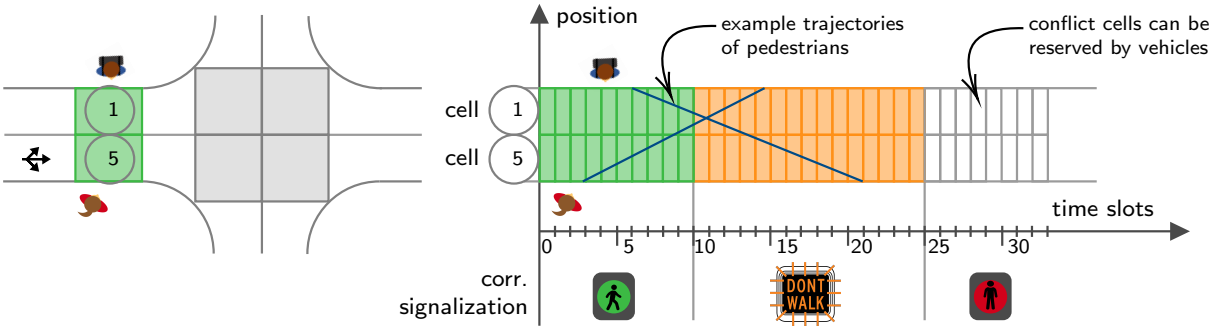

Figure 3.9: Reservation of conflict cells and time slots for pedestrians at the crosswalk of one leg of the intersection.

$$
\begin{aligned}
&Vehicle\ (veh)\ west \rightarrow east:\\
&[C5: \hat{k}_{veh}, \hat{k}(veh)+1;\\
&C6: \hat{k}_{veh}+1^{\Uparrow}, \hat{k}_{veh}+2, \hat{k}_{veh}+3;\\
&C7: \hat{k}_{veh}+2^{\Uparrow}, \hat{k}_{veh}+3, \hat{k}_{veh}+4;\\
&C8: \hat{k}_{veh}+4^{\Uparrow}, \hat{k}_{veh}+5, \hat{k}_{veh}+6].
\end{aligned}
$$

The arrows ($\Uparrow$) indicate that the tile can be reserved during the same time slot by a vehicle with the same origin or destination. This information is specified for the controller which will make the correct checks and consider relevant exceptions. For the sake of simplicity, it is assumed (for now) that all vehicles have the same dimensions and cross the intersection at the same constant speed. This allows for each OD movement to be identified with exactly one combination of space tiles and respective time slots. Note that the space in between two conflict cells (e.g., between the pedestrian crosswalk and the conflict cells in the center) is not considered explicitly, because no conflicts occur there.

Since pedestrians and bicyclists cannot be assumed to cross the intersection at a uniform and constant speed, the tiles are reserved for pedestrian and bicyclist movements for a longer period of time that accounts for the necessary clearance times as well. Figure 3.9 shows an example situation for a pedestrian crosswalk. The corresponding conflict cells are reserved for pedestrians for 25 time slots in total, including a green phase of 9 time slots and 16 time slots of clearance time (depicted by the American "Don't Walk" signal in Figure 3.9), which allows pedestrians to safely finish crossing the street. In contrast to vehicle and bicycle movements, pedestrians can walk in both directions at the same time, i.e., if pedestrians are allowed to cross the western leg of the intersection from south to north, the opposite movement must be allowed as well.

In the following sections, the scheduling policy will be explained in detail for the three user groups vehicles, pedestrians, and bicyclists.

3.4 Scheduling Policy for Vehicle-only Scenarios

The scheduling policy that is implemented for arriving vehicles is an FCFS scheme that is adapted with further rules to integrate pedestrians and bicyclists into the control. In the following, the FCFS scheme for vehicles will be described in Section 3.4.1. The approach also features a routine to reschedule vehicles in case priority is given to VRUs. This routine is explained in Section 3.4.2.

3.4.1 First Come, First Served Policy for Vehicles

As introduced in Section 3.2, vehicles communicate their position, turning information, and earliest arrival time to the intersection controller ahead of time. The intersection controller then knows from the underlying intersection model which space tiles need to be reserved during which time slots as described in Section 3.3. Now, the scheduling routine looks for the pattern to be available in the list of time slots, and the earliest feasible time slot is then reserved for the vehicle. This procedure is shown in Figure 3.10.

Step ① of the figure shows that the earliest possible arrival time for a vehicle veh at the entrance to the intersection is derived from the current position and from the maximum allowed speed (v^{max}) on the approach to the intersection. Technically, kinematic limitations also need to be taken into account if the vehicle is currently not driving at maximum speed and hence needs to accelerate first. However, kinematic limitations can be ignored at this point. It is assumed that, when entering the communication range to the intersection controller, vehicles will drive at maximum speed if possible. If they are not driving at maximum speed, this is because of a vehicle in front of them which will be considered with a separate constraint below. Let t_{veh}^{min} be the earliest possible arrival time communicated by the vehicle. It is clear that the vehicle cannot be scheduled any earlier than this, i.e., the following constraint needs to be respected:

$$t_{veh} \geq t_{veh}^{min}, \tag{3.1}$$

where t_{veh} denotes the arrival time for vehicle veh at the intersection. Since the controller considers discrete time slots instead of continuous time, this constraint is transformed such that the earliest possible time slot is considered instead of the arrival time. Let τ be the step size, and let k be the identifier of the time slot. Then time slot k starts at time $t^k = k \cdot \tau$ and ends when the next time slot starts, i.e., at time $t^{k+1} = (k+1) \cdot \tau$. The earliest possible time slot k_{veh}^{min} for assigning vehicle veh is defined as the earliest time slot that does not start before vehicle veh can arrive at the intersection. This means that Constraint (3.1) is reformulated as follows:

$$k_{veh} \geq k_{veh}^{min} = \min\{k \in \mathbb{N} \mid k \cdot \tau \geq t_{veh}^{min}\}, \tag{3.2}$$

where k_{veh} denotes the time slot for vehicle veh to arrive at the intersection. Additionally, it is assumed that vehicles cannot overtake on the approach to the intersection, and vehicle veh can thus not be scheduled earlier than its preceding vehicle. From the current vehicle position, the controller identifies the vehicle in front of veh on the same approach to the intersection,

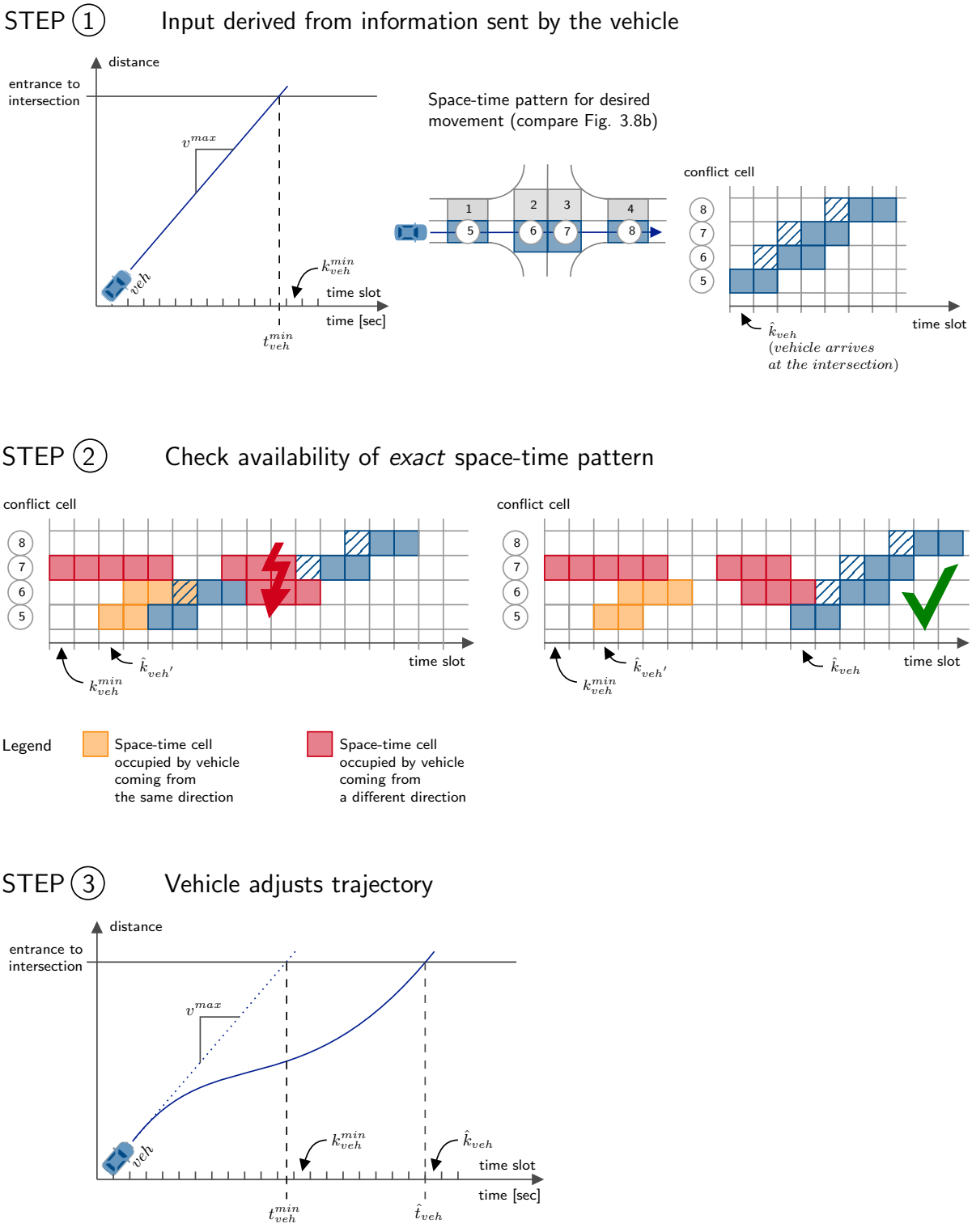

Figure 3.10: Schematic representation of FCFS policy for vehicles in three steps.

denoted here by veh'. Due to the nature of the FCFS procedure, vehicle veh' already has an assigned time slot when vehicle veh signs up. Let this fixed time slot be denoted by $\hat{k}_{veh'}$. Then the following constraint needs to be added:

$$k_{veh} > \hat{k}_{veh'}. \tag{3.3}$$

In addition to the background on how the arrival time constraint is derived from physical limitations, Figure 3.10 also shows the space-time pattern that the intersection controller derives from the received OD information in Step ① as explained in the previous section. In Step ② of the routine, the controller checks for this very pattern to be available in the schedule that contains existing reservations. As shown in Figure 3.10, the whole pattern needs to be available, and it is not possible to insert a time gap as displayed in Step ② on the left (such a time gap would mean that the vehicle would have to disappear for a few time slots). Let the earliest feasible time slot for veh, given the schedule, be denoted by $\hat{k}_{veh}$. This time slot is reserved for vehicle veh and is again transformed into continuous time, i.e., the assigned arrival time for vehicle veh is defined as $\hat{t}_{veh} = \hat{k}_{veh} \cdot \tau$.

After receiving the reserved arrival time, vehicle veh adjusts its speed in order to arrive at exactly the time $\hat{t}_{veh}$ with the predefined speed that remains constant throughout crossing the intersection. In the approach presented in this chapter, this speed corresponds to the maximum allowed speed in order to not block the different conflict cells of the intersection zone for too long. Therefore, the trajectory is adjusted such that vehicles decelerate (if necessary) and accelerate again before entering the intersection. This is schematically displayed in Step ③ of Figure 3.10. The trajectory planning will be described in detail in Chapter 5.

It can be noted that the described procedure follows the general three-step approach shown in Figure 2.9 of the literature section. As raised in Section 2.2.3, the FCFS control can result in a non-globally-optimal solution, where the right of way is given to vehicles coming from different directions in an alternating fashion without forming platoons. This will be further discussed and improved upon in Chapter 4.

3.4.2 Rescheduling Of Vehicles

In the presented approaches, there are situations in which vehicle arrival times need to be rescheduled. The rescheduling of vehicles can be necessary for a number of reasons. The most common one considered in this thesis is that pedestrians or bicyclists are served with priority. Theoretically, a rescheduling might also be necessary if something unexpected happens, for example, if the pedestrian crosswalk is occupied longer than expected. In these situations, the controller replaces the existing schedule with a blank schedule (starting at a specific point in time) and collects new earliest arrival times from all road users that have not finished crossing the intersection by then and thus have "lost" their reservation.

At this point, the earliest possible arrival time might be different from the earliest possible arrival time when the vehicle first signed up. This is shown in Figure 3.11. In this figure, vehicle veh reduces its speed in order to meet the scheduled arrival time. When the schedule

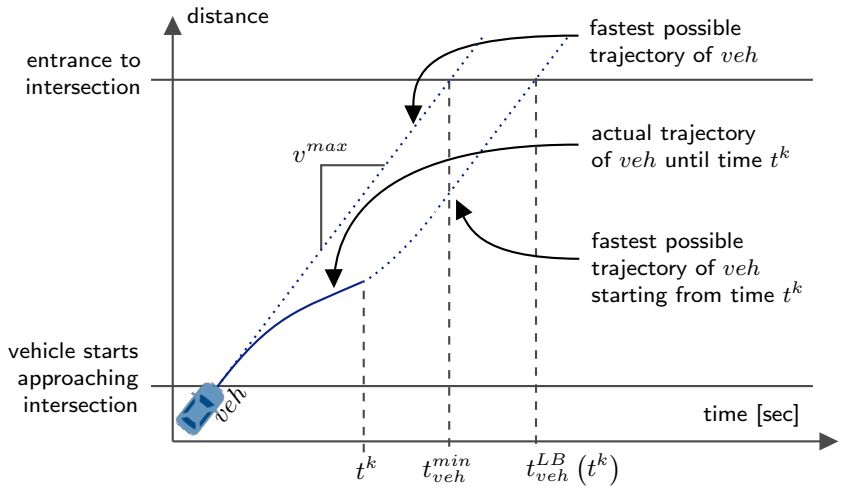

Figure 3.11: The lower bound on the arrival time of vehicle veh, $t_{veh}^{LB}(t^k)$, needs to be updated when vehicle veh is rescheduled.

needs to be reassigned a few seconds later, the earliest possible arrival time has changed. In order to distinguish the different values, the updated earliest arrival time of vehicle veh calculated at time t^k is denoted by $t_{veh}^{LB}(t^k)$. It represents a ***l**ower **b**ound* on the arrival time that is to be scheduled. In this situation, the previously ignored kinematic limitations of vehicle veh (i.e., limited acceleration values) need to be taken into account for the calculation of $t_{veh}^{LB}(t^k)$, because vehicles might have to accelerate as shown in Figure 3.11.

In order to retain the FCFS structure of the approach, vehicles in the rescheduling process are sorted and considered by proximity to the intersection. This means that in the previously described situation, vehicle veh' is scheduled before vehicle veh is assigned a new arrival time.

3.5 Integration of Pedestrians

In contrast to vehicles, pedestrians are not considered individually by the controller. Instead, it is assumed that all pedestrians who are present at a pedestrian crosswalk cross the respective approach together during the pedestrian green phase. Therefore, instead of scheduling individual pedestrian access times, the pedestrian crosswalk activation times are scheduled. Pedestrian crosswalk activation is exclusive, i.e., no vehicle movement is allowed on the crosswalks at the same time. In particular, permitted turning movements, which are common in traffic signal control, are not allowed. The crosswalk activation can be integrated into the scheduling policy in different ways, depending on available information and on the overall control objective at the considered intersection. Three different approaches will be presented and discussed in the following. The first one, described in Section 3.5.1, works with fixed cycle times and hence doesn't require knowledge about pedestrian arrivals at the intersection. The latter two, introduced in Section 3.5.2, represent two slightly different approaches for integrating on-demand signal phases for pedestrians. As discussed in Section 3.1, both mean and maximum waiting times are important for pedestrians and should be within an acceptable range. This is taken into account in the following approaches.

3.5.1 Fixed Cycles for Pedestrian Green Phases

If no information about arriving pedestrians is available or a constant pedestrian demand is assumed, fixed cycles for pedestrian crossings can easily be implemented to guarantee a certain LOS for pedestrians, i.e., to ensure that mean and maximum pedestrian waiting times are below a certain level. In order to implement fixed cycles for pedestrian crossings, the following input is needed:

- The cycle time T – similar to conventional traffic signals.
- The pedestrian green phase duration G in each cycle.
- The clearance time for the pedestrian crosswalk.

The conflict cells that correspond to the pedestrian crosswalk are then blocked for pedestrians upfront (for the combined time slots of green time and clearance time; compare Figure 3.9). All pedestrian crosswalks can be activated at the same time, or they can be activated in alternating or rotational order, for example. The most beneficial setup depends on the layout of the intersection and on the expected turning ratios of the vehicle movement. Since no permitted turns are possible and a small intersection zone as shown in Figure 3.7 is considered here, the alternating activation of pedestrian crosswalks could lead to queues, because there is no separate lane for turning vehicles. Therefore, all four pedestrian crosswalks are activated at the same time in the fixed cycle scenario. This additionally allows for pedestrians to cross the intersection diagonally. The integration of pedestrian crosswalk activation in fixed cycles is easy to understand and implement. Moreover, since the necessary conflict cells of pedestrian crosswalks are blocked upfront, vehicles with a fixed reservation do not need to change their time slot (assuming that no unexpected delays occur).

Just like for traditional fixed-time traffic signals, average and maximum pedestrian waiting times can be calculated analytically in this control scenario. Furthermore, the setup allows for estimating vehicle capacity on an analytical basis by considering only the share of cycle time that is available for vehicle movement at the intersection (if the "saturation flow rate" of vehicle movement at the intersection is known). These properties will be explained in more detail along with the simulation results in Section 3.7. On the other hand, the control is not able to dynamically react to pedestrian demand. This especially reduces efficiency if there are few pedestrians, or if pedestrians only cross at one of the approaches, but all crosswalks are blocked.

3.5.2 Demand-responsive Integration of Pedestrian Green Phases

If information about arriving pedestrians is available, the activation of crosswalks can be integrated on demand. A flowchart of the overall procedure is shown in Figure 3.12. If pedestrians arrive during a green phase, they can immediately start crossing. Otherwise, the control checks whether there are pedestrians already waiting at the crosswalk. In that case, the newly arrived pedestrian joins them and doesn't need to request a new signal phase. Finally, if there are no pedestrians waiting yet, a new pedestrian phase is requested.

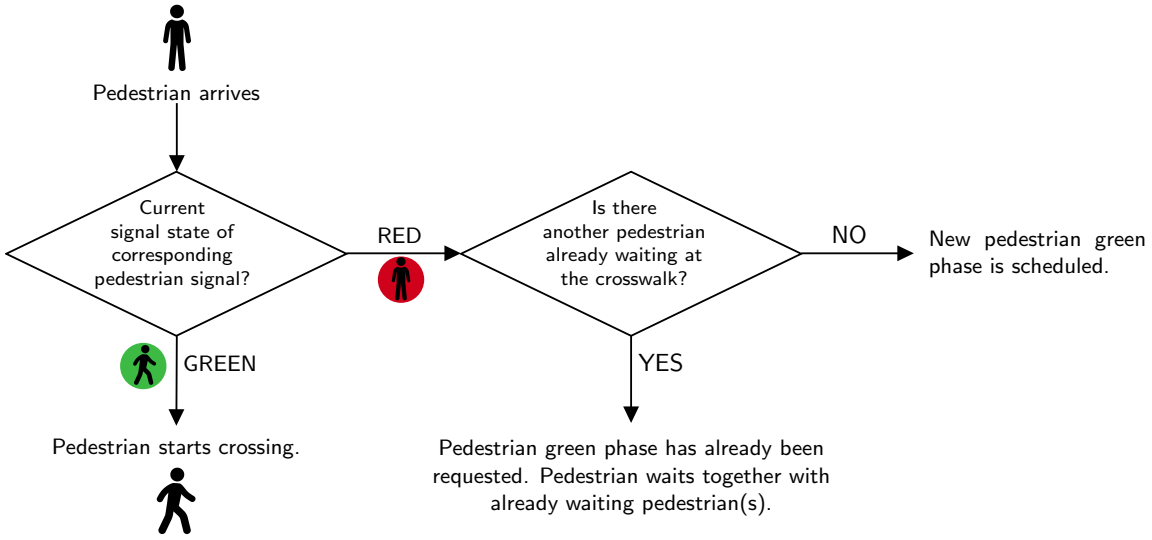

Figure 3.12: Flowchart of on-demand integration of pedestrians.

In principle, this can be done following the same FCFS strategy that was described for vehicles, and necessary space could be blocked as soon as possible. However, this mechanism cannot guarantee that acceptable maximum waiting times are not exceeded. While vehicles reserve their time slot for crossing the intersection several seconds prior to their earliest possible arrival, pedestrians are detected by the necessary infrastructure only when they are at the intersection and ready to cross. Therefore, long waiting times can be expected in such a setup. In order to guarantee a certain LOS for pedestrians and thus make the approach more comparable to conventional traffic signal control, priority will be granted to pedestrian movements.

Similarly to the fixed cycle scenario, some parameters need to be fixed before implementing the policy. First of all, the following two parameters are already known from the fixed cycle setup.

- The pedestrian green phase duration G.
- The clearance time for the pedestrian crosswalk.

If pedestrian signal phases are scheduled with priority, then existing vehicle reservations need to be canceled and the respective vehicles need to receive a new scheduled arrival time as explained in Section 3.4.2. In order to not infringe upon safety, vehicles that are already very close to or even within the intersection are not rescheduled. In such situations, the pedestrian green phase will hence not start immediately. Additionally, if there is vehicle demand at the intersection, pedestrian green phases should not follow one another without allowing vehicle movement in between. These considerations are taken into account via the following parameters:

- The reaction time θ of the control that is needed for allowing vehicles that are currently very close to or crossing the intersection to leave the requested conflict cells. This only applies if there are vehicles very close to or within the intersection.
- The maximum pedestrian waiting time Θ_{ped}.

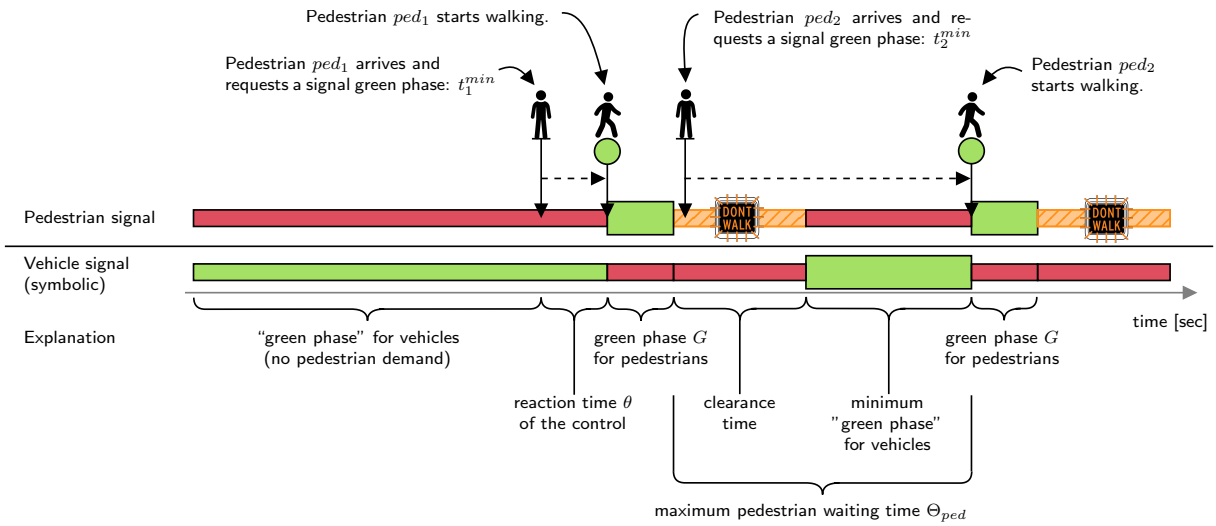

Figure 3.13: Illustration of pedestrian priority policy based on figure in [Niels, Mitrovic, Bogenberger, et al., 2019].

The overall scheduling policy that is applied when a new pedestrian green phase is requested is explained in the illustration in Figure 3.13. The figure shows a time line on the x-axis, and the two superimposed bars represent the allowance of pedestrian and vehicle movement within the considered conflict cells. As explained earlier, no traffic signals are considered for vehicles. The vehicle signal in the illustration is hence merely symbolic, intended to improve understandability. It needs to be noted that the figure and corresponding explanations assume a situation with constant vehicle demand in the intersection. If this is not the case, pedestrian green phases can be scheduled earlier as will be described below. In the figure, the arrival of pedestrian ped_1 at the intersection triggers the request of a new pedestrian green phase. Let t_1^{min} be the arrival time of pedestrian ped_1. It can be seen from the figure that, at time t_1^{min}, vehicle movement has been allowed for a longer consecutive period of time. In this situation, the green phase requested by pedestrian ped_1 is activated as soon as possible, i.e., after vehicles that are currently crossing the intersection have left the respective conflict zones. This means that pedestrian ped_1 can start crossing after the reaction time θ defined above has passed. The green phase lasts for G seconds and is followed by an all-red phase that allows pedestrians to safely finish crossing the street (depicted by the "Don't Walk" symbol). Now, a second pedestrian ped_2 arrives during the clearance time. Allowing pedestrian ped_2 to cross immediately or after the very short waiting time θ could ultimately lead to pedestrian green phases and clearance times being implemented in an alternating fashion without allowing vehicle movement in between. In order for the control to be balanced, vehicle movement will be allowed for a defined minimum duration before activating the pedestrian green phase. Therefore, the next pedestrian green phase is scheduled after the clearance time and the minimum "green phase" for vehicles. It can be seen from the figure that the sum of both equals the maximum pedestrian waiting time Θ_{ped}. This means that, given the clearance time that is defined to fulfill safety criteria (and therefore has a fixed value), the maximum pedestrian waiting time Θ_{ped} can be chosen to provide a certain pedestrian LOS, and the minimum duration of the vehicle phase follows accordingly. For simplification reasons, Θ_{ped} is assumed to be a

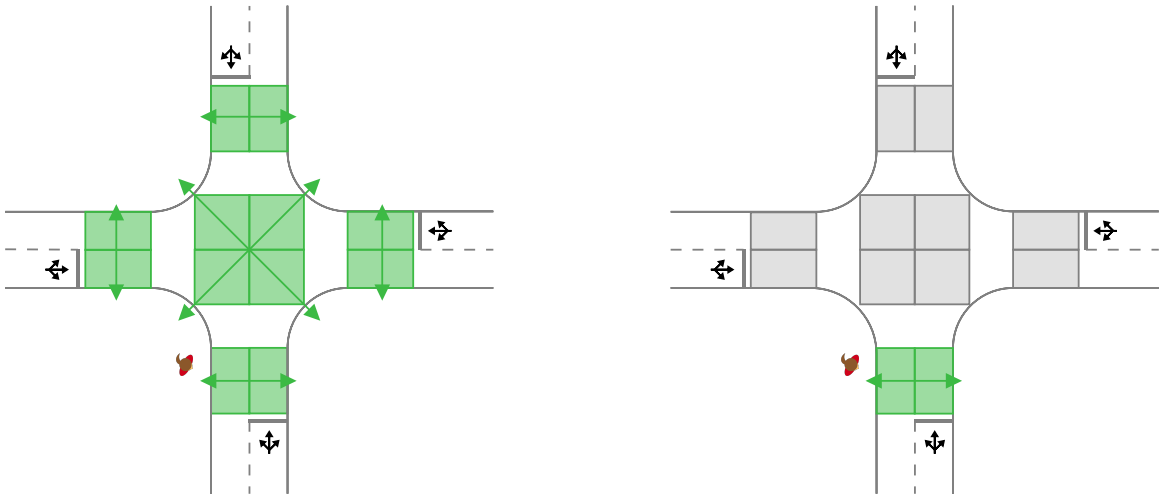

(a) Pedestrian requests apply to the entire intersection zone.

(b) Pedestrian requests apply to one crosswalk only.

Figure 3.14: Schematic representation of the two versions of integrating demand-responsive pedestrian green phases.

constant parameter in this chapter, but it could as well differ depending on pedestrian and vehicle demand or on pedestrian characteristics.

As noted above, the illustrated situation assumes constant vehicle demand. If there is no vehicle demand at the intersection upon the arrival of a pedestrian ped, then the green phase can start immediately, because (i) there are no vehicles that need to leave the intersection safely, and (ii) the minimum green phase for vehicles does not apply in the absence of vehicle demand. The maximum pedestrian waiting time Θ_{ped} hence bounds the pedestrian waiting time in situations with large vehicle demand, but is not utilized if pedestrian green phases can be planned without rescheduling vehicles.

The described policy is implemented in two different versions that are specified below and schematically displayed in Figure 3.14.

1. In the first version, pedestrian requests apply to the entire intersection zone, i.e., the entire intersection is reserved for them and they can cross any leg or cross diagonally. An example situation is displayed in Figure 3.14a.

2. In the second version, pedestrians only request to cross either one leg of the intersection as displayed in Figure 3.14b or, if they want to cross diagonally, the central part of the intersection.

The approaches presented above will be evaluated together with the fixed-cycle approach in Section 3.7. As described previously, discrete time slots are considered in this chapter. Therefore, all introduced time-related parameters (e.g., cycle time T, green phase duration G, reaction time θ of the controller, and maximum pedestrian waiting time Θ_{ped}) will be transformed into time slots when implementing the approach.

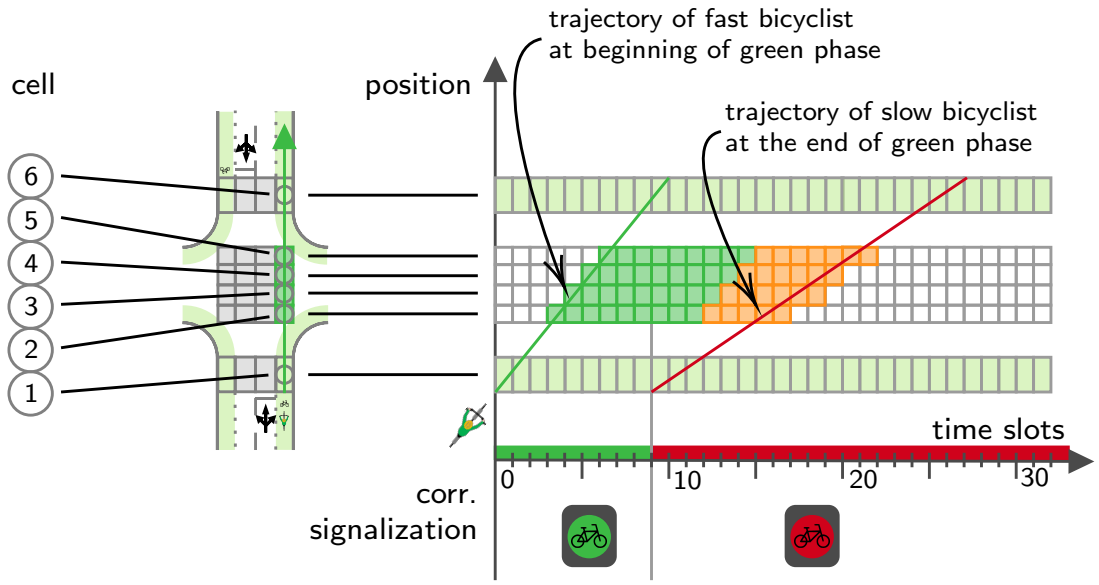

Figure 3.15: Cell occupancy of bicycle through movement.

3.6 Integration of Bicyclists

Similarly as with the integration of pedestrians, bicyclists are not scheduled on an individual basis, but rather signal green phases are planned for them. Again, a fixed cycle scenario, introduced in Section 3.6.1, and two demand-responsive scenarios, explained in Section 3.6.2, are implemented.

3.6.1 Fixed Cycles for Bicycle Green Phases

Just like in the scenario with vehicles and pedestrians, bicycle green phases can be scheduled in fixed cycles. As explained in Section 3.1, the philosophy of the control is to strictly separate vehicle movement from the movement of VRUs, whereas purely inter-VRUs conflicts are not resolved by the control. Therefore, RToR is always allowed for bicyclists. Following the reasoning in Section 3.5, the fixed-cycle approach is implemented such that the entire intersection is reserved for bicycle traffic during the bicycle green phase. The phase thus corresponds to an all-cyclists green phase, comparable to the one applied at some intersections in the Netherlands as described in Section 3.1 [Groningen Cycling City, 2016]. It also allows bicyclists to conduct a direct left turn. In order to implement the policy, the following three input parameters need to be defined:

- The cycle time T – similar to that of conventional traffic signals.
- The duration of the bicycle green phase G in each cycle.
- The clearance time duration that allows bicyclists to leave the intersection zone.

The fixed cycle setup for bicyclists works similarly as with the integration of pedestrian green phases in fixed cycles with the same systemic advantages and disadvantages. These

benefits and limitations will be discussed along with simulation results in Section 3.7. In the following, the implemented strategies for integrating demand-responsive bicycle green phases will be explained.

3.6.2 Demand-responsive Integration of Bicycle Green Phases

The demand-responsive integration of bicycle green phases requires knowledge about bicyclists at the considered intersection zone. Whereas pedestrians are detected and request their green phases when they are at the intersection, bicyclists are already detected on the approach to the intersection. Reasons for this difference are two-fold: on the one hand, bicyclists are easier to detect on the way to the intersection, because they can be assumed to approach the intersection via dedicated lanes, and their movement is easier to predict. On the other hand, detecting bicyclists when they are already at the intersection would require them to stop to request a green phase, which is not considered to be practical. The expected arrival time t_{bic}^{min} of a bicyclist bic is hence calculated based on the time that bicyclist bic crosses the detector, on the distance of the detector to the intersection, and on the expected bicycle speed. Another difference to pedestrian integration, that comes with this detection setup, is the fact that origins of bicyclists are always known.

Additionally, in contrast to pedestrian signals, bicycle signals are dependent on the travel direction of bicyclists, and bicyclists cross several conflict cells on their way through the intersection. Therefore, clearance time is not defined here as one fixed parameter. Instead, the occupation of conflict cells is considered in detail. This is done similarly to the scheduling of vehicle movement (compare Section 3.3). The major difference to planning vehicle movement is that, due to the bicycle green phase that lasts several seconds and the variation in bicycle speed, the conflict cells need to be reserved for a longer period of time. An illustration is provided in Figure 3.15, where the cell occupation of a bicycle green phase for through movement is shown. Details on the modeling and simulation of bicyclist behavior (including variations in speed and acceleration behavior) will be provided in Chapter 5.

Again, pre-defined maximum bicycle waiting times Θ_{bic} shall not be exceeded in this approach. When the intersection controller receives information of an arriving cyclist and a new bicycle green phase needs to be requested, the controller looks for the earliest possible time slot to schedule the green phase. Once this time slot has been found, let it be denoted as $\tilde{t}_{bic}$, the expected waiting time $delay_{bic} = \tilde{t}_{bic} - t_{bic}^{min}$ is calculated. If this waiting time is unacceptably high, i.e., if $delay_{bic} > \Theta_{bic}$, then priority is given to the bicyclist and a green phase after an expected waiting time of Θ_{bic} is implemented, i.e., $\hat{t}_{bic} = t_{bic}^{min} + \Theta_{bic}$. Similarly to the pedestrian integration, this will lead to the rescheduling of vehicles as explained in Section 3.4.2. The respective bicycle signal remains green for at least a minimum duration of a few seconds, which helps bicyclists to meet their green phase even if they are riding at a slower speed. If a new bicyclist bic' crosses the detector and the signal will be green upon the expected arrival of bic' at the stop bar, or a green phase has already been requested for the same signal, no new signal phase is requested. If a bicyclist misses the assigned green phase and has to stop at the stop line, a new green phase will be requested.

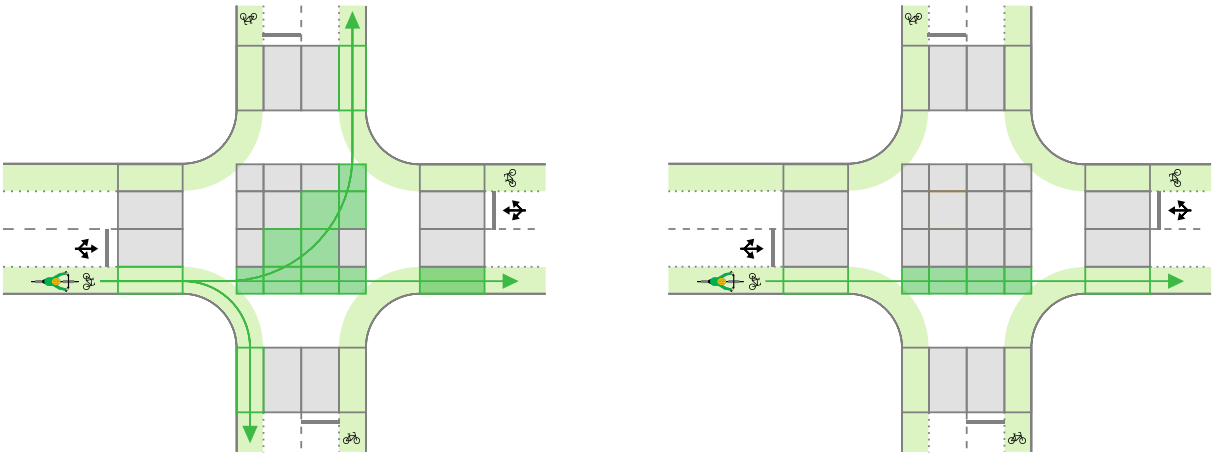

(a) Bike request without knowledge on turning intention.

(b) Bike request with knowledge on turning intention.

Figure 3.16: Schematic representation of the two approaches for integrating on-demand pedestrian green phases.

Again, two different control scenarios for the on-demand integration of bicycle green phases are implemented, schematically displayed in Figure 3.16.

- In the first one, it is assumed that bicyclists are detected on the approach to the intersection, but their turning intention is unknown. The detection thus triggers a bicycle green phase for both through movement and left-turning movement for bicyclists coming from the respective direction. Due to the RToR policy, signal phases for right-turning bicycle movement do not need to be requested. The approach is schematically displayed in Figure 3.16a.
- In the second control scenario, it is assumed that turning intentions of bicyclists are also known. The bicycle request thus only triggers a green phase for the specific turning movement as shown in Figure 3.16b. This is the case if bicyclists enter the intersection zone via dedicated turning lanes, or if video sensors recognize hand gestures that indicate a turning intention.

Independently of the control scenario, each of the bicycle movements has a separate signalization. In addition to the requested green phases, the signal heads will be default to green in the absence of vehicle requests that apply to the relevant conflict cells.

3.7 Simulation-based Evaluation

The presented strategies are implemented and tested using a microsimulation framework. This section presents the obtained results with a focus on measured delays. As described in Chapter 2, the control delay per vehicle or VRU, respectively, is the decisive parameter to evaluate the LOS at signalized intersection zones according to both the American HCM [TRB, 2000] and the German counterpart, the HBS [FGSV, 2015a]. It is also the most

widely used performance indicator when evaluating AIM strategies. In this section, delays for all considered road users are evaluated. First of all, Section 3.7.1 explains how delay is defined in the following evaluations. Section 3.7.2 briefly introduces the simulation setup used for the evaluations. Afterwards, results for vehicle-only scenarios are shown in Section 3.7.3, results for scenarios with vehicles and pedestrians are presented in Section 3.7.4, and results for scenarios with vehicles and bicyclists are discussed in Section 3.7.5.

3.7.1 Definition of Delay

The delay from the road user perspective can be described as the difference in travel time when compared to a scenario without the intersection. For vehicles, this would mean driving at the maximum speed all the way through. In the presented intersection control setup, it is assumed that vehicles cross the intersection zone at the maximum allowed speed. Once a vehicle enters the intersection, it hence does not experience delays caused by the intersection control any more. Therefore, the delay of vehicle veh is calculated as the difference between the earliest possible arrival time of veh at the intersection (denoted by t_{veh}^{min}) and the time it actually enters the intersection area (denoted by $\hat{t}_{veh}$) as shown in Figure 3.17a. The delay of vehicle veh can thus be expressed as follows:

$$delay_{veh} = \hat{t}_{veh} - t_{veh}^{min}. \tag{3.4}$$

The delays of pedestrians are approximated in a similar way. As shown in Figure 3.17b, let t_{ped}^{min} be the time that pedestrian ped arrives at the pedestrian crosswalk and $\hat{t}_{ped}$ the time that pedestrian ped is allowed to start crossing the street. If the pedestrian signal is already green upon the arrival of pedestrian ped, then $\hat{t}_{ped}$ equals t_{ped}^{min} and the delay is zero (compare the situation of ped_3 in Figure 3.17b). Otherwise, $\hat{t}_{ped}$ corresponds to the start of the respective green phase (see ped_1 and ped_2 in the figure). The delay of pedestrian ped can be calculated as follows:

$$delay_{ped} = \hat{t}_{ped} - t_{ped}^{min}. \tag{3.5}$$

The delays of bicyclists are calculated differently. The integration of bicyclists into the control setup features the calculation of the earliest possible arrival time t_{bic}^{min} of a bicyclist bic at the intersection when the bicyclist is detected several meters away from the stop bar. However, this ex-ante calculation is based on an assumed average speed for bicyclists and does not necessarily correspond to the actual arrival time of bicyclist bic at the intersection. For the ex-post evaluation, the delay of bicyclist bic is calculated as the difference between the time bicyclist bic stopped in front of the traffic signal (denoted by t_{bic}^{stop}) and the time bicyclist bic crossed the stop bar (denoted by t_{bic}^{min}). If a bicyclist passes the intersection without stopping, the delay is assumed to be zero. All in all, the delay is defined as

$$delay_{bic} = \left(\hat{t}_{bic} - t_{bic}^{stop}\right) \cdot stop_{bic}, \tag{3.6}$$

where $stop_{bic}$ is a binary variable indicating whether bicyclist bic came to a full stop in front of the signal, i.e.,

$$stop_{bic} = \begin{cases} 1 & \text{if } bic \text{ stopped at the traffic signal,} \\ 0 & \text{otherwise.} \end{cases}$$

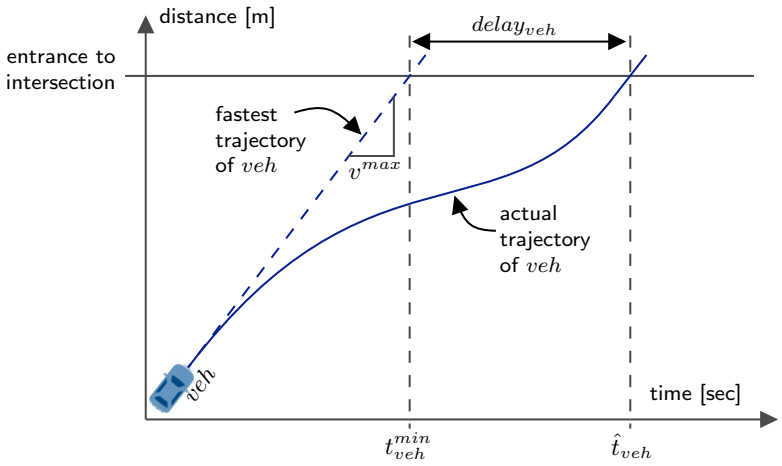

(a) The delay of vehicle veh at the intersection is defined by the earliest possible and the actual arrival time of veh at the intersection.

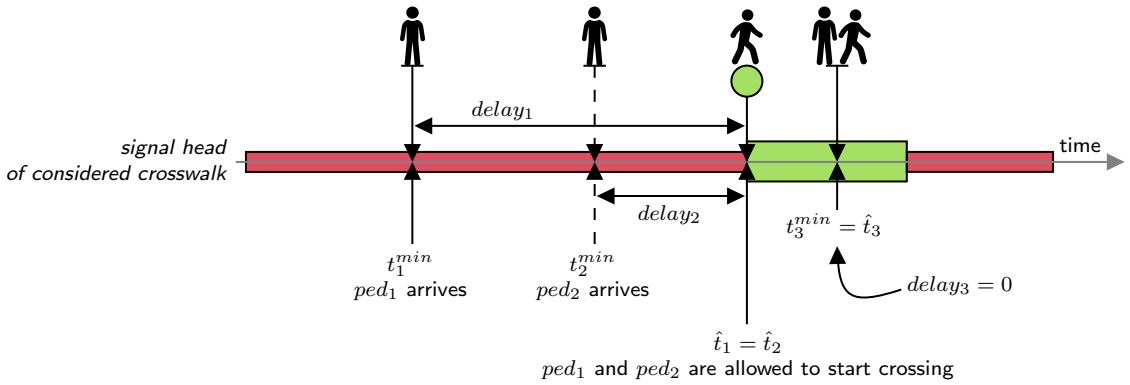

(b) The delay of pedestrian ped is defined by her arrival time at the intersection and the start of her green phase.

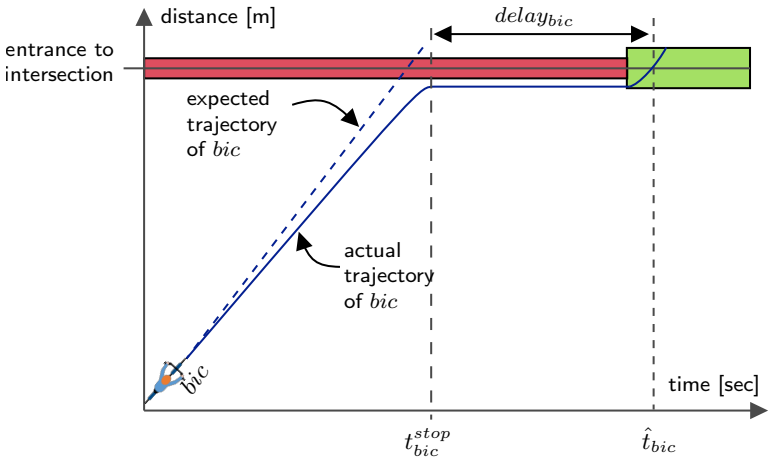

(c) The delay of bicyclist bic is defined by the time bicyclist bic stopped at the intersection and the time she crosses the stop bar.

Figure 3.17: Definition of delay for considered road users: vehicles, bicyclists, and pedestrians.

It needs to be noted that the delay calculation for VRUs does not include delays resulting from reaction times (in the pedestrian case) and the times needed to slow down before stopping and to accelerate until reaching the desired speeds (in the bicycle case). These additional delays are more difficult to quantify and depend on individual behavior. Additionally, they can be reduced independently of the scheduling policy, e.g., by implementing green signal countdown timers at the intersection (compare Section 3.1).

In the following, average delays for each road user group are evaluated. Let $\mathcal{V}$ be the set of vehicles, $\mathcal{P}$ the set of pedestrians, and $\mathcal{B}$ the set of bicyclists that cross the intersection during a specific period of time. Then, the average delays are denoted by $\overline{delay}(\mathcal{V})$, $\overline{delay}(\mathcal{P})$, and $\overline{delay}(\mathcal{B})$, and are calculated as follows:

$$\overline{delay}(\mathcal{V}) = \frac{1}{|\mathcal{V}|} \sum_{veh \in \mathcal{V}} delay_{veh}, \tag{3.7}$$

$$\overline{delay}(\mathcal{P}) = \frac{1}{|\mathcal{P}|} \sum_{ped \in \mathcal{P}} delay_{ped}, \tag{3.8}$$

$$\overline{delay}(\mathcal{B}) = \frac{1}{|\mathcal{B}|} \sum_{bic \in \mathcal{B}} delay_{bic}. \tag{3.9}$$

3.7.2 Simulation Setup

The presented intersection control strategies are tested using the microsimulation platform aimsun.next. In each simulation step, the application programming interface (API) provides the information of all road users that are currently in the network. Additionally, it allows for influencing signal states and vehicle speeds according to user-defined rules. The control logic as presented in the previous sections is implemented in Python. In this chapter, two different example intersections (both displayed in Figure 3.7) are replicated in order to evaluate the strategies. The detailed geometries are shown in Appendix E.1. Given the small size of the intersections and the importance of VRU movement in the described setup, a speed limit of 30 km/h is assumed at the intersections. Additionally, it is assumed that all passenger vehicles have the same dimensions, kinematic limitations, and desired speeds as shown in Table 3.2.

Since the intersections simulated in this chapter are artificial and isolated, the intersection approaches in the simulation can be virtually infinitely long. Based on literature assumptions regarding communication distances that can be reliably achieved with existing V2I technology, it is assumed that vehicles first sign up with the intersection controller when they are at a distance of 300 meters to the intersection [Mannion, 2017]. Based on the speed limit of 30 km/h, vehicles therefore sign up with the intersection control at least 36 seconds prior to their arrival. This position marks the calculation of the earliest possible arrival time t_{veh}^{min} of vehicle veh. This means that queues going beyond this position are not taken into account in the delay calculation, which can lead to an underestimation of delays in situations with very large queues. Nevertheless, these queues only occur in situations with oversaturated demand and will be marked accordingly in the result presentation.

Input Parameters	Values
Vehicle dimensions $(len_{veh} \times wid_{veh})$	$4.00\,\mathrm{m} \times 2.00\,\mathrm{m}$
Maximum allowed speed v^{max}	$8.3\,\mathrm{m/sec}$ $(30\,\mathrm{km/h})$
Vehicle speeds for crossing the intersection $\hat{v}_{veh}$	$8.3\,\mathrm{m/sec}$ $(30\,\mathrm{km/h})$
Min. and max. acceleration acc^{min} | acc^{max}	$-4\,\mathrm{m/sec^2}$ | $3\,\mathrm{m/sec^2}$
Minimum gap for car-following δ^{min}_{follow}	$0.7\,\mathrm{sec}$

Table 3.2: Parameter values for the test scenarios.

Demand on each approach	(veh/h)
Symmetric Scenario x	$0.25 \times x$
Turning ratios	$(\%)$
Through movement	75%
Left	10%
Right	15%

Table 3.3: Vehicle traffic demand for the test scenarios.

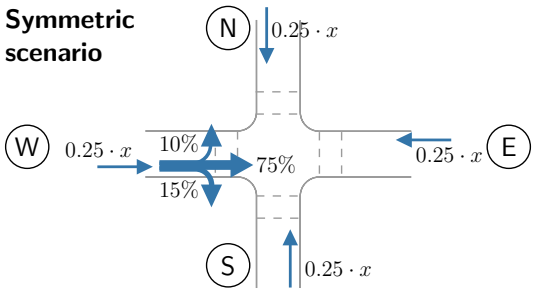

Figure 3.18: Graphical representation of the demand scenarios.

The simulation time step is 0.6 seconds which also corresponds to the size of the time slots in the control approach. This means that within one time slot, vehicles move up to five meters. All simulations presented in the following are run for one full hour with a warm-up phase of 10 minutes that is not considered in the evaluation, and at least 10 replications (with 10 random seeds) are run for each presented scenario. Details on the simulation setup including car-following behavior, trajectory planning, and behavior of pedestrians and bicyclists will be provided in Chapter 5.

3.7.3 Results for Vehicle-only Scenarios

Before analyzing multimodal scenarios, results of the SlotIIC control for vehicle-only scenarios are presented. This brief evaluation is intended to assess the vehicle capacity at the intersection considering an FCFS control without other road users. Obtaining this base capacity will help contextualize the impact of VRU movement in the next steps.

The considered demand scenarios are displayed in Table 3.3 and additionally visualized in Figure 3.18. They are denoted by x, where x is the total number of vehicles per hour considered in the scenario. The scenarios simulated in this chapter can be described as symmetric, i.e., the demand on all approaches is identical with $0.25 \cdot x$ vehicles per hour on each approach. It is assumed that 75% of the vehicles on each approach are through movement, 10% turn left, and 15% turn right as shown in the figure. Further (including non-symmetric) scenarios will be analyzed in Chapters 4 and 5.

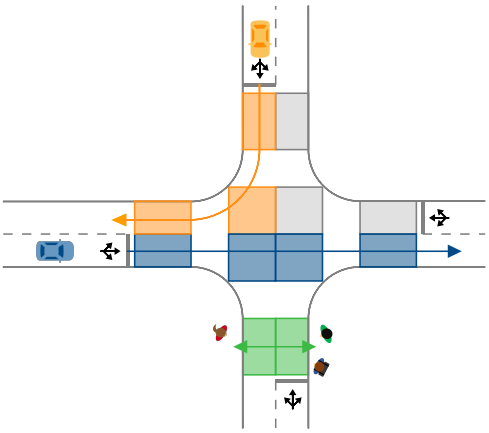

(a) Intersection considered in the presented scenarios.

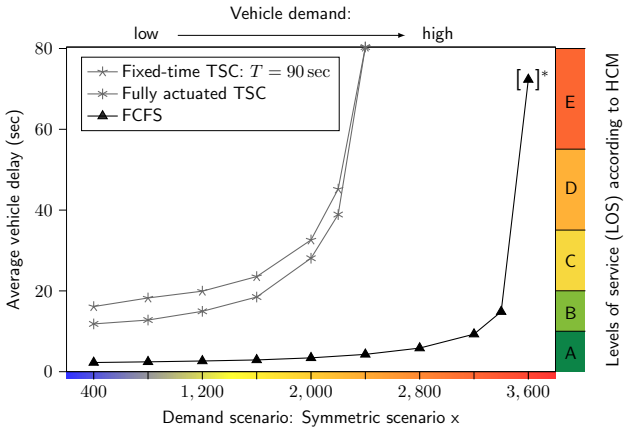

(b) Results for scenarios without pedestrian movement. *The delay in scenario $x = 3,600$ is not accurate, because queues exceed the approach length of 300 meters and throughput falls short of demand.

Figure 3.19: Considered intersection and results for scenarios without pedestrian movement.

The intersection displayed in Figure 3.19a is simulated for this analysis. Average vehicle delays resulting from the SlotIIC approach are compared to those resulting from (i) a fixed-time two-phase traffic signal with a cycle time T of 90 seconds (featuring a green interval of 38 seconds and a yellow interval of 3 seconds in each phase) and (ii) a fully actuated traffic signal with minimum and maximum green intervals of 15 and 38 seconds, thus also featuring a maximum cycle time of 90 seconds. Such a cycle time is very common in urban signal control. According to an analysis by the German Federal Highway Research Institute, cycle times in urban areas range from 30 seconds to 90 seconds; longer cycle times of up to 120 seconds are mostly applied in suburban areas with low VRU demand [Alrutz et al., 2012]. Details on the implementation of the TSC scenarios are provided in Appendix F, Vehicle delays in the TSC scenarios are approximated in the same way as in the SlotIIC scenario (compare Equation 3.4). They hence do not include the vehicle delays that occur after crossing the stop bar (e.g., when left-turning vehicles stop in the middle of the intersection to let oncoming traffic pass). Since such vehicle delays inherently do not occur in the SlotIIC scenario, this comparison slightly "undersells" the benefits of the proposed SlotIIC setup. Nevertheless, the presented results provide a good overall comparison regarding the impact of increased vehicle demand on delays.

Figure 3.19b shows the vehicle demand scenarios on the x-axis and average vehicle delays on the y-axis. It can be seen that the SlotIIC approach (depicted with black triangles) leads to a significant reduction in delays and a larger intersection capacity. The significant improvements of an FCFS control as compared to the considered TSC setups, especially in scenarios with large demand, can be surprising in light of the literature review. It needs to be noted here that the relatively poor performance of the TSC partly results from the small intersection layout where left-turning vehicles stopped within the intersection block the way for vehicles behind them. Many reviewed papers instead consider larger intersections with several lanes and protected left-turning movements. At those intersections, the difference is less striking (compare [Niels, Mitrovic, Dobrota, et al., 2020]).

Let cap^{base} be the approximate vehicle capacity at the intersection following the SlotIIC approach without the consideration of pedestrians. As shown in Figure 3.19b, average vehicle delays increase rather slowly until the capacity limit is reached. The figure shows that the control is not able to handle the demand of 3,600 vehicles per hour at the intersection. Based on the results, the capacity is estimated to be approximately 3,400 vehicles per hour, a demand that can be handled with an average vehicle delay of approximately 15 seconds. This capacity can be used as a baseline in the following evaluations where pedestrians will be integrated into the control and a portion of time will be dedicated to pedestrian movement. It needs to be noted that this capacity, in addition to the intersection geometry and applied control, depends on the demand configuration, i.e., on the demand ratios between different approaches as well as the frequency of turning movements.

3.7.4 Results for Scenarios with Vehicles and Pedestrians

In this section, results for the different described control scenarios featuring vehicles and pedestrians are presented and discussed for a set of demand scenarios. For the following evaluations, it is assumed that the minimum duration of pedestrian green phases is 5.4 seconds. A minimum green phase duration of 5 seconds is prescribed by the German guideline RiLSA and is applied in several German cities as reported by Alrutz et al. [2012]. The green phase is only intended for pedestrians to start crossing, and a longer intergreen phase makes sure that their clearance times are respected. For the calculation of clearance times, pedestrian walking speed is assumed to be 0.8 meters per second. This is relatively slow as compared to the assumption of 1.2 meters per second in the German guideline RiLSA [FGSV, 2015b]. However, it needs to be noted that vehicles will arrive at the intersection at a higher speed. Therefore, pedestrian crosswalks need to be monitored by sensors and, if pedestrians are detected on the street, approaching vehicles need to slow down and request a new time slot for crossing the intersection. If pedestrian clearance times are too short, vehicles need to stop in front of the pedestrian crosswalk and, consequently, cross the intersection with a lower speed. While this last-minute rescheduling process does not infringe upon safety, it is assumed to be uncomfortable for both pedestrians and vehicle passengers and can reduce efficiency at the intersection. In order to reduce the frequency of this occurrence, a slower walking speed is assumed. In practice, the clearance times need to be adapted depending on the prevailing characteristics of pedestrians at the considered intersection. Assuming the intersection depicted in Figure 3.19a, the clearance time assigned for crossing one leg of the intersection (7.5 meters) is 9.4 seconds, whereas the clearance time needed for crossing the central area of the intersection diagonally (15 meters) is 18.8 seconds.[1] Both are rounded up to match the control time step of 0.6 seconds. In the following, results for the integration of pedestrian green phases in fixed cycles will be discussed before presenting results for the demand-responsive integration.

Fixed Cycles for Pedestrians

Before running simulations with vehicles and pedestrians, some analytical calculations for obtaining a suitable cycle time for a given situation are explained. First of all, as described in

[1] The big difference in distances results from the curb turn radii.

	Pedestrians crossing one leg	**Pedestrians crossing diagonally**
Fixed-time SlotIIC		
Pedestrian green phase in each cycle	$15\,\text{sec}$	$5.4\,\text{sec}$
Maximum pedestrian waiting time Θ_{ped}	$T - 15\,\text{sec}$	$T - 5.4\,\text{sec}$
Average pedestrian waiting time $\overline{delay}(\mathcal{P})$	$\frac{(T-15\,\text{sec})^2}{2 \cdot T}$	$\frac{(T-5.4\,\text{sec})^2}{2 \cdot T}$
Fixed-time two-phase TSC		
Pedestrian green phase in each cycle	G	–
Maximum pedestrian waiting time Θ_{ped}	$T - G$	$\frac{1}{2} \cdot T$
Average pedestrian waiting time $\overline{delay}(\mathcal{P})$	$\frac{(T-G)^2}{2 \cdot T}$	$\frac{(T-2 \cdot G)^2}{4 \cdot T} + \frac{G \cdot (T-G)}{T}$

Table 3.4: Analytical calculation of mean and maximum pedestrian waiting times depending on cycle time T and green phase duration G.

Section 3.5.1, the integration of pedestrian green phases in fixed cycles allows for the analytical calculation of mean and maximum pedestrian waiting times. This can be done similarly to with traditional fixed-time TSC. In particular, the maximum pedestrian waiting time Θ_{ped} equals the difference between cycle time T and green phase duration G, i.e., $\Theta_{ped} = T - G$. This corresponds to the time that pedestrians need to wait if they arrive when the signal just turned red. Assuming that a pedestrian arrives at a random point in time, the probability that the traffic signal is currently green equals $\frac{G}{T}$, and the probability of a red signal is $\frac{T-G}{T}$. If the signal is currently green, the waiting time of pedestrians is 0 seconds, since they can already start crossing the intersection. If the signal is currently red, the expected average waiting time is $\frac{1}{2} \cdot (T - G)$. All in all, the average waiting time $\overline{delay}(\mathcal{P})$ of pedestrians can be calculated as

$$\overline{delay}(\mathcal{P}) = \frac{G}{T} \cdot 0 + \frac{T-G}{T} \cdot \frac{1}{2} \cdot (T-G) = \frac{(T-G)^2}{2 \cdot T}. \tag{3.10}$$

Given these simple formulas, the cycle times and green phase durations can be set in such a way that a certain pedestrian LOS (based on both HBS and HCM) can be guaranteed. The calculations for a fixed-time SlotIIC with a minimum green phase of 5.4 seconds and for a fixed-time two-phase TSC can be found in Table 3.4. The table distinguishes between pedestrians who want to cross one leg of the intersection and pedestrians who want to cross the intersection diagonally. In the SlotIIC scenario, green phases on the legs of the intersection can be extended because of the shorter necessary clearance times compared to the central part of the intersection. In the fixed-time two-phase TSC scenario, diagonal crossing is not allowed, but crosswalks are activated in an alternating fashion (i.e., the crosswalks on the northern and southern legs are activated in phase 1, the crosswalks on the eastern and western legs are activated in phase 2). In this scenario, pedestrians wanting to cross diagonally need to cross two of the legs and their waiting times add up. Details on the calculation of waiting times for pedestrians crossing diagonally in the TSC scenario are provided in Appendix F.4.

	Pedestrians crossing one leg	Pedestrians crossing diagonally
Fixed-time SlotIIC		
Max. ped. waiting time Θ_{ped}	45.0 sec	54.6 sec
→ LOS based on HBS [FGSV, 2015a]	C	C
Avg. waiting time $\overline{delay}(\mathcal{P})$	16.9 sec	24.8 sec
→ LOS based on HCM [TRB, 2000]	B	C
Fixed-time two-phase TSC		
Max. ped. waiting time Θ_{ped}	55.0 sec	45.0 sec
→ LOS based on HBS [FGSV, 2015a]	C	C
Avg. waiting time $\overline{delay}(\mathcal{P})$	16.8 sec	22.5 sec
→ LOS based on HCM [TRB, 2000]	B	C

Table 3.5: Mean and max. pedestrian waiting times and corr. LOS for different control strategies with fixed cycles.

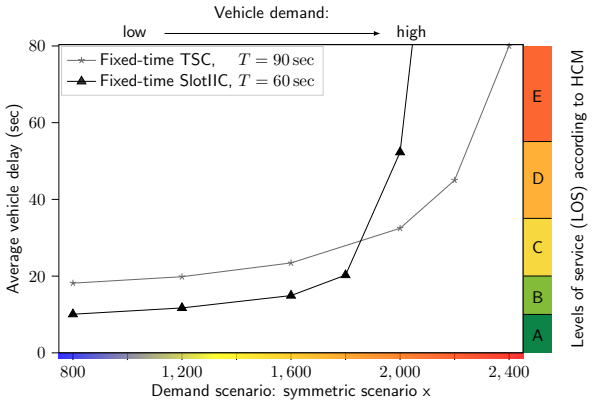

Figure 3.20: Comparison of avg. vehicle delays for the fixed-time two-phase TSC and the fixed-time SlotIIC.

In addition to the pedestrian LOS, a first estimate of the approximate vehicle capacity at the intersection applying the fixed-time SlotIIC approach can be calculated analytically. Assuming that the intersection is reserved for pedestrians for a duration of P seconds in each cycle (including pedestrian green phase and clearance time), the resulting vehicle capacity $cap^{\mathcal{V}}$ can be estimated as

$$cap^{\mathcal{V}} = \frac{T - P}{T} \cdot cap^{base}, \tag{3.11}$$

where cap^{base} is derived from the analysis in Section 3.7.3.

In the following, a fixed-cycle SlotIIC setup is compared to a fixed-time two-phase TSC. The SlotIIC approach features a cycle time T of 60 seconds and allows pedestrians to cross diagonally. Resulting pedestrian mean and maximum waiting times, calculated using the formulas in Table 3.4, are presented in Table 3.5. They are compared to a fixed-time traffic signal with a cycle time of 90 seconds and a pedestrian green phase of 35 seconds in each phase. It can be seen that both setups provide similar waiting times and the same LOS for pedestrians.

Applying Equation 3.11, the vehicle capacity $cap^{\mathcal{V}}$ for the SlotIIC scenario with a cycle time T of 60 seconds and a pedestrian phase P of 24.6 seconds (including a green phase duration of 5.4 seconds plus the clearance time of 19.2 seconds for diagonal crossing) can be calculated. Assuming the base capacity cap^{base} of 3,400 vehicles per hour obtained from Figure 3.19b, $cap^{\mathcal{V}}$ can be estimated as approximately 2,000 vehicles per hour. Figure 3.20 shows the resulting average vehicle delays obtained from the simulations. Results show that the calculations provide a good estimate.

The figure also shows the average vehicle delays resulting from the fixed-time TSC as shown in Figure 3.19b. It can be seen that the SlotIIC approach still performs better than the TSC for scenarios with lower demand (up to 1,800 vehicles per hour). In the scenario with x=2,000 vehicles per hour, average vehicle delay applying the SlotIIC approach exceeds

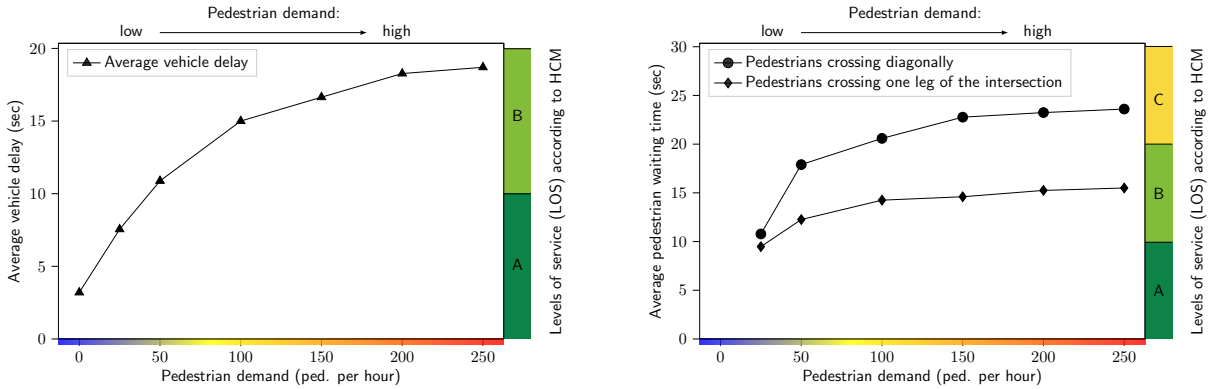

(a) Average vehicle delays depending on pedestrian demand.

(b) Average pedestrian waiting times depending on pedestrian demand.

Figure 3.21: Comparison of vehicle and pedestrian delays for SlotIIC with demand-responsive pedestrian green phases (pedestrian requests apply to the entire intersection).

that of the TSC scenario, and the demand of x=2,200 vehicles per hour cannot be handled by the fixed-time SlotIIC, while the TSC returns an average delay of 45 seconds. It needs to be noted that these scenarios were simulated without simulating pedestrian activity. This makes no difference in the fixed-time SlotIIC scenario, because vehicle and pedestrian movements are strictly separated from each other. On the other hand, it can be assumed that increasing pedestrian activity actually leads to additional delays and reduced capacity in the TSC scenario, because turning vehicles have to yield to pedestrians. Nevertheless, the large capacity increase apparent in Figure 3.19b is now dedicated to pedestrian movement while pedestrian LOS is overall comparable to that of the TSC scenario – at least if we disregard the expected improvements in pedestrian safety that emerge from the strict separation of vehicle and pedestrian movement. Clearly, pedestrian LOS could be further improved by reducing the cycle time at the expense of vehicle capacity at the intersection – and vice versa. If dynamic information on pedestrian arrivals is available, the scheduling can additionally be improved.

Demand-responsive Integration of Pedestrians

If vehicle or pedestrian demand fluctuates or if pedestrian demand mainly applies to one leg of the intersection, the activation of pedestrian green phases in fixed cycles can be inefficient. In the following, the two approaches for integrating demand-responsive pedestrian green phases described in Section 3.5.2 are evaluated. In both scenarios, the reaction time θ of the intersection control that is needed to reschedule conflicting vehicles in order to give priority to pedestrian movement is assumed to be 4.8 seconds.

First, demand-responsive signal phases that apply to the entire intersection zone (including the diagonal crosswalk) are integrated. This means that when a new pedestrian green phase is requested, the entire intersection zone is reserved. In the following, the maximum pedestrian waiting time Θ_{ped} is assumed to be 54.6 seconds which corresponds to the maximum waiting time in the fixed-cycle SlotIIC setup shown in Table 3.5. In the presented scenarios, 20 % of pedestrians are assumed to cross the intersection diagonally.

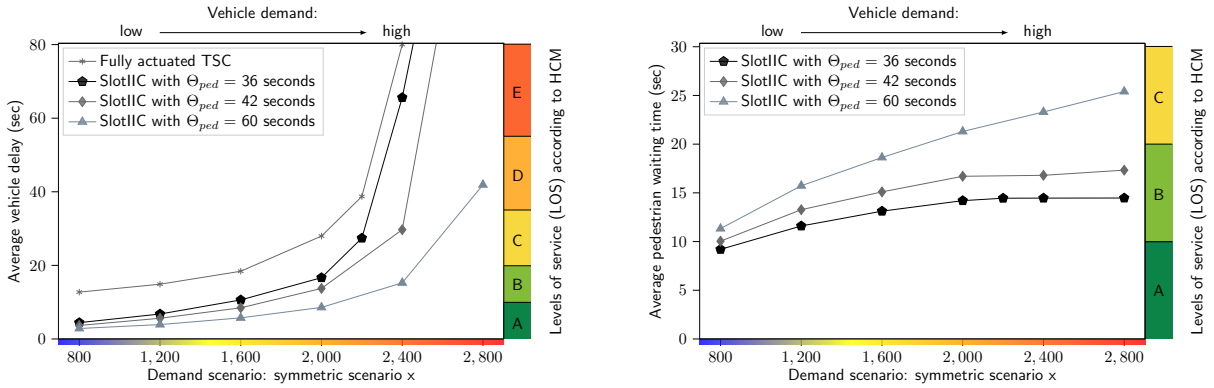

(a) Average vehicle delays depending on vehicle demand.

(b) Average pedestrian waiting times depending on vehicle demand.

Figure 3.22: Comparison of vehicle delays and pedestrian waiting times for the demand-responsive integration of pedestrian green phases with different values of Θ_{ped}.

Figure 3.21 shows average vehicle delays (Figure 3.21a) and pedestrian waiting times (Figure 3.21b) for the demand scenario with x=1,800 vehicles per hour and an increasing pedestrian demand. First of all, it can be seen that lower pedestrian demand allows for both shorter vehicle delays (because fewer pedestrian green phases are scheduled) and shorter pedestrian waiting times. The latter effect is more interesting. If pedestrian demand is low, then pedestrian requests are more likely to appear at a moment when vehicle movement has already been allowed within the intersection for some time. In these situations, pedestrians are allowed to cross after the very short waiting time θ (compare Figure 3.13). With increasing pedestrian demand, it is likely that a new pedestrian request directly follows a pedestrian green phase and the minimum "green phase" for vehicles needs to be respected. The approach hence converges to the fixed-cycle setup that was evaluated previously. Additionally, Figure 3.21b shows that average waiting times are longer for pedestrians crossing diagonally compared to pedestrians crossing one leg of the intersection. This results from two considerations: firstly, the clearance time for the diagonal crosswalk is longer. Therefore, when the diagonal signal turns red, the signal on the legs can still remain green for a few seconds. Secondly, the default to green that applies in the absence of vehicle demand is more likely to apply to the crosswalks on the legs, because fewer conflict zones need to be considered. Therefore, the probability of arriving during a pedestrian green phase (and hence experiencing no delay) is larger for pedestrians crossing only one leg of the intersection.

If pedestrian requests only apply to the area of the intersection that pedestrians actually want to cross, the performance can further be improved. In the following analysis, a pedestrian demand of 200 pedestrians per hour per leg with no diagonal crossings is assumed. Maximum pedestrian waiting time Θ_{ped} is altered from 42 seconds (comparable to the SlotIIC scenario in Table 3.5) to 60 seconds (comparable to the TSC scenario in Table 3.5) and 36 seconds. Figure 3.22 shows resulting vehicle delays (Figure 3.22a) and pedestrian waiting times (Figure 3.22b). As expected, vehicle delays increase with increasing vehicle demand. The resulting delays follow a similar curve as the ones shown in Figures 3.19 and 3.20 with exact values

Strategy	Benefits	Limitations
Fixed Cycles	+ No pedestrian detection necessary. + Vehicle capacity and pedestrian LOS can be calculated analytically. + Highest level of safety, because entire intersection is reserved for pedestrians. + Vehicles don't need to be rescheduled.	– Can be inefficient, if demand fluctuates or if VRU activity only applies to one part of the intersection.
Demand-responsive integration (no information on OD)	+ Dynamic, reacts to fluctuations in demand. + Highest level of safety, because entire intersection is reserved for pedestrians.	– Pedestrian detection necessary. – Frequent rescheduling of vehicles can become necessary. – Can be inefficient, if VRU activity only applies to one part of the intersection.
Demand-responsive integration (OD-specific)	+ Dynamic, reacts to fluctuations in demand.	– Pedestrian detection necessary. – Frequent rescheduling of vehicles can become necessary.

Table 3.6: Comparison of the different characteristics of the SlotIIC scheme.

depending on the parameter value Θ_{ped}. On the other hand, with increasing vehicle demand, pedestrian waiting times converge to a fixed-cycle setup. If vehicle demand is low, then pedestrians can often start crossing without any waiting time, because the crosswalks are not reserved for vehicles. In such a situation, the different maximum pedestrian waiting times do not play an important role as shown in Figure 3.22b for the scenario with 800 vehicles per hour. If vehicle demand increases, pedestrian requests are more likely to conflict with existing vehicle reservations. In these situations, pedestrian priority needs to be granted more often. In situations with frequent pedestrian requests, the minimum "green phase" for vehicles, that increases with increasing values of Θ_{ped}, needs to be respected. Therefore, the SlotIIC with larger values of Θ_{ped} can handle more vehicles, but leads to larger average waiting times in scenarios with heavy vehicle and pedestrian demand. In comparison to the fixed-cycle setup shown in Figure 3.20, vehicle capacity can be increased while providing a comparable pedestrian LOS. Even though pedestrian demand with 200 pedestrians per hour per leg is relatively high, the scenario with 2,400 vehicles per hour is now feasible with an average vehicle delay of 29.7 seconds applying a maximum pedestrian waiting time Θ_{ped} of 42 seconds. As shown in Figure 3.22a, all SlotIIC scenarios presented there outperform the fully actuated TSC that is also shown in the figure. It needs to be noted that the situation could look different if diagonal crossing was allowed and requested. However, it is also conceivable that pedestrians wanting to cross diagonally will have to cross two consecutive crosswalks as it is usually the case at today's signalized intersections. An approach with explicit consideration of double-crossing will briefly be described in Section 3.8.

Conclusion

The SlotIIC approaches with pedestrian integration allow for balancing vehicle delays and pedestrian waiting times by setting suitable cycle times or maximum pedestrian waiting times.

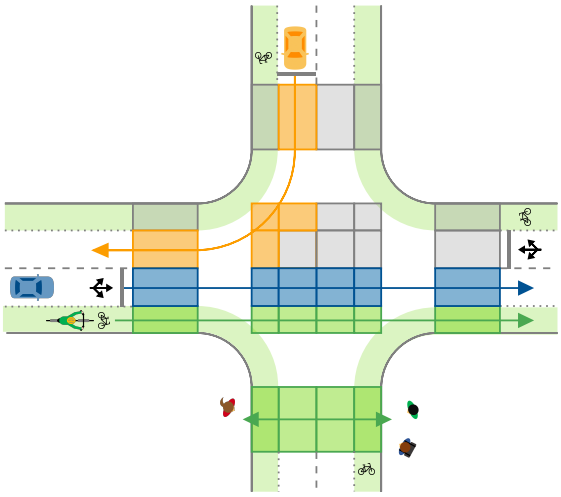

Figure 3.23: Intersection considered in the presented scenarios.

Demand on each approach	(bic/h)
Symmetric Scenario x	$0.25 \cdot x$
Turning ratios	$(\%)$
Through movement	75%
Left	10%
Right	15%

Table 3.7: Bicycle demand for the test scenarios.

The fixed-cycle setup can be used to obtain a first estimate of pedestrian waiting times and vehicle capacity on an analytical basis. The cycle times can then be transformed into maximum pedestrian waiting times for the demand-responsive setup. Depending on the demand at the intersection, the demand-responsive approaches can reduce both vehicle and pedestrian delays as compared to the fixed-time SlotIIC. With increasing vehicle and pedestrian demand, they converge to the fixed-time setup. A comparison of the different characteristics of the presented SlotIIC scheme (fixed-time as well as demand-responsive with and without knowledge of pedestrian ODs) is shown in Table 3.6. The most suitable setup depends on available infrastructure and expected demand at the intersection. The most flexible control strategy provides the best LOS and was able to outperform the fully actuated TSC in the considered demand scenarios. More simulation results for different scenarios (including different cycle times and vehicle turning ratios) can be found in Niels, Mitrovic, Bogenberger, et al. [2019], and an extension of the approach for a larger intersection zone with pedestrian refuge islands will briefly be presented in Section 3.8.

3.7.5 Results for Scenarios with Vehicles and Bicyclists

The integration of bicyclists follows the same overall concept as the integration of pedestrians. This especially applies to the integration of green phases in fixed cycles, which has been discussed in detail in the previous section. The evaluation presented in this section will hence be condensed and focus on the demand-responsive integration of bicyclists. More scenarios with vehicles and bicyclists are presented in Niels, Bogenberger, et al. [2020].

Demand-responsive Integration of Bicyclists

The intersection shown in Figure 3.23 is simulated in this section. It features a bicycle lane on each approach, and a separate phase is implemented for each turning movement. Vehicle demand in this evaluation is equal to the previous scenarios and, as shown in Table 3.7, the

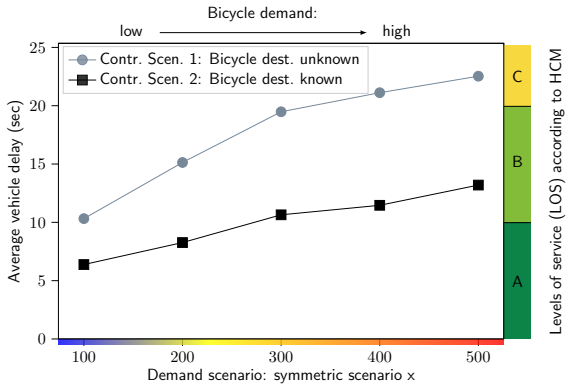

(a) Avg. vehicle delay depending on bicycle demand.

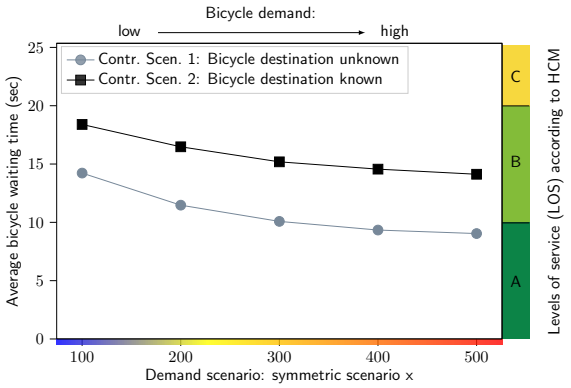

(b) Avg. bicycle delay depending on bicycle demand.[1]

Figure 3.24: Comparison of average vehicle delays and bicycle waiting times for the two different demand-responsive strategies and an increasing bicycle demand.

considered bicycle demand follows the same distribution. If bicycle arrivals at the intersection can be detected, the respective green phases can be scheduled on demand. In the demand-responsive setup evaluated here, bicycle detectors are assumed to be placed at a distance of 50 meters from the entrance to the intersection zone. Assuming a mean speed of 5.2 meters per second (almost 19 kilometers per hour), the expected arrival time t_{bic}^{min} of bicyclist bic at the traffic signal is calculated. For the reservation of conflict cells, a maximum bicycle speed of 8.3 meters per second (approximately 30 kilometers per hour) and a minimum speed of 2.7 meters per second (approximately 10 kilometers per hour) are assumed. As has been shown in Figure 3.15, the cells that bicyclists will cross need to be blocked for the time span between an assumed fast cyclist crossing the stop bar at the beginning of a green phase and an assumed slow cyclist starting at the end of the green phase. Again, assumed minimum and maximum speeds are more restrictive than in the German guideline RiLSA [FGSV, 2015b], because vehicles enter the intersection at a larger speed than in conventional TSC scenarios. More details on bicycle behavior modeling will be provided in Chapter 5.

The two different demand-responsive scenarios displayed in Figure 3.16 are simulated in this section. In the first scenario, destinations of approaching bicyclists are unknown. When approaching bicyclists cross the detector, green phases for both turning movements are requested, i.e., almost the entire intersection will be reserved for them (compare Figure 3.16a). In the second scenario, it is assumed that bicycle destinations are known. Bicyclists then only request a green phase for one particular turning movement or, if they want to turn right, none at all (compare Figure 3.16b). Similarly to that of the pedestrian signals, the minimum green phase for bicyclists in the following scenarios is 5.4 seconds, and bicycle signals remain green if the respective conflict cells are not reserved by vehicles.

[1] Average bicycle delay is calculated considering only through movement and left-turning movement. Due to the RToR policy, right-turning bicyclists do not need to wait.

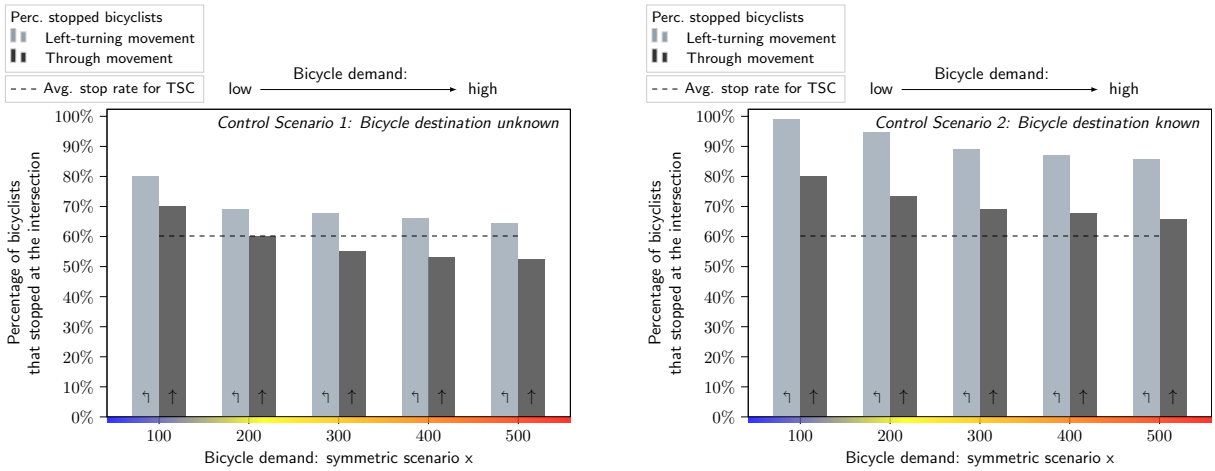

(a) Bicycle destination unknown.

(b) Bicycle destination known.

Figure 3.25: Percentages of stopped bicyclists for the two demand-responsive scenarios.

Figure 3.24 shows average vehicle delays and bicycle waiting times for the two different scenarios with a maximum bicycle waiting time Θ_{bic} of 42 seconds. The vehicle demand scenario x=2,000 with 500 vehicles per hour on each approach is simulated. Bicycle demand is increased as shown on the x-axis of the figures. As can be seen in Figure 3.24a, vehicle delays increase with increasing bicycle demand, because green phases for bicyclists are scheduled more frequently. Clearly, reserving both turning movements for bicyclists with each request occupies more intersection space. Therefore, vehicle delays are larger in this scenario. On the other hand, average bicycle delays are shorter in the scenario where both turning movements are reserved. This is because the reservation of almost the entire intersection for one bicyclist is beneficial for other bicyclists, too. First of all, bicyclists coming from the same direction at the same time do not have to request their own signal phase, independently of their intended turning movement. Additionally, bicyclists from other directions can also profit. As an example, a green phase for all bicyclists coming from the west (i.e., the situation shown in Figure 3.16a) allows for a northbound bicyclist approaching from the south to cross as well.

Additionally, average bicycle delays decrease with increasing bicycle demand, because arriving bicyclists benefit from other bicyclists already having requested a green phase (see Figure 3.24b). This is different from the pedestrian waiting times presented in Figure 3.21b, because the setup explained in Section 3.5 gives almost immediate priority to pedestrians if vehicle movement has been allowed in the intersection for some time. All in all, bicycle waiting times fall into LOS category A or B for all evaluated scenarios.

Figure 3.25 shows the percentages of stopped bicyclists at the intersection distinguished between through movement and left-turning movement. Figure 3.25a shows results for the control scenario without knowledge on bicycle destinations (Control Scenario 1), and Figure 3.25b displays the results for OD-specific green phase requests (Control Scenario 2). First of all, it can be seen that, even though bicyclists are detected before they arrive at the intersection, the majority of them needs to stop. Scenario 1 allows more bicyclists to pass without

stopping than Scenario 2, and left-turning bicyclists are more likely to stop than bicyclists going straight. Bicyclists going straight benefit from having fewer conflicts, and they can often pass together with parallel vehicle through movement such that vehicles do not necessarily have to be rescheduled. By contrast, a left-turning bicycle movement almost always needs to request priority in a scenario with rather large vehicle demand. In the scenario with x=100 bicyclists per hour, there are 25 bicyclists on each approach of which (on average) 2.5 want to turn left.

Regarding these few left-turning requests and the large vehicle demand at the intersection, it is conceivable that 99 % of left-turning bicyclists need to stop in Control Scenario 2. By contrast, in Control Scenario 1, all 25 bicyclists per hour per approach are assumed to possibly turn left, and their requests will also help bicyclists coming from other directions. With a larger share of left-turning bicyclists, the two control scenarios will hence look more alike. If few bicyclists turn left, however, Control Scenario 2 can be the better choice to balance delays. Considering the scenario with a bicycle demand of x=500 bicyclists per hour, average vehicle and bicycle delays are similar under Control Scenario 2 (approximately 13 seconds for vehicles and 14 seconds for bicyclists as shown in Figure 3.24). At the same time, it is questionable whether the direct left turns actually lead to an improvement for bicyclists here. The average delay of bicycle through movements in this scenario is 13 seconds; left-turning bicyclists wait 22 seconds on average. Requiring left-turning bicyclists to cross in two steps while at the same time implementing more frequent green phases for through movement could be beneficial for all bicyclists and still leave enough room for vehicle movement.

Overall, the demand-responsive integration of bicycle green phases shows promising results with respect to both vehicle delays and bicycle waiting times, but bicycle stops are not reduced as compared to a fixed-time TSC, at least for bicycle through movement. Figures 3.25a and 3.25b additionally show the analytically calculated average stop rate for bicycle through movement at a fixed-time TSC with a cycle time of 90 seconds and a green phase of 38 seconds in each cycle as a dashed line. Control Scenario 1 performs similar to the TSC, and Control Scenario 2 even increases the percentage of stopped bicyclists. This situation could possibly be improved by providing a stricter priority to bicyclists, i.e., strictly decreasing maximum bicycle waiting times, which would in turn affect vehicle delays and vehicle capacity. Additionally, countdown timers and GLOSA applications could inform bicyclists about their scheduled green phases and mitigate stops. However, the discussion should take into account that the bicycle arrivals at the intersection are not realistically distributed in this comparison. The simulation considers an isolated intersection with Poisson-distributed arrivals of bicyclists. If bicyclists instead arrive in flocks (starting at adjacent intersections during the respective green phases), these flocks could be assigned to cross the intersection together – possibly reducing bicycle stops. The consideration of surrounding intersections (that could be assumed to also be equipped with detection infrastructure) would additionally allow for an earlier estimation of bicycle arrivals. This would also be beneficial when planning green phase durations. While increasing bicycle demand helps bicyclists to pass the intersection without stopping, queues can occur if demand is increased further and more bicyclists are assigned to the same signal phase. In these situations, green phase durations would have to be extended.

Conclusion

The SlotIIC approaches with bicycle integration use similar mechanisms to balance vehicle delays and bicycle waiting times as the previously presented strategies with vehicles and pedestrians. Bicycle delays are successfully bounded and resulting LOS are satisfactory, but, even though bicyclists are detected before they arrive at the stop bar, results show that the majority of them need to stop at the intersection. The consideration of surrounding intersections could provide (i) more realistic arrival patterns of bicyclists at the considered intersection zone, and (ii) the possibility to provide a green wave for bicyclists that cross several consecutive intersections and travel at a common average speed. This will be further analyzed in Chapter 4.

In the following, an extension of the SlotIIC approach for vehicles and pedestrians to larger intersections is demonstrated before the chapter is summarized in Section 3.9.

3.8 Extension to Intersection Zone with Several Vehicle Lanes

The SlotIIC approaches can also be adapted for larger intersections with multiple lanes coming from each direction. In order to apply the control at the intersection displayed in Figure 3.26, two extensions need to be made to the approaches presented so far. The first extension applies to the vehicle scheduling policy, the second extension integrates pedestrian refuge islands into the approach. These two extensions will briefly be explained in Sections 3.8.1 and 3.8.2. A snapshot of the results will be presented in Section 3.8.3. Details can be found in Niels, Mitrovic, Dobrota, et al. [2020].

3.8.1 Extension of the Scheduling Policy for Vehicles

At multi-lane intersections that can currently be found in the field, the assignment of turning movements is relatively restricted. At an intersection such as the one shown in Figure 3.26, turning movements are usually only allowed from the rightmost or leftmost lane. Additionally, left-turning movements are often assigned an exclusive lane, because the movement is either assigned a separate phase (if the movement is protected) or vehicles need to wait for oncoming traffic (if the movement is permitted). While this kind of lane assignment improves the safety and efficiency at signalized intersections, it can be relaxed in the SlotIIC scenario. In this scenario, vehicles can, in principle, perform any turning movement coming from any lane as long as all cells that they pass on their way are reserved for them. Allowing the controller to assign each vehicle with an entry lane gives the controller more flexibility, especially in combination with the activation of pedestrian crosswalks. For example, if the crosswalk on the southern leg is activated (as shown in Figure 3.26), then the right-turning vehicles coming from the west need to slow down, and other movements can be assigned to the remaining lanes. If there are a lot of left-turning movements, both remaining lanes can be used to perform turning movements in parallel (similarly to the right-turning vehicles coming from the north in Figure 3.26). Nevertheless, it is generally preferable that left-turning vehicles use the leftmost lane and right-turning vehicles use the right lane. As can be seen for the marked right-turning

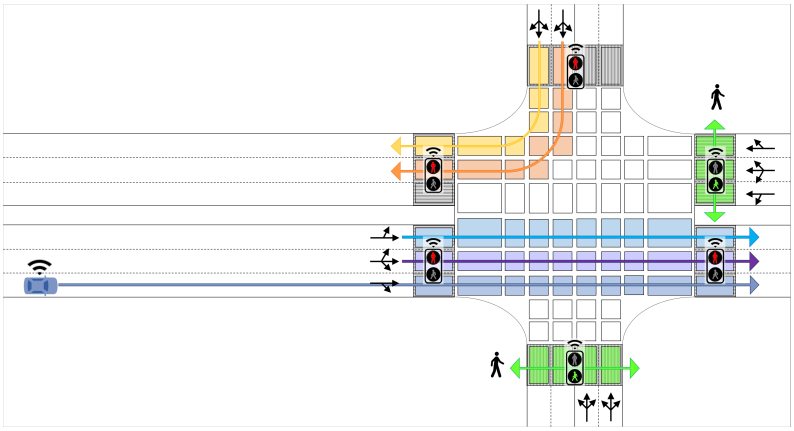

Figure 3.26: Intersection layout of a larger intersection with several vehicle lanes on each approach and pedestrian refuge islands on the major road. Illustration based on figure in [Niels, Mitrovic, Dobrota, et al., 2020].

movements in Figure 3.26, turning movements from other lanes lead to a greater number of cell reservations and longer intersection crossing times.

The overall scheduling approach for the intersection follows the FCFS scheme introduced in Section 3.4 with the difference that the controller compares the availability of the required cells and computes feasible arrival times for all possible lanes that the vehicle could use to enter the intersection. For the blue vehicle in Figure 3.26, for example, the controller will compute three different cell occupancies and arrival times, assuming that the vehicle can enter the intersection from all three eastbound lanes. Only one lane and the respective arrival time is then assigned to the vehicle. In order to avoid unnecessary lane changes, vehicles are assigned to a different lane than the one they are currently in only if the lane change improves their travel time by at least a pre-defined threshold. A different rule applies to turning vehicles: the controller usually assigns them to their traditional turning lane (left- or rightmost lane, respectively), and deviates from this default assignment only if this reduces their delay by more than the defined threshold.

Due to computational complexity, the intersection controller does not compute a complete trajectory for every vehicle including possibly necessary lane changes. Instead, the controller informs each vehicle veh about their assigned arrival time $\hat{t}(veh)$ and, additionally, about the lane $\hat{l}(veh)$ that they shall use for entering the intersection and their assigned leader and follower vehicle. By considering necessary time gaps between vehicles entering the intersection from the same lane, the control implicitly makes sure that there is room on the lane that vehicle veh is assigned to. Vehicles then cooperate on the approach to the intersection to make sure that necessary lane changes can be performed. In particular, they follow a protocol for adjusting their trajectories that includes sharing positions and speeds with surrounding vehicles. The interested reader is referred to Niels, Mitrovic, Dobrota, et al. [2020] for more details.

3.8.2 Consideration of Pedestrian Refuge Islands

In order to integrate pedestrians into the control, the previously presented approaches are adapted in such a way that pedestrian refuge islands are considered and pre-defined maximum waiting times are still not exceeded. As can be seen in Figure 3.26, pedestrians who want to cross the major road need to reserve two consecutive crosswalks that are separated by a median refuge island. These two parts are reserved individually, and waiting times for pedestrians can occur both before crossing the street and when reaching the median refuge island. In this approach, the following two constraints hold: (i) the green phase at the second crosswalk that pedestrian ped needs to pass shall not start before pedestrian ped has crossed the first crosswalk, and (ii) the sum of waiting times experienced by pedestrian ped shall not exceed the maximum acceptable waiting time Θ_{ped}. This approach is further extended to integrate pedestrians who want to cross to the diagonally opposite corner and thus need to reserve three consecutive crosswalks.

Again, vehicles need to be rescheduled if pedestrians are given priority. The rescheduling of vehicles in the setup with several lanes is more complex due to the number of involved vehicles and the necessary lane changes. In order to avoid vehicle rescheduling, the overall pedestrian integration approach is improved. Instead of scheduling pedestrian green phases after the fixed time spans of the reaction time θ required by the controller or the maximum pedestrian waiting time Θ_{ped}, the number of pedestrian-vehicle conflicts is calculated for all different time slots that the pedestrian green phase could be assigned to. Among all those feasible time slots, the one with the minimum number of conflicts is chosen.

3.8.3 Simulation-based Evaluation

Similarly to the previously presented scenarios, the control was tested against a fully actuated TSC setup using the microsimulation platform aimsun.next in combination with its API and Python for a set of sixteen different scenarios (comprised by the combination of four different levels of vehicle demand and four different levels of pedestrian activity). Maximum pedestrian waiting times in the SlotIIC approach were defined such that the resulting pedestrian LOS was comparable to results obtained from the TSC. The vehicle delays resulting from the presented SlotIIC approach were significantly lower than vehicle delays in the TSC scenario in three out of four evaluated vehicle demand scenarios. However, integrating pedestrian activities into the SlotIIC approach with a very large vehicle demand exceeded intersection capacity. In these scenarios, the TSC setup showed better results.

3.8.4 Conclusion

The approach shows that the presented SlotIIC scheme can be extended and applied at larger intersections with several lanes on each approach with promising results. Nevertheless, it has already been suggested by some researchers that FCFS controls are most beneficial in rather low to medium demand scenarios and can be problematic for high demand levels, because they tend to assign the right of way in alternating order without taking advantage of platoon formation [Levin, Boyles, and Patel, 2016]. A similar effect was shown here. This could

be overcome by applying more sophisticated scheduling algorithms such as the ones presented in the next chapter. More details and results regarding the presented approach can be found in Niels, Mitrovic, Dobrota, et al. [2020], and a video of the control is available via Niels, Mitrovic, Dobrota, et al. [2019].

3.9 Summary

The SlotIIC strategies presented in this chapter show that it is possible to integrate pedestrians and bicyclists into AIM – both with fixed cycles and in a demand-responsive way. The control strategies are designed following the conceptual decisions justified in Section 3.1 and fulfill the overarching goal of designing a **multimodal** AIM scheme. Different strategies were presented that can be applied to intersections with or without VRU detection equipment. All presented strategies require the reservation of conflict cells by vehicles and VRU signal groups, and ensure the strict separation of vehicles and VRUs within the intersection zone. Conflicts involving vehicles are hence resolved by the control which makes the setup **safe by design**.

The presented approaches can compete with traffic signals regarding **efficiency**. The direct comparison of the vehicle-only FCFS control showed a significant decrease in delays and increase in capacity as compared to two common TSC setups (Figure 3.19b), at least for a small intersection zone without separate turning lanes. In the multimodal scenarios, vehicle capacity is reduced according to the portion of time that is dedicated to VRU movement. When implementing a VRU service quality that is comparable to today's traffic signals, vehicle delays are shorter than in the TSC setup for demand scenarios with low to medium vehicle demand. The TSC can even be outperformed for scenarios with large vehicle demand if pedestrians are integrated in a demand-responsive way (compare Figure 3.22). Nevertheless, in scenarios with large vehicle demand, the alternating right-of-way assigned by the FCFS-based vehicle control can be inefficient. At the larger intersection shown in Section 3.8, the TSC setup shows a better performance in multimodal scenarios with very large vehicle demand. In the next chapter, the scheduling approach will be further improved.

The strategies can be modeled in a VRU-friendly way and guarantee that pre-defined maximum waiting times are not exceeded for pedestrians and bicyclists. Setting suitable upper bounds on VRU waiting times allows for **balancing** delays of different road users at the intersection. The determination of suitable upper bounds can be obtained by analytical calculations assuming a fixed-cycle integration of VRUs. In the demand-responsive setup, the guarantee of limited waiting times is obtained by overwriting (pre-)assigned vehicle arrival times. If a VRU signal phase needs to be scheduled that interferes with existing vehicle reservations, vehicles loose their assigned time slots for crossing and new reservations are requested for them. In principle, the **integration of policies** and prioritization of individual road users can be implemented in a similar way. However, the repeated overwriting of (pre-)assignments leads to a complex structure of rules. Additionally, different road user priorities cannot be balanced in a comprehensive way. Instead, the overwriting of existing assignments implies an absolute priority of the newly requested movement. Therefore, in the next chapter, an optimization-based approach is implemented that enables the integration of policy goals via the objective function.

Requirement	Evaluation	
Multimodality	✓	Pedestrians and bicyclists are integrated into the control strategy.
Safety by Design	✓	Only fully protected movements are allowed – except for conflicts without the involvement of motorized vehicles.
Efficiency	(✓)	The LOS improvements depend on the considered control strategy and on the level of demand. While the strategies outperform traditional traffic signal control in most of the scenarios, it is assumed that efficiency can further be improved by including optimization techniques.
Balance	✓	In general, FCFS is presumed to be fair. Additionally, waiting times for pedestrians and bicyclists can be bounded.
Policy Integration	✗	Policies (other than limiting maximum VRU waiting times) cannot easily be integrated.
Demand Responsiveness	✓	The control is able to respond to current demand.
Low-Tech	✓	The simplest control strategies work even without knowledge about VRU activity. The performance can be improved with detection of VRUs at the intersection.
Heterogeneity	(✓)	Including heterogeneous vehicles with various dimensions and speeds would be possible by adjusting the reservation of space-time. However, the discrete space and especially the discrete time slots are inconvenient for such a setup.
Transferability	(✓)	The control schemes can be applied to different intersection zones, including those with several lanes on each approach and pedestrian refuge islands. However, a lot of manual work is needed to set up the conflict cells for each individual intersection, especially for possible non-symmetric layouts in real world scenarios.

Table 3.8: List of requirements and their evaluation regarding the SlotIIC strategies.

The presented strategies work with and without knowledge about VRU activity, depending on the applied scenario. As discussed in Section 3.7, the **demand-responsive** integration of VRU phases (if suitable detection measures are available) can increase the efficiency of the control. In either scenario, VRUs are not required to be connected to the infrastructure, such that the strategies can be considered to be **low-tech**. Additionally, the rule-based nature makes the strategies easy to understand and they can be implemented without the necessity of solving an optimization problem such that computation times are not an issue.

In the presented setup, all vehicles are homogeneous, i.e., they have identical dimensions, desired speeds, and kinematic limitations. This implies that each vehicle movement through the intersection has exactly one space-time pattern that needs to be reserved (compare Figure 3.10), which makes it easy to understand and implement. In principle, vehicles of different dimensions and intersection crossing speeds could be considered as well. However, in that

case, the controller needs to develop an individual pattern for each vehicle, which requires a lot of effort. Additionally, the combination of heterogeneous vehicles with discrete time slots implies that not all safety gaps will be equally large. For example, the headway between two vehicles entering the intersection must always be a multiple of the considered time step. In the approaches presented in this chapter, the time step was 0.6 seconds, the vehicle length was 4 meters, and the speed for crossing the intersection was 30 kilometers per hour (approximately 8.3 meters per second). Assuming that a minimum time gap of 0.7 seconds needs to be respected, vehicles can enter the intersection with a headway of at least two time steps (1.2 seconds).[1] If the front vehicle is longer, the gap resulting from a 1.2 second-headway will quickly fall below the minimum gap. Therefore, a headway of 1.8 seconds (three time steps) would have to be required. Small deviations in vehicle size could thus lead to a rather inefficient setup. This could only be overcome by a significant reduction in time step size which, in turn, would further increase the complexity of the approach. All in all, **heterogeneity** cannot easily be implemented in the presented strategies. In order to overcome the described difficulties, both intersection modeling and time frame will be changed from discrete to continuous in the next section. This will also improve transferability. As explained in Section 3.8, the concept can be extended to more general intersection zones and is hence **transferable**. However, the division into discrete cells has to be considered for each intersection zone individually and cannot intuitively be derived from the pure intersection geometry. Therefore, a conflict-point based approach is proposed in the next chapter.

Table 3.8 gives a short summary of the evaluation of the presented strategies regarding each of the requirements defined in Section 1.2. To sum up, the strategies presented in this chapter are very promising, since VRUs can be integrated into the control in a demand-responsive way and results in most scenarios are satisfactory. They thus provide a first answer to Research Question 1: *"How can pedestrians and bicyclists be integrated into automated intersection control in a safe and efficient way?"* On the other hand, the overall setup including the rigid conflict cell partitioning, the discretization of time, and the rule-based character of scheduling algorithms implies several limitations, and the control cannot fulfill all requirements defined in Section 1.2. All in all, the results are encouraging to further refine the strategies which will be done in the next chapter.

[1] $gap\,[\mathrm{sec}] = headway\,[\mathrm{sec}] - \frac{length(front\ vehicle)\,[\mathrm{m}]}{speed\,[\mathrm{m/sec}]} = 1.2\,\mathrm{sec} - \frac{4\,\mathrm{m}}{8.3\,\mathrm{m/sec}} = 0.72\,\mathrm{sec}$

Chapter 4

Optimization-based Integrated Intersection Control Strategies

This chapter extends the approaches presented in Chapter 3 and develops new optimization-based integrated intersection control (OptIIC) approaches to overcome the limitations of the SlotIIC methods. The chapter roughly follows the same structure as Chapter 3, but focuses on those parts where new concepts are implemented: in particular, the intersection is modeled with a more flexible conflict point-based concept instead of fixed cells, the discretization of time is relaxed, and the scheduling policy is improved. The main new contributions will be the increased flexibility resulting from the consideration of continuous space and time, the enhanced efficiency by including optimization, and the possibility to integrate policy objectives. Additionally, bicycle movement will be analyzed taking adjacent intersections into account. Section 4.1 presents the overall control architecture and the communication protocol. The intersection modeling and identification of conflicting movements is described in Section 4.2. Since the integration of optimization techniques increases the complexity, the multimodal scheduling policy is described in several sections: Section 4.3 provides background on the considered optimization problem and defines the objective function. Section 4.4 explains the optimization problem for vehicle-only scenarios and Section 4.5 explains the corresponding rolling horizon framework. The integration of VRUs into the scheduling policy is explained in Section 4.6. Finally, Section 4.7 presents the simulation-based evaluation of presented concepts at a symmetric intersection zone. The chapter is concluded with a summary in Section 4.8.

This chapter forms the basis for the following Chapter 5 which presents the simulation-based evaluation of the control strategies considering a real intersection zone with realistic multimodal demand. While Chapter 4 presents theoretical thoughts and introduces the important parameters and their effects on the performance measures, Chapter 5 focuses on the simulation setup and on the applicability in a realistic scenario.

4.1 Traffic Coordination

The traffic coordination concept applied in the OptIIC strategies remains unchanged from the previously presented SlotIIC strategies. This can be seen in Figure 4.1, where the overall control architecture is displayed. Again, a centralized intersection controller schedules all arriving vehicles and the green phases of the pedestrian and bicycle signalization. The figure also

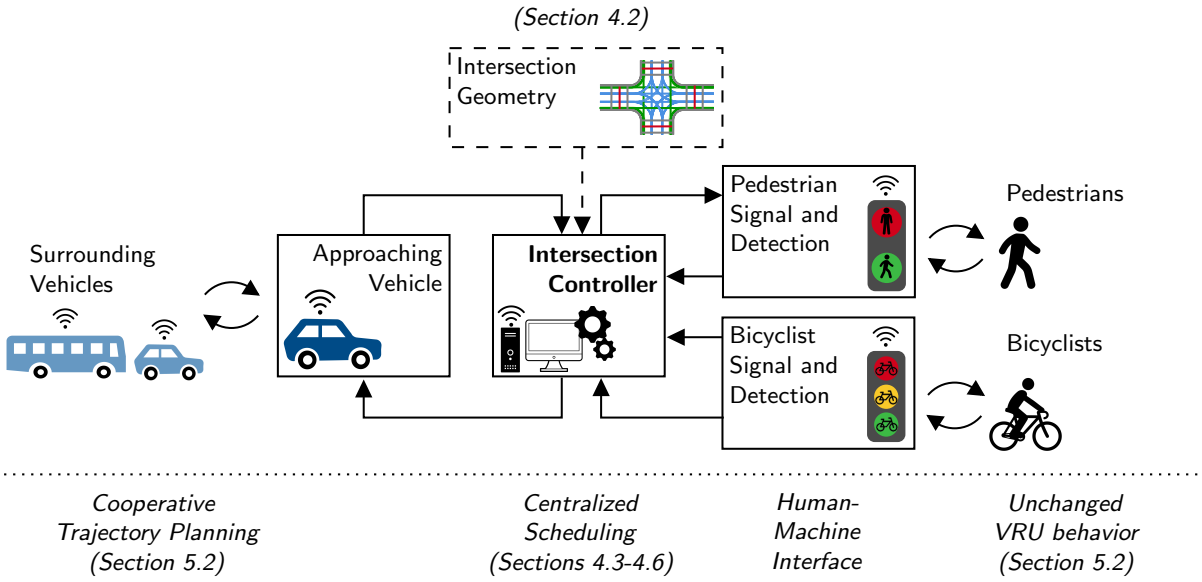

Figure 4.1: Intersection control architecture.

indicates the sections in which each part of the signal control is explained in detail (except for the HMI, which has been motivated in Section 3.1).

First of all, the intersection geometry is handed to the intersection controller as a static input. It contains information about paths and conflict points within the intersection zone and the lengths and speed limits of its approaches. This information is needed by the intersection controller to inform vehicles and resolve conflicts. The modeling of the intersection geometry is described in Section 4.2.

4.1.1 Coordination of Approaching Vehicles

Approaching vehicles communicate directly with the intersection control as shown in Figures 4.1 and 4.2. Since a larger degree of flexibility is considered here in comparison to the approaches presented in Chapter 3, more information is exchanged. In particular, vehicles can have different dimensions, they can cross the intersection at their preferred speed, and they can be prioritized based on the implemented control policy. The intersection controller first provides the approaching vehicles with the static information needed to plan their trajectory, such as the exact geographic position of the entrance to the intersection zone, relevant speed limits, and turning radii. With this information, vehicles can derive their earliest possible arrival time at the entrance to the intersection zone depending on their current position and speed, and on their kinematic limitations. This information is needed in order to assign a feasible time slot for the vehicle and to calculate the vehicle's delay. In order to simplify the control, it is assumed that vehicles maintain a constant speed throughout crossing the intersection. With the information about turning radii, vehicles can decide on their comfort speed for their intended turning movement. Current vehicle position, earliest arrival time, and desired turning movement and speed are passed to the intersection control along with the vehicle dimensions

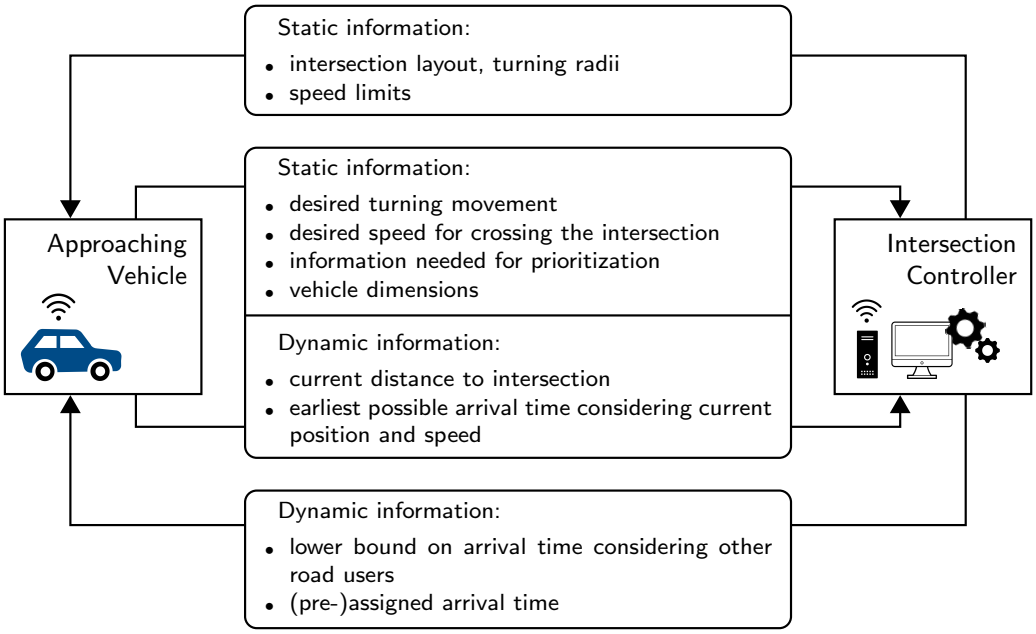

Figure 4.2: Information that is exchanged between approaching vehicles and the intersection controller.

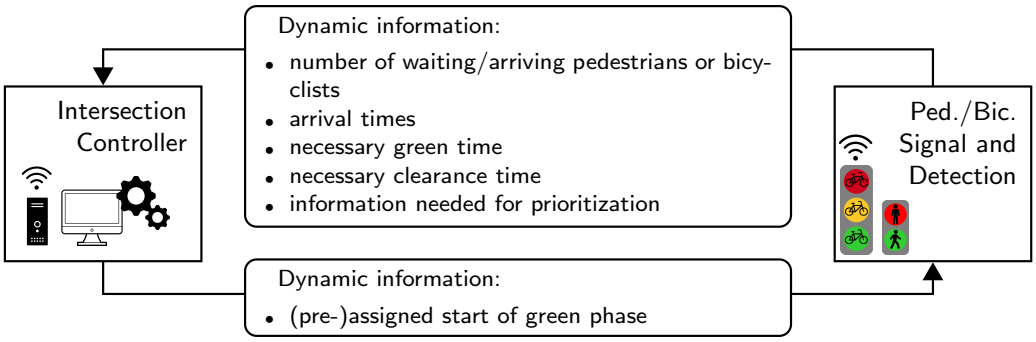

Figure 4.3: Information that is exchanged between the intersection controller and the pedestrian/bicyclist signalization.

and the information needed to determine the prioritization factor of the vehicle. This information depends on the implemented policy, but might include vehicle type (e.g., passenger vehicle, bus or emergency vehicle), occupancy, and fuel type, among others.

The controller processes all information obtained by vehicles and infrastructure. On the approach to the intersection, each vehicle keeps the controller updated about whether the earliest possible arrival time at the intersection has changed. It has to be noted that this arrival time is an ego perspective of the vehicle without considering other road users. On the other hand, the intersection control entity returns to the vehicle a lower bound on its scheduled arrival time that considers other previously scheduled road users. Additionally, the intersection controller returns a pre-assigned arrival time to the vehicle that can be subject to change, if for example a prioritized vehicle with a conflicting path appears. If the vehicle arrival

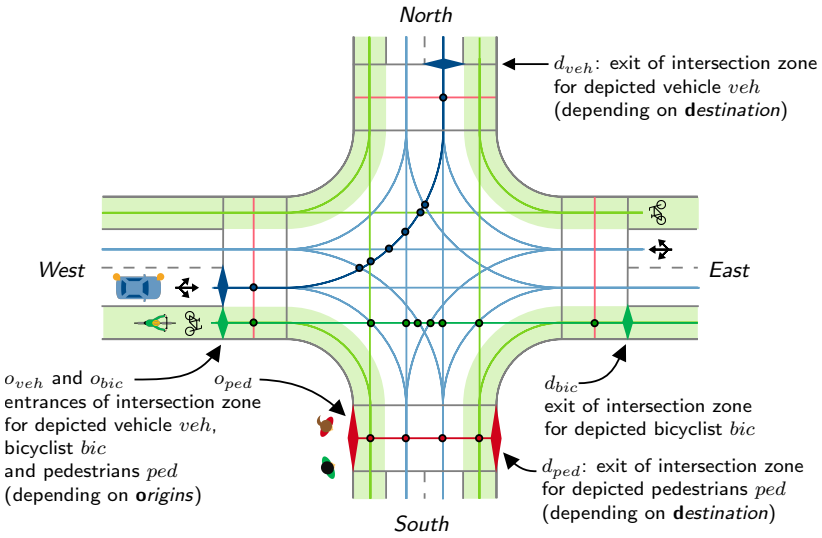

Figure 4.4: Intersection modeling showing possible conflict points and entrance and exit points of different road users.

time has been fixed, the assigned arrival time is sent to the vehicle. The vehicle adjusts its speed on the approach to the intersection zone individually while making sure that it arrives at the intersection zone with the pre-defined speed. The information that is exchanged between vehicles and intersection controller can be seen in Figure 4.2.

4.1.2 Coordination of Pedestrians and Bicyclists

As described previously, pedestrians and bicyclists are not generally required to be connected to the infrastructure. They are detected by suitable detectors and are assumed to cross the intersection together when given the right of way. In principle, optimization-based vehicle scheduling could be combined with fixed cycles for VRU movement, similar to the fixed cycle approach in Chapter 3. However, in order to explore the full potential of optimization-based integrated control, pedestrian and bicycle signal phases will be scheduled on demand in this chapter. In order to do so, the intersection controller receives information about waiting or approaching VRUs from the infrastructure, as well as necessary green times, clearance times, and information that is needed for prioritization. The communication between the intersection controller and VRU detection and signal infrastructure is displayed in Figure 4.3.

4.2 Intersection Modeling

The intersection model is needed by the controller to identify and resolve conflicts between different road user movements. Instead of dividing the intersection into a fixed set of discrete tiles as described in Chapter 3, a more flexible approach is applied here. This will facilitate the integration of heterogeneous road users and improve the transferability to other intersection layouts. Equivalently to the previous chapter, all road users are assumed to roughly travel through the intersection along predefined paths. Having these paths at hand, conflict points

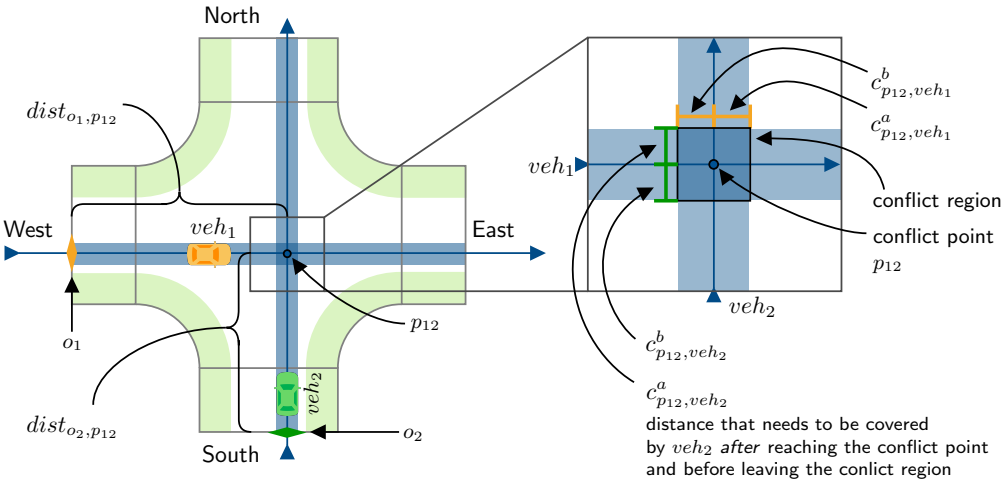

Figure 4.5: Example calculation of conflict region.

between merging, diverging and crossing movements can be determined. A similar determination of conflict points takes place when planning current signalized intersections [FGSV, 2015b].

An example intersection zone is shown in Figure 4.4. The figure shows all possible paths for vehicles (blue), bicyclists (green), and pedestrians (red), and displays conflict points for selected movements. For reasons of simplicity, the intersection does not feature direct left-turning for bicyclists or diagonal crossing for pedestrians, but the determination of conflict points for these movements would be straight-forward. The diamond shapes display entrance and exit points for the depicted example vehicle veh, bicyclist bic and pedestrians ped. Distances between the entrance points to the intersection and relevant conflict points (always along the paths) are stored by the controller in a conflict matrix. Of course, a conflict point is not one-dimensional, but represents a conflict area, which is spanned by the overlap of conflicting paths, and depends on vehicle or lane widths. In the following, this is explained in more detail for the different possible conflicts: vehicle-vehicle conflicts are described in Section 4.2.1, and conflicts involving VRUs are described in Section 4.2.2.

4.2.1 Conflict Points and Conflict Regions for Vehicle-Vehicle Conflicts

Similarly to in the slot-based approach, vehicles' enhanced information and capability to follow pre-defined trajectories are used in this approach. In particular, (i) the turning maneuver of each vehicle is known beforehand, (ii) vehicles are assumed to exactly follow the path defined by entrance and exit lane, and (iii) vehicles are assumed to arrive at the entrance to the intersection at their assigned time and maintain a constant pre-announced speed from entering until leaving the intersection zone. Therefore, the time a vehicle arrives at a specific conflict point can be obtained from the intersection geometry, the predefined speed, and the time that the vehicle enters the intersection zone. Figure 4.5 shows the conflict point and corresponding conflict region for an example with two vehicles (veh_1 and veh_2). The origins

and destinations of vehicles veh_1 and veh_2 with respect to the current intersection zone (i.e., west-east and south-north) are denoted by OD_1 and OD_2. Let o_1 and o_2 be the points where vehicles veh_1 and veh_2 enter the intersection (derived from their ***origins***), and let p_{12} be their common conflict point as marked in the figure. The distances between intersection entrance points and conflict point are denoted by $dist_{o_1,p_{12}}$ and $dist_{o_2,p_{12}}$, respectively. The conflict between vehicles veh_1 and veh_2 does not only have to be resolved at this one-dimensional point, but the two movements span a conflict area. Given two conflicting ODs, the dimensions of the conflict area depend on the widths (wid_1 and wid_2) of involved vehicles as shown in the figure. The distance that vehicle veh_1 covers within the conflict area can be calculated as $c^b_{p_{12},veh_1} + c^a_{p_{12},veh_1}$, where $c^{\mathbf{b}}_{p_{12},veh_1}$ denotes the distance that vehicle veh_1 covers within the conflict region ***before*** reaching the conflict point, and $c^{\mathbf{a}}_{p_{12},veh_1}$ is the distance that vehicle veh_1 covers within the conflict region ***after*** passing the conflict point. As can be seen in the figure (on the right), the conflict region from the perspective of veh_1 hence starts at a distance of $dist_{o_1,p_{12}} - c^b_{p_{12},veh_1}$ and ends at a distance of $dist_{o_1,p_{12}} + c^a_{p_{12},veh_1}$ (from the entrance to the intersection). It is easy to see that the conflict region from the perspective of veh_2 can be calculated in a similar way. The dimensions of the conflict region and how they depend on the vehicle widths are stored in the conflict matrix along with the position of the conflict point.

Now, let $\hat{t}_1$ and $\hat{t}_2$ be the assigned arrival times of veh_1 and veh_2 at the intersection zone, that is, the front bumper of veh_1 arrives at o_1 and the front bumper of veh_2 arrives at o_2, respectively. Both vehicles travel at pre-defined speeds that remain constant until the vehicles leave the intersection zone. The time that veh_1 arrives at conflict point p_{12} within the intersection zone can then be calculated as $\hat{t}_{1,p_{12}} = \hat{t}_1 + \frac{dist_{o_1,p_{12}}}{\hat{v}_1}$, where $\hat{v}_1$ is the speed of veh_1 when crossing the intersection. The calculation of $\hat{t}_{2,p_{12}}$ is analogous. In order to separate vehicle movements, both vehicles should arrive at p_{12} with a sufficient time headway Δ^{min}_{12} to make sure that the first vehicle has left the conflict region before the second vehicle arrives, and a sufficient additional time gap δ^{min}_{12} is respected. This is shown with the following calculations. Let veh_1 be the vehicle that crosses p_{12} first in this small example. Then, the following needs to hold:

$$\hat{t}_{2,p_{12}} = \hat{t}_2 + \frac{dist_{o_2,p_{12}}}{\hat{v}_2} \tag{4.1}$$

$$= \overbrace{\hat{t}_2 + \frac{dist_{o_2,p_{12}} - c^b_{p_{12},veh_2}}{\hat{v}_2}}^{veh_2 \text{ enters the conflict region (see Figure 4.6a)}} + \frac{c^b_{p_{12},veh_2}}{\hat{v}_2} \tag{4.2}$$

$$\overset{!}{\geq} \overbrace{\hat{t}_1 + \frac{dist_{o_1,p_{12}} + c^a_{p_{12},veh_1} + len_1}{\hat{v}_1}}^{veh_1 \text{ has left the conflict region entirely (see Figure 4.6a)}} + \frac{c^b_{p_{12},veh_2}}{\hat{v}_2} + \delta^{min}_{12} \tag{4.3}$$

$$= \hat{t}_1 + \frac{dist_{o_1,p_{12}}}{\hat{v}_1} + \underbrace{\frac{c^a_{p_{12},veh_1} + len_1}{\hat{v}_1} + \frac{c^b_{p_{12},veh_2}}{\hat{v}_2} + \delta^{min}_{12}}_{=\Delta^{min}_{12} \text{ (minimum gap between } veh_1 \text{ and } veh_2 \text{ at } p_{12})} \tag{4.4}$$

$$= \hat{t}_{1,p_{12}} + \Delta^{min}_{12}, \tag{4.5}$$

where len_1 denotes the length of vehicle veh_1.

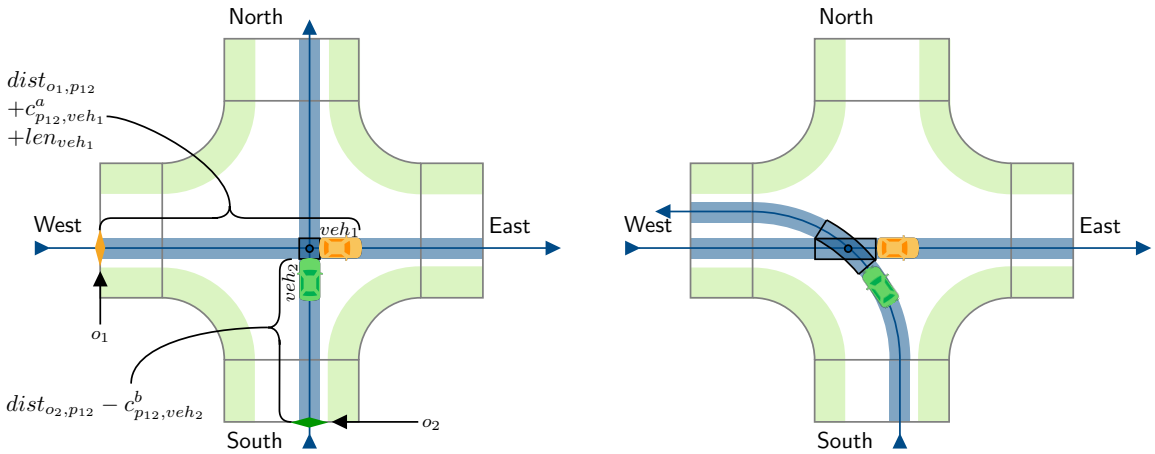

(a) Conflict situation shown in Figure 4.5.

(b) Other conflict situations can lead to a different extent of the conflict region.

Figure 4.6: Example illustration of different vehicle-vehicle conflicts.

It is easy to see that the size of the conflict region depends on how the vehicle paths overlap. The conflict region shown in Figure 4.6b is larger due to the involved turning movement and the angle at which the movements cross. Additionally, minimum headways depend on the lengths, widths, and speeds of involved vehicles. Therefore, for each pair of vehicles veh_i and veh_j, the minimum headways Δ_{ij}^{min} and Δ_{ji}^{min} need to be calculated individually, and Δ_{ij}^{min} does not necessarily equal Δ_{ji}^{min}. The formula for calculating Δ_{ij}^{min} for two vehicles with crossing conflicts can be derived from Equation (4.4):

$$\Delta_{ij}^{min} = \frac{c^a_{p_{ij},veh_i} + len_i}{\hat{v}_i} + \frac{c^b_{p_{ij},veh_j}}{\hat{v}_j} + \delta_{ij}^{min} \tag{4.6}$$

It can also be seen from these considerations that platooning is in fact efficient, at least if the minimum gap δ is not significantly larger for car-following situations than for crossing situations. The reason is that the "conflict region" in the car-following situation is one-dimensional, i.e., vehicle movements have to be separated *only* at one single point. As previously described in Figure 2.2, for veh_i and veh_j with $o_i = o_j$, the minimum headway Δ_{ij}^{min} can be calculated as $\Delta_{ij}^{min} = \frac{len_i}{\hat{v}_i} + \delta_{ij}^{min}$. The same holds for merging vehicles that come from different directions but have the same destinations. In car-following situations, special attention is required if the control allows different vehicle speeds within the intersection. In general, it can be assumed that vehicles going straight will cross the intersection at the maximum allowed speed, as it is currently the case if traffic conditions allow. Depending on the turning radii, the speeds of turning vehicles, especially right-turning vehicles, might differ. Now consider, for example, a vehicle that goes straight and merges behind a slower right-turning vehicle. The slower vehicle will be required to accelerate after leaving the intersection, and the necessary headway needs to be respected at the location where both are traveling at their final speed (instead of the location where their paths first meet). This location additionally depends on the acceleration rate of the slower vehicle. The situation is different if the slower right-turning vehicle follows

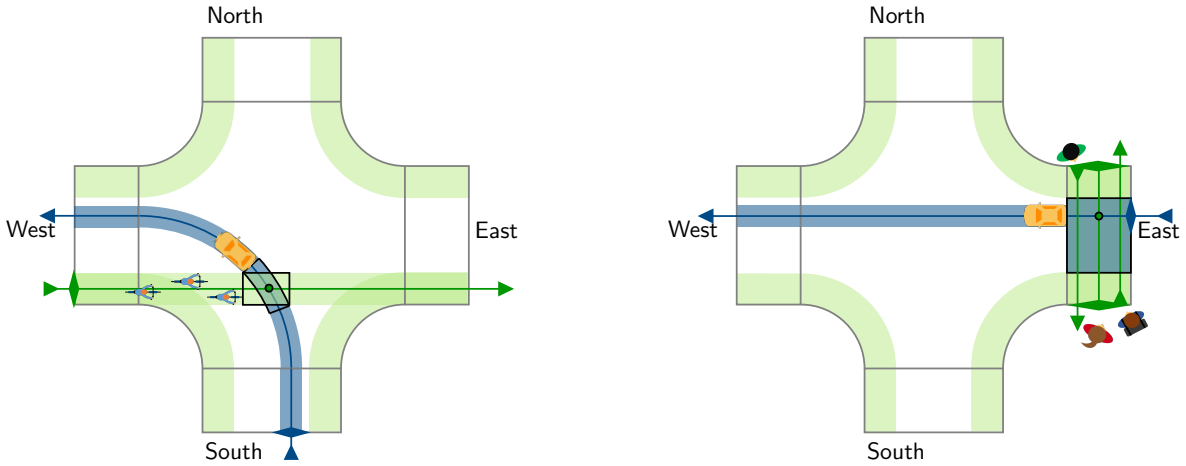

(a) Example illustration of vehicle-bicyclist conflict.

(b) Example illustration of vehicle-pedestrian conflict.

Figure 4.7: Example illustration of conflict points and conflict regions for vehicle-bicyclist and vehicle-pedestrian conflicts.

the faster vehicle: in this case, the conflict needs to be resolved at the location where their paths merge. For the sake of simplicity and in order for the scenarios to be comparable to the ones analyzed in Chapter 3, it is assumed that all vehicles will travel through the intersection at the same constant speed in this chapter. However, it can be seen that the integration of heterogeneous vehicle speeds within the intersection is rather easy in the described setup. Such heterogeneity will be explicitly considered in Chapter 5.

All in all, compared to the approaches presented in Chapter 3, the exact arrival times in the approaches presented here are continuous, and the conflict zones are not static, but are dynamically defined by individual conflicting movements. The same holds for conflicts involving VRUs, as will be described below. Section 4.4 explains how the minimum headways will be considered as constraints in the optimization problem.

4.2.2 Conflict Points and Conflict Regions for Conflicts Involving VRUs

Bicyclists and pedestrians are also assumed to (roughly) cross the intersection along predefined paths, at least within their specified lanes or the pedestrian crosswalks. Therefore, conflict points and regions of vehicle-bicycle and vehicle-pedestrian conflicts can be calculated similarly to the vehicle-vehicle conflicts described above. Figure 4.7 shows two examples. Similarly to what has been described in Chapter 3, the major differences are that the exact entrance times of pedestrians and bicyclists are not well defined (after their signal turns green, reaction times differ), and their speeds cannot be assumed to be constant and known beforehand. Additionally, several bicyclists and pedestrians are assumed to cross the intersection together during a green phase. Therefore, the calculation of necessary headways will take the green phase durations as well as minimum and maximum speeds of VRUs into account. In the following,

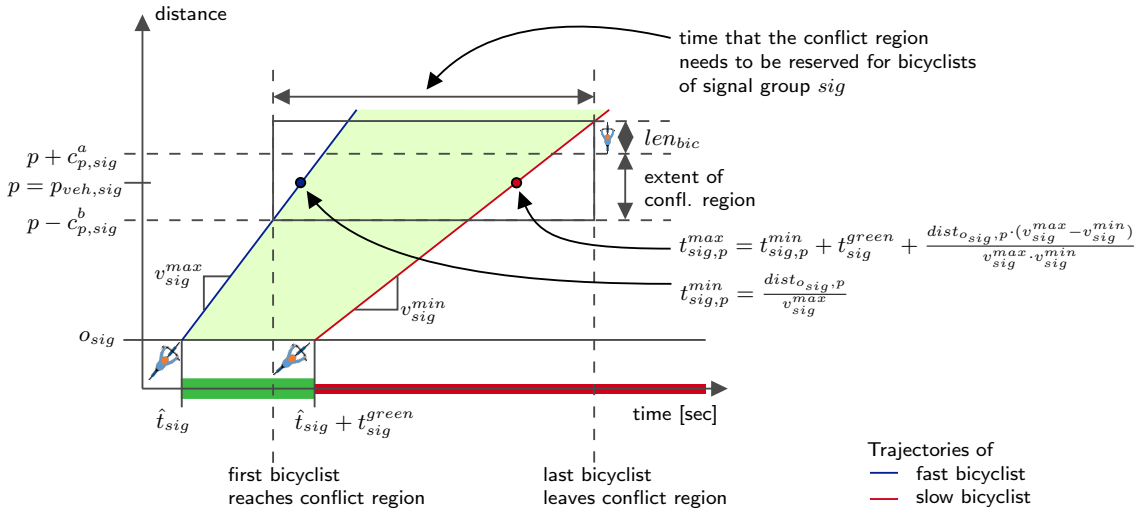

Figure 4.8: Example trajectories of bicyclists through the intersection and resulting time that a specific conflict region needs to be reserved for them.

bicycle-vehicle and pedestrian-vehicle conflicts are described in detail. As explained in Section 3.1, conflicts without the involvement of motorized vehicles are not explicitly modeled in this thesis.

Vehicle-Bicycle Conflicts

In principle, conflict points and regions for conflicting movements of vehicles and bicyclists are defined similarly to vehicle-vehicle conflicts, as shown in Figure 4.7a. The main difference is that $\hat{v}_{bic}$, i.e., a pre-defined speed for bicyclist bic, does not exist. Instead, the actual speed v_{bic} lies within a range of speeds from minimum assumed cyclist speed v^{min}_{bic} to maximum assumed speed v^{max}_{bic}. Additionally, as stated above, a group of bicyclists can cross the intersection together. Therefore, it would be inefficient to model the conflict points for each individual cyclist. Instead, let $sig \in S^{\mathcal{B}}$ be a bicycle green phase, where $S^{\mathcal{B}}$ is the set of all bicycle green phases in a considered time period. Let us assume that bicyclist bic is assigned to signal phase sig, i.e., $bic \in \mathcal{B}_{sig}$, where $\mathcal{B}_{sig}$ is the set of all bicyclists assigned to signal phase sig. Signal phase sig inherits parameters from bic, for instance $v^{min}_{sig} = v^{min}_{bic}$ and $v^{max}_{sig} = v^{max}_{bic}$. Let $\hat{t}_{sig}$ be the start and t^{green}_{sig} be the duration of the green phase. The earliest possible arrival time of a bicyclist in phase sig at the conflict zone with vehicle veh is defined by a fast cyclist who starts crossing the intersection when the signal turns green. This is shown by the blue trajectory in Figure 4.8. The figure also shows that a minimum and maximum arrival time of bicyclists in phase sig at the considered conflict point is calculated, denoted by $t^{min}_{sig,p} = \frac{dist_{o_{sig},p}}{v^{max}_{sig}}$ and $t^{max}_{sig,p} = t^{min}_{sig,p} + t^{green}_{sig} + \frac{dist_{o_{sig},p} \cdot (v^{max}_{sig} - v^{min}_{sig})}{v^{max}_{sig} \cdot v^{min}_{sig}}$, where p denotes the conflict point $p_{veh,sig}$. Any conflicting vehicle veh that is assigned to pass the conflict point before the bicycle green phase must have left before this very fast bicyclist arrives at the entrance to the conflict region, i.e., covers the distance $dist_{o_{sig},p} - c^b_{p,sig}$ (compare the blue trajectory in Figure 4.8). Therefore,

$\Delta^{min}_{veh,sig}$ can be calculated as follows (compare Equation 4.6):

$$\Delta^{min}_{veh,sig} = \frac{c^a_{p,veh} + len_{veh}}{\hat{v}_{veh}} + \frac{c^b_{p,sig}}{v^{max}_{sig}} + \delta^{min}_{veh,sig}. \tag{4.7}$$

On the other hand, if bicyclists are assumed to leave the conflict region before vehicle veh arrives, a slow bicyclist needs to be considered, and this cyclist could start crossing at the end of the green phase with a very low speed. This is displayed by the red trajectory in Figure 4.8. In order to ensure safety, $\Delta^{min}_{sig,veh}$ is calculated as follows:

$$\Delta^{min}_{sig,veh} = t^{green}_{sig} + \frac{dist_{o_{sig},p} \cdot (v^{max}_{sig} - v^{min}_{sig})}{v^{max}_{sig} \cdot v^{min}_{sig}} + \frac{c^a_{p,sig} + len_{bic}}{v^{min}_{sig}} + \frac{c^b_{p,veh}}{\hat{v}_{veh}} + \delta^{min}_{sig,veh} \tag{4.8}$$

Again, the minimum time gaps described here will be needed when scheduling bicycle signal phases in Section 4.6.

Vehicle-Pedestrian Conflicts

Similarly to bicyclists, a group of pedestrians shares the same signal green phase. Therefore, pedestrians are also not considered individually, but their signal phase inherits minimum and maximum walking speeds just as described above. Similarly to in the previous subsection, $S^{\mathcal{P}}$ denotes the set of pedestrian signal phases in a considered time period. Let $sig \in S^{\mathcal{P}}$ be the signal phase that pedestrian ped is assigned to, i.e., $ped \in \mathcal{P}_{sig}$. The main difference to the consideration of bicyclists is that pedestrians starting from two different sides of the crosswalk share the same signal. Additionally, in order to fulfill the objective of developing a control scheme that is easily understandable and safe for everyone, vehicles should have left the pedestrian crosswalk when the signal turns green. Therefore, the distances described in the previous subsections are not calculated analogously for pedestrians. Instead, in order to ensure that the signal turns green only after the vehicle has left the intersection, $dist_{o_{sig},p}$ and $c^b_{p,sig}$ are artificially set to zero for any conflict point $p = p_{veh,sig}$. From the vehicle perspective, the conflict point p lies in the middle of the pedestrian crosswalk, i.e., both $c^b_{p,veh}$ and $c^a_{p,veh}$ equal half the width of the crosswalk. For $\Delta^{min}_{veh,sig}$, this leads to:

$$\Delta^{min}_{veh,sig} = \frac{c^a_{p,veh} + len_{veh}}{\hat{v}_{veh}} + \delta^{min}_{veh,sig}. \tag{4.9}$$

This assumption is in line with the SlotIIC approach presented in Chapter 3 (i.e., the conflict region can either be reserved by a vehicle *or* by a pedestrian signal). If applied in practice and safety considerations allow, this conservative assumption could be relaxed and the signal could already turn green when the vehicle is still on the crosswalk, or an entry time for pedestrians could be considered (as done by RiLSA [FGSV, 2015b]).

At the end of the pedestrian green phase, a slowly walking pedestrian needs to be able to enter the road and cross all vehicle lanes entirely. This is displayed by the red trajectories in Figure 4.9b. Therefore, as shown in Figure 4.9a, depending on the layout, two different distances $c^{a1}_{p,sig}$ and $c^{a2}_{p,sig}$ are calculated. The larger one, denoted by $c^a_{p,sig}$ is used for the

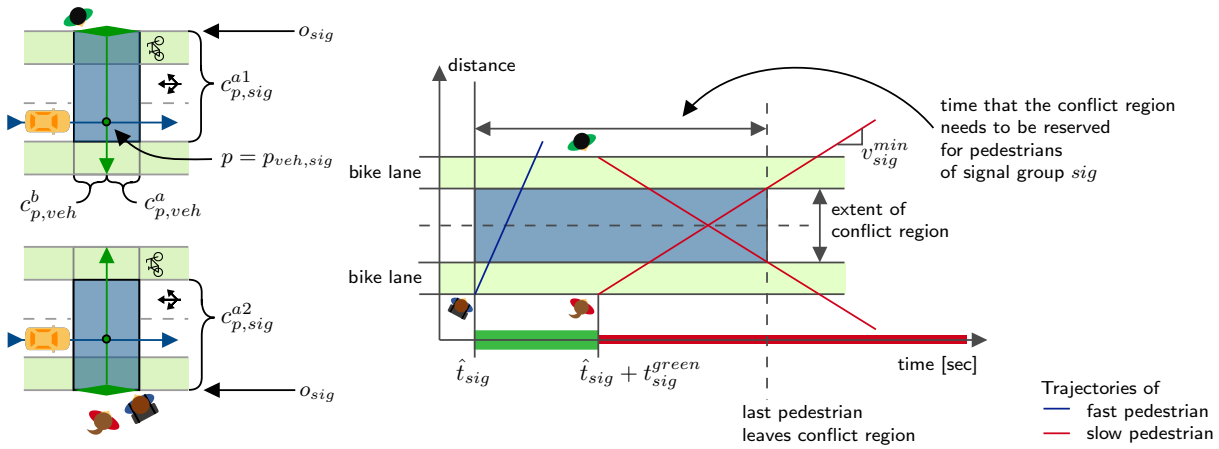

(a) Conflict point and region from pedestrian perspective.

(b) Example trajectories of pedestrians crossing the street.

Figure 4.9: Example illustration of conflict points and conflict regions for vehicle-pedestrian conflicts.

calculation of $\Delta^{min}_{sig,veh}$. If the road layout is symmetric, then the two regions are equally large (as shown in Figure 4.9a). Now, $\Delta^{min}_{sig,veh}$ can be calculated as follows:

$$\Delta^{min}_{sig,veh} = t^{green}_{sig} + \frac{c^{a}_{p,sig}}{v^{min}_{sig}} + \frac{c^{b}_{p,veh}}{\hat{v}_{veh}} + \delta^{min}_{sig,veh} \tag{4.10}$$

Figure 4.9b also shows the trajectory of a fast pedestrian, but it is easy to see that the maximum assumed walking speed is in fact not needed to be considered here. The reason is that it is assumed that pedestrians do not need to cover any distance before entering the conflict region.

4.2.3 Summary

Conflict points and conflict regions depend on the conflicting movements. Since every road user follows a predefined movement, these movements can be stored in a conflict matrix. In particular, for each combination of movements OD_i and OD_j with a conflict point and at least one vehicle involved, the conflict matrix contains the following information: $dist_{o_i,p}$, $c^{b}_{p,i}$, $c^{a}_{p,i}$ and $dist_{o_j,p}$, $c^{b}_{p,j}$, $c^{a}_{p,j}$, where $p = p_{ij}$ denotes the common conflict point. The necessary headways Δ^{min}_{ij} and Δ^{min}_{ji} can then be calculated ad hoc with the information on speeds, vehicle or bicycle lengths, and minimum time gaps δ. The necessary formulas have been introduced above. In the following, these headways are used as an input to the optimization-based scheduling program that will be explained in the next sections. Table 4.1 provides an overview on the variables that have been introduced in this chapter so far.

Symbol	Description
veh, $\mathcal{V}$	Vehicle and set of vehicles.
bic, $\mathcal{B}$	Bicyclist and set of bicyclists.
ped, $\mathcal{P}$	Pedestrian and set of pedestrians.
sig, $\mathcal{S}$	Pedestrian or bicycle signal phase and set of signal phases $\mathcal{S} = S^{\mathcal{B}} \cup S^{\mathcal{P}}$. $S^{\mathcal{B}}$ and $S^{\mathcal{P}}$ denote the sets of pedestrian and bicycle signal phases, respectively. $\mathcal{B}_{sig}$ denotes the set of bicyclist assigned to signal phase sig. Analogously for $\mathcal{P}_{sig}$.
OD_{veh}	Origin & destination of vehicle veh w.r.t. the current intersection zone (e.g., north→south). Analogously for OD_{bic} and OD_{ped}.
o_{veh}	Point, where vehicle veh enters the intersection zone, i.e., the position of the stop bar that veh crosses in order to enter the intersection. Analogously for o_{bic} and o_{ped}, compare Figure 4.4.
d_{veh}	Point, where vehicle veh leaves the intersection zone. Analogously for d_{bic} and d_{ped}, compare Figure 4.4.
p_{ij}	Position of conflict point for movements of veh_i and veh_j. Analogously for pedestrian ped_i, bicyclist bic_i or signal phase sig_i.
$dist_{o_i,p_{ij}}$	Distance between the point, where veh_i enters the intersection, and the conflict point with veh_j, following the prescribed vehicle path. Analogously for pedestrian ped_i, bicyclist bic_i or signal phase sig_i.
$c^b_{p_{ij},veh_i}$	Distance that needs to be covered by veh_i from entering the conflict region around p_{ij} until reaching the conflict point p_{ij} (***b**efore* the conflict point). Analogously for pedestrian ped_i, bicyclist bic_i or signal phase sig_i.
$c^a_{p_{ij},veh_i}$	Distance that needs to be covered by veh_i from conflict point p_{ij} until leaving the conflict region around it (***a**fter* the conflict point). Analogously for pedestrian ped_i, bicyclist bic_i or signal phase sig_i.
$\hat{v}_{veh}$	Speed of vehicle veh when crossing the intersection zone: veh needs to enter the intersection zone with a speed of $\hat{v}_{veh}$ and keep the speed constant until leaving the intersection zone.
v^{min}_{bic}	Minimum speed of bicyclist bic when crossing the intersection zone. Analogously for v^{min}_{ped}. Several pedestrians or bicyclists in one signal phase sig can pass the information on to v^{min}_{sig}.
v^{max}_{bic}	Maximum speed of bicyclist bic when crossing the intersection zone. Analogously for v^{max}_{ped}. Several pedestrians or bicyclists in one signal phase sig can pass the information on to v^{max}_{sig}.
t^{green}_{sig}	Duration of green phase for signal phase sig.
$\hat{t}_{veh}$	Scheduled arrival time of vehicle veh. Analogously for the start of a green phase $\hat{t}_{sig}$ and for pedestrians or bicyclists assigned to the green phase: $\hat{t}_{bic}$, $\hat{t}_{ped}$.
$\hat{t}_{veh,p}$	Time that vehicle veh arrives at position p, given the assigned arrival time at the intersection, the prescribed speed, and the distance between o_{veh} and p following the prescribed vehicle path.
δ^{min}_{ij}	Minimum safety time gap after veh_i has left and before veh_j enters the conflict region. Analogously for pedestrian ped_i or ped_j, bicyclist bic_i or bic_j, and signal phase sig_i or sig_j.
Δ^{min}_{ij}	Minimum time headway for veh_i and veh_j to arrive at the common conflict point p_{ij}. Analogously for pedestrian ped_i or ped_j, bicyclist bic_i or bic_j, and signal phase sig_i or sig_j.

Table 4.1: List of variables used in this section.

4.3 Optimization-based Scheduling Policy

Just as in the previous chapter, the scheduling policy is the center of the intersection control. It combines all relevant information and applies optimization techniques in order to achieve the objective of providing a safe and efficient schedule for road users to cross the intersection. Similarly to the FCFS scheme presented in Chapter 3, the scheduling policy not only returns the order in which vehicles are supposed to enter the intersection, but also assigns the exact arrival time for each vehicle and the start times of green phases for each traffic signal. In the following, the scheduling policy is explained in detail. Due to the complexity and importance of the policy concepts, their description is stretched over several sections. First of all, a brief background on optimization is provided in Section 4.3.1 and the objective function is defined in Section 4.3.2. Section 4.4 presents vehicle-only scenarios: necessary constraints are defined and the problem is formally set up. In Section 4.5, the rolling-horizon implementation is explained.The detailed explanations in the limited vehicle-only scenario set the ground for explaining the integration of pedestrians and bicyclists into the scheduling policy in Section 4.6. The results of the implementation of the OptIIC schemes are presented in Section 4.7.

4.3.1 Background on the Optimization Problem

Similar to existing studies on the optimization-based scheduling of conflicting vehicle movements at intersection zones (and scheduling problems in general), the problem is formulated as an MILP, an optimization problem that consists of a linear objective function and a set of linear constraints with the additional restriction that some of the decision variables need to be integers. A very brief background on these optimization problems based on Williams [2013] is given here.

In general, a linear optimization problem can be written as

$$\begin{aligned} &\min z = c^T x \\ &\text{subject to } Ax \geq b \end{aligned}$$

with z being called the objective function with objective $c \in \mathbb{R}^n$ and decision variables $x \in \mathbb{R}^n$. $A \in \mathbb{R}^{m \times n}$ is a given constraint matrix and $b \in \mathbb{R}^m$ is a given right hand side of the constraints. A solution x is said to be *feasible* with respect to the program if it fulfills all specified constraints. A solution is *optimal* if it is feasible and its objective function value is the smallest value that z can take over the set or region of feasible solutions. When setting up and attempting to solve such a model, it is necessary to check that the model is (i) feasible, i.e., there exists at least one feasible solution, and that it is (ii) bounded, i.e., there exists a finite minimum objective value over the feasible region. If these conditions are fulfilled, the model is said to be *solvable*, i.e., at least one finite optimal solution exists.

Linear optimization problems are very popular, mainly because they can be solved rather easily. The geometric properties of the feasible region and the objective function allow for searching the optimal solution only among the vertices of the feasible region and, starting from an arbitrary vertex, one can find a path along the edges such that objective values in the

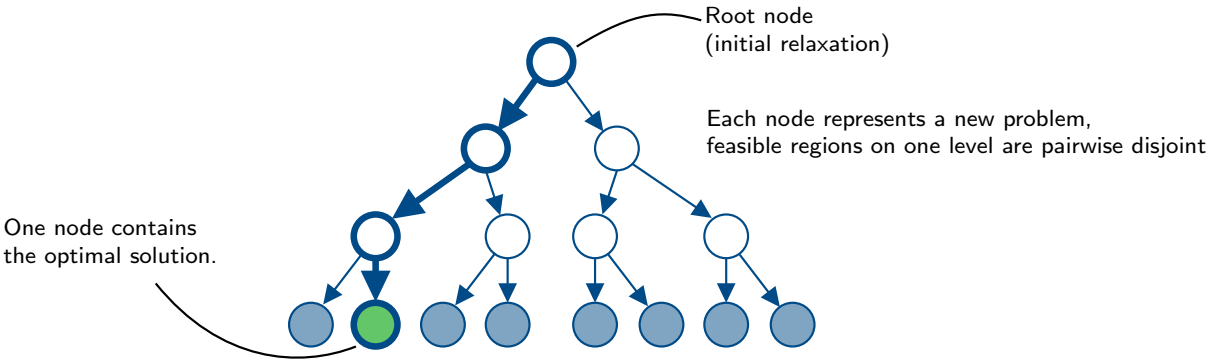

Figure 4.10: Schematic representation of the branch and bound (B&B) methodology.

respective vertices are strictly decreasing. These features are smartly exploited by the famous simplex algorithm which dates back to a work by George B. Dantzig in 1947 [Karloff, 1991]. If some or all decision variables are required to be integers, these favorable geometric properties no longer hold. Despite immense efforts, no comparable general algorithm has emerged for solving a wide range of integer programs. In fact, there is theoretical evidence that such an algorithm does not exist [Williams, 2013].

With that being said, many promising heuristics exist that can often achieve good (approximate or optimal) solutions for practical problems. The most widely used algorithms for solving integer problems are branch and bound (B&B) algorithms. B&B techniques are not classical algorithms, but can rather be referred to as a framework or solution procedure that uses other algorithms. A good introduction is given by Morrison et al. [2016]. The B&B methodology works by forming several subproblems that can be solved more easily than the original problem. These subproblems are arranged in the form of a tree as shown in Figure 4.10, where each of the nodes is a new subproblem. Usually, an initial *relaxation* is defined by removing some of the constraints of the original problem. This new relaxed problem should be easily solvable, but since some of the constraints are omitted, the optimal solution might not be feasible for the original problem. Anyhow, the objective value can work as a *lower bound* to the overall problem, since imposing more constraints will only decrease the quality of the solution. On the other hand, the objective value of any feasible solution to the original problem can be considered as an *upper bound*, i.e., the solution is feasible, but there might still be a better one. Now, starting from the so-called root node with the relaxed problem, children can be created by partitioning the solution space into disjoint regions, called *branching*. By applying suitable rules, nodes or entire branches can be cut off, since their solution spaces are provably suboptimal. The performance of B&B heavily depends on good initial solutions and bounds, that can be obtained by heuristics. Additionally, the search strategy (i.e., in which order the nodes are explored), the branching strategy, (i.e., how new subproblems are created), and the pruning rules (i.e., how suboptimal regions of the tree are identified and removed), all contribute to the performance of the method [Morrison et al., 2016]. Today, many commercial and open source solvers exist that use B&B methods with ever-improving run times. They often feature parallelism, i.e., several nodes of the search tree can be explored simultaneously and the multiple cores of state-of-the-art computers are used [Ralphs et al., 2018]. In this

thesis, such a commercial solver will be used, which is why the interested reader is referred to literature for more details on B&B, e.g., MORRISON et al. [2016].

4.3.2 Objective of the Scheduling Policy

As explained previously, the control delay per vehicle or VRU, respectively, is the decisive performance measure to evaluate the LOS at signalized intersection zones, and it is used as the key performance indicator for evaluating the strategies presented in this thesis as well. It is hence the objective of the scheduling policy to minimize the total delay at the intersection zone. Additionally, the optimization shall be able to include dynamic prioritization of road users.

Definition of Delay

The definition of delay has been explained in more detail in Section 3.7 and the same formulas are used here. As a reminder, the delay of vehicle veh is calculated as the difference between the earliest possible arrival time t_{veh}^{min} of vehicle veh at the intersection and the time it actually enters the intersection area $\hat{t}_{veh}$. The delay of pedestrian ped is analogously approximated as the difference between the time t_{ped}^{min} that pedestrian ped arrives at the pedestrian crosswalk, and the time $\hat{t}_{ped}$ that pedestrian ped is allowed to start crossing the street, i.e., the beginning of the respective green phase. In the bicycle case, the scheduling has to rely on the a-priori calculation of the bicycle waiting times as explained in Section 3.6. In this approach, the expected arrival time t_{bic}^{min} of bicyclist bic is calculated based on detector measurements captured at a distance to the intersection and on an assumed progression speed. Again, $\hat{t}_{bic}$ denotes the start of the green phase and the delay is approximated as the difference between the two points in time. If the signal is already green upon the (expected) arrival of bic or ped, then $\hat{t}_{bic}$ or $\hat{t}_{ped}$ are set equal to t_{bic}^{min} or t_{ped}^{min}, respectively. Their delays can thus be expressed as follows:

$$delay_{veh} = \hat{t}_{veh} - t_{veh}^{min} \qquad \forall\ veh \in \mathcal{V} \tag{4.11}$$

$$delay_{bic} = \hat{t}_{bic} - t_{bic}^{min} \qquad \forall\ bic \in \mathcal{B} \tag{4.12}$$

$$delay_{ped} = \hat{t}_{ped} - t_{ped}^{min} \qquad \forall\ ped \in \mathcal{P} \tag{4.13}$$

where $\mathcal{V}$, $\mathcal{B}$ and $\mathcal{P}$ are the sets of all vehicles, bicyclists, and pedestrians that cross the intersection during a considered period of time.

Prioritization

The delays of the different road users, i.e., vehicles, pedestrians, and bicyclists, need to be combined in the objective function. Additionally, it is one requirement of the control to dynamically integrate policy considerations. This means that the scheduling algorithm should allow for prioritizing individual or groups of road users. Such a prioritization could depend on emissions, prioritized routes, or on the occupancy of vehicles. This also provides the opportunity to minimize the average person delay instead of the average vehicle delay. Rather than minimizing the simple sum of all delays, the delays of vehicles, pedestrians and bicyclists

are thus first multiplied with an individual prioritization factor. The higher this factor, the higher the weight of the corresponding delay in the overall objective function.

Objective Function

Combining the considerations described above, the (linear) objective function for the scheduling problem can be defined as follows:

$$\min \left(\sum_{veh \in \mathcal{V}} \gamma_{veh} \cdot delay_{veh} + \sum_{bic \in \mathcal{B}} \gamma_{bic} \cdot delay_{bic} + \sum_{ped \in \mathcal{P}} \gamma_{ped} \cdot delay_{ped} \right) \tag{4.14}$$
$$\text{with } \gamma_{veh}, \gamma_{bic}, \gamma_{ped} \in \mathbb{R}_0^+ \; \forall \; veh \in \mathcal{V}, bic \in \mathcal{B}, ped \in \mathcal{P}$$

where γ_{veh}, γ_{bic} and γ_{ped} are the priority indicators (weighting factors) for each vehicle veh, bicyclist bic, and pedestrian ped. All weighting factors should be greater than or equal to zero, as otherwise a larger delay of a particular road user is "rewarded" and the problem can possibly become unbounded. The objective function is very flexible in the sense that weighting factors can be defined individually and changed in different demand situations. The effect of different weighting factors will be discussed with the help of results in Section 4.7.

4.4 Optimization Problem for Vehicle-only Scenarios

The optimization problem is first set up for vehicle-only scenarios. The introduced concept is similar to those of existing optimization-based AIM schemes (e.g., E. R. Müller et al. [2016b] and Levin and Rey [2017]). First, necessary constraints are explained in Section 4.4.1. Afterwards, the optimization problem is formally set up in Section 4.4.2. A rolling horizon approach will be applied to the program in Section 4.5 and pedestrians and bicyclists will be integrated in Section 4.6.

4.4.1 Constraints

Several constraints need to be considered when scheduling vehicle arrival times at the intersection zone. In particular, physical restrictions bound the arrival time of a vehicle at the intersection zone, and conflicting vehicle movements need to be resolved.

First of all, a vehicle veh_i cannot be scheduled earlier than its earliest possible arrival time (denoted by t_i^{min}) considering its current distance and speed, its kinematic limitations, and the maximum allowed speed on the approach to the intersection zone. Secondly, it is assumed that vehicles cannot overtake on the approach to the intersection zone. Therefore, if two vehicles veh_i and veh_j are approaching the intersection zone from the same direction, then the vehicle which is already closer to the intersection zone needs to be scheduled to arrive at the intersection first. Furthermore, a minimum temporal headway needs to be respected between two adjacent vehicles. These assumptions lead us to the first sets of linear constraints:

$$t_i \geq t_i^{min} \qquad \forall \; veh_i \in \mathcal{V} \tag{4.15}$$
$$t_i \geq t_j + \Delta_{ji}^{min} \qquad \forall \; veh_i, veh_j \in \mathcal{V} \mid o_i = o_j \;\&\; dist_i > dist_j. \tag{4.16}$$

where $dist_i$ and $dist_j$ denote the distances of vehicles veh_i and veh_j to the intersection at the time the program is solved. The minimum headway Δ_{ji}^{min} includes the time that is needed for the front vehicle veh_j to cross the stop bar and a minimum time gap as explained in Section 4.2.1.

Additionally, vehicle movements that have crossing paths within the intersection zone need to arrive at the respective conflict points with a sufficient time gap in order to ensure collision-free passing. In contrast to the previous constraints, the decision of which vehicle passes the conflict point first can be considered as the true improvement compared to a pure FCFS control. Usually, vehicle following time gaps are smaller than time gaps between crossing movements. Additionally, the conflict regions in which vehicle movements need to be separated are larger for crossing situations. Therefore, as explained in Section 4.2.1, assigning vehicle platoons to cross together can lead to capacity gains.

The possibility to have either vehicle cross first leads to two distinct constraints where exactly one of them needs to hold in order to generate a feasible solution. Let veh_i and veh_j be two vehicles that approach the intersection from two different directions and let p_{ij} be the conflict point of the paths of veh_i and veh_j. If veh_i is assigned to arrive at the conflict point first, then the following constraint needs to hold:

$$t_i + \frac{dist_{o_i,p_{ij}}}{\hat{v}_i} + \Delta_{ij}^{min} \leq t_j + \frac{dist_{o_j,p_{ij}}}{\hat{v}_j} \qquad \text{if } t_i + \frac{dist_{o_i,p_{ij}}}{\hat{v}_i} \leq t_j + \frac{dist_{o_j,p_{ij}}}{\hat{v}_j}, \tag{4.17}$$

where the position of p_{ij} and the measures $dist_{o_i,p_{ij}}$ and $dist_{o_j,p_{ij}}$ are derived from the conflict matrix presented in Section 4.2, and the minimum headway Δ_{ij}^{min} is calculated according to Equation 4.6 (defined in Section 4.2.1) for some minimum time gap δ_{ij}^{min}. In order to simplify the expression, Equation (4.17) is reformulated as follows:

$$t_i + \underbrace{\frac{dist_{o_i,p_{ij}}}{\hat{v}_i} - \frac{dist_{o_j,p_{ij}}}{\hat{v}_j}}_{=\tau_{ij}} + \Delta_{ij}^{min} \leq t_j \qquad \text{if } t_i + \tau_{ij} \leq t_j \tag{4.18}$$

and the new variable $\tau_{ij} = \frac{dist_{o_i,p_{ij}}}{\hat{v}_i} - \frac{dist_{o_j,p_{ij}}}{\hat{v}_j}$ is introduced. It represents the difference in time needed for vehicles veh_i and veh_j to reach the conflict point p_{ij} starting from their respective entrance points to the intersection, o_i and o_j. If τ_{ij} is positive, then vehicle veh_i needs more time to get from o_i to p_{ij} than veh_j needs to get from o_j to p_{ij}, and vice versa.

On the other hand, if veh_j is assigned to arrive at the conflict point first, the above constraint is obviously violated, but the following constraint needs to hold:

$$t_i + \tau_{ij} \geq t_j + \Delta_{ji}^{min} \qquad \text{if } t_i + \tau_{ij} \geq t_j. \tag{4.19}$$

The logical condition cannot directly be included into the linear program. In general, an optimization model requires that all constraints need to be fulfilled at the same time. In order to overcome this issue, binary auxiliary variables are introduced. They allow for reformulating the constraints in such a way that all constraints hold true at the same time with some of them

being redundant. This is a well-known trick in mathematical programming that can be applied to include practical conditions of a logical type into optimization problems [Williams, 2013]. In this case, similarly to in the approaches presented in existing studies [E. R. Müller et al., 2016a; Levin and Rey, 2017; Fayazi and Vahidi, 2018; Yao et al., 2020], the binary auxiliary matrix $I \in \{0,1\}^{(|\mathcal{V}|\times|\mathcal{V}|)}$ indicates whether vehicle veh_i is supposed to arrive at the conflict point p_{ij} before veh_j. Additionally, a large scalar $\mathcal{M}$ is introduced. The previously defined constraints can then be rewritten as follows:

$$t_i + \tau_{ij} + \Delta_{ij}^{min} \leq t_j + \overbrace{(1 - I_{ij}) \times \mathcal{M}}^{=0,\text{ if } I_{ij}=1;\ \mathcal{M},\text{ otherwise}} \qquad \forall\ veh_i, veh_j \in \mathcal{V} \tag{4.20}$$

$$t_i + \tau_{ij} + \overbrace{I_{ij} \times \mathcal{M}}^{=0,\text{ if } I_{ij}=0;\ \mathcal{M}\text{ otherwise}} \geq t_j + \Delta_{ji}^{min} \qquad \forall\ veh_i, veh_j \in \mathcal{V} \tag{4.21}$$

$$I_{ij} \in \{0,1\} \qquad \forall\ veh_i, veh_j \in \mathcal{V}$$

If $I_{ij} = 1$, then Inequality (4.20) equals Inequality (4.18), and Inequality (4.21) is redundant and always holds true if $\mathcal{M}$ is big enough. On the other hand, if $I_{ij} = 0$, then Inequality (4.21) equals Inequality (4.19), and Inequality (4.20) is redundant. This means that, without explicitly stating it, I_{ij} indicates whether veh_i is supposed to arrive at the conflict point p_{ij} before veh_j:

$$I_{ij} \in \{0,1\} \text{ with } I_{ij} = 1 \Leftrightarrow t_i + \tau_{ij} \leq t_j \qquad \forall\ veh_i, veh_j \in \mathcal{V}.$$

In other words, I_{ij} equal to 1 indicates that veh_i arrives at the conflict point before veh_j, and I_{ij} equal to 0 indicates that veh_j arrives at the conflict point before veh_i.

This method is also sometimes referred to as the "Big-$\mathcal{M}$"-method [Fayazi and Vahidi, 2018]. As the name suggest, $\mathcal{M}$ needs to be big – but how big? In order for the redundant constraints to hold true, it has to be ensured that $|\hat{t}_i - \hat{t}_j| < \mathcal{M}$ for all veh_i and veh_j considered in the optimization. In order to ensure that this constraint is not violated, an additional constraint is introduced that sets an upper bound Θ_{veh} on the delay of each individual vehicle veh:

$$t_{veh} \leq t_{veh}^{min} + \Theta_{veh} \qquad \forall\ veh \in \mathcal{V} \tag{4.22}$$

Then, the following holds:

$$\begin{aligned}
\max_{veh_i, veh_j \in \mathcal{V}} |\hat{t}_i - \hat{t}_j| = &\max_{veh_i \in \mathcal{V}} \hat{t}_i - \min_{veh_j \in \mathcal{V}} \hat{t}_j \\
&\overset{(4.15)}{\leq} \max_{veh_i \in \mathcal{V}} \hat{t}_i - \min_{veh_j \in \mathcal{V}} t_j^{min} \\
&\overset{(4.22)}{\leq} \max_{veh_i \in \mathcal{V}} \left(t_i^{min} + \Theta_i\right) - \min_{veh_j \in \mathcal{V}} t_j^{min} \\
&\overset{!}{<} \mathcal{M}
\end{aligned} \tag{4.23}$$

Now, the expression in Inequality (4.23) can be limited by the time period considered in the optimization and by the defined maximum delay Θ_{veh}. Additionally, Constraints (4.22) can be

used for limiting the delay for vehicles in order to ensure fairness. However, one needs to be careful not to limit the delay of vehicles too strictly, since this can lead to infeasibility if no schedule is found that can fulfill all the constraints. In this thesis, the upper bound Θ_{veh} is chosen large enough to make Constraints (4.22) redundant. This is further described in the next subsection.

The binary requirement of the auxiliary variable I converts the otherwise linear program into an MILP. As described in Section 4.3.1, this makes solving the problem harder, but promising approaches exist to approximate or solve the problem, even in standard optimization packages [Williams, 2013].

4.4.2 Formulation of the Optimization Problem

The overall optimization problem for vehicle-only movement at the intersection can then be formulated as follows:

Problem I (Intersection Control Optimization for Vehicle-Only Scenarios)**.**

$$\min \left(\sum_{veh_i \in \mathcal{V}} \gamma_i \cdot delay_i \right) \tag{4.24}$$

subject to

$$delay_i = t_i - t_i^{min} \qquad \forall\ veh_i \in \mathcal{V} \tag{4.25}$$

$$t_i \geq t_i^{min} \qquad \forall\ veh_i \in \mathcal{V} \tag{4.26}$$

$$t_i \leq t_i^{min} + \Theta_i \qquad \forall\ veh_i \in \mathcal{V} \tag{4.27}$$

$$t_i \geq t_j + \Delta_{ji}^{min} \qquad \forall\ veh_i, veh_j \in \mathcal{V} \mid o_i = o_j\ \&\ dist_i > dist_j \tag{4.28}$$

$$t_i + \tau_{ij} + \Delta_{ij}^{min} \leq t_j + (1 - I_{ij}) \times \mathcal{M} \qquad \forall\ veh_i, veh_j \in \mathcal{V} \tag{4.29}$$

$$t_i + \tau_{ij} + I_{ij} \times \mathcal{M} \geq t_j + \Delta_{ji}^{min} \qquad \forall\ veh_i, veh_j \in \mathcal{V} \tag{4.30}$$

$$I_{ij} \in \{0, 1\} \qquad \forall\ veh_i, veh_j \in \mathcal{V}$$

If veh_i and veh_j are such that their movements do not conflict with each other, then $\tau_{ij} = \Delta_{ij}^{min} = \Delta_{ji}^{min} = 0$ in Constraints (4.29) and (4.30). As described in Section 4.3.1, an optimization problem is solvable, if it is *feasible* and *bounded*. Both characteristics are fulfilled for Problem I. The formal proof can be found in Appendix B. Given these necessary characteristics, the following remark substantiates that resulting schedules are in fact valid from a practical point of view.

Remark. *The schedule resulting from the optimization does not lead to gridlocks.*

Since the constraints allow for multiple vehicles with conflicting movements to be within the intersection zone at the same time, it is theoretically conceivable that gridlocks could occur. However, this is not the case. The key is that the scheduling algorithm *only* assigns the exact time $\hat{t}_{veh}$ for each vehicle veh to enter the intersection. The time that veh arrives at any potential conflict point p within the intersection zone then only depends on $\hat{t}_{veh}$ and

the pre-defined distances between the entrance to the intersection o_{veh} and p, and on the also pre-defined vehicle speed $\hat{v}_{veh}$. The remark is proven by contradiction and the proof can be found in Appendix B.

4.5 Rolling Horizon Strategy

With the objective function and the presented constraints for vehicle movements, the scheduling program can be set up for vehicle-only scenarios as defined in Problem I. However, the intersection controller does not have all relevant information, such as the earliest arrival times t_{veh}^{min} for *all* vehicles, from the start. Instead, the controller is only aware of those vehicles that are currently approaching the intersection. Therefore, a rolling horizon strategy is applied, in which the optimization is run repeatedly with the information that is available at that time. A brief background on rolling horizon decision making is given in Section 4.5.1. Section 4.5.2 describes how the rolling horizon strategy is applied in this thesis, and Section 4.5.3 formally sets up the problem formulation.

4.5.1 Background on Rolling Horizon Strategies

Rolling horizon decision making is motivated by many real-world planning problems such as production planning, energy supply and demand planning, airplane scheduling, and vehicle routing. It is also commonly used in adaptive TSC [A. Stevanovic, 2010]. The rolling horizon scheme tackles two issues that arise in practice: the first issue is that decisions for the current time period are of immediate importance, but input data are only known a certain amount of time in advance and forecasts can be inaccurate. The second issue is that data for a larger time horizon are available, but the overall problem size is too large to be solved within an acceptable time frame. As an approach to tackle both of these challenges, the problem is repeatedly modeled and solved for a certain (smaller) period of time, called *projection horizon* or *forecast horizon*. After solving a problem instance, the returned decisions are applied only for the most immediate decisions within an even shorter period, called *roll period* or *decision horizon*. After the roll period, the program is modeled and solved again. In this subsequent iteration, all decisions that were applied in the previous iteration are considered as fixed, but possible new data that improve on the forecast quality can be incorporated. The scheme thus allows for making immediate decisions while revising decisions for future time periods when more data are available. At the same time, the sizes of the subproblems that are solved iteratively are narrowed, hence accounting for limited run times. Overall, the projection horizon "gets rolled over," which justifies the term [Sethi and Sorger, 1991]. The ideas on forecast horizons and solving a sequence of problems date back to the work on production planning by Modigliani and Hohn [1955].

Glomb et al. [2020] formally define their rolling horizon approach as a finite sequence of coupled optimization problems $\{P_0, \dots, P_K\}$, where each of the problems belongs to a time period t^k with $k \in \{0, \dots, K\}$ and $K \in \mathbb{N}_0$. Each problem contains initial state variables that correspond to the end state of the previous time period. In particular, the applied decisions of the previous time period are considered as fixed in the next iteration. The idea is

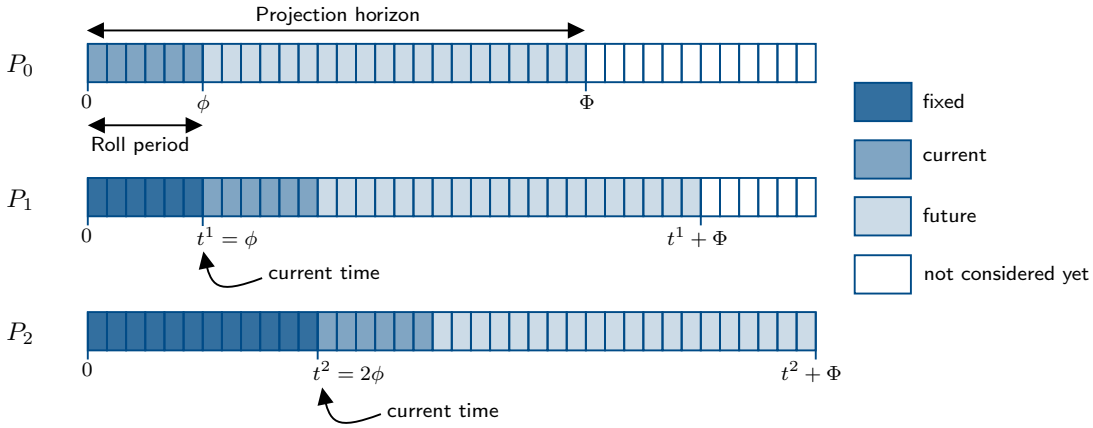

Figure 4.11: Schematic representation of rolling horizon decision making based on Gartner et al. [2001] and Glomb et al. [2020].

schematically displayed in Figure 4.11. In the figure, the roll period is denoted by ϕ and the projection horizon is denoted by Φ. The program is hence modeled and run every ϕ time units – depending on the use case, these could be a few seconds or several weeks. The overall time horizon is divided into several periods in which decisions are either 'fixed' (decisions taken in the previous time period), 'current' (decisions that will be applied in the current time period), 'future' (information is considered in the optimization problem, but decisions are not applied yet), or 'not considered yet'.

Depending on the nature of a problem, it can be modeled as a *finite-horizon* (such as the one described by Glomb et al. [2020]) or an *infinite-horizon* problem. Roll period and projection horizon can be static or dynamic, and data incorporated into the decision can be deterministic or stochastic. Chand et al. [2002] provide a good overview on the various horizon types, model types, and solution methods. Their paper also features a literature review on horizon research which attempts to analyze how future data impacts initial decisions. While more data and longer projection horizons can improve the decision making, forecasts further into the future seem to have a minor effect on the quality of immediate decisions. Additionally, forecasts further into the future are less reliable and more costly. Setting up the program for a larger projection horizon also leads to a larger instance that needs to be solved, which can lead to program runtime issues. The projection horizon should thus be chosen carefully. In the following, the rolling horizon strategy for the intersection scheduling problem is described.

4.5.2 Rolling Horizon Strategy for Vehicle-only Scenarios

As described above, the optimization problem for scheduling vehicle arrival times at the intersection is modeled repeatedly with the information that is currently available. In principle, this corresponds to the information of all vehicles which are currently communicating with the intersection controller. The level of information thus depends on the communication range of the controller and on the length of the approach to the intersection. This is schematically displayed in Figure 4.12a, where the controller can consider the arrival times of the blue vehicles in the optimization. At the same time, some of the vehicles (colored orange in Figure 4.12a)

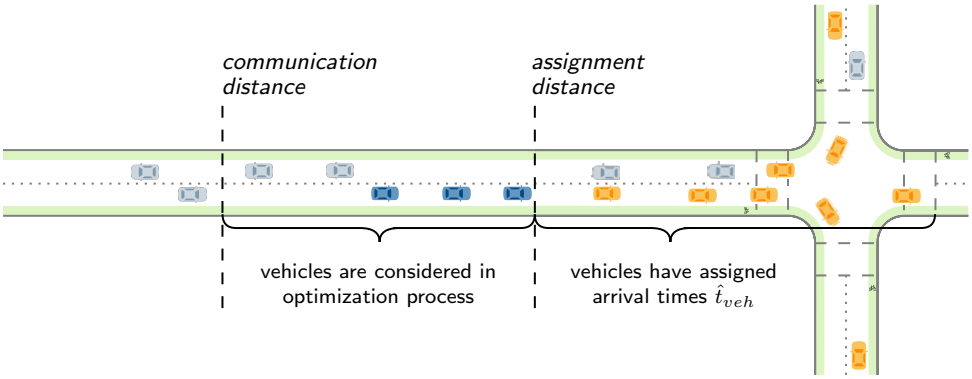

(a) Schematic representation of communication distance and assignment distance.

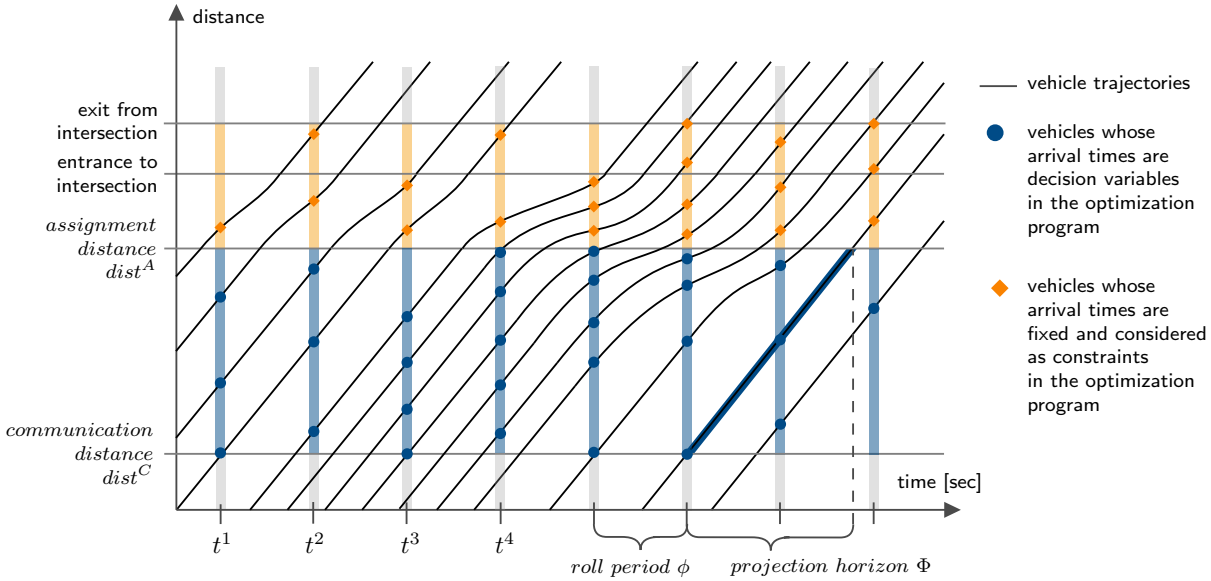

(b) Example trajectories and schematic representation of roll period ϕ and projection horizon Φ.

Figure 4.12: Representation of the relationship between spatial distance and time horizon.

have already started crossing the intersection zone or are about to do that, and their arrival times should not be changed any more. This is reflected by defining an assignment distance, after which arrival times of vehicles are fixed. It is clear that vehicles which have not yet left the intersection still need to be considered in the optimization problem as constraints for safety reasons. Vehicles that are not considered in the scheduling process at all are colored gray in Figure 4.12a.

Figure 4.12b shows how these distance-wise considerations relate to the temporal dimension. The figure schematically shows trajectories of vehicles on the approach to and within the intersection zone. It is assumed that the optimization is run in fixed intervals of ϕ seconds, which corresponds to a fixed roll period. Alternatively, optimization runs could be triggered by vehicles entering the communication range of the intersection controller leading to variable roll periods. At the time the program is solved (denoted as t^1, t^2, etc., in Figure 4.12b), the

controller takes a snapshot of the situation. The information of the blue and orange vehicles is then considered in the optimization as described above. The number of vehicles considered as decision variables thus depends on the length of the stretch between communication distance and assignment distance, on the number of incoming lanes, and on the vehicle densities on these lanes. In the figure, communication distance and assignment distance remain fixed, but the densities change: at time t^1, only three blue vehicles are considered in the optimization problem, at time t^4, there are five blue vehicles in the considered area. As can be seen in the figure, the projection horizon Φ can be defined as the time needed to traverse the stretch between communication and assignment distance at maximum allowed speed. It is clear that the roll period ϕ needs to be less than or equal to the projection horizon Φ. Otherwise, a vehicle could cross the assignment distance without having a scheduled arrival time. This needs to be taken into account when determining the combination of communication range, assignment distance, and roll period.

Formally speaking, let $t^k = k \times \phi$ for $k \geq 0$ denote the times in which the optimization problem is modeled and solved. It is assumed that, at time t^k, the controller has (i) a list of all vehicles with a fixed time slot that have not yet left the intersection (orange vehicles in Figure 4.12), denoted by $\hat{\mathcal{V}}^k$, and (ii) a list of all vehicles within the communication distance but without a fixed time slot (blue vehicles in Figure 4.12), denoted by $\mathcal{V}^k$. For all vehicles $\widehat{veh}$ in the first list $\hat{\mathcal{V}}^k$, the controller has all the information that is needed to resolve conflicts with newly arriving vehicles. This includes the assigned arrival times $\hat{t}_{\widehat{veh}}$, origins and destinations $OD_{\widehat{veh}}$, vehicle speeds $\hat{v}_{\widehat{veh}}$ for crossing the intersection, and vehicle dimensions $len_{\widehat{veh}}$ and $wid_{\widehat{veh}}$. For all vehicles veh in the second list $\mathcal{V}^k$, the controller has all relevant information for computing an optimal schedule, namely the earliest possible arrival times t^{min}_{veh}, weighting factors γ_{veh}, origins and destinations OD_{veh}, vehicle speeds v_{veh}, and vehicle dimensions len_{veh} and wid_{veh}.

In this chapter, it is assumed that vehicles drive at maximum possible speed (considering the speed limits and vehicles in front of them), and only adjust their trajectory after their assigned arrival time is fixed, i.e., after crossing the assignment distance. If they slow down earlier, this is due to a queuing effect on the approach to the intersection. Nevertheless, to allow for more flexible trajectory planning approaches later on, the variable $t^{LB}_{veh}(t^k)$ is calculated for vehicles in the second list $\mathcal{V}^k$. As introduced in Section 3.4, it denotes the earliest possible arrival time of veh at the intersection at time t^k and thus serves as a lower bound. The measure t^{min}_{veh}, which was presented in the Section 4.3.2, is calculated only once for each vehicle approaching the intersection zone. In contrast to that, $t^{LB}_{veh}(t^k)$ is affected by the actual trajectory of veh on the way to the intersection zone and thus includes possible disturbances. Assuming that vehicle speeds never exceed the maximum allowed speed, it is easy to see that $t^{LB}_{veh}(t^k) \geq t^{min}_{veh}$ at all times t^k and for all vehicles veh.

All in all, the controller determines the optimal arrival times of vehicles veh at the intersection considering the current situation, but the arrival times are not fixed immediately. Only when vehicles are close to the intersection zone is the arrival time assigned and the vehicle adjusts its speed in order to fulfill the schedule obtained by the controller. This assignment

policy is somewhat similar to what LEVIN and REY [2017] describe as their policy called "as late as possible." Even though they tested a few values for roll period and projection horizon in their work, the overall influence of the different parameters has not been fully explored yet. Additionally, the setup in this thesis is different, since the spatial dimensions of communication and assignment distance are considered and vehicle trajectories are simulated in detail, whereas LEVIN and REY [2017] directly generate earliest possible arrival times at the intersection from Poisson processes. The detailed microscopic simulation setup allows for the analysis of queuing effects and vehicle density, for example. It is clear that, in the setup presented here, the following parameters can have an influence on the overall performance of the control – regarding both solution quality and program run time: (i) the length of the stretch between communication distance and assignment distance, and (ii) the roll period ϕ. These effects will be further explored in Section 4.7. Additionally, it needs to be noted that having vehicles drive at the maximum allowed speed until the assigned arrival time is fixed is only one possible strategy. Instead, vehicles could already adjust their trajectory based on pre-assigned arrival times which are derived in every simulation run. This could lead to smoother trajectories, but would limit the flexibility of the scheduling program (because $t_{veh}^{LB}(t^k)$ will increase if vehicle veh decelerates early on). An analysis of the trade-off will be left for future work.

4.5.3 Formulation of the Rolling-Horizon Optimization Problem

At time t^k, let $\widehat{\mathcal{V}}^k$ and $\mathcal{V}^k$ be the list of approaching vehicles with ($\widehat{\mathcal{V}}^k$) and without ($\mathcal{V}^k$) an assigned arrival time as described above. The optimization problem can then be defined as follows:

Problem II (Intersection Control Optimization for Vehicle-Only Scenarios at Time t^k)**.**

$$\min \left(\sum_{veh_i \in \mathcal{V}^k} \gamma_i \cdot delay_i \right)$$

subject to

$$\begin{aligned}
delay_i &= t_i - t_i^{min} && \forall\ veh_i \in \mathcal{V}^k \\
t_i &\geq t_i^{LB}(t^k) && \forall\ veh_i \in \mathcal{V}^k \quad (4.31) \\
t_i &\leq t_i^{min} + \Theta_i && \forall\ veh_i \in \mathcal{V}^k \\
t_i &\geq t_j + \Delta_{ji}^{min} \ \forall\ veh_i, veh_j \in \mathcal{V}^k \mid o_i = o_j \ \&\ dist_i(t^k) > dist_j(t^k) && \\
t_i &\geq \hat{t}_l + \Delta_{li}^{min} && \forall\ veh_i \in \mathcal{V}^k, veh_l \in \widehat{\mathcal{V}}^k \mid o_i = o_l \quad (4.32) \\
t_i + \tau_{ij} + \Delta_{ij}^{min} &\leq t_j + (1 - I_{ij}) \times \mathcal{M} && \forall\ veh_i, veh_j \in \mathcal{V}^k \\
t_i + \tau_{ij} + I_{ij} \times \mathcal{M} &\geq t_j + \Delta_{ji}^{min} && \forall\ veh_i, veh_j \in \mathcal{V}^k \\
t_i + \tau_{il} + \Delta_{il}^{min} &\leq \hat{t}_l + (1 - I_{il}) \times \mathcal{M} && \forall\ veh_i \in \mathcal{V}^k, veh_l \in \widehat{\mathcal{V}}^k \quad (4.33) \\
t_i + \tau_{il} + I_{il} \times \mathcal{M} &\geq \hat{t}_l + \Delta_{li}^{min} && \forall\ veh_i \in \mathcal{V}^k, veh_l \in \widehat{\mathcal{V}}^k \quad (4.34) \\
I_{ij} &\in \{0, 1\} && \forall\ veh_i, veh_j \in \mathcal{V}^k \\
I_{il} &\in \{0, 1\} && \forall\ veh_i \in \mathcal{V}^k, veh_l \in \widehat{\mathcal{V}}^k \quad (4.35)
\end{aligned}$$

The problem formulation is similar to Problem I. Constraints (4.31) have been changed to incorporate the earliest possible arrival time at time t^k as explained above. Constraints (4.32), (4.33), (4.34), and (4.35) resolve conflicts between already scheduled and newly arriving vehicles. Constraints (4.32) make sure that vehicle veh_i in $\mathcal{V}^k$ is scheduled to arrive later than veh_l in $\widehat{\mathcal{V}}^k$ with a sufficient headway, where veh_l is on the same approach as veh_i. Note that veh_l already having a scheduled arrival time $\hat{t}_l$ implies that veh_l is closer to the intersection than veh_i. Constraints (4.33), (4.34), and (4.35) resolve crossing conflicts. Here, the new vehicle veh_i can be assigned to cross a conflict point p_{il} before or after an already assigned vehicle veh_l. Therefore, the big-$\mathcal{M}$ method is used again. All other constraints are identical to the respective constraints in Problem I with $\mathcal{V}$ being replaced by $\mathcal{V}^k$.

Again, necessary properties such as the feasibility and boundedness of the program need to hold for Problem II in order to ensure its solvability, given the start states. These characteristics can be transferred from Problem I.

4.6 Integration of Pedestrians and Bicyclists

The integration of pedestrians and bicyclists follows the overall concept described in the previous sections with three major differences that have already been described in Section 4.2 and are consistent with the approaches presented in Chapter 3:

(i) Pedestrians and bicyclists coming from the same direction are supposed to cross the intersection zone roughly at the same time, i.e., when their respective signal head turns green.

(ii) The speeds of pedestrians and bicyclists when crossing the intersection zone are unknown and cannot be assumed to be constant. Instead, they are bounded by assumed minimum and maximum speeds.

(iii) Conflicting movements of pedestrians and bicyclists without the involvement of motorized vehicles are not resolved by the control.

Based on these assumptions, it does not make sense to consider each individual bicyclist and pedestrian in the optimization problem separately, but instead consider several bicyclists and pedestrians with the same origin and destination and roughly the same arrival time at the intersection zone together. This means that, when formulating the constraints, they are not set for each bicyclist bic and pedestrian ped individually, but for each signal phase sig. These constraints then protect all pedestrians and bicyclists assigned to this phase. In order to do so, each VRU needs to be assigned to a signal phase in the first place. This is done based on the OD information of the pedestrian or bicyclist, and on their arrival time at the intersection. In order to exploit the full potential of the optimization-based control, VRUs are considered in a demand-responsive way. Similarly to what has been described in Chapter 3, signal phases are thus requested by the infrastructure when pedestrians and bicyclists are detected. Therefore, the rolling horizon approach comes into play again.

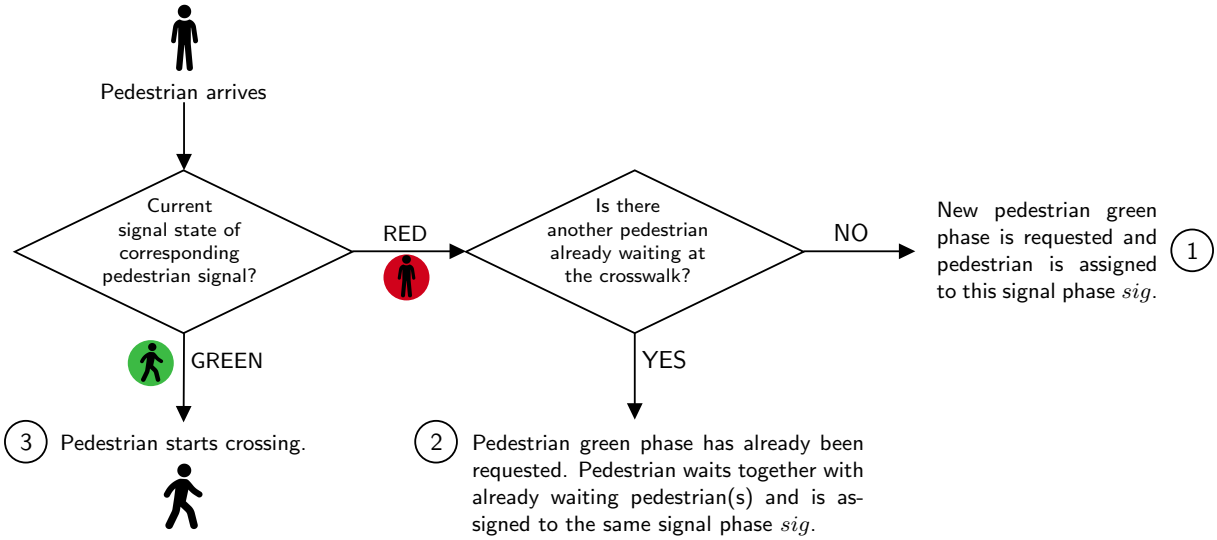

Figure 4.13: Flowchart of on-demand integration of pedestrians.

Section 4.6.1 describes how pedestrians and bicyclists are detected and how their signal phases are integrated into the rolling horizon approach. Section 4.6.2 presents the updated objective function that includes signal phases instead of individual VRUs, and Section 4.6.3 explains necessary constraints. The multimodal problem in the rolling horizon context is formulated in Section 4.6.4.

4.6.1 Integration of Pedestrians and Bicyclists into the Rolling Horizon Approach

In multimodal traffic scenarios with pedestrians and bicyclists, it is even more apparent that full information about road users at the intersection is not available from the start. By contrast, while vehicles communicate with the controller in every time step once they are within the communication range of the intersection controller, arrival times of pedestrians and bicyclists are not precisely determined ahead of time. As motivated in Section 3.1, VRUs are not assumed to be connected to the infrastructure. Therefore, their presence at the intersection needs to be detected by suitable infrastructure, and a look-ahead time horizon can only be applied if the infrastructure detects VRUs ahead of time. In the following, the integration of pedestrians and bicyclists is described separately.

Integration of Pedestrians into the Rolling Horizon Approach

Similarly to the approach presented in Chapter 3, pedestrians are detected when they are already at the crosswalk. Figure 4.13 repeats the flowchart shown in Section 3.5: if the signal is green upon their arrival, pedestrians directly start crossing the street. Otherwise, they are assigned to an already requested signal phase sig or, if their signal is currently red and there are no other pedestrians waiting, a new green phase sig is requested and the pedestrian is assigned to this new green phase.

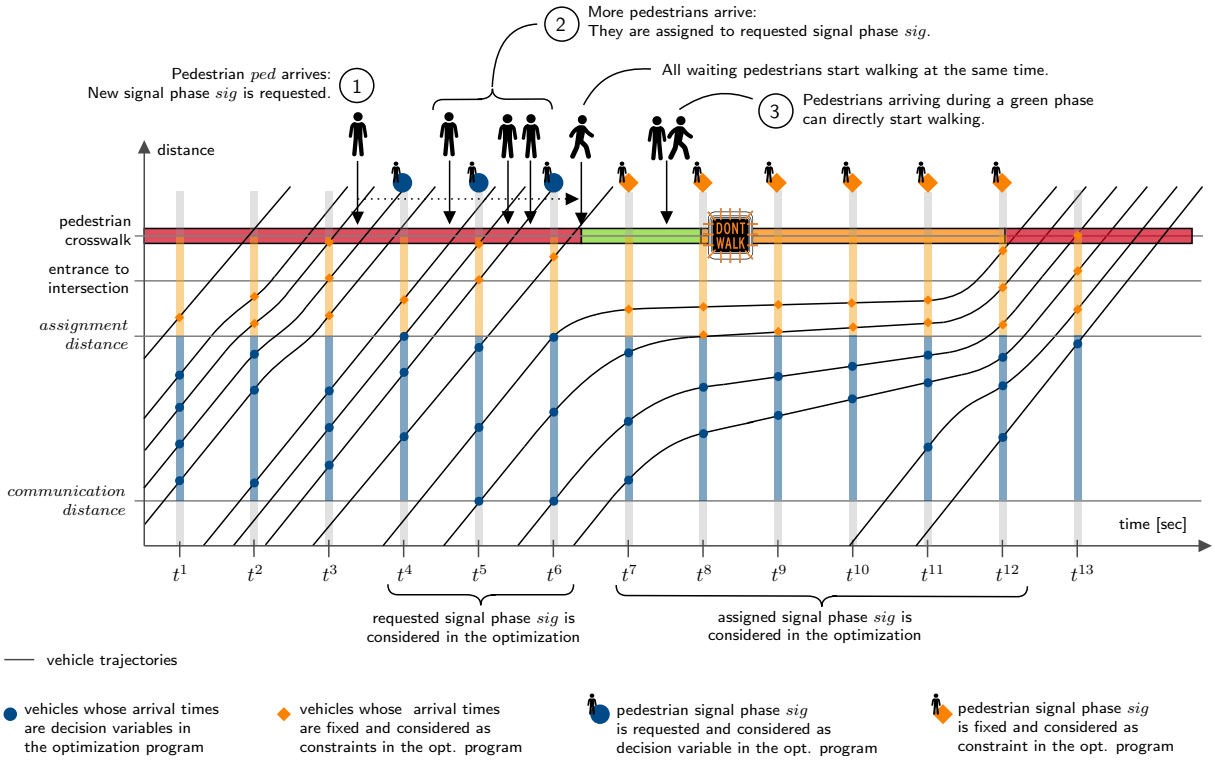

Figure 4.14: Example trajectories and schematic representation of the consideration of a requested pedestrian signal phase.

Figure 4.14 shows the three situations described above in the rolling horizon setup. Similarly to Figure 4.12 in Section 4.5, it schematically displays trajectories of vehicles on the approach to and within the intersection zone. Additionally, it features the on-demand integration of a pedestrian signal phase. As explained in Section 4.5, the optimization problem is set up and solved in fixed intervals of ϕ seconds, i.e., at times $t^k = k \cdot \phi$ that are displayed on the x-axis. At the time the problem is solved, the controller takes a snapshot of the current situation which is marked vertically, and considers approaching vehicles and requested signal phases in the optimization. It can easily be seen that, in contrast to the vehicle case, no look-ahead time is used for pedestrians. In particular, in the situation shown in the figure, no pedestrian green phase is considered when the optimization is run at times t^1, t^2, and t^3. The first pedestrian ped to request a pedestrian green phase sig arrives shortly after t^3, denoted as Situation ① in the figure. Pedestrian ped is assigned to the newly requested signal phase sig, i.e., $ped \in \mathcal{P}_{sig}$. The start time of sig is first considered as a decision variable in the optimization problem at time t^4 (depicted by the larger blue dot). Depending on the objective function and necessary constraints that will be explained in the following sections, green phase sig is scheduled after at least one round of optimization. Note that those vehicles that already have an assigned arrival time or are currently crossing the intersection (depicted as orange diamonds) cannot be rescheduled. Therefore, depending on the vehicle demand, if the signal is red upon the arrival of ped, a waiting time that allows assigned vehicles to finish crossing will occur. In the situation shown in the figure, the green phase is scheduled shortly after t^6. In the mean time,

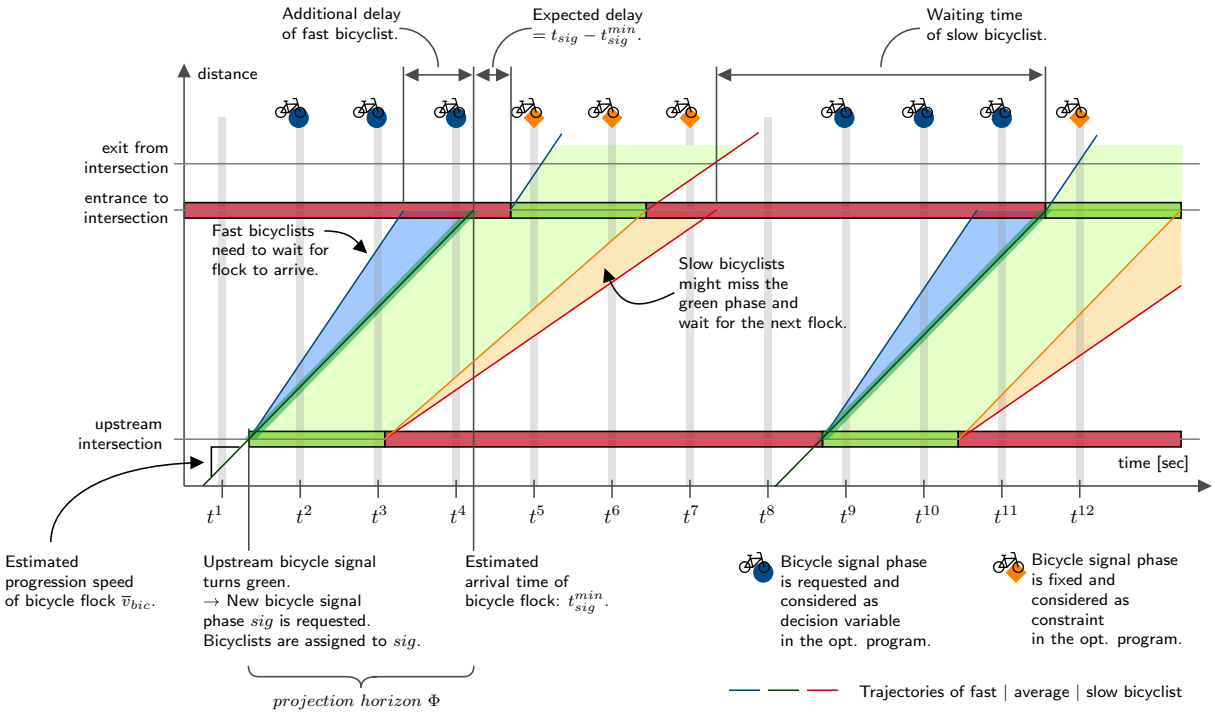

Figure 4.15: Example bike trajectories and schematic representation of the consideration of requested bike signal phases.

more pedestrians arrive and are assigned to the same signal phase sig, denoted as Situation ② in the figure. From the given setup, it becomes apparent that input parameters such as the roll period ϕ and the assignment distance as well as the communication distance (which determines how many vehicles are considered in each round of optimization) implicitly affect pedestrian LOS. Finally, when the signal green phase starts, all waiting pedestrians are allowed to start walking at the same time. If pedestrians arrive during the green phase, they can start walking without any waiting time (compare Situation ③). Current or recently ended green phases still need to be considered in the optimization problem with necessary constraints to ensure safe crossing for all assigned pedestrians. This is depicted by the large orange diamond shapes in the figure.

Integration of Bicyclists into the Rolling Horizon Approach

The approach for integrating bicyclists into the rolling horizon approach is slightly different. In particular, bicyclists are not only detected when they are already at the intersection, but the intersection controller additionally communicates with adjacent intersections. Each upstream intersection sends a notification when the bicycle signal leading to the considered intersection turns green, including the number of cyclists that are crossing the signal during the green phase and are now on their way to the considered intersection. This notification initializes the request for a bicycle green phase on behalf of the bicycle flock. The motivation behind this different approach is two-fold: first of all, cyclists have to expend energy to reach their desired speed, which makes stop and go situations exhausting for them. Secondly, unlike pedestrians,

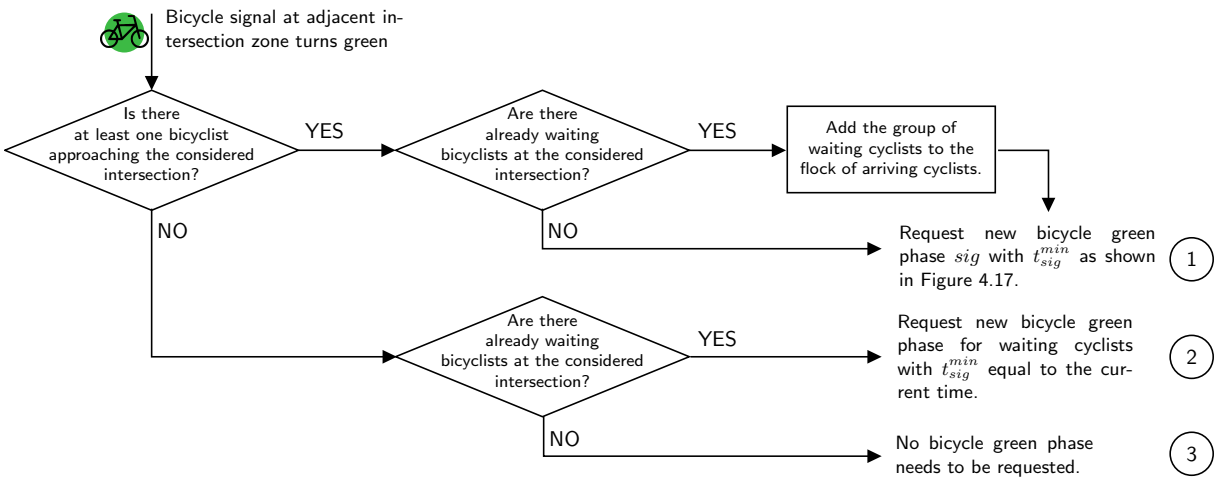

Figure 4.16: Flowchart of on-demand integration of bicyclists.

bicyclists are more likely to cross multiple successive intersections. As discussed based on the SlotIIC results in Section 3.7, the consideration of adjacent intersections can provide a more realistic arrival pattern of bicyclists and allow the control setup to implement a green wave for bicyclists that travel at a common average speed.

The procedure is schematically displayed in Figure 4.15. In this figure, bicycle trajectories are displayed instead of vehicle trajectories. In order to simplify the explanations in the following description and in the result discussion, it is assumed for now that the bicycle signals at adjacent intersections turn green in fixed cycles. When the upstream bike signal turns green (shortly after t^1 in the figure), the bicycle green phase is requested. The arrival time of the bicycle flock at the considered intersection, denoted as t_{sig}^{min}, is calculated based on the distance between the two adjacent intersections and the assumed progression speed. Depending on the objective function and the relevant constraints, the bike signal is scheduled to start any time after t_{sig}^{min}. Consequently, the bike signal phase is already considered in the optimization at t^2, even though the flock is considered to arrive after t^4. As shown in the figure, the distance between the two adjacent intersections is similar to the communication distance in the vehicle scenarios and thus relates to the projection horizon Φ. The main difference to the vehicle scenario is that the exact speed of cyclists is not known. Due to the variation in speed, cyclist flocks will diverge over distance, i.e., a larger distance between two intersections will lead to a wider flock of cyclists. Figure 4.15 schematically displays that very fast cyclists (blue trajectories) arrive before t_{sig}^{min} and therefore need to wait for an additional amount of time, and slow cyclists (red trajectories) might miss the assigned green phase. Infrastructure at the considered intersection detects waiting bicyclists who missed their assigned green phase or are just starting their ride. For the sake of simplicity, in the implemented simulation scenarios, these bicyclists will wait for the next bicycle flock and will be reassigned to the next bicycle green phase. Therefore, when the adjacent signal turns green (in fixed cycles), both bicyclists at the adjacent intersection and already waiting bicyclists are taken into account and assigned to the newly requested phase. The corresponding flowchart is shown in Figure 4.16. Situation ① corresponds to the one explained in Figure 4.15. Whether still waiting bicyclists are

added to the group of approaching bicyclists or not only affects the duration of the requested green phase. By contrast, if there are no approaching but waiting bicyclists (Situation ②), there is no need to wait for an arriving flock and the requested signal phase can theoretically start immediately. Finally, if there are neither approaching nor waiting bicyclists (Situation ③), no bicycle green phase is requested.

Clearly, once such a control is applied in reality, it will most likely be implemented along an entire corridor and the neighboring intersection will not be controlled in fixed cycles. In this situation, slower bicyclists who missed their assigned green phase could directly request a new phase that can start immediately and is bounded by a defined maximum waiting time (similarly to the request of pedestrian green phases). Additionally, the problem could be mitigated by dynamically adjusting the green phase durations if slow bicyclists are detected, and by providing the bicyclists with dynamic information such as GLOSA.

All in all, the presented scheduling optimization will take the *expected* delay of cyclists that are not yet at the intersection into account, whereas the *actual* delay of each individual cyclist might differ. This is consistent with the approach presented in Chapter 3, but it has a larger impact because of the longer distance between bicycle detection and entrance to the intersection zone. In order to actually minimize bicycle delays, it is thus important to have a good estimation of cyclist arrival times at the intersection and schedule green phases that are long enough to accommodate a large portion of a bicycle flock.

4.6.2 Updated Objective Function

The objective function defined in Section 4.3.2 contains the delay times and weighting factors of each individual vehicle, bicyclist, and pedestrian with their respective weighting factors:

$$\min \left(\sum_{veh \in \mathcal{V}} \gamma_{veh} \cdot delay_{veh} + \sum_{bic \in \mathcal{B}} \gamma_{bic} \cdot delay_{bic} + \sum_{ped \in \mathcal{P}} \gamma_{ped} \cdot delay_{ped} \right)$$
$$\text{with } \gamma_{veh}, \gamma_{bic}, \gamma_{ped} \in \mathbb{R}_0^+ \; \forall \; veh \in \mathcal{V}, bic \in \mathcal{B}, ped \in \mathcal{P},$$

where γ_{veh}, γ_{bic} and γ_{ped} are the priority indicators (weighting factors) for each vehicle veh, bicyclist bic, and pedestrian ped. Since signal phases are considered instead of individual VRUs, the objective function is reformulated in such a way that the delays and weighting factors of signal phases represent the delays and weighting factors of the VRUs that are assigned to these phases. In particular, let $\mathcal{B}_m$ and $\mathcal{P}_m$ be the sets of bicyclists and pedestrians assigned to signal phase sig_m, let γ_m be the weighting factor of sig_m, and let $delay_m$ be the delay, i.e.:

$$\gamma_m \cdot delay_m = \sum_{bic \in \mathcal{B}_m} \gamma_{bic} \cdot delay_{bic} + \sum_{ped \in \mathcal{P}_m} \gamma_{ped} \cdot delay_{ped}. \tag{4.36}$$

Note that each VRU signal phase accommodates either pedestrians or bicyclists, which means that one of the two sums in Equation (4.36) is always zero. The objective function can be

rewritten as follows:

$$\min \left(\sum_{veh \in \mathcal{V}} \gamma_{veh} \cdot delay_{veh} + \sum_{sig \in S} \gamma_{sig} \cdot delay_{sig} \right) \quad \text{with } \gamma_{veh}, \gamma_{sig} \in \mathbb{R}_0^+ \; \forall \; veh \in \mathcal{V}, sig \in S. \tag{4.37}$$

4.6.3 Constraints

Constraints that are necessary for scheduling signal phases are set up similarly to the constraints for vehicle scheduling. First of all, a specific signal phase should not be scheduled earlier than the assumed arrival time of assigned VRUs:

$$t_{sig} \geq t_{sig}^{min} \qquad \forall \; sig \in S. \tag{4.38}$$

Note that, in practice, this is especially relevant for bicycle signals, because their signal green phases are requested ahead of time.

Additionally, it is a requirement of the control strategy that pedestrians' and bicyclists' waiting times should not exceed predefined maximum waiting times that guarantee a required LOS for VRUs at the intersection. This can be ensured by adding the following constraints that are also already known from the vehicle-only scenarios:

$$t_{sig} \leq t_{sig}^{min} + \Theta_{sig} \qquad \forall \; sig \in S. \tag{4.39}$$

Constraints to Resolve Conflicts Between Vehicles and VRUs

Similarly to vehicle-vehicle conflicts, the optimized schedule either allows a considered vehicle or the VRUs of a certain signal phase to cross a common conflict point first. Therefore, we again obtain two distinct constraints where exactly one of them needs to hold in order to generate a feasible solution. Let the VRUs of signal phase sig and a vehicle veh be such that $p = p_{sig,veh}$ is the conflict point of their paths. If the VRUs of sig are assigned to arrive at the conflict point first, then the following constraint needs to hold:

$$t_{sig} + \frac{dist_{o_{sig},p}}{v_{sig}^{max}} + \Delta_{sig,veh}^{min} \leq t_{veh} + \frac{dist_{o_{veh},p}}{\hat{v}_{veh}}, \quad \text{if } t_{sig} + \frac{dist_{o_{sig},p}}{v_{sig}^{max}} \leq t_{veh} + \frac{dist_{o_{veh},p}}{\hat{v}_{veh}}. \tag{4.40}$$

The position of p and the measures $dist_{o_{sig},p}$ and $dist_{o_{veh},p}$ are derived from the conflict matrix described in Section 4.2. Since VRUs do not have an assigned speed $\hat{v}$ for crossing the intersection, the assumed maximum speed v_{sig}^{max} is applied that depends on the VRUs that use the considered signal. Additionally, the minimum headway $\Delta_{sig,veh}^{min}$ is calculated according to Equation (4.8) or (4.10) (depending on whether bicyclists or pedestrians are considered at the intersection as described in Section 4.2.2) for an assumed speed range including minimum *and* maximum speeds of considered VRUs, a pre-defined green duration t_{sig}^{green}, and some minimum

time gap $\delta^{min}_{sig,veh}$. In order to simplify the expression, Constraint (4.40) is reformulated as follows:

$$t_{sig} + \underbrace{\frac{dist_{o_{sig},p}}{v^{max}_{sig}} - \frac{dist_{o_{veh},p}}{\hat{v}_{veh}}}_{=\tau_{sig,veh}} + \Delta^{min}_{sig,veh} \leq t_{veh} \qquad \text{if } t_{sig} + \tau_{sig,veh} \leq t_{veh} \tag{4.41}$$

and the new variable $\tau_{sig,veh} = \frac{dist_{o_{sig},p}}{v^{max}_{sig}} - \frac{dist(o_{veh},p)}{\hat{v}_{veh}}$ is introduced. The variable $\tau_{sig,veh}$ represents the difference in time needed to cover the distance between the entrance to the intersection and the common conflict point – here, the difference between a fast VRU assigned to signal phase sig (traveling at v^{max}_{sig}) and a vehicle veh is calculated.

On the other hand, if vehicle veh is assigned to arrive at the conflict point first, the above constraint is obviously violated, but the following constraint needs to hold:

$$t_{sig} + \tau_{sig,veh} \geq t_{veh} + \Delta^{min}_{veh,sig}, \qquad \text{if } t_{sig} + \tau_{sig,veh} \geq t_{veh}. \tag{4.42}$$

The minimum headway $\Delta^{min}_{veh,sig}$ is now calculated according to Equation (4.7) or (4.9), again depending on whether bicyclists or pedestrians are assigned to the considered signal phase.

Similarly to what has been described for vehicle-only scenarios, the big-$\mathcal{M}$-method introduced in Section 4.4.1 is used and the previously defined constraints are rewritten as follows:

$$t_{sig} + \tau_{sig,veh} + \Delta^{min}_{sig,veh} \leq t_{veh} + \overbrace{(1 - I_{sig,veh}) \times \mathcal{M}}^{=0, \text{ if } I_{sig,veh}=1;\ \mathcal{M}, \text{ otherwise}} \quad \forall\ sig \in S, veh \in \mathcal{V} \tag{4.43}$$

$$t_{sig} + \tau_{sig,veh} + \overbrace{I_{sig,veh} \times \mathcal{M}}^{=0, \text{ if } I_{sig,veh}=0;\ \mathcal{M} \text{ otherwise}} \geq t_{veh} + \Delta^{min}_{veh,sig} \quad \forall\ sig \in S, veh \in \mathcal{V} \tag{4.44}$$

$$I_{sig,veh} \in \{0, 1\} \quad \forall\ sig \in S, veh \in \mathcal{V}$$

If $I_{sig,veh} = 1$, then Constraint (4.43) equals Constraint (4.41), and Constraint (4.44) is redundant and always holds true if $\mathcal{M}$ is big enough. On the other hand, if $I_{sig,veh} = 0$, then Constraint (4.44) equals Constraint (4.42), and Constraint (4.43) is redundant. In other words, $I_{sig,veh}$ equal to 1 indicates that the VRUs of signal phase sig arrive at the conflict point before vehicle veh, and $I_{sig,veh}$ equal to 0 indicates that vehicle veh arrives at the conflict point before the VRUs assigned to signal phase sig.

Constraints to resolve conflicts between different VRUs

As discussed in Section 3.1, conflicts between bicyclists and pedestrians without the involvement of vehicles are not resolved by the control in this thesis. If desired otherwise, adding constraints to resolve these conflicts is straight forward applying the same concepts as for vehicle-vehicle and vehicle-VRU conflicts.

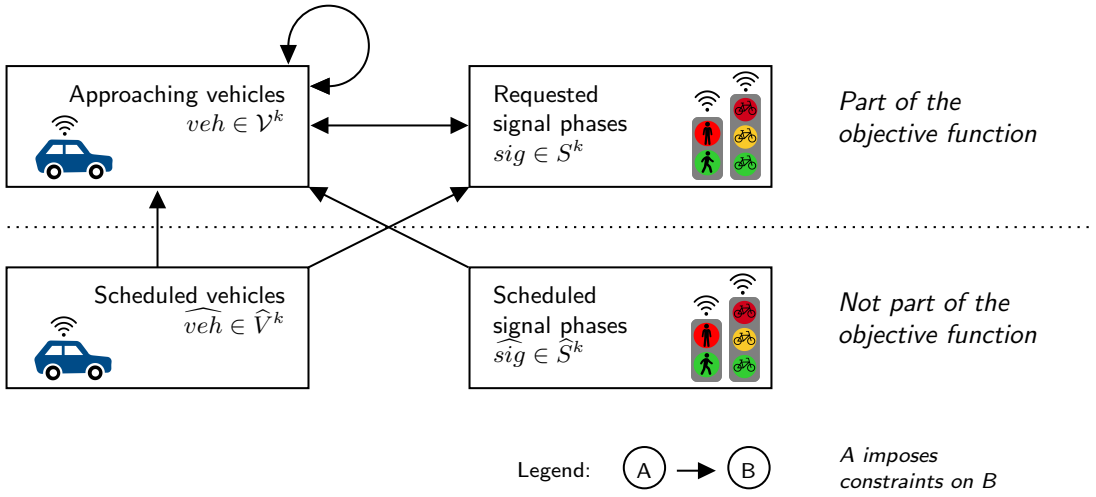

Figure 4.17: Schematic illustration of the elements of the objective function and the set of constraints at time t^k.

4.6.4 Formulation of the Multimodal Rolling-Horizon Optimization Problem

Finally, the integrated optimization problem at time t^k is formulated similarly to the optimization problem for vehicle-only scenarios. In addition to the lists $\mathcal{V}^k$ and $\widehat{\mathcal{V}}^k$ explained in Section 4.5 and the information about vehicles therein, the controller now has two new lists S^k and $\widehat{S}^k$ with requested (S^k) and assigned or current signal phases ($\widehat{S}^k$). The information about current signal phases $\widehat{sig}$ in $\widehat{S}^k$ contains the assigned start time $\hat{t}_{\widehat{sig}}$ and safety constraints such as conflict points and information to calculate necessary headways. For each requested signal phase sig in S^k, the controller has information about the (expected) earliest arrival time of assigned VRUs t_{sig}^{min}, the earliest possible start of the green phase $t_{sig}^{LB}\left(t^k\right)$, the maximum waiting time of assigned VRUs Θ_{sig}, the weighting factor γ_{sig}, and necessary constraints. The lower bound for the start time of the green phase t^{LB} makes sure that the signal phase is not assigned to start earlier than the current time, i.e., $t_{sig}^{LB}\left(t^k\right) = max\left(t_{sig}^{min}, t^k\right)$. Recall Figure 4.14, where the first pedestrian arrives shortly after t^3. When the optimization is run at time t^4, the control can only make decisions for the present and future, i.e., t^4 is the earliest possible start time of the green phase.

Figure 4.17 shows how the different input lists are linked in the overall problem formulation: Lists $\mathcal{V}^k$ and S^k are considered in the objective function. When requesting time slots, approaching vehicles "compete" with each other (compare Section 4.4.1) and with requested signal phases (compare constraints presented in Section 4.6.3). Already scheduled vehicles impose constraints on the scheduling of approaching vehicles and on currently requested signals. Already scheduled signal phases impose constraints on approaching vehicles. Since conflicts without the involvement of vehicles are not resolved by the scheduling algorithm, neither scheduled nor requested signal phases generate any constraints for other requested signal phases. The overall optimization problem can now be defined as follows:

Problem III (Intersection Control Optimization for Multimodal Scenarios at Time t^k)**.**

$$\min \left(\sum_{veh_i \in \mathcal{V}^k} \gamma_i \cdot delay_i + \sum_{sig_m \in S^k} \gamma_m \cdot delay_m \right)$$

subject to

$$delay_i = t_i - t_i^{min} \qquad \forall\ veh_i \in \mathcal{V}^k$$

$$\gamma_m \cdot delay_m = \sum_{bic \in \mathcal{B}_m} \gamma_{bic} \cdot \left(t_m - t_{bic}^{min}\right) + \sum_{ped \in \mathcal{P}_m} \gamma_{ped} \cdot \left(t_m - t_{ped}^{min}\right) \qquad \forall\ sig_m \in S^k \quad (4.45)$$

$$t_i \geq t_i^{LB}(t^k) \qquad \forall\ veh_i \in \mathcal{V}^k$$

$$t_m \geq t_m^{LB}(t^k) \qquad \forall\ sig_m \in S^k \quad (4.46)$$

$$t_i \leq t_i^{min} + \Theta_i \qquad \forall\ veh_i \in \mathcal{V}^k$$

$$t_m \leq t_{sig}^{min} + \Theta_m \qquad \forall\ sig_m \in S^k \quad (4.47)$$

$$t_i \geq t_j + \Delta_{ji}^{min} \quad \forall\ veh_i, veh_j \in \mathcal{V}^k \mid o_i = o_j\ \&\ dist_i(t^k) > dist_j(t^k)$$

$$t_i \geq \hat{t}_l + \Delta_{li}^{min} \qquad \forall\ veh_i \in \mathcal{V}^k, veh_l \in \widehat{\mathcal{V}}^k \mid o_i = o_l$$

$$t_i + \tau_{ij} + \Delta_{ij}^{min} \leq t_j + (1 - I_{ij}) \times \mathcal{M} \qquad \forall\ veh_i, veh_j \in \mathcal{V}^k$$

$$t_i + I_{ij} \times \mathcal{M} \geq t_j + \tau_{ji} + \Delta_{ji}^{min} \qquad \forall\ veh_i, veh_j \in \mathcal{V}^k$$

$$t_i + \tau_{im} + \Delta_{im}^{min} \leq t_m + (1 - I_{im}) \times \mathcal{M} \qquad \forall\ veh_i \in \mathcal{V}^k, sig_m \in S^k \quad (4.48)$$

$$t_i + I_{im} \times \mathcal{M} \geq t_m + \tau_{mi} + \Delta_{mi}^{min} \qquad \forall\ veh_i \in \mathcal{V}^k, sig_m \in S^k \quad (4.49)$$

$$t_i + \tau_{il} + \Delta_{il}^{min} \leq \hat{t}_l + (1 - I_{il}) \times \mathcal{M} \qquad \forall\ veh_i \in \mathcal{V}^k, veh_l \in \widehat{\mathcal{V}}^k$$

$$t_i + I_{il} \times \mathcal{M} \geq \hat{t}_l + \tau_{li} + \Delta_{li}^{min} \qquad \forall\ veh_i \in \mathcal{V}^k, veh_l \in \widehat{\mathcal{V}}^k$$

$$t_i + \tau_{in} + \Delta_{in}^{min} \leq \hat{t}_n + (1 - I_{in}) \times \mathcal{M} \qquad \forall\ veh_i \in \mathcal{V}^k, sig_n \in \widehat{S}^k \quad (4.50)$$

$$t_i + I_{in} \times \mathcal{M} \geq \hat{t}_n + \tau_{ni} + \Delta_{ni}^{min} \qquad \forall\ veh_i \in \mathcal{V}^k, sig_n \in \widehat{S}^k \quad (4.51)$$

$$t_m + \tau_{ml} + \Delta_{ml}^{min} \leq \hat{t}_l + (1 - I_{ml}) \times \mathcal{M} \qquad \forall\ sig_m \in S^k, veh_l \in \widehat{\mathcal{V}}^k \quad (4.52)$$

$$t_m + I_{ml} \times \mathcal{M} \geq \hat{t}_l + \tau_{lm} + \Delta_{lm}^{min} \qquad \forall\ sig_m \in S^k, veh_l \in \widehat{\mathcal{V}}^k \quad (4.53)$$

$$I_{ij} \in \{0, 1\} \qquad \forall\ veh_i, veh_j \in \mathcal{V}^k$$

$$I_{im} \in \{0, 1\} \qquad \forall\ veh_i \in \mathcal{V}^k, sig_m \in S^k \quad (4.54)$$

$$I_{il} \in \{0, 1\} \qquad \forall\ veh_i \in \mathcal{V}^k, veh_l \in \widehat{\mathcal{V}}^k$$

$$I_{in} \in \{0, 1\} \qquad \forall\ veh_i \in \mathcal{V}^k, sig_m \in \widehat{S}^k \quad (4.55)$$

$$I_{ml} \in \{0, 1\} \qquad \forall\ sig_m \in S^k, veh_l \in \widehat{\mathcal{V}}^k \quad (4.56)$$

Constraints that have already been explained in the vehicle-only case in Section 4.5 are not numbered. Constraints (4.45) represent the definition of signal delay and weighting factor.

Input Parameters	Values
Vehicle dimensions: Passenger vehicle $(len_{veh} \times wid_{veh})$	$4.00\,\mathrm{m} \times 2.00\,\mathrm{m}$
Vehicle dimensions: Bus $(len_{veh} \times wid_{veh})$	$12.00\,\mathrm{m} \times 2.50\,\mathrm{m}$
Maximum allowed speed v^{max}	$8.3\,\mathrm{m/sec}$ $(30\,\mathrm{km/h})$
Vehicle speeds for crossing the intersection $\hat{v}_{veh}$	$8.3\,\mathrm{m/sec}$ $(30\,\mathrm{km/h})$
Min. and max. acceleration acc^{min} | acc^{max}	$-4.0\,\mathrm{m/sec^2}$ | $3.0\,\mathrm{m/sec^2}$
Min. and max. bicycle speeds v_{bic}^{min} | v_{bic}^{max}	$2.7\,\mathrm{m/sec}$ | $8.3\,\mathrm{m/sec}$
Min. and max. pedestrian speeds v_{ped}^{min} | v_{ped}^{max}	$0.8\,\mathrm{m/sec}$ | $1.5\,\mathrm{m/sec}$
Min. gaps for car-following and crossing movements δ_{follow}^{min} | δ_{cross}^{min}	$0.7\,\mathrm{sec}$ | $1.0\,\mathrm{sec}$
Simulation time step τ	$0.6\,\mathrm{sec}$
Weighting factors γ_{veh}, γ_{bic}, and γ_{ped} (if not stated otherwise)	1

Table 4.2: Parameter values for the test scenarios.

Constraints (4.46) and (4.47) make sure that earliest and latest times for scheduling a requested signal phase are respected. Conflicts between arriving vehicles and requested signal phases are resolved by Constraints (4.48) and (4.49). Constraints (4.50) and (4.51) resolve conflicts between scheduled signal phases and arriving vehicles, and Constraints (4.52) and (4.53) resolve conflicts between scheduled vehicles and requested signal phases. Finally, Constraints (4.54), (4.55), and (4.56) ensure the binarity of the auxiliary matrix.

Feasibility and boundedness of the program can be proven similarly to the vehicle-only case. Analogously to the vehicle-only case, the resulting schedules are valid and do not lead to gridlocks. Again, it is especially important to carefully choose the limits Θ_{sig} and Θ_{veh} large enough. In contrast to the vehicle-only case, Θ_{sig} shall not be chosen in such a way that Constraints (4.47) are redundant, but in order to effectively limit the VRU waiting times. On the other hand, Θ_{sig} cannot limit the waiting times too narrowly, because vehicles that already have an assigned arrival time, i.e., vehicles in list $\widehat{\mathcal{V}}^k$, cannot be rescheduled. In the practical application, the optimization solver allows for adjusting these limits if no feasible schedule is found.

4.7 Simulation-based Evaluation

This section presents results of the implementation of the presented OptIIC schemes and explores the effects of different parameter settings. The control is tested using a microscopic simulation of the four-way intersection zone described in Section 4.2 and displayed in Figure 4.4. The detailed intersection geometry is shown in Appendix E.1. Section 4.7.1 briefly introduces the simulation setup. Section 4.7.2 presents results for vehicle-only scenarios and justifies parameter settings that are applied in the multimodal scenarios. Results for scenarios with vehicles and pedestrians are explained in Section 4.7.3, and Section 4.7.4 discusses results for scenarios with vehicles and bicyclists. The evaluations set the basis for the fully multimodal scenarios presented in Chapter 5.

Scenario	Vehicle demand and turning ratios			
	veh/h	*Through (%)*	*Left (%)*	*Right (%)*
Symmetric Scenario x				
Demand on each approach	$0.25 \times x$	75%	10%	15%
Asymmetric Scenario x				
Demand on minor road (each approach)	$0.2 \times x$	70%	12%	18%
Demand on major road (each approach)	$0.3 \times x$	80%	8%	12%

Table 4.3: Vehicle traffic demand for the test scenarios.

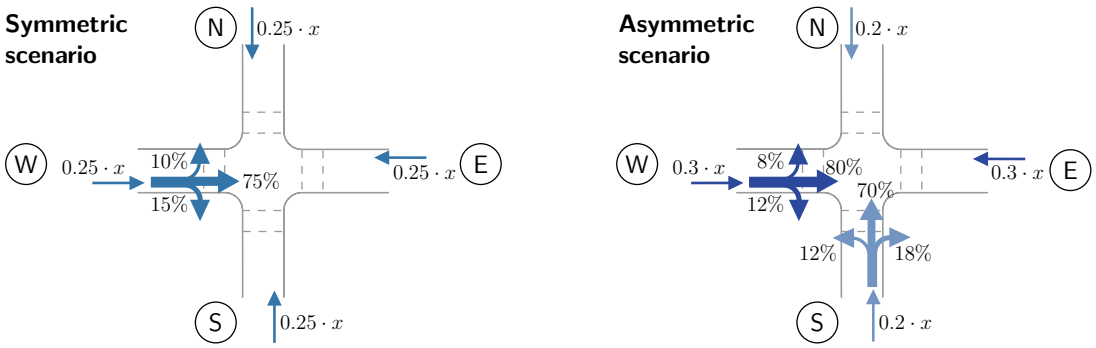

Figure 4.18: Graphical representation of the demand scenarios.

4.7.1 Simulation Setup

The presented intersection control strategies are again tested using the microsimulation platform aimsun.next together with the API and Python. The scheduling optimization problem is solved using gurobi. The overall setup will be explained in detail in Chapter 5 along with the justification of assumed parameter values. Where possible, input parameters and demand scenarios are consistent with those assumed in Chapter 3 to enable a comparison of SlotIIC and OptIIC approaches. In particular, vehicle dimensions, kinematic limitations, and desired speeds are as defined in Section 3.7. This also holds for assumed minimum and maximum speeds of VRUs. A tabular overview of the parameter values is shown in Table 4.2. All weighting factors γ_{veh}, γ_{bic}, and γ_{ped} are equal to one if not stated otherwise in the following evaluation. Again, simulations are run for one full hour with a warm-up phase of 10 minutes that is not considered in the evaluation. At least five replications are run for each presented scenario. Independently of the communication range $dist^C$, which will be varied in the following evaluations, the earliest possible arrival time of vehicles is always calculated when they are at a distance of 300 meters to the intersection. This allows for the comparison of vehicle delays in the different scenarios.

4.7.2 Results for Vehicle-only Scenarios

The results for vehicle-only scenarios presented in this section feature a comparison of the OptIIC concept to FCFS and the analysis of implications of control-specific input parameters, such as projection horizon and weighting factors. As displayed in Table 4.3 and Figure 4.18, several

different vehicle demand scenarios are implemented for the evaluation. They are denoted by x, where x is the total number of vehicles per hour considered in the scenario. Scenarios can be categorized as symmetric (i.e., the demand on all approaches is identical) or asymmetric (i.e., there is one major road with higher demand and one minor road with lower demand). In the symmetric scenarios, 75 % of the vehicles on each approach are through movement, 10 % turn left, and 15 % turn right. In the asymmetric scenarios, demand on the approaches of the major road is assumed to be 1.5 times the demand on the approaches of the minor road. On the major road, 80 % through movement, 8 % left-turning, and 12 % right-turning movement are assumed. On the minor road, turning ratios are assumed to be 12 % for left-turning movement and 18 % for right-turning movement, and consequently 70 % for through movement. The total vehicle demand at the intersection, given in vehicles per hour, is increased in steps of 400 vehicles per hour in the symmetric scenarios (i.e., in steps of 100 vehicles per hour on each approach) and 500 vehicles per hour in the asymmetric scenarios (i.e., in steps of 100 vehicles per hour on minor roads and 150 vehicles per hour on major roads). The symmetric demand scenarios are consistent with the scenarios evaluated in Chapter 3.

Comparison to FCFS

First of all, the presented OptIIC scheme is compared to an FCFS control for vehicle-only scenarios. To this end, an FCFS control is implemented that is comparable to the vehicle-only SlotIIC scenario evaluated in Section 3.7, but applies the conflict-point intersection modeling with continuous time described in this chapter. In principle, the FCFS implementation presented in this section applies the optimization scheme described in Problem II. The major differences are that (i) the optimization is run each time a vehicle signs up with the controller, and (ii) the vehicle is directly assigned with a scheduled arrival time. This means that no look-ahead time is used, i.e., the communication range $dist^C$ equals the assignment distance $dist^A$. Recalling Problem II, list $\widehat{\mathcal{V}}$ contains all vehicles that are currently approaching or crossing the intersection and list $\mathcal{V}$ contains *only* the one single vehicle that has just entered the communication range.

For the OptIIC scenario, a communication range $dist^C$ of 100 meters and an assignment distance $dist^A$ of 50 meters are set. With $dist^C$, $dist^A$, and the maximum allowed speed v^{max} being fixed, the projection horizon Φ can be calculated as follows:

$$\text{Projection horizon } \Phi\,[sec] = \frac{dist^C - dist^A}{v^{max}}. \tag{4.57}$$

In the presented setup, this leads to a projection horizon Φ of 6.02 seconds. A roll period ϕ of 3 seconds is set, such that each vehicle is considered in at least two rounds of optimization. If vehicles decelerate on the approach to the intersection, they take more time to traverse the stretch between $dist^C$ and $dist^A$ and are thus considered in more optimization rounds.

Results are displayed in Figure 4.19. Figure 4.19a shows average vehicle delays for symmetric scenarios, and Figure 4.19b shows average vehicle delays for asymmetric scenarios. It can be seen that, for both FCFS and OptIIC, average vehicle delays are very low for demand scenarios with low vehicle demand. In these scenarios, the optimization-based control cannot yield

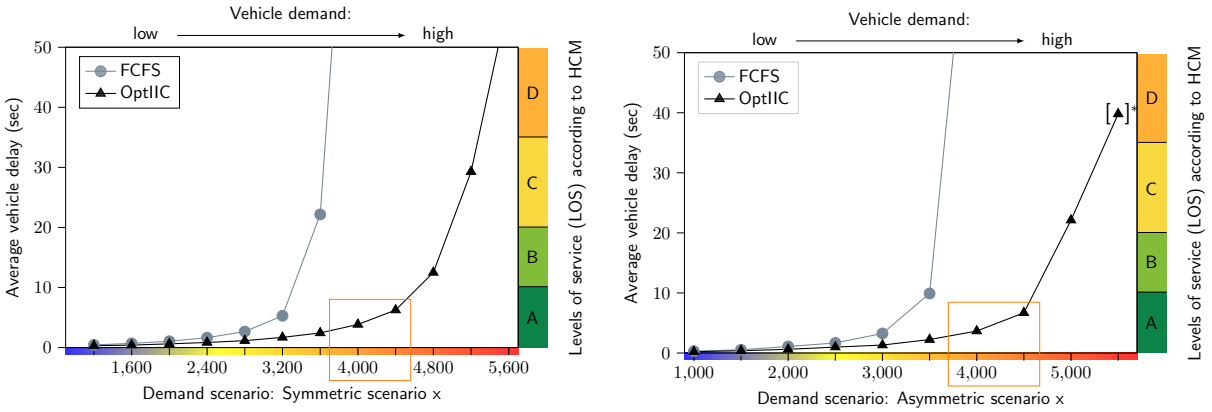

(a) Comparison of vehicle delays for different symmetric scenarios.[1]

(b) Comparison of vehicle delays for different asymmetric scenarios.
*The delay in scenario $x = 5,500$ is not accurate due to a spillover effect as described below.

Figure 4.19: Comparison of vehicle delays for the FCFS and OptIIC schemes.

significant improvements, simply because there is not much to improve. However, major improvements can be achieved in scenarios with larger demand: it is easy to see that the capacity can be increased significantly using the optimization-based control. In the symmetric scenarios shown in Figure 4.19a, the FCFS control is not able to handle the demand of x=4,000 vehicles per hour at the intersection, while this demand can be handled by the optimization-based control scheme with an average vehicle delay of only 3.8 seconds. A similar behavior can be observed in the asymmetric case: here too, the scenario with x=4,000 vehicles per hour is beyond the capacity limits of the FCFS-based control. Average vehicle delay in the OptIIC scenario with the same demand is only 3.7 seconds.

Once demand exceeds capacity, average delays increase very rapidly, essentially jumping from rather low values to unacceptably high values. This holds for both control scenarios. In all scenarios with delays that are not within the scale of up to 50 seconds, demand exceeds capacity. The same holds for the asymmetric scenario with x=5,500 vehicles per hour. In this scenario, the major road is filled, such that no more vehicles can enter the road. Virtual queues are formed in the simulation and the full vehicle demand does not enter the network. On the minor road, this spillover effect does not occur, vehicles can enter the communication range of the intersection and are served by the control. Overall, average vehicle delay is not meaningful in situations where throughput falls short of demand, which is why the respective delay value is parenthesized.

As explained in Section 3.7, the vehicle-only analysis can be used to estimate the base vehicle capacity cap^{base} given a certain demand pattern and control setup without the consideration of VRU demand. Essentially, the intersection capacity can be significantly increased from ap-

[1] Results of the FCFS scenario are roughly comparable to the vehicle-only SlotIIC approach presented in Section 3.7. Deviations result from the larger intersection zone considered here and from the setup with continuous space and time.

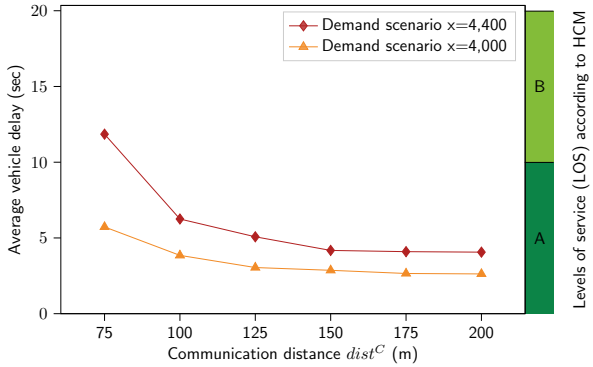

(a) Effects of increased communication distance on average vehicle delay for two symmetric demand scenarios (x=4,000 and x=4,400).

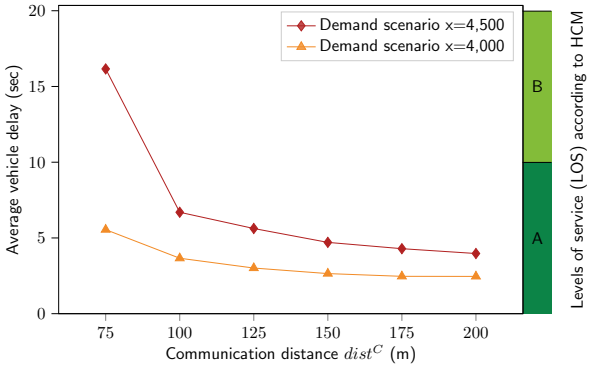

(b) Effects of increased communication distance on average vehicle delay for two asymmetric demand scenarios (x=4,000 and x=4,500).

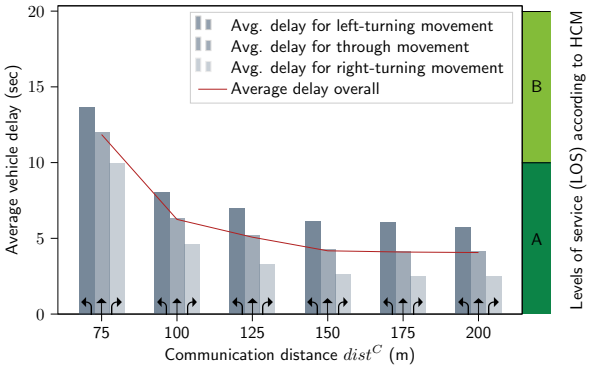

(c) Average vehicle delay depending on turning movement for the symmetric demand scenario x=4,400.

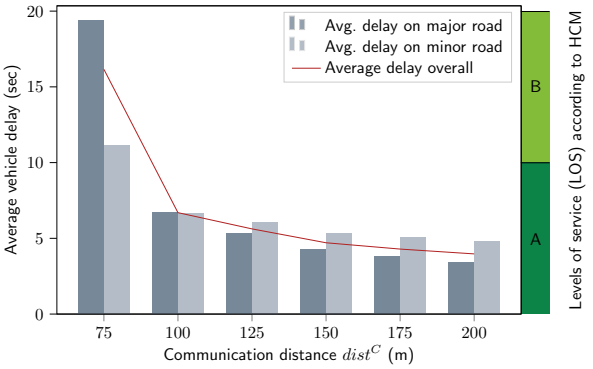

(d) Average vehicle delay depending on minor and major road for the asymmetric demand scenario x=4,500.

Figure 4.20: Comparison of average vehicle delay for increasing communication distances.

proximately 3,600 to approximately 5,200 vehicles per hour in the symmetric scenario and from approximately 3,500 to approximately 5,000 vehicles per hour in the asymmetric scenario – an improvement of more than 40 % in both scenarios. This increased base capacity can be used later on to increase vehicle capacity in a multimodal scenario, or to dedicate a larger portion of time to other modes. The capacities and average delays resulting from the OptIIC scenario further depend on control parameters that will be analyzed in the following subsections. For the following analyses, the symmetric scenarios with x=4,000 and x=4,400, and the asymmetric scenarios with x=4,000 and x=4,500 vehicles per hour (marked in Figure 4.19) will be considered. These scenarios are beyond the capacity limits of FCFS, but below the capacity limits of OptIIC.

Implications of Communication Distance

In this subsection, a comparison of results based on different communication distances is conducted. The assignment distance $dist^A$ of 50 meters is fixed, and the communication

range $dist^C$ is varied from 75 to 200 meters using steps of 25 meters. Resulting projection horizons Φ given by applying Equation (4.57) are as follows:

$$\text{Projection horizon } \Phi\,[sec] = \frac{dist^C - 50\,\mathrm{m}}{8.3\,\mathrm{m/sec}} = \begin{cases} 3.01\,\mathrm{sec}, & \text{for } dist^C = \ \ 75\,\mathrm{m} \\ 6.02\,\mathrm{sec}, & \text{for } dist^C = 100\,\mathrm{m} \\ 9.04\,\mathrm{sec}, & \text{for } dist^C = 125\,\mathrm{m} \\ 12.05\,\mathrm{sec}, & \text{for } dist^C = 150\,\mathrm{m} \\ 15.06\,\mathrm{sec}, & \text{for } dist^C = 175\,\mathrm{m} \\ 18.07\,\mathrm{sec}, & \text{for } dist^C = 200\,\mathrm{m} \end{cases}$$

As discussed previously, the roll period ϕ cannot be larger than the projection horizon (i.e., $\phi \leq \Phi$). The roll period ϕ will be fixed with three seconds in this subsection. Again, the symmetric and asymmetric demand scenarios displayed in Table 4.3 are considered.

Figures 4.20a and 4.20b show a delay comparison for different communication ranges $dist^C$. The communication range is displayed on the x-axis, and the average vehicle delay is shown on the y-axis. The two graphs in each figure correspond to the two considered demand scenarios in the symmetric setup (shown in Figure 4.20a) and in the asymmetric setup (shown in Figure 4.20b). In all four considered demand scenarios, average vehicle delays decrease with increasing communication distance. As described in Section 4.5.1, it is expected that the extension of the communication distance has a diminishing effect, the larger the communication distance gets. The effect scale additionally depends on the considered demand scenario: Effects are larger in scenarios with large demand. The consideration of symmetric and asymmetric demand patterns has a minor impact, both figures show similar shapes.

Larger capacities and decreased delays in the OptIIC scenarios are achieved by implicitly forming platoons and accommodating turning movements when it is most suitable. Figures 4.20c and 4.20d provide a more detailed look at how average delays are distributed among movements. Left-turning movement at an intersection in right-hand traffic has more conflict points with other movements than through movement, and right-turning movement has no crossing conflict at all, such that only the smaller headways for car-following behavior need to be considered. Therefore, right-turning vehicles are easier to accommodate by the control algorithm. The resulting effect is that lower delays are experienced by right-turning vehicles, and larger delays by left-turning vehicles. As can be seen in Figure 4.20c, this effect holds for all considered communication distances. While absolute differences between average delays for left-turning, right-turning and through movement remain almost constant, relative differences increase. Figure 4.20d displays how average delays on the minor and major road differ in asymmetric demand scenarios. Due to the larger demand on the major road, the formation of platoons is easier and more efficient there. Vehicles on the major road will benefit from this process, while vehicles on the minor road will have to wait for platoons on the major road to pass. Therefore, the average delay on the minor road is expected to be larger than the delay on the major road. This can be seen in Figure 4.20d for communication distances of at least 125 meters. Here, both absolute and relative differences in delay increase with an increasing communication distance. In principle, the effect holds for the scenarios

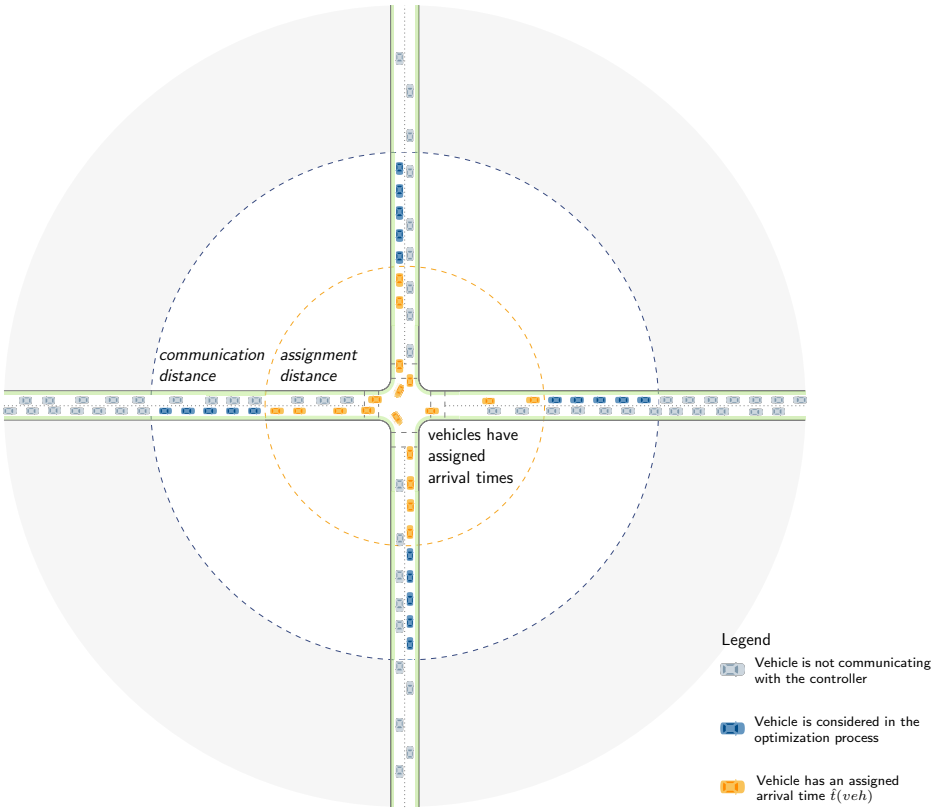

Figure 4.21: Schematic representation of communication and assignment distance.

with lower communication range as well. The difference is that vehicles on the major road experience a larger delay before even reaching the communication range. Considering the scenario with a communication distance $dist^C$ of 75 meters, the average delay on the major road is 19.4 seconds, while the average delay on the minor road is 11.1 seconds. Vehicles are only considered in the optimization scheme when they are at a distance of 75 meters to the entrance of the intersection. Until reaching that distance, vehicles on the major road have already experienced 10.2 seconds of delay, while vehicles on the minor road reach the communication range with an average delay of only 2 seconds. This, however, is not considered in the optimization problem. The reason is that the control algorithm is not aware of those vehicles that are not within the communication distance. In Figure 4.21, an example situation is shown where the east-west direction of a four-way intersection is the major road with larger demand. However, since the vehicles in the gray area are not visible to the controller, the control will consider five arriving vehicles from each direction, i.e., it assumes the demand to be equal on each approach. This can lead to suboptimal schedules from the global perspective. It needs to be noted here, that the scenarios shown in Figure 4.20d do not exceed capacity limits, i.e., formed queues are only temporary.

In order to include the global demand perspective, weighting factors could be changed such that already experienced delay is considered, or vehicles in the back of a queue are implicitly taken into account. This is proposed by the so-called max-pressure approach presented by

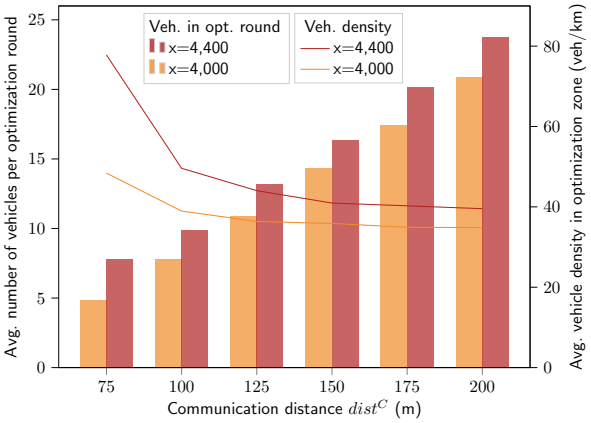

(a) Average number of vehicles considered per optimization round and average vehicle density in optimization zone for two symmetric demand scenarios (x=4,000 and x=4,400).

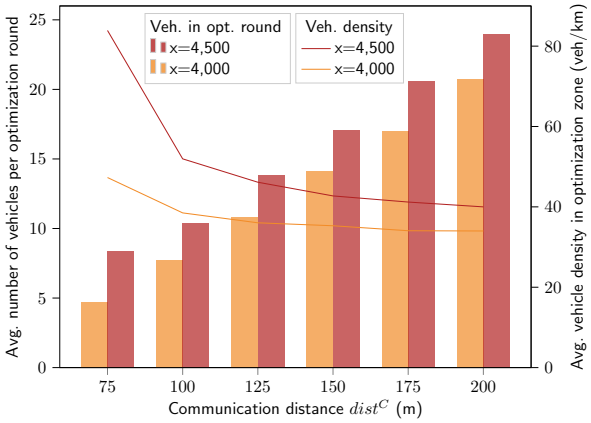

(b) Average number of vehicles considered per optimization round and average vehicle density in optimization zone for two asymmetric demand scenarios (x=4,000 and x=4,500).

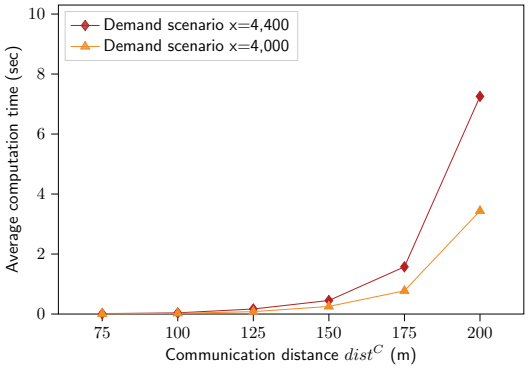

(c) Average computation times per optimization round in symmetric demand scenarios (x=4,000 and x=4,400).[1]

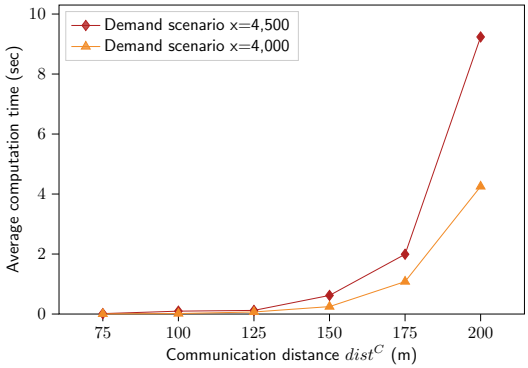

(d) Average computation times per optimization round in asymmetric demand scenarios (x=4,000 and x=4,500).[1]

Figure 4.22: Comparison of number of vehicles considered in the optimization run and computation times for increasing communication distances.

R. Chen et al. [2020]. They calculate the weighting factor for each vehicle according to the number of vehicles queued in their incoming lane and the number of vehicles queued in the downstream link, and achieve stable vehicle queues in a symmetric network with symmetric demand. However, they implement a larger communication range of 150 meters and thus do not consider an additional disadvantage of the small communication range, namely that only very few vehicles are considered in each round of the optimization, which makes it difficult to identify platoons.

The bars in Figures 4.22a and 4.22b display how many yet unscheduled vehicles are considered in each optimization round (on average), depending on the vehicle demand and on

[1]The optimization was run on a Lenovo G4-i3it with Intel(R) Core(TM) i7-8665U CPU with 4 kernels, 2.11 GHz and 32 GB RAM.

the projection horizon. Recalling Problem II, this corresponds to the size of $\mathcal{V}^k$ in each time step $t^k = \phi \times k$. The size of $\mathcal{V}^k$ reflects the average density of vehicles on the stretch of the road between communication distance and assignment distance: Let $|\mathcal{V}^k|$ be the number of vehicles considered in the optimization round. All vehicles veh in $\mathcal{V}^k$ are currently on one of the incoming lanes and within a distance of $dist^A < dist_{veh}(t^k) \leq dist^C$. Therefore, the average density in vehicles per kilometer can be calculated as

$$density\left[\frac{veh}{km}\right] = \frac{|\mathcal{V}^k|}{(dist^C - dist^A) \times (no.\ of\ lanes)} \times 1,000.$$

Average densities are displayed by the line plots in Figures 4.22a and 4.22b. Vehicle densities are larger in the scenarios with shorter communication distance, since the larger delays lead to a queuing effect and thus higher densities on the incoming lanes. It can be seen that the shapes of the lines clearly resemble the delay plots in Figures 4.20a and 4.20b. Nevertheless, in the considered demand scenarios, the absolute number of vehicles considered in the optimization problem predominantly depends on the communication range.

Unfortunately, the increased benefits of a larger communication distance in scenarios with large demand are countered by the costly optimization process. Figures 4.22c and 4.22d show that the linear increase in the number of vehicles considered in the optimization problem results in an exponential increase in computation times. As a trade-off between computation times and delay reduction, a communication distance of 150 meters, i.e., a projection horizon of 12.05 seconds seems like a good compromise in the scenarios considered so far: (i) the number of vehicles within a communication distance of 150 meters could be handled by the control with low computation times (compare Figure 4.22), and (ii) delay reductions were significant for an initial increase in communication range of up to 150 meters, but marginal, if the communication range was further increased (compare Figure 4.20). In the future, communication distance could be adjusted dynamically in order to consider as many vehicles as possible without exceeding acceptable computation times. Acceptable computation times depend on further parameter settings, which in turn are related to various considerations as explained below.

Parameter Settings for Further Scenarios

In the following, the impact of two other input parameters, the assignment distance $dist^A$ and the roll period ϕ, will be discussed qualitatively before fixing parameter settings for multimodal scenarios.

Assignment distance $dist^A$: In terms of optimization performance, the assignment distance $dist^A$ cannot be analyzed in an isolated manner, but only in combination with the communication range $dist^C$. As defined by Equation (4.57), those two parameters together specify the projection horizon Φ that has a significant influence on runtime and results as discussed previously. In practical applications, the assignment distance needs to be large enough to allow for vehicles to adjust their speed in order to reach the intersection zone at the assigned time and speed without compromising safety. In addition, pedestrians and cyclists should be able

to understand the approaching behavior of vehicles. A larger assignment distance can thus be beneficial for smooth and emission-friendly trajectory planning. On the other hand, those vehicles within the assignment distance cannot change their assigned arrival time. Increasing the assignment distance thus has a negative influence on LOS for VRUs, especially on pedestrians, because they might have to wait for more vehicles with assigned arrival times to pass.

Roll period ϕ: The roll period ϕ determines in which interval the optimization is set up and solved. It is necessary that the roll period ϕ is smaller than the projection horizon Φ. Otherwise, a vehicle could traverse the entire stretch from the start of the communication distance until crossing the assignment distance without being considered in any optimization round. On the other hand, in order to be implementable in practice, the roll period ϕ needs to be larger than the optimization runtime: If the optimization is run at time t^k, then the results of the previous run at time t^{k-1} need to be available as an input. Running the optimization more frequently increases the flexibility, since vehicles are dynamically reassigned using the new information in each optimization run. According to Levin and Rey [2017], the roll period has a minor impact on overall results, however. Own simulations showed that the impact depends on the number of times each vehicle is considered in the optimization formulation with a decreasing tendency: if roll period and projection horizon are equal, each vehicle is considered in at least one round of optimization. Decreasing the roll period such that each vehicle is considered at least twice significantly improves the results. Further reducing the roll period has a decreasing effect. Nevertheless, it needs to be noted that a small roll period also helps pedestrians. As previously shown in Figure 4.14, pedestrians need to wait for the next optimization run after arriving at the crosswalk. The roll period should thus be small enough to make this waiting time negligible.

For the following scenarios, an assignment distance $dist^A$ of 50 meters is chosen. This allows for vehicles to slow down and accelerate without compromising safety. Note that with the parameters considered here (maximum allowed speed, kinematic limitations), vehicles need up to 25 meters to decelerate and accelerate again before entering the intersection. Additionally, vehicles will decelerate early enough to make VRUs feel safe [Ackermann et al., 2019]. The roll period ϕ is chosen to be 3 seconds. This allows for the control to run up to 3 seconds to find the optimal result. Considering the projection horizon Φ of 12.05 seconds defined by the communication distance $dist^C$ of 150 meters and the assignment distance $dist^A$ of 50 meters, each vehicle is considered in at least four optimization rounds.

Consideration of Weighting Factors

In the scenarios presented so far, all vehicles have the same weighting factor $\gamma_{veh} = 1$. However, it is one research goal to integrate policy objectives into the control strategies and this can be realized by choosing appropriate weighting factors.

The generic selection of weighting factors in a similar setup has been described by Levin and Rey [2017]: They state that if $\gamma_{veh} = 1$ for all vehicles, the objective is to maximize intersection throughput. If γ_{veh} instead depends on the earliest possible arrival time of veh, then the objective is fairness-based. As described previously, R. Chen et al. [2020] use weighting

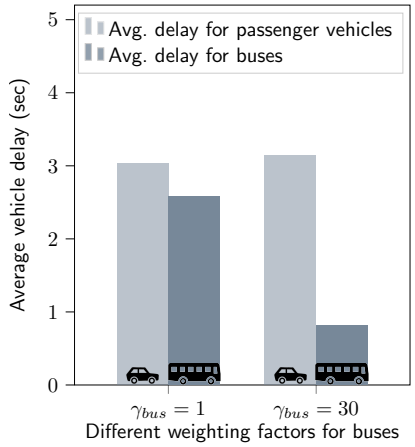

(a) Average delays in the asymmetric demand scenarios (x=4,000) with buses running on the major road.

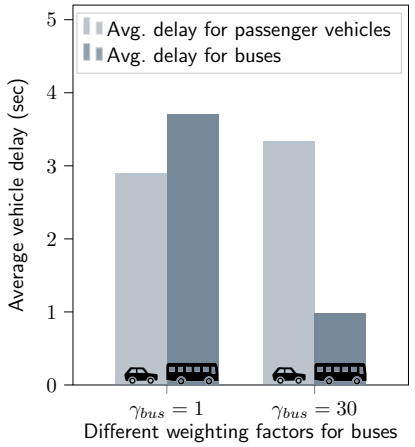

(b) Average delays in the asymmetric demand scenarios (x=4,000) with buses running on the minor road.

Figure 4.23: Impact of prioritizing PT vehicles by assigning a higher weighting factor.

factors that correspond to queues on incoming and outgoing lanes with the objective of obtaining queue stability.

In this thesis, it is desired to apply weighting factors as an individual policy prioritization for specific road users. To this end, the current scenario setup is extended by integrating a bus line that runs every five minutes on one of the roads. The asymmetric demand scenario with 4,000 passenger vehicles per hour is considered, and a communication range of 150 meters is applied. Figure 4.23 shows the resulting average delays of passenger vehicles and buses for two different bus weighting factors. In the scenarios displayed in Figure 4.23a, the bus runs on the major road, whereas in the scenarios displayed in Figure 4.23b the bus runs on the minor road. Since average delays have been shown to be shorter on the major road, in Figure 4.23a, the average delay for buses is slightly lower than the average delay for passenger vehicles, even if the bus is not treated with priority. Prioritizing the bus by assigning a higher weighting factor of $\gamma_{bus} = 30$, while weighting factors for all other vehicles remain, significantly reduces the bus delay. At the same time, the average delay of other vehicles is only slightly increased. If the bus runs on the minor road, average bus delay is higher than passenger vehicle delay in the scenario with $\gamma_{bus} = 1$. In the scenario with $\gamma_{bus} = 30$, bus delay is reduced similarly to the scenario with the bus on the major road, but both bus and vehicle delay are slightly larger.

All in all, the intended prioritization is effective in the considered scenarios. Since the idea of individual prioritization can undermine the goal of overall efficiency, effects of weighting factors on overall delays need to be carefully evaluated for each specific scenario.

Conclusion

The analysis of vehicle-only scenarios featured a comparison of the improved OptIIC setup with FCFS and revealed a significant capacity increase of more than 40 % for both considered

Input Parameters	Values
Communication range and assignment distance $dist^C$ | $dist^A$	$150\,\mathrm{m}$ | $50\,\mathrm{m}$
Roll period ϕ	$3\,\mathrm{sec}$
Green phase duration t_{ped}^{green}	$5.4\,\mathrm{sec}$
Maximum pedestrian waiting time Θ_{ped} (if not stated otherwise)	$42\,\mathrm{sec}$
Weighting factor γ_{ped} (if not stated otherwise)	1
Pedestrian demand	200 pedestrians per hour per leg

Table 4.4: Parameter values for the test scenarios with vehicles and pedestrians.

demand configurations (symmetric and asymmetric demand). The performance of the OptIIC scheme further depends on parameter settings, first and foremost on the communication distance to the intersection controller (corresponding to the projection horizon in the rolling horizon setup). Clearly, an increasing projection horizon can improve the performance of the scheduling algorithm. This improvement, however, comes at the cost of increased computation times, because more vehicles need to be considered in each round of the optimization – a good trade-off needs to be found that depends on the demand scenario. The detailed result analysis additionally showed that vehicle movements with fewer conflicts experience shorter delays because they are easier to schedule, and vehicles on the major road benefit from the implicit platoon formation of the scheduling algorithm. These effects especially become apparent if the communication distance of the intersection controller is increased. If the projection horizon is too small and queues are larger than the communication range, vehicles in the back of the queue are not considered by the algorithm. This could be overcome in the future by incorporating queues on incoming and outgoing lanes into the weighting factors as described by R. Chen et al. [2020]. Finally, larger weighting factors for buses were applied and show that they are in fact effective and allow the control setup to integrate policy objectives. This will be further explored when evaluating multimodal scenarios in the following.

4.7.3 Results for Scenarios with Vehicles and Pedestrians

In the OptIIC scenarios, there are three different dials that can be adjusted in order to balance pedestrian waiting times and vehicle delays: (i) the bounded maximum pedestrian waiting times Θ_{ped}, (ii) the duration of a green phase t_{ped}^{green}, and (iii) the pedestrian weighting factor γ_{ped}. All of these parameters ultimately influence what portion of time is dedicated to pedestrian movement. In the following, their impacts are analyzed by implementing test scenarios that are based on the analysis of presented SlotIIC scenarios in Section 3.7. Before going into detail, it is worth noting that the larger capacity resulting from the optimization-based control as compared to FCFS that was revealed in Figure 4.19 can be used in the multimodal scenarios. Considering a fixed vehicle demand, the larger vehicle capacity essentially allows for dedicating a larger portion of time to pedestrian movement without exceeding vehicle capacity. On the other hand, considering a fixed LOS for pedestrians, the larger vehicle capacity allows for serving a larger number of vehicles.

In addition to the assumptions listed in Sections 4.7.1 and 4.7.2, further parameters that are necessary for the considered multimodal control are displayed in Table 4.4. In particular,

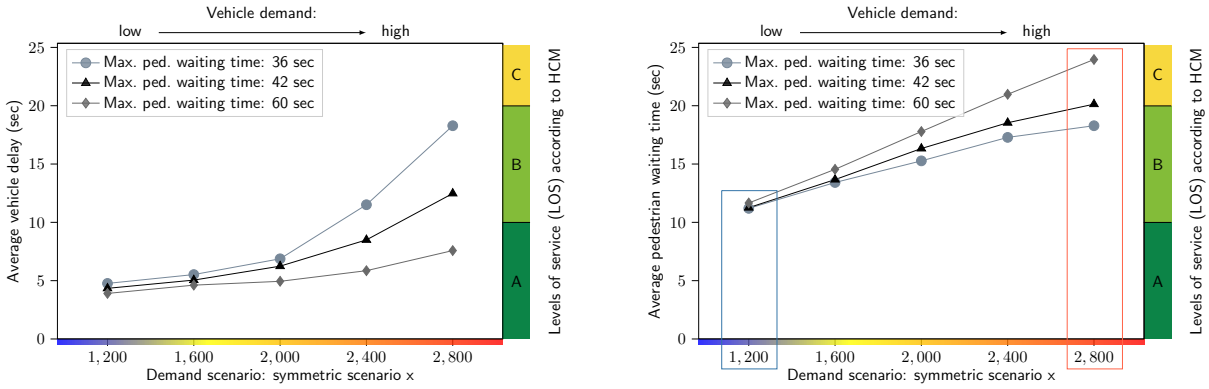

(a) Avg. vehicle delay depending on vehicle demand and Θ_{ped}.

(b) Avg. ped. waiting times depending on vehicle demand and Θ_{ped}.

Figure 4.24: Average vehicle delays and pedestrian waiting times depending on vehicle demand and maximum pedestrian waiting time Θ_{ped}.

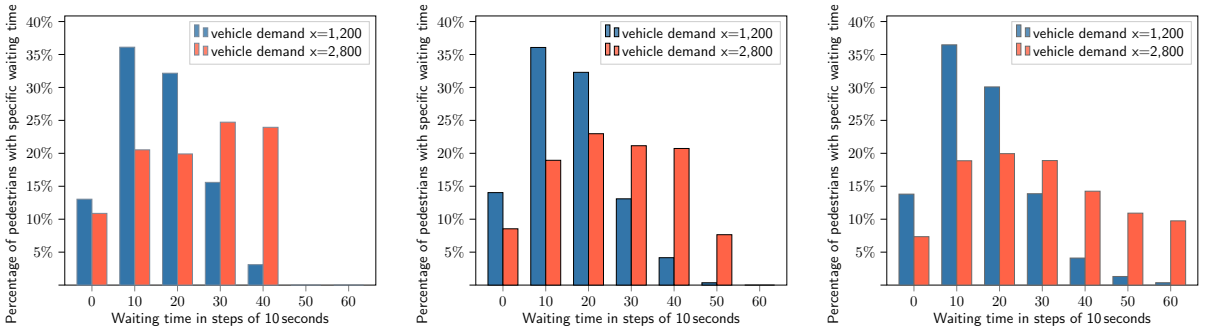

(a) Histogram of ped. waiting times for $\Theta_{ped} = 36$ sec.

(b) Histogram of ped. waiting times for $\Theta_{ped} = 42$ sec.

(c) Histogram of ped. waiting times for $\Theta_{ped} = 60$ sec.

Figure 4.25: Histogram of pedestrian waiting times for different maximum pedestrian waiting times Θ_{ped}.

the maximum pedestrian waiting time Θ_{ped} is 42 seconds and all pedestrians have the same weighting factor γ_{ped} of one if not stated otherwise. Just like in Section 3.7, the duration of the pedestrian green phase is 5.4 seconds. Again, the green phase is only intended for pedestrians to start crossing, and a longer clearance time makes sure that they can finish crossing the street safely. Finally, pedestrian demand is assumed to be 200 pedestrians per hour per leg. For the sake of simplicity, the following analyses focus on pedestrians crossing only one leg of the intersection – pedestrians who cross diagonally or rather twice are not considered.

Impact of Maximum Pedestrian Waiting Times

Limiting pedestrian waiting times by imposing upper bounds Θ_{ped} was the method used to prioritize pedestrian movement and to ensure a pre-defined pedestrian LOS in the slot-based strategies presented in Chapter 3. The constraint makes sure that when a new pedestrian green phase is requested, this phase is started after at most Θ_{ped} seconds. The impact of

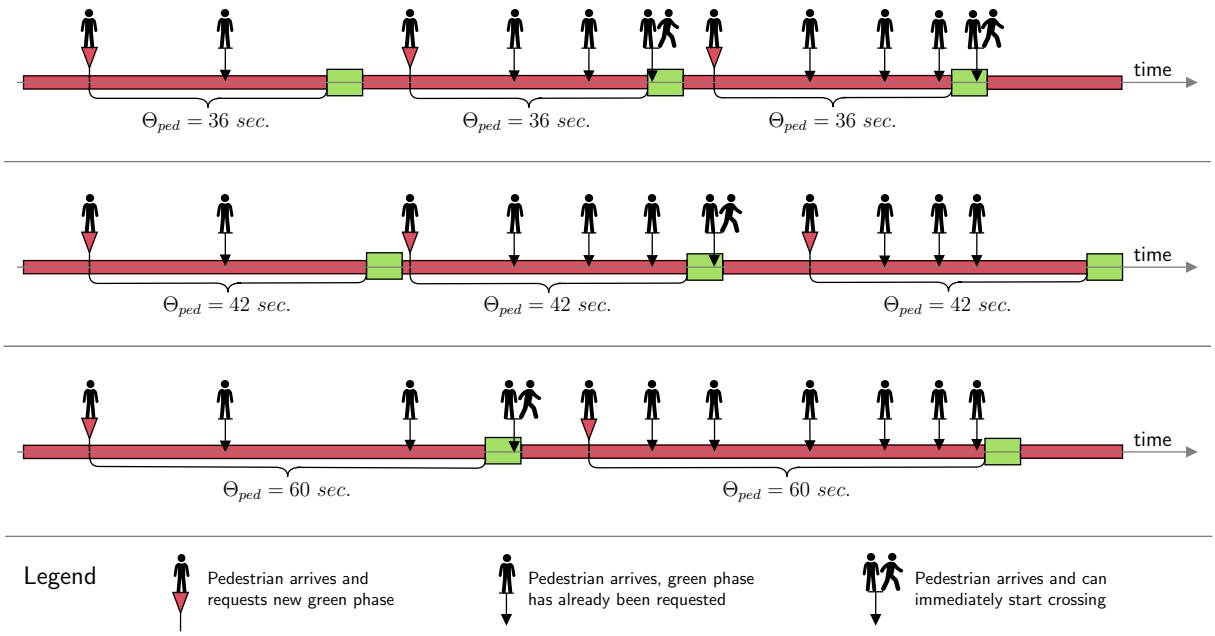

Figure 4.26: Schematic representation of pedestrian green phases depending on Θ_{ped}.

adjusting maximum pedestrian waiting times in the OptIIC strategy is shown in Figure 4.24. Figure 4.24a shows average vehicle delays for an increasing vehicle demand and different maximum pedestrian waiting times, while Figure 4.24b presents average pedestrian waiting times for the same scenarios. The maximum pedestrian waiting time Θ_{ped} is altered from the base scenario with 42 seconds to 36 and 60 seconds. Similarly to the results that were presented in Chapter 3 (Figure 3.22 in Section 3.7), Figure 4.24 shows that upper bounds on pedestrian waiting times have an increasing effect with increasing vehicle demand: if vehicle demand is large, then pedestrian green phases are more often *only* scheduled after the maximum pedestrian waiting time. On the other hand, if vehicle demand is low, these upper bounds are more often redundant, because it is optimal from the control perspective to start the green phase earlier anyways.

These effects can be seen from the histograms in Figure 4.25, where the percentages of pedestrians with a specific waiting time (in steps of 10 seconds) for two different vehicle demand scenarios (x=1,200 and x=2,800) are shown for the three different values of Θ_{ped}, i.e., 36 seconds in Figure 4.25a, 42 seconds in Figure 4.25b, and 60 seconds in Figure 4.25c. It can be seen that histograms for the scenario with low vehicle demand (blue bars) look very similar for all three control scenarios. The situation changes in the scenario with large demand (orange bars): here, the full bandwidth of allowed waiting times is used. Figure 4.26 schematically shows how the maximum pedestrian waiting time influences the timing of green phases in a situation where the maximum allowed waiting time is always fully utilized by the controller. Here, smaller values of Θ_{ped} lead to more frequent green phases. This leads to more green time overall which allows for a larger percentage of pedestrians to luckily arrive during a green phase and thus experience no delay. It also means that more pedestrians request a new green phase and their delay thus matches Θ_{ped}. Both effects are visible in the histograms considering

	Demand scenario $x = 1,200$			*Demand scenario* $x = 2,400$		
	SlotIIC	OptIIC	Diff. (%)	SlotIIC	OptIIC	Diff. (%)
Max. pedestrian waiting time $\Theta_{ped} = 36\,\text{sec}$						
Avg. vehicle delays [sec]	6.8	4.8	-29%	65.6	11.5	-82%
Avg. pedestrian waiting times [sec]	11.6	11.2	$-\ 3\%$	14.5	17.3	$+19\%$
Max. pedestrian waiting time Θ_{ped}*= 42sec*						
Avg. vehicle delays	5.6	4.3	-23%	29.7	8.5	-71%
Avg. pedestrian waiting times [sec]	13.3	11.3	-15%	16.8	18.5	$+10\%$
Max. pedestrian waiting time Θ_{ped}*= 60sec*						
Avg. vehicle delays	3.9	3.9	$\pm\ 0\%$	15.3	5.9	-61%
Avg. pedestrian waiting times [sec]	15.7	11.7	-25%	23.3	21.0	-10%

Table 4.5: Comparison of results with vehicles and pedestrians (SlotIIC and OptIIC)[1]

the scenario with large demand. All in all, a smaller upper bound on pedestrian waiting times leads to more frequent pedestrian green phases and thus larger vehicle and smaller pedestrian delay, especially in scenarios with larger vehicle demand. This trend is expected and similar to what has been observed in Chapter 3.

In comparison to the SlotIIC results presented in Chapter 3, average vehicle delays are smaller and vehicle capacities are larger in the scenarios presented here. The comparison provided in Table 4.5 features all three applied parameter values for Θ_{ped} and two demand scenarios for each control setup. As an example, the scenario with Θ_{ped} of 42 seconds showed a vehicle delay of approximately 30 seconds for x=2,400 vehicles (and capacity was exceeded for x=2,800 vehicles) when applying the most flexible SlotIIC strategy. In comparison, average vehicle delays are below 15 seconds even in the scenario with x=2,800 vehicles for the comparable OptIIC strategy as shown in Figure 4.24a. Pedestrian waiting times are comparable overall. Differences result from the different way pedestrians are integrated. In Chapter 3, the crosswalk is activated as soon as possible while respecting a minimum vehicle "green time." If a pedestrian arrives and vehicle movement has been allowed for a while already (let's say for 10 seconds), then the pedestrian does not have to wait for a maximum of Θ_{ped}, but $\Theta_{ped} - 10$ seconds, even with saturated conditions. On the other hand, this same waiting time also applies if vehicle demand is rather low (at least if the pedestrian green phase cannot be scheduled earlier without having to reschedule an existing vehicle reservation). Pedestrians thus do not profit from low vehicle demand that much in the SlotIIC strategy – average pedestrian waiting times for different demand scenarios thus stay in a tighter range for SlotIIC as compared to the OptIIC setup (compare Table 4.5). As an example, in the scenario with Θ_{ped}=42 seconds and vehicle demand of x=1,200, average pedestrian waiting times were

[1]The SlotIIC and OptIIC approaches are tested on two different intersection geometries – compare Figures 3.7a and 3.7b. The intersection simulated to test the OptIIC is larger because it features bicycle paths. Therefore, necessary pedestrian clearance times are larger. Other than than, the two setups are comparable.

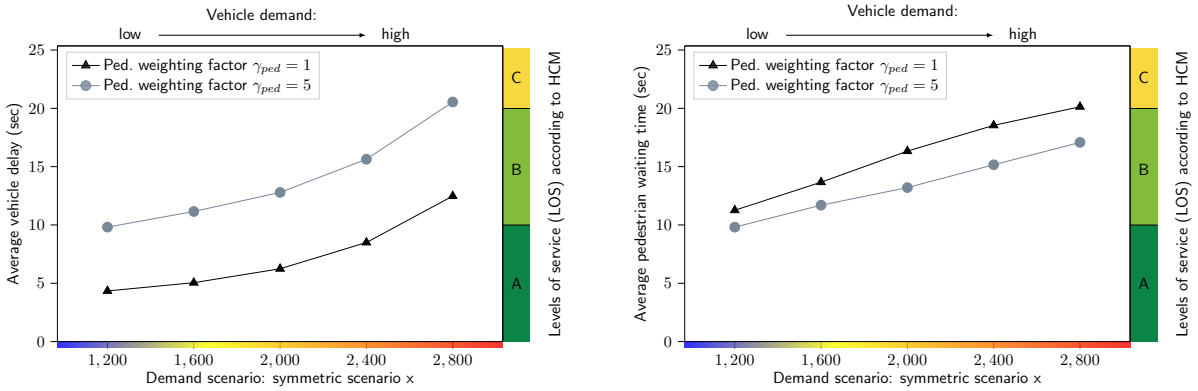

(a) Avg. vehicle delays depending on vehicle demand and γ_{ped}.

(b) Avg. ped. waiting time depending on vehicle demand and γ_{ped}.

Figure 4.27: Average vehicle delays and pedestrian waiting times depending on vehicle demand and pedestrian weighting factor γ_{ped}.

12.8 seconds in the SlotIIC scenario, and 11.3 seconds in the OptIIC scenario. In the demand scenario with x=2,400 vehicles, average pedestrian waiting times were 16.8 seconds for SlotIIC and 18.5 seconds for OptIIC.

It needs to be noted here that smaller maximum pedestrian waiting times Θ_{ped} might not always be respected in the OptIIC approach, since imposing a very tight bound can lead to infeasibility. In contrast to the approaches presented in Chapter 3, vehicles are not rescheduled in the OptIIC strategies. Therefore, if vehicles are already closer to the intersection zone than the assignment distance $dist^A$, their arrival times are fixed. In the practical implementation, if the conflicting movements do not allow activating signal sig within the next Θ_{sig} seconds, then the constraint $t_{sig} \leq t_{sig}^{min} + \Theta_{sig}$, i.e., Constraint (4.47) in Problem III is relaxed. Therefore, the maximum waiting time is not guaranteed here – in contrast to the SlotIIC approaches, where the pre-defined maximum waiting time is never exceeded and conflicting vehicle reservations can be canceled and rescheduled. In the scenarios presented in Figures 4.24 and 4.25, this was not an issue.

Impact of Pedestrian Weighting Factor

As described above, upper bounds on pedestrian waiting times Θ_{ped} do not have a significant influence in situations with low vehicle demand. In order to balance pedestrian waiting times for all considered vehicle demand scenarios, altered pedestrian weighting factors γ_{ped} are tested. Figure 4.27 shows results for the basic scenario with γ_{ped} equal to 1 and a scenario with pedestrian weighting factor γ_{ped} equal to 5. Again, average vehicle delay is shown in Figure 4.27a and average pedestrian waiting time is shown in Figure 4.27b. It can be seen that for all considered scenarios, the larger pedestrian weighting factor increases vehicle delay and reduces pedestrian waiting time. Since the larger weighting factor leads to a prioritized scheduling of pedestrian green phases, green phases are scheduled more frequently. However, similarly to the analysis of weighting factors in the vehicle case, the effect cannot necessarily

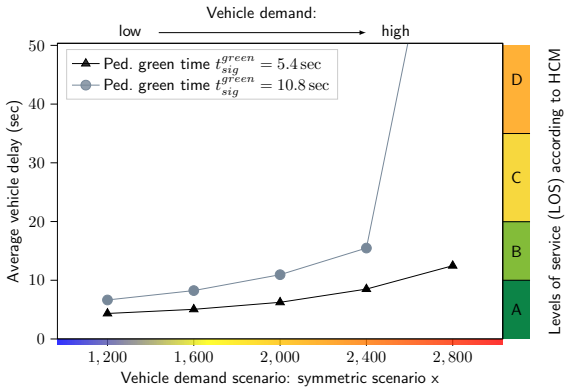

(a) Avg. vehicle delays depending on vehicle demand and t_{sig}^{green}.

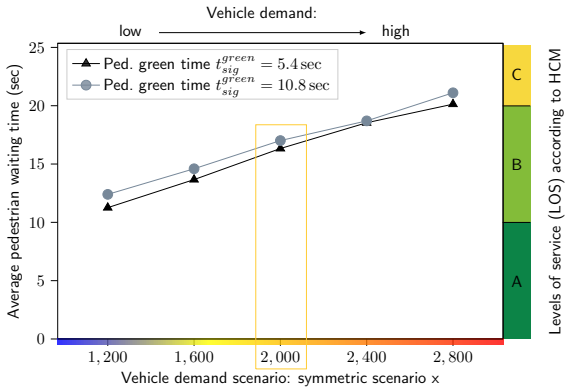

(b) Avg. ped. waiting times depending on vehicle demand and t_{sig}^{green}.

Figure 4.28: Average vehicle delays and pedestrian waiting times depending on vehicle demand and pedestrian green phase duration t_{sig}^{green}.

(a) Histogram of ped. waiting times in steps of 5 seconds for t_{sig}^{green}=5.4 seconds and symmetric vehicle demand x=2,000.

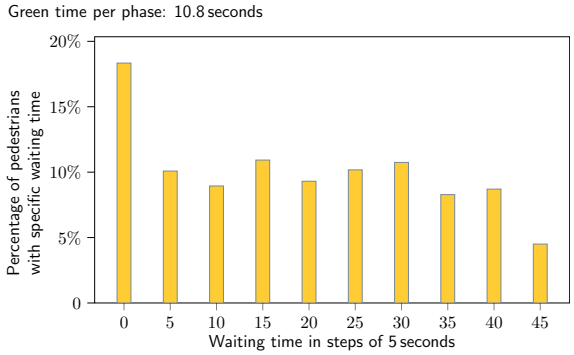

(b) Histogram of ped. waiting times in steps of 5 seconds for t_{sig}^{green}=10.8 seconds and symmetric vehicle demand x=2,000.

Figure 4.29: Histograms of pedestrian waiting times.

be generalized: If the more frequent scheduling of pedestrian signal phases at some point leads to queues in the incoming vehicle lanes, the larger number of vehicles could lead to an opposite effect and decrease the pedestrian LOS. In addition, the effect of changing pedestrian demand needs to be analyzed. If there are several pedestrians waiting at a pedestrian crosswalk, their weighting factors are added up, which also changes the overall situation. All in all, it is critical to balance weighting factors such that pedestrians are prioritized (if desired), but the increased weighting factor doesn't turn into the opposite by provoking vehicle queues.

Impact of Pedestrian Green Phase Duration

In the scenarios analyzed so far, each requested pedestrian signal phase has a green phase duration of 5.4 seconds. If a green phase is set to be longer, then the probability of a pedestrian arriving during the green phase increases. Figure 4.28 shows average vehicle delays and

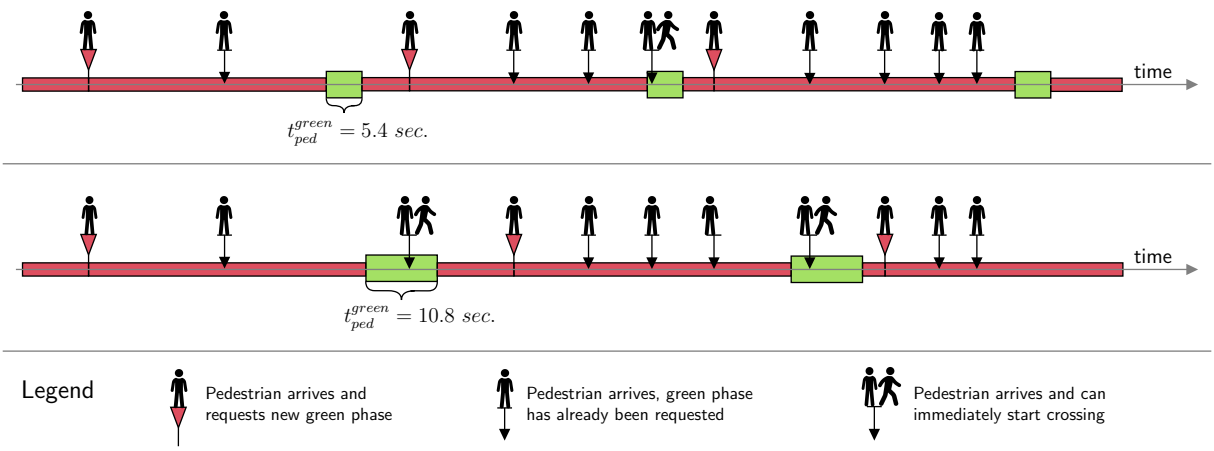

Figure 4.30: Schematic representation of green phases depending on t_{sig}^{green}.

average pedestrian waiting times for increasing vehicle demand and two different green phase durations t_{sig}^{green}: 5.4 seconds and 10.8 seconds. As expected, vehicle delay increases with increased pedestrian green phase durations (see Figure 4.28a). The scenario with 2,800 vehicles per hour and pedestrian green phase durations of 10.8 seconds even exceeds vehicle capacity. It might be somewhat unexpected that average pedestrian waiting times are not reduced – they are even slightly higher in the scenario with larger green phase durations. The reason is that larger pedestrian green times with otherwise unchanged parameters lead to less frequent green phases, as scheduling a longer green phase is more costly from the optimization point of view. Therefore, average pedestrian waiting times are similar, but the distribution is different.

In order to better understand the phenomenon, the scenario with 2,000 vehicles per hour is analyzed in more detail. Here, the scenario with green phase durations of 5.4 seconds leads to approximately 75 green phases per hour per leg (i.e., a total green time of 405 seconds per hour per leg), while the scenario with green phase durations of 10.8 seconds results in approximately 64 green phases per hour per leg (i.e., a total green time of approximately 690 seconds per hour per leg). Adding the necessary clearance times, this means that each leg is blocked from vehicle movement for a total duration of 1,215 seconds in the first scenario and 1,380 seconds in the second scenario, respectively, which explains the difference in vehicle delay shown in Figure 4.28a.

The corresponding average pedestrian waiting times are further disaggregated in Figure 4.29, where the histograms of pedestrian waiting times are shown in steps of 5 seconds. The direct comparison shows that there are in fact more "lucky pedestrians" who arrive during a green phase in the scenario with green phase durations of 10.8 seconds (displayed in Figure 4.29b). At the same time, 21.5% of pedestrians wait for more than 30 seconds in comparison to only 16% in the scenario with green phase durations of 5.4 seconds. The effects of green phase durations on the timing of signal phases are schematically shown in Figure 4.30. Again, it needs to be noted that results cannot be generalized: if pedestrian demand is larger, there will be more "lucky pedestrians" in both scenarios, which will change the overall average pedestrian delay.

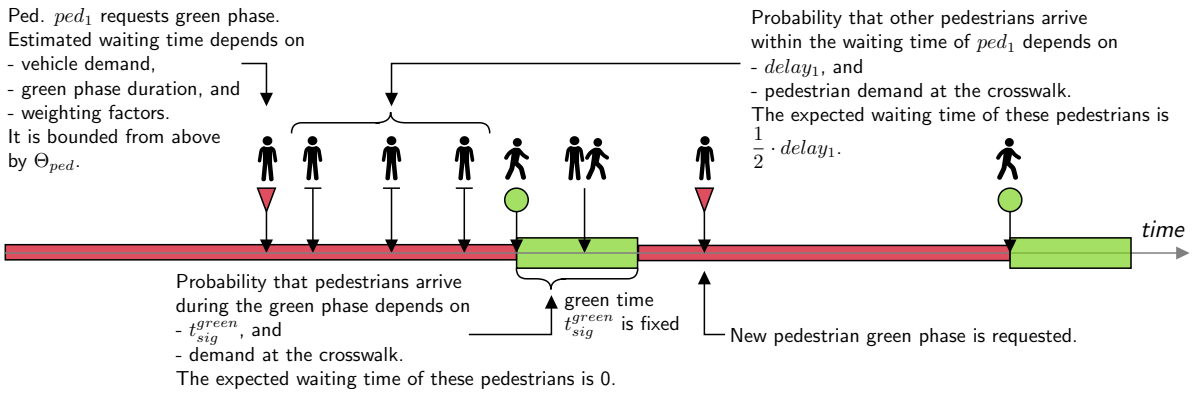

Figure 4.31: Schematic representation of the influence of control parameters and demand scenario on average pedestrian waiting times.

Conclusion

From the discussions on the last few pages, it becomes clear that effects of parameter adjustments need to be evaluated in detail. It is especially critical to observe that effects on average waiting times depend on the interaction between control parameters and considered demand scenario – including both vehicle and pedestrian demand. This context is schematically displayed in Figure 4.31. In the figure, the first pedestrian ped_1 requests a pedestrian green phase. Now, her waiting time depends on control parameters such as weighting factors and green phase duration, but also on the situation at the intersection, i.e., the current vehicle demand. In the extreme scenario, if there are no approaching vehicles, the pedestrian green phase can be scheduled to start immediately when the optimization is run. Additionally, the waiting time is bounded from above by Θ_{ped}. Now, the probability that other pedestrians arrive during the time that ped_1 is waiting depends on her waiting time and on the pedestrian demand. If pedestrian demand is large, more pedestrians are likely to arrive and, since their expected waiting time is shorter than the waiting time of ped_1, the overall average pedestrian waiting time will be lower. Not to mention that additional pedestrians will increase the weighting factor of the requested signal phase, thus possibly providing for an earlier start of the green phase. Finally, the probability that pedestrians arrive during the green phase depends on the duration of the green phase and the demand at the crosswalk. Obviously, these pedestrians do not experience delay. All in all, if ped_1 is the only pedestrian, then the average waiting time will equal the waiting time of ped_1, if more pedestrians arrive until the end of the green phase, the average delay will be reduced. Finally, the frequency and duration of pedestrian green phases will also influence vehicle delays. Due to the complexity of the interdependencies, once the estimated demand situation and policy objectives are clear, parameters need to be tuned for the specific situation.

4.7.4 Results for Scenarios with Vehicles and Bicyclists

As explained in Section 4.6.1, the integration of bicyclists into the OptIIC control scheme follows the overall idea of providing a bicycle green wave. Therefore, upper bounds Θ_{bic} on (expected) waiting times of bicyclists arriving from surrounding intersections are chosen to be

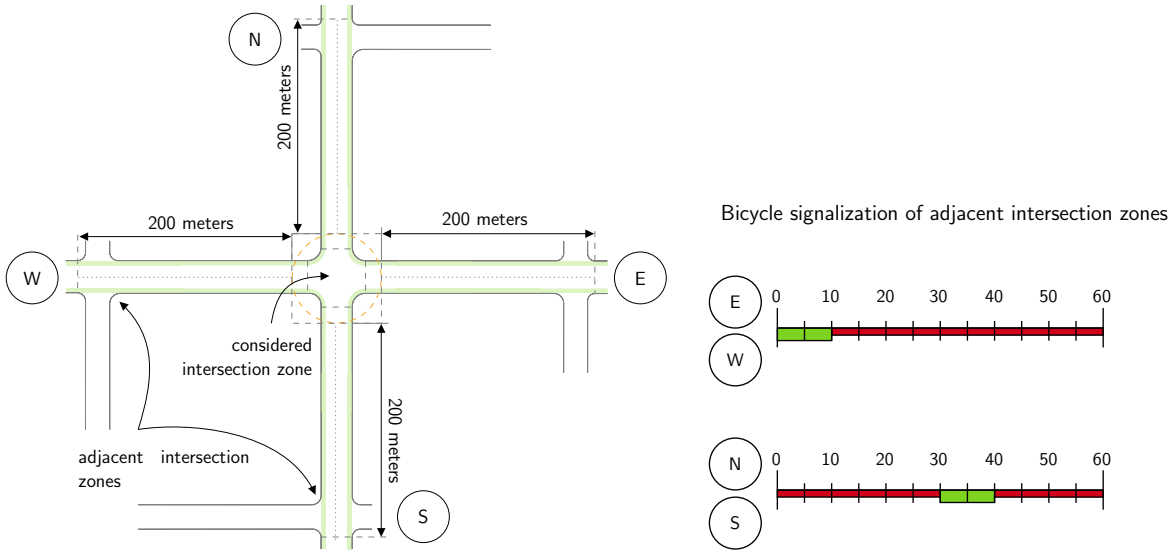

Figure 4.32: Considered grid of intersections and bicycle signalization at adjacent intersections.

very small. For this reason, weighting factors γ_{bic} are expected to have little influence, because they can only affect the start of bicycle green phases within the narrow time frame between the expected bicycle arrival time t_{bic}^{min} and $t_{bic}^{min} + \Theta_{bic}$. Therefore, in the following, the impact of minimum bicycle green phase durations t_{sig}^{mingr} will be analyzed. In contrast to pedestrian green phases, the green phase durations of bicycle signals depend on the number of bicyclists considered in the respective phase. If bicycle demand is larger, green phases are extended to facilitate the crossing of a larger number of bicyclists. In particular, let t_{sig}^{mingr} be the minimum green phase duration. It is assumed to be sufficiently long for a capacity of cap bicyclists. If there are more than cap bicyclists assigned to green phase sig, then the phase is extended by the assumed time needed t_{bic}^{needed} per each additional cyclist. Let $\mathcal{B}_{sig}$ be the set of bicyclists and $|\mathcal{B}_{sig}|$ be the number of cyclists assigned to signal phase sig. Then the resulting green phase t_{sig}^{green} can be calculated as follows:

$$t_{sig}^{green} = \begin{cases} t_{sig}^{mingr} & \text{if } |\mathcal{B}_m| \leq cap, \\ t_{sig}^{mingr} + t_{bic}^{needed} \cdot (|\mathcal{B}_m| - cap) & \text{otherwise.} \end{cases} \tag{4.58}$$

It needs to be noted that results additionally depend on the distances of the considered intersection to adjacent intersections (compare Section 4.6.1) and on how these intersections are controlled. This will be explained together with the discussion of results. In the test scenario considered here, the intersection lies within a grid of intersections with link lengths of 200 meters (compare Figure 4.32). It is assumed that the adjacent signals turn green in fixed cycles of 60 seconds with green phase durations of 10 seconds. Due to the artificially wide waiting area for cyclists, capacity is not an issue at the adjacent intersection zones. In the scenarios presented in the following, vehicle demand is kept constant (with x=2,000 vehicles in the symmetric demand scenario), and bicycle demand is increased with demand scenarios shown in Table 4.6. It is assumed that direct left turns are not allowed for bicyclists, and left-turning bicyclists will hence cross the first street together with the bicycle through movement and then join the flock on the other approach. In order to simplify result discussions,

Symmetric Bicycle Scenario x	**Bicycle demand and turning ratios**			
	bic/h	*Through (%)*	*Left (%)*	*Right (%)*
Demand on each approach	$0.25 \times x$	85%	0%	15%

Table 4.6: Bicycle traffic demand for the test scenarios.

Input Parameters	**Values**
Distance to adjacent intersections	$200\,\text{meters}$
Bicycle signal control at adj. intersections	According to Figure 4.32
Bicycle green phase t_{sig}^{green}	According to Equation (4.58) with
Scenario 1	$t_{sig}^{mingr} = 5.4\,\text{sec}$, $cap = 2\,\text{bic}$, $t_{bic}^{needed} = 1.2\,\text{sec}$
Scenario 2	$t_{sig}^{mingr} = 10.8\,\text{sec}$, $cap = 4\,\text{bic}$, $t_{bic}^{needed} = 1.2\,\text{sec}$
Maximum bicyclist waiting time Θ_{bic}	$10\,\text{sec}$
Weighting factor γ_{bic}	1
Vehicle demand	$2,000$ vehicles per hour (symm. demand scenario)

Table 4.7: Parameter values for the test scenarios with vehicles and bicyclists.

left-turning bicyclists are not included into the simulation. Right-turning bicyclists are simulated to make the flock progression behavior more realistic, but, because of the RToR policy for bicyclists, they do not experience delay and are hence not considered in the evaluation. In addition to these assumptions and to the parameter values applied in Sections 4.7.1 and 4.7.3, it is assumed that the maximum estimated bicycle waiting time Θ_{bic} for bicyclists arriving from adjacent intersections is 10 seconds and that all bicyclists have the same weighting factor γ_{bic} of one. The parameters are additionally listed in Table 4.7.

When evaluating the mixed scenarios with vehicles and bicyclists, we are again interested in average vehicle delays and bicycle waiting times, but also in the percentage of bicyclists that had to stop at the traffic signal. These results are displayed in Figure 4.33. Figure 4.33a shows the average vehicle delay for increasing bicycle demand and two different minimum green phase durations t_{bic}^{mingr}: 5.4 seconds and 10.8 seconds. First of all, it can be seen from the figure that, as expected, larger bicycle green phase durations negatively affect vehicle delay. Vehicle delays additionally increase with rising bicycle demand in both control scenarios, because bicycle green phase durations depend on the number of bicyclists, and larger bicycle demand leads to more frequent bicycle green phases. In the scenario with 200 bicyclists per hour, for example, there are only 50 bicyclists per hour on each approach, such that not every green phase at the adjacent intersections leads to the request of a new green phase at the considered intersection. In comparison to the results presented in Chapter 3 (compare Figure 3.24 in Section 3.7), vehicle delays are again significantly reduced. Nevertheless, it needs to be noted that the two setups are not fully comparable, because no adjacent intersections were taken into account for the SlotIIC approach.

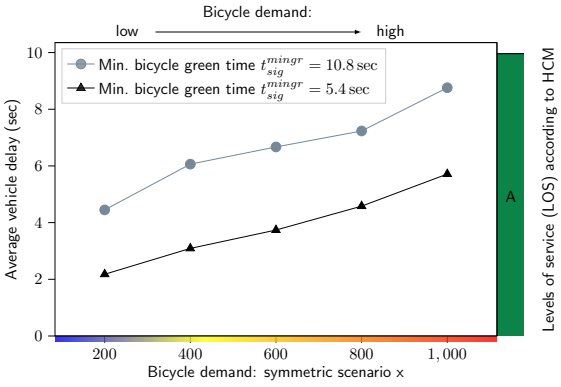

(a) Avg. vehicle delays depending on bicycle demand and minimum bicycle green phase.

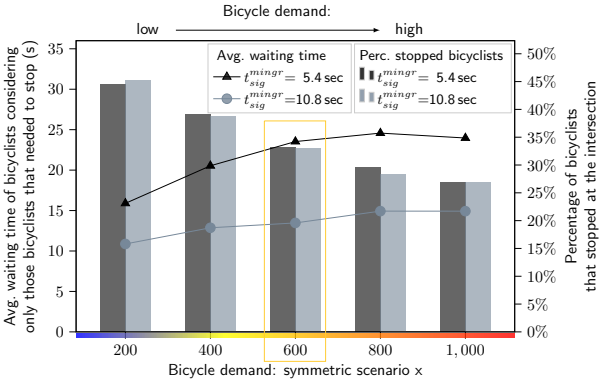

(b) Avg. percentage of bicyclists that stopped at the intersection and their avg. waiting time depending on bicycle demand and t_{sig}^{mingr}.

Figure 4.33: Average vehicle delays and bicycle waiting times depending on bicycle demand and minimum bicycle green phase durations t_{sig}^{mingr}.

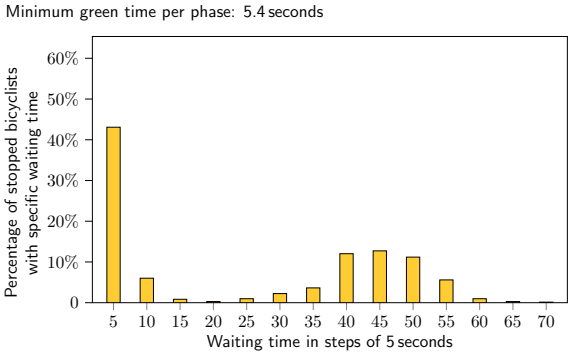

(a) Histogram of bic. waiting times in steps of 5 seconds for t_{sig}^{mingr}=5.4 seconds and symmetric bicycle demand x=600.

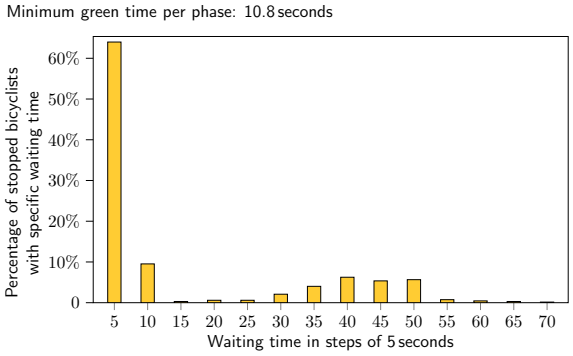

(b) Histogram of bic. waiting times in steps of 5 seconds for t_{sig}^{mingr}=10.8 seconds and symmetric bicycle demand x=600.

Figure 4.34: Histograms of bicycle waiting times.

Figure 4.33b shows the percentage of bicyclists that stopped at the intersection (bar plots) and the average waiting times considering only the stopped bicyclists (line plots). First of all, the percentage of stopped bicyclists is significantly reduced compared to Section 3.7. It seems somewhat surprising, however, that the minimum green phase duration does not significantly affect the percentage of cyclists that catch the green wave. On the other hand, it does have an influence on average waiting times. It can be noticed that waiting times for the scenarios with t_{sig}^{mingr} of 10.8 seconds are smaller than for the scenarios with t_{sig}^{mingr} of 5.4 seconds, independently of the considered demand. Figure 4.34 shows the histograms of bicycle delays in steps of five seconds for the demand scenario with 600 bicyclists per hour and minimum green times of 5.4 seconds (Figure 4.34a) and 10.8 seconds (Figure 4.34b). Again, only those bicyclists who had to stop at the intersection, i.e., whose waiting times are larger than zero, are considered. It can be seen that in the scenario with a minimum green time of 5.4 seconds more longer delays occur, while the vast majority of delays in the scenario with a minimum

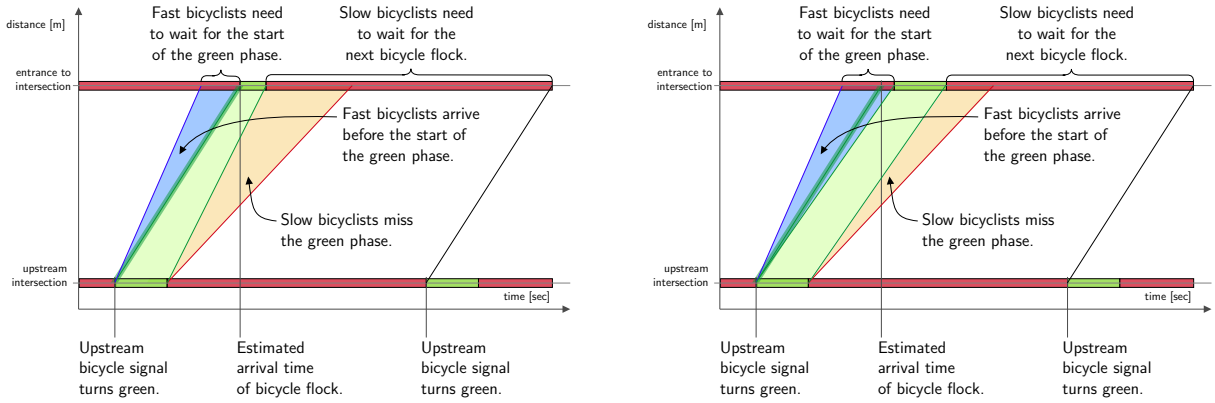

(a) Schematic representation of bicycle green phases for a shorter t_{sig}^{green}.

(b) Schematic representation of bicycle green phases for a longer t_{sig}^{green}.

Figure 4.35: Schematic representation of bicycle green phases for different values of t_{sig}^{green}.

green time of 10.8 seconds are below 5 seconds. Consequently, the average delay of stopped bicyclists in the situation shown in Figure 4.34a is 23.5 seconds and in the situation in Figure 4.34b is 13.5 seconds.

The explanation for this phenomenon is shown in Figure 4.35: Figure 4.35a shows a situation with a short bicycle green phase. Due to the short green phase, slower bicyclists miss their assigned phase and need to wait for the next bicycle flock. If a longer green phase is considered, however, the green phase tends to start slightly later. As previously discussed for pedestrian green phases, implementing longer green phase durations is more costly for the control. Therefore, more fast bicyclists need to stop (for a few seconds), but fewer slow bicyclists miss the green wave as shown in Figure 4.35b. Cyclist behavior is simulated without the support of GLOSA, signal countdown timers, or adaptive behavior that can be assumed for cyclists who regularly use the same route. The decreasing trend in percentages of stopped bicyclists displayed by the bar plots in Figure 4.33b results from the longer bicycle green phases combined with an earlier green phase start due to larger accumulated weighting factors, but also from the speed harmonization effect of larger cycle flocks: faster cyclists are slowed down such that they can now pass without stopping. In fact, average waiting times of stopped bicyclists increase, because an increasing portion of the group of stopped bicyclists are slower cyclists. All in all, more than 50 % of bicyclists cross the intersection without stopping in the scenario with low bicycle demand and more than 70 % in the scenario with very high bicycle demand - a significant improvement compared to the uncoordinated SlotIIC approach. Average waiting times considering all bicyclists with through movement range between 4 and 8 seconds in all scenarios and are hence very low – and again significantly lower than the waiting times measured in Section 3.7 (ranging between 9 and 18 seconds).

The histograms in Figure 4.34 also show that, in both control scenarios, the maximum waiting time of bicyclists is 70 seconds. This results from the fact that bicyclists who miss the green phase assigned for their flock need to wait for the next flock. Since the bicycle signal at the adjacent intersection turns green every 60 seconds, the next flock will arrive approximately

60 seconds later and will wait for a maximum of Θ_{bic} which is set to be 10 seconds. This correlation already indicates that the signalization of adjacent intersection zones impacts the LOS at the intersection zone that is considered here. If the cycle time is larger, the maximum waiting time for slower cyclists will also be larger with the given control setup. Additionally, longer green phases at the adjacent intersection zone can lead to more dispersed bicycle flocks.

Conclusion

The consideration of adjacent intersections allowed for more realistic bicycle arrival patterns and enabled more bicyclists to cross the intersection without stopping as compared to the setup in Chapter 3. However, due to the interconnection of the considered intersection zone with adjacent intersection zones and the stochastic cyclist behavior, it is even more difficult to comprehensively evaluate the effect of control parameters in the presented scenarios. Overall, the results not only depend on specified input parameters and demand scenarios, but also on how well the arrival times of bicyclists can be estimated. This, in turn, depends on the distance to the upstream intersection and the length of the green phase there as well as the heterogeneity of bicyclists. The simulation of bicycle behavior will be explained in more detail in Chapter 5. As a summary, it can be stated that longer green times at the considered intersection (both as an ex ante control setting or in response to larger bicycle demand) allow slower bicyclists to catch the green wave and thus avoid the occurrence of very long waiting times. Maximum waiting times can additionally be reduced by decreasing the cycle times at adjacent intersections.

4.8 Summary

The OptIIC strategies presented in this chapter are based on the **multimodal** control strategies developed in Chapter 3. They take on the previously presented reservation concept, but additionally apply an optimization scheme within a rolling horizon approach to minimize the sum of weighted delays. Due to the more flexible intersection modeling approach that features dynamic conflict points and regions instead of fixed cells, vehicles of different dimensions such as PT vehicles can easily be integrated. All vehicles and signal groups need to reserve conflict areas, and conflicts involving vehicles are resolved by the control. This means that the control is **safe by design**.

Overall, the OptIIC strategies are more **efficient** than the SlotIIC strategies presented in Chapter 3. As expected, applying the presented optimization results in reduced delays and waiting times as compared to the more naive FCFS-based approach. The direct comparison of the two approaches for vehicle-only scenarios additionally revealed a significant increase in capacity as shown in Figure 4.19. This capacity gain can be used to increase capacity in the multimodal scenarios as well. The integration of VRU signal phases into the optimization problem additionally facilitates an efficient scheduling of green phases. The optimization setup features numerous possibilities to **balance** delays and waiting times of the considered road users via parameters such as weighting factors and upper bounds on waiting times. Optimization parameter settings can also be used to **integrate policy considerations** and prioritize

specific road users, e.g., PT vehicles or VRUs. The effectiveness of the prioritization can be seen from the results presented in Section 4.7. As discussed in the same section, the exact effect of parameter settings is difficult to predict and depends on the considered demand scenario. Therefore, the settings need to be evaluated in detail for each relevant scenario.

The control is fully **demand responsive** and integrates all considered road users into the control in a dynamic way. Vehicles and bicyclists are considered by the controller ahead of time in a rolling-horizon approach, whereas pedestrians are detected and integrated into the scheduling policy when they arrive at the intersection zone. Pedestrians and bicyclists do not need to carry connected devices, and VRU signalization principally works as today, such that the control can still be considered as **low-tech**. In order to leverage the full optimization potential, the demand-independent integration of pedestrians and bicyclists is not considered in this chapter. Nevertheless, such a hybrid model (fixed cycles for VRUs, optimization-based scheduling around these fixed cycles for vehicles) is conceivable.

The dynamic calculation of conflict regions and the consideration of continuous time instead of discrete time slots make the **integration of heterogeneous road users** much more intuitive. In this chapter, PT vehicles with a different size than the previously considered passenger vehicles have already been integrated. In the next chapter, both intersection crossing speeds and vehicle dimensions will be heterogeneous to demonstrate the compatibility of the approach with realistic conditions. The intuitive definition of conflict points and regions also increases the **transferability** of the strategy to other (possibly asymmetric) intersection zones. An extension to larger intersection zones with several lanes on each approach is conceivable as well. On the other hand, the larger number of vehicles would increase computation times. Additionally, if the optimal lane assignment and more complex pedestrian paths (such as the ones including a pedestrian refuge island) shall be integrated, the scheduling program would require modification and include even more decision variables. Furthermore, it needs to be noted that the control scheme is not easily applicable to street designs where bicyclists use the road together with vehicles.

The requirements defined in Section 1.2 and the evaluation considering the OptIIC strategies are additionally summarized in Table 4.8. As described above, appropriate parameter settings can be used to balance delays and apply policy objectives. This chapter thus offers an answer to Research Question 2: *"How can policy objectives be integrated into automated intersection control?"*. The detailed results shown and discussed in Section 4.7 demonstrate the effectiveness of prioritization measures. Clearly, the presented strategies only show one possible way to integrate policy objectives while many others may exist – such as the auction-based systems introduced in Section 2.2 or machine learning strategies that apply larger rewards for prioritized road users.

In the next chapter, the implementation and the microscopic traffic simulation are explained in detail, including the modeling of road user behavior and the trajectory planning for vehicles crossing the intersection zone. Additionally, the presented OptIIC scheme is compared to a state of the art TSC assuming a realistic intersection with measured demand.

Requirement	Evaluation	
Multimodality	✓	Pedestrians and bicyclists are integrated into the control strategy. Additionally, PT vehicles are integrated.
Safety by Design	✓	Only fully protected movements are allowed – except for conflicts without the involvement of motorized vehicles.
Efficiency	✓	Efficiency is improved significantly compared to the strategies presented in Chapter 3. The LOS improvements depend on the considered control strategy and on the level of demand. A comparison with a state of the art TSC will be provided in Chapter 5.
Balance	✓	The control strategies can be balanced by adjusting a set of parameters.
Policy Integration	✓	Policies can be integrated by putting upper bounds on VRU waiting times, adapting VRU green phase durations, and assigning suitable weighting factors for different road users.
Demand Responsiveness	✓	The control is able to respond to current demand.
Low-Tech	(✓)	In this scenario, VRUs need to be detected at the intersection. They are not required to be connected to the infrastructure. In principle, the optimization-based strategies for vehicle-only scenarios could be combined with fixed cycles for VRUs and thus not require knowledge about VRU activity. However, only the fully optimized scenario is analyzed, where VRU signal phases are fully integrated into the optimization.
Heterogeneity	✓	Due to the dynamic calculation of conflict regions and necessary headways, including heterogeneous vehicles with various dimensions and speeds is possible. This will be further explored when considering realistic demand in Chapter 5.
Transferability	(✓)	Due to the intuitive definition of conflict points and conflict regions, the control schemes can easily be applied to different intersection zones. The large computation times could be burdensome in a scenario with several vehicle lanes coming from each direction. Additionally, the optimization problem would require modification, if the optimal lane assignment and more complex pedestrian paths (such as the ones including a pedestrian refuge island) should be integrated. The control scheme is not easily applicable to street designs where bicyclists use the road together with vehicles.

Table 4.8: List of requirements for the control and their evaluation regarding the OptIIC family.

Chapter 5

Simulation-based Evaluation Considering a Real Intersection Zone

This chapter describes the setup of the microsimulation and the implementation of the control strategies introduced in Chapters 3 and 4, and presents a simulation study where the OptIIC strategy is applied to a real intersection zone with measured demand. The overall microsimulation setup and implementation is described in Section 5.1. Section 5.2 focuses on the behavior modeling of considered road users. The trajectory planning for CAVs on the approach to the intersection is explained in Section 5.3. In order to obtain smooth trajectories, an optimal control problem is presented that is repeatedly solved for vehicles approaching the intersection. The intersection zone considered in this final simulation study is presented in Section 5.4. It features a realistic layout with measured demand, and the currently implemented actuated TSC is used as a benchmark. Simulation results are presented in Section 5.5. In addition to the comparison of road user delays, the energy consumption of passenger vehicles at the intersection is analyzed, and maximum applied acceleration and deceleration values are presented. Finally, the chapter is summarized in Section 5.6.

5.1 Microsimulation Setup and Implementation

The microsimulation platform aimsun.next[1] is used for conducting the simulations in this thesis [Aimsun, 2020]. The platform allows for simulating vehicles, pedestrians, and bicyclists with their specific behavior. Additionally, the road user behavior and signal states can be manipulated using the API. This is needed for implementing the novel control strategies and overwriting the default driving behavior by a new trajectory planning approach. The overall setup is shown in Figure 5.1: road user arrivals and movements are simulated using aimsun.next which is connected to Python via the API. The Python program contains the rules for controlling the intersection and adjusting vehicle trajectories. If the OptIIC scheme presented in Chapter 4 is applied or trajectories of vehicles on the approach to the intersection are optimized, the Gurobi optimization solver is used to set up and solve the respective problem. The results are returned to Python and translated into the commands to change vehicle speeds and signal states, which are again sent back to the simulation platform. In the following, the implementation is described in more detail.

[1] The simulation studies presented in Chapters 4 and 5 were conducted using version 20. The SlotIIC approaches presented in Chapter 3 were simulated using version 8.4 with the same settings.

Figure 5.1: Basic setup used for the simulation study.[1]

The detailed flowchart of the simulation and implementation is shown in Figure 5.2. It is divided into the four steps (i) simulation setup, (ii) pre-processing, (iii) simulation run, and (iv) post-processing. All four steps are described below.

Simulation Setup: First of all, the considered intersection zone is modeled in aimsun.next. This can be done both for generic intersections that were presented previously or for realistic intersection zones as will be presented in Section 5.4. Geographic information system (GIS) data, aerial photos, or site maps can be used to accurately replicate the intersection. At the same time, the division of the intersection into a set of tiles (as introduced in Section 3.3) or the definition of a conflict matrix (as introduced in Section 4.2) is set up and stored in Python.

Pre-processing: Before running simulations, a set of scenarios is generated. Scenarios are defined by the considered demand, the assumed road user behavior, and the control settings that shall be tested. Demand scenarios comprise vehicle, pedestrian and bicycle movements and are specified via OD-matrices which are loaded into aimsun.next. Again, this demand can be both generic or measured at the site. Additionally, road user-related parameters need to be defined, such as vehicle dimensions or the distribution of bicycle speeds. From the control perspective, time gaps for conflicting movements need to be defined and the maximum allowed speed needs to be fixed. As discussed in Chapter 2, these settings can significantly influence resulting performance measures and thus need to be defined as realistically as possible. The road user behavior and safety-related input parameters applied in this thesis will be explained in Section 5.2. Finally, the control scenario needs to be defined. This includes the information, whether a SlotIIC or OptIIC scheme shall be applied, and how decisive parameters, e.g., the maximum waiting times for VRUs or the roll period ϕ are set. Additionally, the trajectory planning procedure that applies for vehicles on the approach to the intersection needs to be defined. Different trajectory planning options will be introduced in Section 5.3. Control-related information is specified in Python, where control decisions will be taken during the simulation run. A single scenario is run with at least five different "random seeds", i.e., with five different stochastic arrival distributions. Each simulation runs for one full hour with a warm-up time of ten minutes that is not considered in the final evaluation.

Simulation Run: The simulation applies discrete time steps with a length of $\tau = 0.6\,\text{seconds}$. During the simulation run, aimsun.next generates all considered road users from Poisson processes based on the demand data that apply for the considered scenario. In the beginning

[1] aimsun.next logo: `https://en.wikipedia.org/wiki/File:Aimsun_Next.png`
Python logo: `https://de.wikipedia.org/wiki/Datei:Python_logo_and_wordmark.svg`
Gurobi logo: `https://www.gurobi.com/`

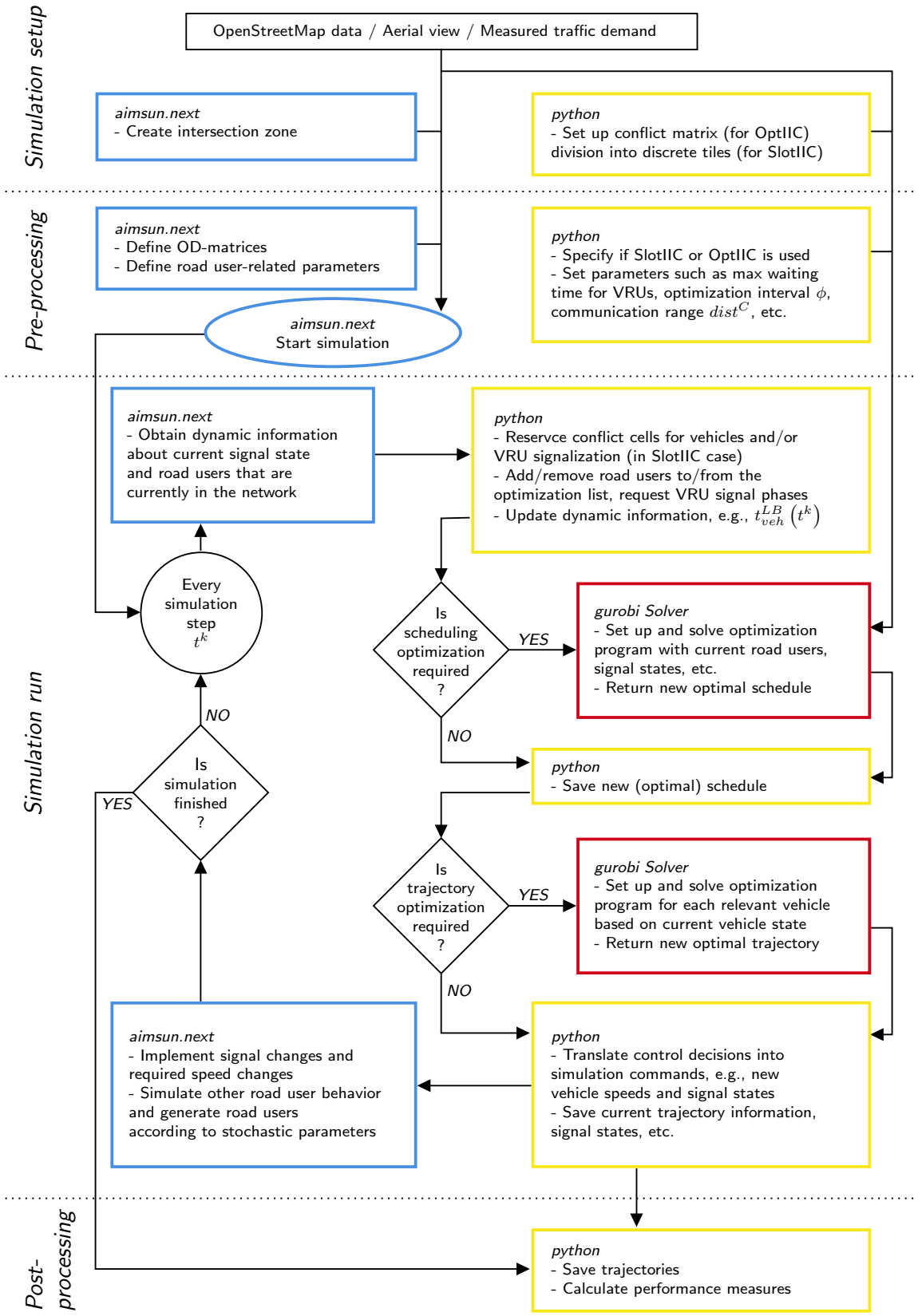

Figure 5.2: Flowchart of the simulation and implementation.

of each simulation step, aimsun.next exports a snapshot of the current situation to Python via the API. Let k be the current simulation step. At time $t^k = k \cdot \tau$, the snapshot includes the positions and speeds of all road users that are currently in the network and current signal states of the VRU signalization. In Python, these data are processed and used as input for control decisions. If the OptIIC scheme is applied and the optimization is run, i.e., every ϕ seconds, the optimization problem for the Gurobi solver is set up using the current lists of approaching and scheduled vehicles, as well as current and requested signal phases. The resulting optimized schedule is returned to Python, where it is saved for future simulation steps and final evaluations. The scheduled arrival times are used for planning trajectories for vehicles on the approach to the intersection. The trajectory planning approach can again be performed in a rule-based manner or applying an optimal control problem (applying Gurobi). Subsequently, the Python program translates the schedule and control decisions into specific actions which are sent to aimsun.next and will be applied in simulation step k (i.e., from the current time until time t^{k+1}). With these commands, the speeds of vehicles are changed or the phases of VRU signalization are switched. This communication loop is repeated at the beginning of every simulation step.

Post-processing: After the simulation run, trajectories of all road users are saved, results are processed, and performance measures are calculated.

The necessary input for the simulation study, i.e., the behavior modeling of considered road users, the considered intersection, and the benchmark intersection control are presented in the following sections.

5.2 Behavior Modeling of Considered Road Users

This section describes how the road user behavior is modeled. In this thesis, all vehicles at the intersection are assumed to be connected and automated, i.e., human-driven vehicles are not simulated. If vehicles are not within the communication range of the intersection controller or if the benchmark scenario with actuated traffic signal control is applied, trajectories are obtained from the car-following model which is implemented in aimsun.next. In Section 5.2.1, the car-following behavior is introduced briefly, and parameter values are sustained. The behavior modeling of bicyclists is explained in Section 5.2.2, and the behavior of pedestrians is described in Section 5.2.3. In the integrated intersection control scenarios, vehicle trajectories are adjusted in such a way, that vehicles arrive at the intersection at the assigned time and with a pre-defined speed. The applied trajectory optimization scheme is explained in Section 5.3.

5.2.1 Behavior Modeling of Connected Automated Vehicles

In general, a car-following model based on the Gipps model is implemented in aimsun.next [Gipps, 1981; Gipps, 1986]. Drivers are assumed to drive at their desired speed if possible, which (in addition to personal preferences) depends on the speed limit of a link and on geometric characteristics of the road. The car-following model describes driver behavior in situations where the driver is following another vehicle, and driving at the desired speed would

lead to a collision. In such "constrained" driving situations, the drivers try to adjust their speed in order to maintain or obtain a safe gap to their leader. What gap is considered safe depends on the reaction time of the follower. Several parameter adjustments can be made to the model, such as reaction times of drivers, how well the speed and acceleration of the leader vehicle can be estimated, and what acceleration and deceleration rates feel comfortable to the driver, among others. These values vary for human drivers – not only among different drivers, but also for one single driver in different situations. When the model is calibrated, i.e., the "correct" statistical distribution of these parameter values is implemented, the model is able to reproduce characteristics of real traffic flow, see e.g., Papathanasopoulou et al. [2016].

For CAVs, these values can be assumed to be different from human drivers. Especially with increasing communication technology, vehicles can inform their followers about current speed, acceleration and deceleration, and the following vehicle can almost immediately perform the same actions. This will most likely allow for smaller headways and a uniform driving behavior in the future. As for now, there is a lack in information about parameter values that are being planned to be implemented in CAVs in the future, and the "ground truth" for future traffic simulations cannot be measured in reality yet [Calvert et al., 2017]. In the following, the most important input parameters used in this thesis are sustained.

Time Gaps for Car-following Behavior

Assumed vehicle time gaps for CAVs in literature range from 0.1 seconds [Mavromatis et al., 2020] to 1.5 seconds [Olstam et al., 2020]. While smaller time gaps can increase traffic throughput, they can also lead to the amplification of disturbances caused by velocity variations of the first vehicle in a platoon. A platoon or 'string' of vehicles can be considered to be 'stable', if disturbances are instead attenuated in upstream direction [Ploeg et al., 2011], an important prerequisite for automatic car-following. Ploeg et al. [2011] show a theoretical correlation between communication latency and feasible time gaps yielding string stability. They validate these theoretical results with a fleet of six vehicles that are equipped with ex-factory ACC functions using long-range radar sensors, and upgraded with a GPS receiver and a WLAN device. Their results show that a time gap of 0.7 seconds is technically feasible and yields string stable behavior in their test scenario.

Based on these findings, a car-following time gap of 0.7 seconds is assumed for all motorized vehicles in this thesis. The time gap is kept constant for all simulation scenarios in order to obtain consistent results that allow for a comparison between different control strategies. Depending on the development of communication performance, even shorter time gaps might be implementable in the future. In order to increase safety for crossing movements, time gaps are set to be 1.0 seconds for conflicting vehicles coming from different directions.

Reaction Times

The microsimulation platform aimsun.next allows for specifying several reaction times: (i) the classical *reaction time* is the time it takes a vehicle to react to speed changes in the preceding vehicle, (ii) the *reaction time at stop* is the time it takes for a stopped vehicle (in a queue)

Vehicle Parameters	**Chosen values**	
Dimensions ($len_{veh} \times wid_{veh}$)	Passenger cars:	$len_{veh} \in [3.50,\ 4.50],\ mean = 4.00\,\mathrm{m}$
		$wid_{veh} \in [1.60,\ 2.00],\ mean = 1.80\,\mathrm{m}$
	Buses:	$12.00\,\mathrm{m} \times 2.50\,\mathrm{m}$
	Trucks:	$len_{veh} \in [6.00, 10.00],\ mean = 8.00\,\mathrm{m}$
		$wid_{veh} \in [2.60,\ 2.80],\ mean = 2.25\,\mathrm{m}$
Desired speeds v_{veh}	Maximum allowed speed: $8.3\,\mathrm{m/sec}$ ($30\,\mathrm{km/h}$)	
	On curves depending on radii with acc^{lat} of $3\,\mathrm{m/sec^2}$	
Min. and max. acceleration $acc^{min} \mid acc^{max}$	Passenger cars:	$-4.0\,\mathrm{m/sec^2} \mid 3.0\,\mathrm{m/sec^2}$
	Bus:	$-2.0\,\mathrm{m/sec^2} \mid 1.2\,\mathrm{m/sec^2}$
	Trucks:	$-3.5\,\mathrm{m/sec^2} \mid 1.2\,\mathrm{m/sec^2}$
Minimum gaps for car-following / crossing	$0.7\,\mathrm{sec}$ / $1.0\,\mathrm{sec}$	
Minimum clearance for car-following	$3.0\,\mathrm{m}$	

Table 5.1: Parameter values for CAV behavior modeling.

to react to the acceleration of the vehicle in front, and (iii) the *reaction time at traffic light* is the time it takes for the first vehicle at a traffic signal to react to the start of the green phase. Under the precondition that all vehicles are connected with each other and with the infrastructure, all three types of reaction times depend on the communication latency. With this respect, very promising results have been reported in literature. Liu et al. [2018], for example, present results of test drives with two vehicles in different road scenarios. They measured a mean latency of 1.3 ms and a PDR of 0.15% using DSRC communication [Liu et al., 2018]. Due to the negligible transmission latency, it is assumed here that vehicles react to speed changes of the preceding vehicle, a dissolving queue in front of them, and a signal phase change immediately.

Desired Speeds

If driving in free-flow conditions and the maximum allowed speed is less or equal to their desired speed, CAVs are assumed to drive at (exactly) the maximum allowed speed. Comfortable turning speeds depend on the turning radius and the maximum lateral acceleration that feels comfortable to the passenger. For the purposes of a simplified control explanation and result interpretation, this was ignored in the previous chapters and all motorized vehicles passed the intersection at the same speed. In order to be implementable at realistic intersections with possibly small turning radii, the control needs to be able to handle different crossing speeds. In this chapter, the maximum lateral acceleration is set to $3\,\mathrm{m/sec^2}$, following the results by Schimmelpfennig and Nackenhorst [1985]. The vehicle speeds for crossing the intersection can then be calculated according to the formula $v = \sqrt{R * acc_{lat}}$ depending on the comfortable lateral acceleration acc_{lat} and the curve radius R. For simplicity reasons, the same maximum lateral acceleration is assumed for all passenger vehicles, buses, and trucks, but implementing various different lateral acceleration values is straight-forward.

Other Parameter Values

In order to demonstrate feasibility in a realistic environment, vehicle dimensions are assumed to be heterogeneous in this final evaluation. The default values suggested by aimsun.next with distributions as shown in Table 5.1 are used. Maximum acceleration and deceleration are fixed per vehicle class with the mean values as suggested by aimsun.next. Stronger accelerations and decelerations can be assumed for passenger vehicles, while these acceleration rates will feel uncomfortable for passengers of PT vehicles or might not be realizable by heavier trucks. The minimum acceleration values listed in Table 5.1 apply for regular driving conditions. Emergency breaking can lead to stronger decelerations.

5.2.2 Behavior Modeling of Bicyclists

The default microsimulation behavior for bicyclists in aimsun.next is defined equivalently to the vehicle driving behavior with adapted parameters such as dimensions and kinematic limitations. In order to model queue dissipation and intersection crossing behavior more realistically, the default model is partially replaced by own implementations that follow the findings of current bicycle research. In the following, these considerations and how they are used in the implementation are explained for free-flow situations and situations in which bicyclists accelerate from a stop. Additionally, further parameters and resulting example trajectories are presented.

Bicyclists in Free-flow Conditions

Each bicyclist bic has an individual mean desired cruising speed v_{bic}^{des}, which is assigned when the bicyclist enters the simulation. Following the analyses by Twaddle and Grigoropoulos [2016], v_{bic}^{des} is taken from a truncated normal distribution with a mean of 5.23 m/sec and a standard deviation of 1.25 m/sec. Values are bounded from below by 2.7 m/sec, which is the lowest value observed in the "German Naturalistic Cycling Study" [Schleinitz et al., 2017] and from above by 8.3 m/sec, which corresponds to the maximum allowed speed in the considered scenarios. The resulting probability density and cumulative distribution functions are shown in Figure 5.3a. Bicyclists do not usually keep a constant speed, even in free-flow conditions. Instead, their speed fluctuates around their comfortable speed with accelerations and decelerations in the range of $\pm 0.2\,\mathrm{m/sec^2}$ and speeds between $0.8 \cdot v_{bic}^{des}$ and $1.15 \cdot v_{bic}^{des}$ [Twaddle and Grigoropoulos, 2016]. Therefore, for each bicyclist in free-flow conditions, an acceleration value between -0.2 m/sec^2 and 0.2 m/sec^2 is chosen from a truncated normal distribution with a mean value of 0.0 m/sec^2 in each time step. If necessary, this acceleration value is adjusted to guarantee that bicyclists do not leave their range of acceptable speeds.

Acceleration from a Stop

Bicyclists are assumed to be accelerating, if their current speed $v_{bic}(t)$ at time t is significantly lower than their desired speed v_{bic}^{des}, i.e., if $v_{bic}(t) < 0.8 \cdot v_{bic}^{des}$. Once the bicyclists have reached a speed of $v_{bic}(t) \geq 0.95 \cdot v_{bic}^{des}$, they are assumed to have reached their free-flow speed and thus leave the "acceleration mode". While accelerating, bicycle acceleration is not

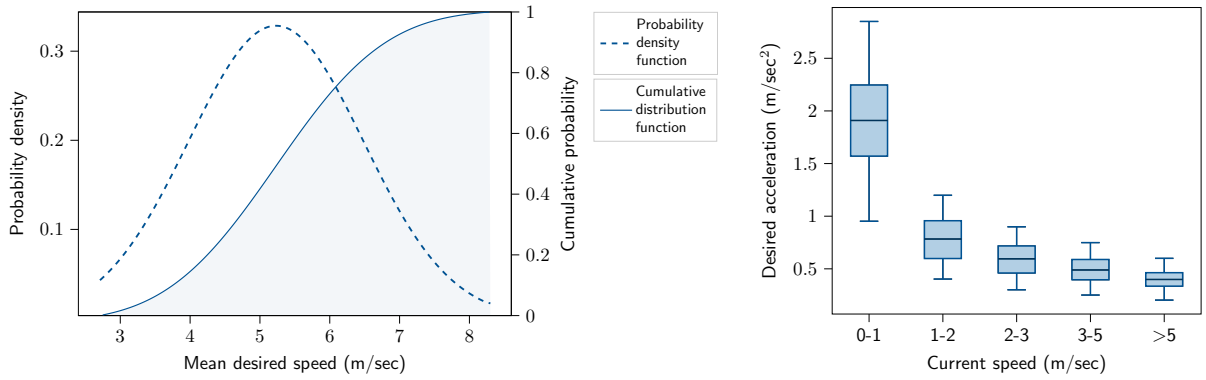

(a) Desired speed of bicylists: probability density and cumulative distribution function.

(b) Desired acceleration of bicyclists depending on current speed.

Figure 5.3: Desired speeds of bicyclists and desired accelerations depending on current speed.

constant over time, but depends on their current speed and tends to decrease as their speed increases [Figliozzi et al., 2013]. H. Kaths, Keler, et al. [2021] present distributions of acceleration values depending on the momentary speed of cyclists which they collected during a bicycle simulator experiment. In this thesis, a simplified approach based on their findings is implemented: in each time step, an acceleration value $acc_{bic}(t)$ for bic is taken from truncated normal distributions with parameters (mean value and bounds) that depend on the current speed $v_{bic}(t)$ of bic. Mean accelerations $\overline{acc}(v)$ range from 1.9 m/sec^2 (for current speeds v of 0-1 m/sec) to 0.4 m/sec^2 (for current speeds v of 5-7 m/sec) [H. Kaths, Keler, et al., 2021]. The authors show individual standard deviations and lower and upper bounds on the acceleration values for the different current speeds. To reduce the model complexity, the standard deviation is chosen to be 0.2 m/sec^2 and values are bounded by $0.5 \cdot \overline{acc}(v)$ and $1.5 \cdot \overline{acc}(v)$ for all current speeds in this thesis. Resulting boxplots for acceleration values depending on the current speed are shown in Figure 5.3b.

Other Parameter Values

Following the analyses by H. Kaths, Keler, et al. [2021], minimum time gaps are again assigned following a truncated normal distribution with a mean value of 0.7 seconds and further parameters shown in Table 5.2. If bicyclists approach a red light or cannot cycle at their desired speed without violating the gap to the cyclist in front of them, their speed is restricted by the aimsun.next car-following model. Reaction times for bicyclists stopped at the traffic signal are also assigned stochastically as shown in Table 5.2 with a mean value of 1.2 seconds. Resulting trajectories and speed curves for cyclists that are stopped at a traffic signal are shown in Appendix C, and it can be seen that the demand-dependent green phase durations implemented in Chapter 4 are long enough for all assigned waiting and arriving cyclists to cross the stop bar. The heterogeneity of bicycle behavior makes it difficult to validate the model. Nevertheless, with these settings, the queue dissipation times and intersection crossing speeds approximately match those indicated by H. Kaths, Keler, et al. [2021] and Twaddle and Grigoropoulos [2016]. The described implementation is hence assumed to be realis-

Bicycle Parameters	**Chosen values**
Dimensions ($len_{bic} \times wid_{bic}$)	1.30 m × 0.60 m
Desired speeds v_{bic}	Figure 5.3a
Acceleration (free-flow conditions)	Truncated normal distribution with
	μ: 0.0 m/sec^2, σ: 0.1 m/sec^2, min: -0.2 m/sec^2, max: 0.2 m/sec^2
Acceleration from a stop	Figure 5.3b
Minimum time gap	Truncated normal distribution with
	μ: 0.7 sec, σ: 0.2 sec, min: 0.1 sec, max: 2.5 sec
Reaction time at stop	Truncated normal distribution with
	μ: 1.2 sec, σ: 0.4 sec, min: 0.1 sec, max: 2.5 sec

Table 5.2: Parameter values for bicycle behavior modeling.

tic enough for the given purpose, i.e., simulating the progression behavior of a flock of cyclists and measuring bicycle delay in the simulation. It needs to be noted, however, that profound safety analyses require further considerations such as lane discipline to be taken into account.

In addition to the current setup, the bicycle traffic signal could be equipped with green signal countdown timers. As described in Section 3.1, this additional dynamic information has the potential to increase the probability of bicyclists to cross the signal without stopping and thus improve cycling comfort. However, there has not yet been a consistent conclusion on the effect of countdown-timers on bicyclist behavior and safety. On the contrary, H. Kaths, Grigoropoulos, et al. [2019] report both an increase and a decrease in red-signal violations, depending on where the countdown timer is installed. Therefore, no such behavior was simulated in this thesis.

5.2.3 Behavior Modeling of Pedestrians

Pedestrians are simulated using the default behavior that is implemented in aimsun.next. In the simulations, their entrance and exit points are defined in such a way that they appear directly at the crosswalk that they would like to cross and disappear after crossing the street. They hence arrive at the intersection following a Poisson-process with parameters specified by the OD matrix. Jaywalking is not simulated, i.e., pedestrians wait to cross the intersection until their signal head turns green. All pedestrians assigned to the same signal phase cross the street at roughly the same time, and the entire crosswalk is blocked for them from the start of the green phase until the end of the clearance time. Therefore, the exact distribution of walking speeds is not relevant for this thesis. Most importantly, (i) green phases need to be long enough to allow all waiting pedestrians to *start* crossing the street, and (ii) clearance times need to be long enough to allow all pedestrians to *finish* crossing the street safely.

All pedestrian green phases implemented in this thesis last for at least 5 seconds. This duration corresponds to the minimum required green time according to the German guideline RiLSA [FGSV, 2015b] and is applied in several German cities [Alrutz et al., 2012]. According to HCM, a reasonable value for estimating pedestrian capacity is 75 pedestrians per minute

of effective green time and meter of crosswalk width ($\frac{75\ ped}{min \cdot m}$). Additionally, a start-up time of up to 3 seconds needs to be considered for capacity calculations [TRB, 2000]. A pedestrian crosswalk area with a width of 6 meters (as applied in Chapters 3 and 4) thus has a capacity of $75 \frac{ped}{min \cdot m} \cdot \frac{5-3}{60} \frac{sec}{sec/min} \cdot 6\,\mathrm{m} = 15$ pedestrians per green phase if the green phase duration is exactly 5 seconds. This is sufficient for the scenarios evaluated in this thesis. If a larger pedestrian demand is considered, the green phase durations have to be increased accordingly. Additionally, green times can be extended to increase the probability of pedestrians arriving during a green phase (compare Section 4.7.3).

The clearance time is calculated such that slow pedestrians can start crossing the street at the end of the green time and finish crossing safely. The assumed speed suggested for this purpose by RiLSA is 1.2 meters per second. A survey among German cities revealed that all of the respondents work with assumed speeds between 1 and 1.5 meters per second, depending on prevailing pedestrian characteristics [Alrutz et al., 2012]. However, slower pedestrian speeds can also be measured in the field, especially if pedestrians need assistive devices such as wheeled walkers [Alrutz et al., 2012]. As described in Chapter 3, in the presented AIM scenarios, vehicles will arrive at the intersection at a higher speed. Therefore, pedestrian crosswalks need to be monitored and, if pedestrians are detected on the streets, approaching vehicles are required to slow down and eventually stop. In these situations, they will have to request a new time slot and will cross the intersection at a lower speed.

The rescheduling procedure does not infringe upon safety, but is assumed to be uncomfortable for both pedestrians and vehicle passengers. Additionally, a frequent occurrence of this process can reduce efficiency. Therefore, a lower pedestrian speed of 0.8 meters per second and, consequently, longer clearance times are assumed in this thesis. The speed of 0.8 meters per second is just below the 10th percentile of low-density walking speeds obtained from field measurements as reported by Hoogendoorn and Daamen [2006]. The rescheduling process described above has been implemented for test purposes but does not come into play in the evaluations presented in this thesis (the aimsun.next pedestrian model with default values applies walking speeds between 1.08 and 1.6 meters). A "trade-off" analysis of different clearance times is left for future research. Additionally, when being implemented in the field, pedestrian speeds could be measured at the site to find the most suitable clearance time. Finally, dynamic displays such as pedestrian countdown timers could allow faster pedestrians to start crossing the street at a later point in time.

5.2.4 Conclusion

The behavior modeling of road users is intended to replicate traffic at the considered intersection zones as realistically as necessary to draw a valid comparison with existing control setups, while at the same time keeping the complexity of the models tractable. The introduced model parameters can have a significant influence on simulation results and are therefore founded in literature results. The behavior modeling of VRUs particularly reflects the heterogeneity found at urban intersections. Vehicle time gaps and VRU speeds are chosen in such a way that the control strategies are safe by design.

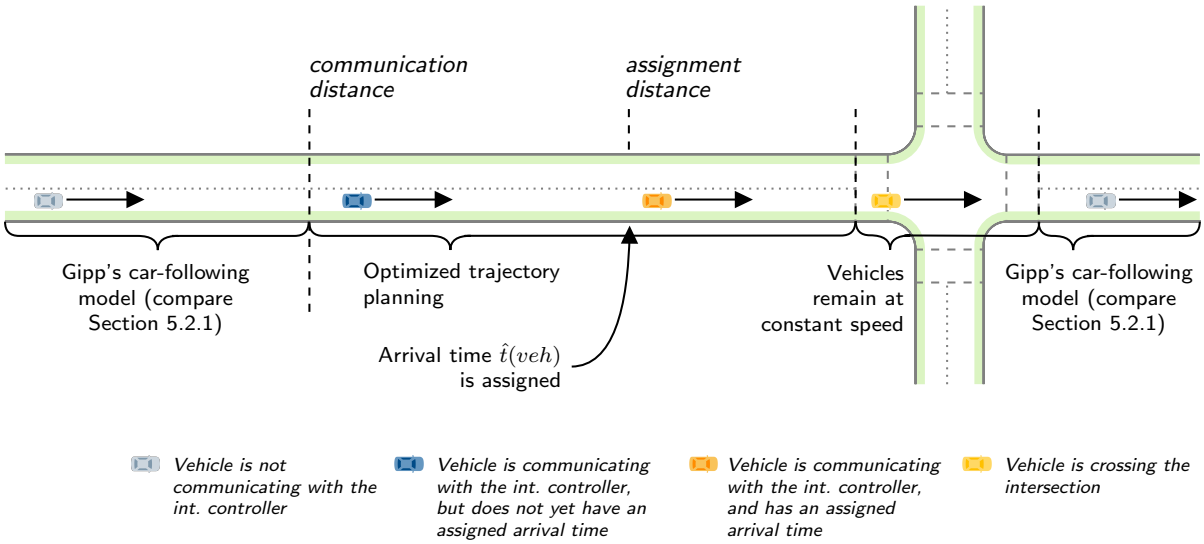

Figure 5.4: Area in which the trajectory optimization approach is applied.

5.3 Optimized Trajectory Planning

As described in the previous section, it is assumed that all motorized vehicles considered at the intersection zone (i.e., passenger vehicles, buses, and trucks) are connected and automated. In particular, it is assumed that they are able to send and receive accurate information about their current state and the states of surrounding vehicles in every time step, and that they are able to react to this information and information provided by the central controller immediately. Before the vehicles start communicating with the intersection controller and after they have crossed the intersection, the car-following model implemented in aimsun.next with the parameter values described in Section 5.2.1 is applied. While crossing the intersection, the constant predefined speed is maintained. The trajectory optimization approach presented in this section hence focuses on those vehicles that are currently on the approach to the intersection and are communicating with the intersection controller (see Figure 5.4). The trajectory planning is implemented in Python and overwrites the default vehicle driving behavior in aimsun.next.

The knowledge about the current vehicle state and the required arrival time and speed at the intersection can be used to formulate an optimal control problem to provide a trajectory that makes the vehicle approach the intersection as smoothly as possible. Such approaches have already been presented in literature, e.g., by Ntousakis et al. [2016] and Typaldos et al. [2020], and they allow for applying different objective functions. In principle, the optimized trajectory planning presented in this section requires vehicles to have a fixed arrival time at the intersection. If the SlotIIC strategy is applied, vehicles receive a scheduled arrival time upon their first contact with the intersection controller. This is not the case for vehicles that have not yet crossed the assignment distance in the OptIIC scenario, e.g., for the blue vehicle in Figure 5.4. Nevertheless, it is beneficial that vehicle speeds, if necessary, are reduced as early as possible. The intersection controller can provide the vehicle with a lower bound on its arrival time that takes existing reservations into account. For example, if the pedestrian

crosswalk that vehicle veh needs to pass has a current or scheduled pedestrian green phase and it is physically not possible for the vehicle to pass before the start of the green phase, it is already clear that the vehicle cannot be scheduled any earlier than after the respective green and clearance time. Additionally, the vehicle cannot be scheduled any earlier than its leader vehicle. This knowledge can already be used to adjust the trajectory early on and avoid that the vehicle travels at maximum speed until reaching the assignment distance, where it then needs to drastically reduce its speed. It needs to be noted that this early trajectory adaptation does not infringe upon the flexibility of the scheduling controller – the vehicle only reduces its speed if an earlier scheduled arrival time is not possible. If new information is available, the intersection controller will update the lower bound accordingly. This setup implies that it can be necessary to run the trajectory optimization algorithm multiple times for one vehicle as will be explained later on. First of all, the problem formulation for one individual vehicle veh at time t^k is explained in the following.

5.3.1 Optimized Trajectory Planning for Vehicle veh at Time t^k

The microscopic simulation that is used to evaluate the control strategies in this thesis applies discrete time steps of fixed duration. Therefore, a discrete-time optimal control formulation similar to the one presented by Typaldos et al. [2020] is applied. In their approach, initial and final positions and speeds are fixed, and vehicle acceleration in each time step is used as the control input. The objective of the optimal control problem is that the vehicle, based on its current state, adjusts its acceleration in such a way that the final conditions are met and a given function f is minimized that can represent, for example, passenger discomfort or fuel or energy consumption. A broader background on optimal control problems is given by Papageorgiou, Leibold, et al. [2015].

Let τ be the simulation step size and let $t^k = k \cdot \tau$ be the simulation time where $k \in \mathbb{N}$ is the simulation step. The state information used in the trajectory adjustment procedure for vehicle veh at time t^k consists of the vector $[dist, v, t^{end}, \hat{v}]$, where $dist_{veh}(t^k)$ is the distance of vehicle veh to the entrance of the intersection at time t^k (corresponding to the position of the front bumper of veh and given in meters) and $v_{veh}(t^k)$ describes the velocity of vehicle veh at time t^k in meters per second. The variable $t^{end}_{veh}(t^k)$ corresponds to the assigned arrival time $\hat{t}_{veh}$ at the intersection or, if the arrival time is not yet fixed, a lower bound on $\hat{t}_{veh}$ as explained above. Finally, $\hat{v}_{veh}$ is the predefined speed for crossing the intersection that depends on the turning intention of the vehicle and is independent of the assigned arrival time.

The trajectory will be optimized for the time horizon $H_{veh}(t^k) = t^{end}_{veh}(t^k) - t^k$ (abbreviated by H in the following), which is the time that remains until vehicle veh is supposed to reach the entrance to the intersection. Vehicle veh shall hence cover a distance of $dist_{veh}(t^k)$ within the time horizon H and reach the position $dist_{veh}(t^k)$ with a speed of $\hat{v}_{veh}$. It needs to be noted that the OptIIC scheme works in continuous time and the time horizon H is hence not necessarily a multiple of the simulation step size τ. Therefore, the (discretized) trajectory will be planned for the next $N_{veh}(t^k) = \left\lfloor \frac{H}{\tau} \right\rfloor$ simulation steps (abbreviated by N), and the discretized problem is formulated in such a way that vehicle veh reaches the speed of $\hat{v}_{veh}$ and

covers a distance of

$$x_{veh}^{end}(t^k) = dist_{veh}(t^k) - (H - N \cdot \tau) \cdot \hat{v}_{veh}\,[\mathrm{m}] \tag{5.1}$$

within N simulation steps. The vehicle then uses the remaining $H - N \cdot \tau$ seconds to cover the remaining distance of $(H - N \cdot \tau) \cdot \hat{v}_{veh}$ meters with the assigned speed $\hat{v}_{veh}$ until arriving at the intersection at time $t_{veh}^{end}(t^k) = t^k + H$. This means that for the optimal control problem formulation, the initial position will be defined as $x_{veh}^{0}(t^k) = 0$, and the final position $x_{veh}^{end}(t^k)$ will be as defined in Equation (5.1).

Let f be the cost function that shall be minimized. The overall trajectory optimization problem for vehicle veh at time t^k can then be defined as follows:

Problem IV (Trajectory Optimization Problem for Vehicle veh at Time t^k)**.**

$$\min \left(\sum_{l=k}^{k+N-1} f(l) \right) \tag{5.2}$$

subject to

$$v(k) = v_{veh}(t^k) \tag{5.3}$$

$$x(k) = 0 \tag{5.4}$$

$$v(k+N) = \hat{v}_{veh} \tag{5.5}$$

$$x(k+N) = x_{veh}^{end}(t^k) \quad \textit{(end pos. given by Equation (5.1))} \tag{5.6}$$

$$v(l+1) = v_l + acc(l) \cdot \tau \qquad \forall\, l \in [k, \ldots, k+N-1] \tag{5.7}$$

$$x(l+1) = x(l) + v(l) \cdot \tau + \frac{1}{2} \cdot acc(l) \cdot \tau^2 \qquad \forall\, l \in [k, \ldots, k+N-1] \tag{5.8}$$

$$acc(l) \in [acc_{veh}^{min}, acc_{veh}^{max}] \qquad \forall\, l \in [k, \ldots, k+N-1] \tag{5.9}$$

$$v(l+1) \in [0, v^{max}] \qquad \forall\, l \in [k, \ldots, k+N-1] \tag{5.10}$$

Constraints (5.3)-(5.6) fix the initial and final positions and speeds, and Constraints (5.7)-(5.8) represent the state equations for all time steps within the time horizon. Additionally, acceleration and speed are bounded (compare Constraints (5.9)-(5.10)).

In this thesis, the sum of squares of the acceleration (both positive and negative) will be minimized, i.e., $f(l) = acc(l)^2$ for all l in $[k, \ldots, k+N-1]$. Acceleration is directly related to engine power, and reducing acceleration is thus assumed to be emission-friendly [Rios-Torres et al., 2015]. Additionally, acceleration can be considered as an estimation of driving comfort. Reducing acceleration will especially be important in a future with self-driving shuttle buses, where passengers don't have a fastened seat belt or might even be standing [Bae et al., 2019]. The described setup also allows for applying other objective functions in the future. These could put more focus on passenger comfort by integrating jerk (compare [Ntousakis et al., 2016]), or apply a fuel consumption model (compare [Typaldos et al., 2020]) or an energy consumption model (compare [Hu et al., 2021]). However, the quadratic objective function puts us into the comfortable position of being able to solve the program easily and

fast. If one of the other objective functions suggested above is used instead, the program formulation and the solution approach need to be more sophisticated. For example, TYPALDOS et al. [2020] reduce the number of decision variables and constraints of the program by removing the final conditions from the list of constraints and instead adding them to the objective function with suitable penalty weights.

The optimization returns the trajectory that the vehicle should follow in order to reach the intersection at the required time and speed, and with minimum accelerations on the way. The result consist of a list of acceleration values $[acc^*_{veh}]$, speeds $[v^*_{veh}]$, and positions (converted to the distances to the intersection $[dist^*_{veh}]$) that will be saved and compared to the actual vehicle states in the following simulation steps.

5.3.2 Repeated Setup of the Optimal Control Problem

As explained above, it can be necessary to run the trajectory optimization for vehicle veh multiple times. First of all, the trajectory optimization is already run when the arrival time of the vehicle is still up for changes. Additionally, the trajectory optimization procedure considers one single vehicle without taking surrounding vehicles into account. The vehicle might hence deviate from its assigned trajectory in order to maintain a safe gap to its leader vehicle. The overall procedure applied in each simulation step for each vehicle on the approach to the intersection is shown in Figure 5.5 and explained in the following.

Let vehicle veh be a vehicle on the approach to the intersection at time t^k. In order to adjust its speed, the procedure first checks whether the vehicle already has a planned trajectory. If the vehicle has just entered the communication range of the intersection controller, a plan first needs to be established. If the vehicle does have a planned trajectory, it needs to be checked whether it was planned for the currently expected arrival time $t^{end}_{veh}(t^k)$. If the lower bound has changed or the vehicle has crossed the assignment distance and the assigned arrival time differs from the previously calculated lower bound, a new plan needs to be calculated. Finally, if the final state has not changed, it needs to be checked whether the vehicle is following its planned trajectory and current distance and speed are as planned, i.e., whether $v_{veh}(t^k) = v^*_{veh}(t^k)$ and $dist_{veh}(t^k) = dist^*_{veh}(t^k)$. If this is the case, vehicle veh should continue following this trajectory. Otherwise, a new trajectory needs to be calculated based on the new initial state. As a fallback option, if no feasible trajectory can be found, the vehicle needs to update its earliest possible arrival time and possibly request a new time slot for crossing the intersection. Finally, the new desired acceleration $acc^*_{veh}(t^k)$ that shall be applied is taken from the existing or newly calculated trajectory plan.

Before returning this acceleration to the simulation, it needs to be checked whether it can be safely implemented. In particular, the program compares the gap of vehicle veh to its leader vehicle veh' and checks if the implementation of the proposed acceleration is feasible without violating necessary safety constraints in the next time step. To this end, let $clear_{veh',veh}(t^k)$ be the current clearance, i.e., the spacial gap between the back of vehicle veh' and the front

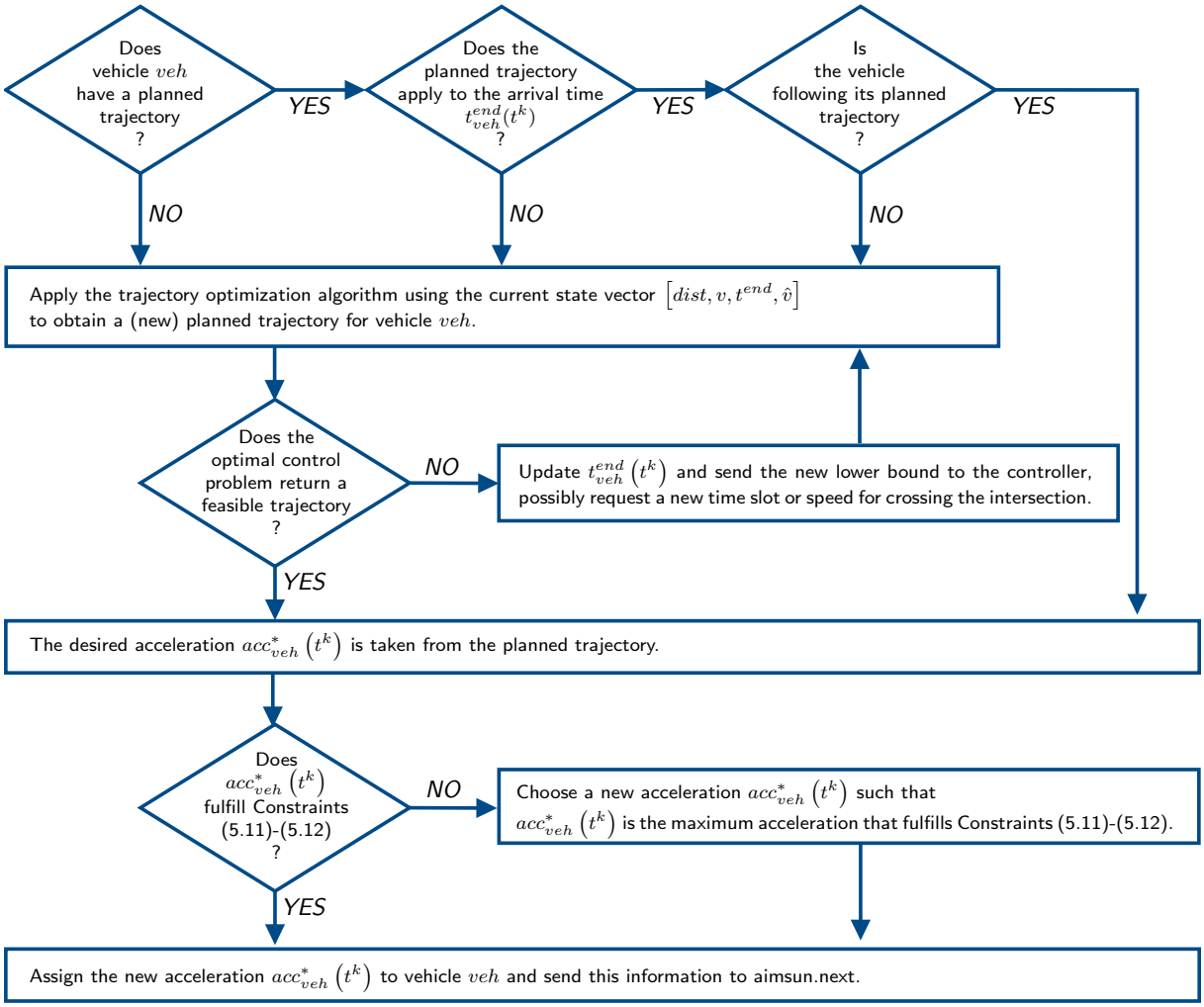

Figure 5.5: Trajectory adjustment procedure run for vehicle veh at time t^k.

of vehicle veh at time t^k. The clearance at time t^{k+1} can then be calculated as

$$\begin{aligned} clear_{veh',veh}(t^{k+1}) = clear_{veh',veh}(t^k) \\ + \left(v_{veh'}(t^k) \cdot \tau + \frac{1}{2} \cdot acc_{veh'}(t^k) \cdot \tau^2 \right) \\ - \left(v_{veh}(t^k) \cdot \tau + \frac{1}{2} \cdot acc_{veh}^{*}(t^k) \cdot \tau^2 \right), \end{aligned}$$

where it is assumed that both speed $v_{veh'}(t^k)$ and acceleration $acc_{veh'}(t^k)$ of the leader vehicle are known. The proposed acceleration for vehicle veh has to fulfill the following two constraints:

$$clear_{veh',veh}(t^{k+1}) \geq \delta_{follow}^{min} \cdot (v_{veh}(t^k) + acc_{veh}^{*}(t^k) \cdot \tau \geq 0, \tag{5.11}$$

$$clear_{veh',veh}(t^{k+1}) \geq clear^{min}. \tag{5.12}$$

Constraint (5.11) ensures that the time gap is fulfilled, and Constraint (5.12) requires that a minimum spacial gap is respected that comes into play for very low speeds (in these situations,

the time gap converges to zero). If the constraints are not fulfilled for $acc^*_{veh}(t^k)$, the proposed acceleration will be overwritten by a lower value that fulfills these constraints. In this case, vehicle veh deviates from the proposed trajectory. Therefore, in the next time step, a new optimal trajectory given the new state will be calculated.

In a real-world application, it is assumed that vehicles will monitor the gap to the vehicle in front in real time and share their speeds and accelerations. In the simulation setup, the procedure is run sequentially for vehicles in upstream direction to account for the relatively large simulation steps. Let the vehicles be sorted by proximity to the intersection. When the feasible acceleration for vehicle veh is calculated, the applied acceleration of veh' is already known. The necessary gap can thus already be calculated taking the new speed of veh' into account. If vehicle veh can have access to the entire trajectory of vehicle veh' (which is scheduled before vehicle veh), the entire trajectories could be compared directly upon the calculation of the trajectory for vehicle veh. In this case, if a conflict will occur at any point in time, the entire trajectory can directly be recalculated and the repetitive calculation while approaching the intersection is unnecessary – at least if the arrival times of both vehicles are fixed. This is done, for example, by Y. Wang et al. [2020]. However, the fast and efficient calculation of the trajectory allows for the implementation of the presented approach, which can also take further disturbances into account and doesn't require vehicles to share their entire trajectory plan.

Nevertheless, adding yet another layer to the overall program does slow down the simulation. This especially applies for the scenarios close to the capacity limit that were analyzed in Chapters 3 and 4. Therefore, in the previous two chapters, a simplified rule-based (non-optimized) version was used that works with fixed acceleration and deceleration rates, and the trajectory planning approach was only applied to those vehicles with an assigned arrival time at the intersection. The trajectories resulting from the simplified procedure are also feasible in the sense that deceleration and acceleration values are bounded, vehicles maintain a safe distance to their leader, and they arrive at the intersection at the assigned time with the assigned speed. Therefore, the approach was viable for a comparison of road user delays in the previous chapters. This chapter additionally features a comparison of maximum acceleration values and resulting energy consumption in Section 5.5. The simplified approach is briefly shown in Appendix D.

5.4 Simulation Setup of the Test Intersection

This section describes the intersection zone that is simulated in this chapter. The considered intersection (on Theresien and Arcis Street in Munich) is located next to the main building of Technical University of Munich (TUM) in the central area of Munich. The position of the intersection in Munich as well as the replication of the intersection in aimsun.next are shown in Figure 5.6. Section 5.4.1 describes the characteristics of the intersection zone, Section 5.4.2 specifies the OptIIC control scenario that will be tested, and Section 5.4.3 briefly introduces the currently applied TSC that will be used here as a benchmark.

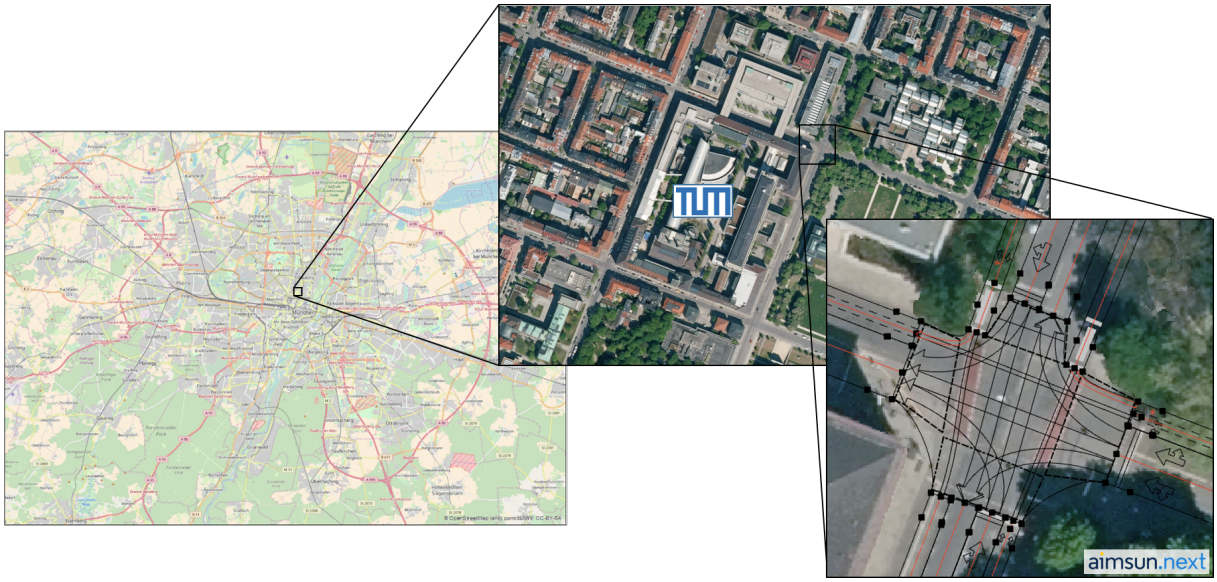

Figure 5.6: Considered intersection zone.[1]

5.4.1 Characteristics of the Intersection Zone

The major street of this intersection is Arcis Street, a one-way westbound street with two lanes. Average daily traffic on Arcis Street is about 11,500 vehicles with a heavy traffic share of around 3%. For this simulation, the peak hours in the morning (between 8:30 and 9:30 a.m.) and evening (between 5:30 and 6:30 p.m.) are simulated, when up to 1,675 vehicles per hour cross the intersection. The exact numbers of vehicle traffic volume considered in the simulations are taken from manual counts provided by the municipality of Munich and are listed in Table 5.3a. In addition to the passenger vehicles and trucks, a public bus runs westbound on Arcis street every 5 minutes. As the surroundings of the intersection comprise the major universities as well as several museums and restaurants, there is also a large number of pedestrians and bicyclists. Since no exact numbers on VRU activity were available, demand was estimated based on measurements at an intersection in the neighborhood and manual short-period counts of 15 minutes. Values are listed in Table 5.3b for bicyclists and Table 5.3c for pedestrians. To account for the estimation inaccuracy and in order to explore the effects of changing VRU demand, in addition to the estimated demand (denoted as "medium"), two scenarios with lower and higher demand are analyzed as indicated in the tables. Similarly to the evaluation in Chapter 4, left-turning bicyclists are not considered in the simulation study. The intersection is flat and normal conditions are assumed for the simulation study, i.e., regular visibility and a dry street surface.

5.4.2 Settings for the Applied OptIIC Strategy

As shown in Figure 5.6, the intersection zone is, in contrast to those modeled in the previous chapters, not symmetric: curve radii, distances for crossing the intersection zone and widths

[1]The map is taken from OpenStreetMap. The arial view of the intersection and surroundings was kindly provided by the Bavarian Agency for Digitisation, High-Speed Internet and Surveying.

Scenario	**Vehicle Demand in veh/h (Passenger Vehicles | Trucks)**							
	Westbound			**Southbound**		**Northbound**		**Total**
	Through	*Left*	*Right*	*Through*	*Right*	*Through*	*Left*	
Morning Peak	760 | 20	40 | 5	50 | 5	530 | 10	60 | 5	90 | 5	30 | 0	1560 | 50
Evening Peak	980 | 5	40 | 5	70 | 0	300 | 5	80 | 0	140 | 0	50 | 0	1660 | 15

(a) Vehicle Traffic.

Scenario	**Bicycle demand in bic/h**					
	Westbound		**Southbound**		**Northbound**	**Total**
	Through	*Right*	*Through*	*Right*	*Through*	
Morning Peak *Medium*	320	20	212	24	48	624
Low | *High*	160 | 480	10 | 30	106 | 318	12 | 36	24 | 72	312 | 936
Evening Peak *Medium*	408	28	120	32	76	664
Low | *High*	204 | 612	14 | 42	60 | 180	16 | 48	38 | 114	332 | 996

(b) Bicycle demand.

Scenario	**Pedestrian Activity in ped/h**				
	South	**East**	**North**	**West**	**Total**
Morning Peak *Medium*	86	72	84	70	312
Low | *High*	43 | 129	36 | 108	42 | 126	35 | 105	156 | 468
Evening Peak *Medium*	109	57	109	57	332
Low | *High*	55 | 164	29 | 86	54 | 163	28 | 85	166 | 498

(c) Pedestrian activity.

Table 5.3: Demand at the considered intersection.

of pedestrian crosswalks depend on the considered OD movement. These specifications can easily be handled with the intersection modeling approach presented in Section 4.2. Due to the narrow curve radii, speeds for through movement and turning movement differ. Exact radii and assumed speeds are shown in Appendix E.2. As briefly raised in Section 4.2, the consideration of different speeds within the intersection needs to be taken into account when resolving conflicts where vehicle paths merge or diverge. This is considered with adapted conflict regions and resulting minimum time headways as also shown in Appendix E.2. To simplify the approach, turning vehicles are assumed to accelerate with a fixed acceleration rate of $1.2\,\mathrm{m/sec^2}$ (the maximum acceleration value for buses and trucks) from leaving the intersection until reaching the maximum speed.

Again, a green wave is desired for bicyclists. Therefore, the signal is coordinated with surrounding intersections which are controlled in fixed cycles similarly to in the setup that was shown in Figure 4.32. The locations of the adjacent intersections are modeled based on the georeferenced photo shown in Figure 5.6. Other than the described adaptations, the input parameters for the OptIIC strategy are set similar to the ones that were established in Chapter 4. These values are displayed in Table 5.4.

Input Parameters	Values
Communication distance $dist^C$	150.0 meters
Assignment distance $dist^A$	50.0 meters
Roll period ϕ	3.0 seconds
Green phase durations t_{ped}^{green}	5.4 seconds
$t_{bic}^{mingreen}$	5.4 seconds *(with dynamic green phase durations as shown in Table 4.7)*
Maximum waiting times Θ_{ped} | Θ_{bic}	40.0 seconds | 10.0 seconds
Weighting factors γ_{veh} | γ_{bus} | γ_{bic} | γ_{ped}	$1 \mid 30 \mid 1 \mid 1$

Table 5.4: Parameter values for the test scenarios.

5.4.3 Benchmark Intersection Control

The OptIIC strategy is compared against a fully actuated traffic signal control that features vehicle detectors on each approach as well as PT prioritization. The fully actuated signal control scenario was implemented using the actuated traffic signal functionality of aimsun.next, which follows the National Electrical Manufacturers Association (NEMA) standards [NEMA, 2003]. It is modeled as realistically as possible based on the information which was kindly provided by the municipality of Munich. Figures of the detector placements and the traffic signal setup can be found in Appendix F.3. There are no exclusive pedestrian or bicycle phases, but pedestrian and bicycle signals are activated concurrently to the vehicle signal phases. The initial cycle time is 90 seconds, but green phase durations and cycle times vary depending on the demand. Since the intersection is considered here in isolation, the existing coordination with surrounding signals is not modeled. Bicycle phases at adjacent intersections are activated in fixed cycles in order to be consistent with the OptIIC scenarios, and the offset is chosen in such a way that a green wave for bicyclists is provided initially. However, due to the fluctuating cycle times resulting from the non-coordinated actuated signal control, there is no dynamic green wave for bicyclists which makes it difficult to compare their waiting times.

5.5 Simulation Results

The OptIIC strategy with the settings described in Section 5.4.2 is tested against the actuated TSC introduced in Section 5.4.3 for the six described demand scenarios. In the following, resulting delays for all road users are discussed in Section 5.5.1. Additionally, energy consumption models for electric vehicles (EVs) are briefly explained, and the energy consumption at the intersection is compared in Section 5.5.2. Section 5.5.3 presents maximum applied acceleration and deceleration values of passenger vehicles at the intersection as an estimation of smoothness of their trajectories.

5.5.1 Road User Delay

First of all, average road user delays are evaluated for all six considered demand scenarios. Results are displayed in Figure 5.7 with each subfigure representing one road user group. Fig-

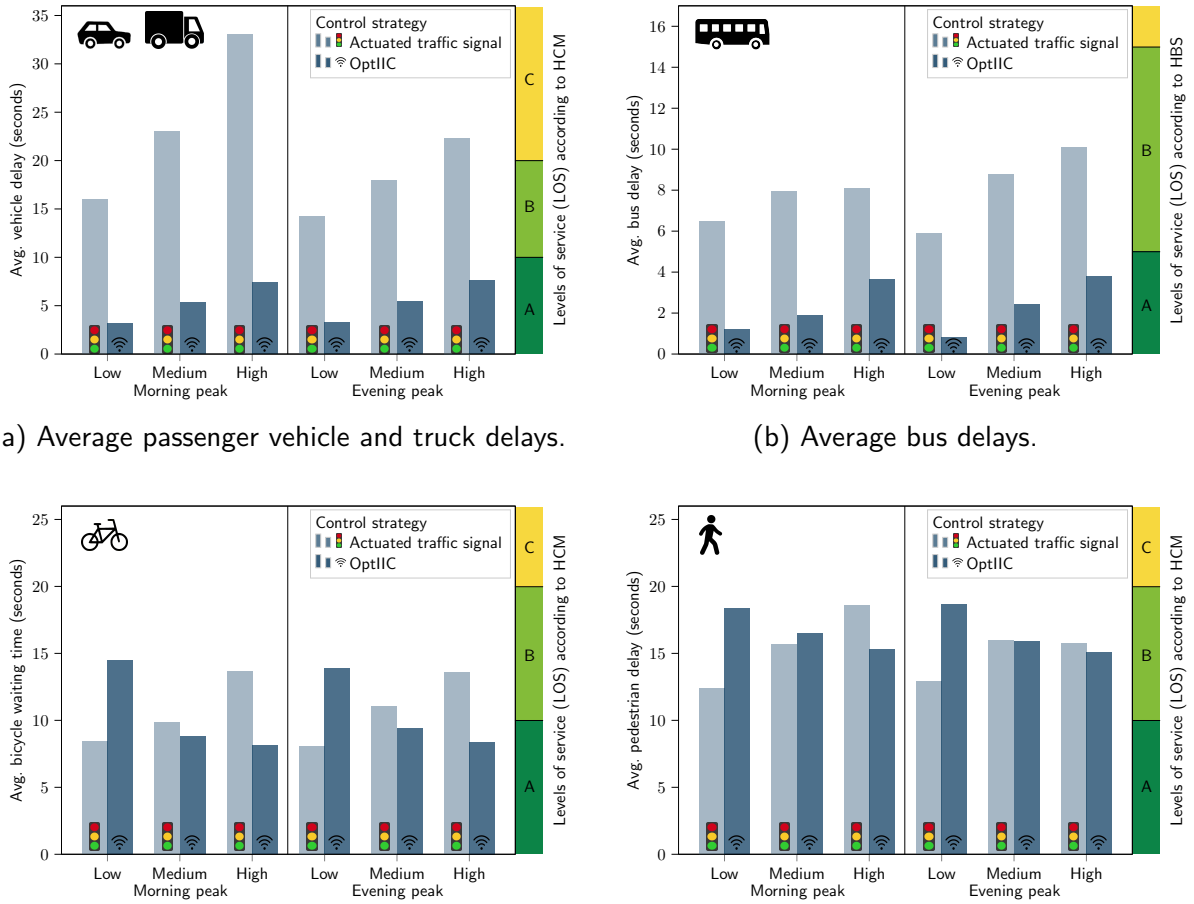

(a) Average passenger vehicle and truck delays.

(b) Average bus delays.

(c) Average bicycle waiting times.

(d) Average pedestrian waiting times.

Figure 5.7: Average road user delay at the considered realistic intersection: Default settings.

ure 5.7a shows average delays of passenger vehicles and trucks, Figure 5.7b shows average bus delays, Figure 5.7c shows average bicycle waiting times, and Figure 5.7d shows average pedestrian waiting times. All road user delays are calculated applying the formulas presented in Section 3.7.1. Again, vehicle delays are measured at the stop bar, which can underestimate delays in the TSC scenario, where vehicles sometimes have to yield to VRUs or oncoming traffic within the intersection. It needs to be noted, however, that the interaction between CAVs and VRUs is not modeled in detail. Depending on the field of view, occlusions, and possible support by infrastructure sensors, reaction times and acceleration values in the TSC scenario can change [Pechinger et al., 2021].

Figure 5.7a shows that the implemented OptIIC strategy significantly reduces vehicle delays as compared to the TSC setup for all considered demand scenarios with reductions between 62 and 78 %. In both control scenarios, larger VRU demand increases vehicle delays: in the OptIIC scenario, because vehicles compete with VRU green phases, and in the TSC scenario, because turning vehicles have to yield to pedestrians and bicyclists. Vehicle delays in the TSC scenario are larger in the morning than in the evening, even though the total demand is slightly

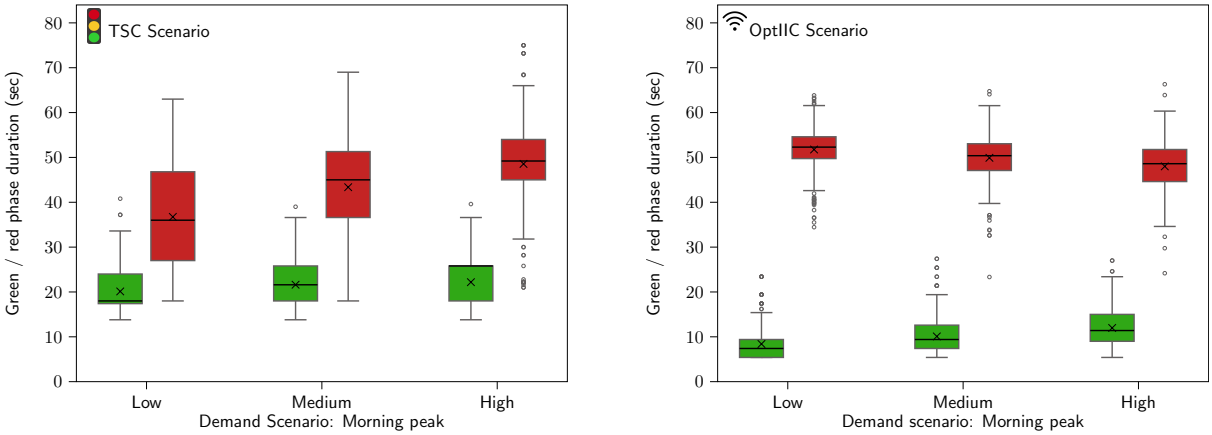

(a) Green and red phase durations of bicycle signals (TSC scenario).

(b) Green and red phase durations of bicycle signals (OptIIC scenario).

Figure 5.8: Green and red phase durations of bicycle signals.

lower. This results from the distribution of demand: in the morning, a larger portion of vehicle demand comes from the north. In the TSC scenario, delays are larger for vehicles coming from the north, because right-turning vehicles need to yield to bicyclists and, due to the narrow space, block the way for vehicle through movement on the same approach. In the evening, the vehicle demand on the northern approach is lower and the vast majority of vehicles travel on the main road featuring two vehicle lanes. The OptIIC scenario, in contrast, works equally well in the morning and evening. Here, conflicting movements of vehicles and VRUs are strictly separated.

As shown in Figure 5.7b, the bus prioritization works in both control scenarios (note that the scales of the different figures differ). Again, the OptIIC scenario significantly improves upon delay with reductions between 53 and 86 %. Bus delays are affected by VRU demand similarly to vehicle delays. However, since buses only travel on the main road, there are no significant differences between morning and evening peak hour. It needs to be noted that the existing coordination with the upstream intersection on the main road is not modeled. Vehicle and bus delays in the TSC scenario can thus be expected to be lower in reality – at least on the main road and if the coordination is applied for vehicle traffic.

Figure 5.7c shows that both the TSC or the OptIIC control can lead to lower bicycle waiting times, depending on the demand scenario. Both control scenarios feature the activation of bicycle green phases at adjacent intersections in fixed cycles. A dynamic bicycle green wave is only implemented in the OptIIC scenario. In the TSC scenario, the cycle times at the considered intersection change depending on vehicle detector data – measured cycle times range between 40 and 100 seconds. Nevertheless, the longer green phases in the TSC scenario, where bicyclists are given the right of way simultaneously to vehicle movement, lead to a similar bicycle LOS overall. Boxplots of bicycle green and red phase durations in the morning peak hour are shown in Figure 5.8. Figure 5.8a shows bicycle green and red phase durations in the TSC scenario. It can be seen that both green and red phase durations increase with

increasing VRU demand. This results from increased vehicle delays (and queues) which lead to extended vehicle green phases and increased cycle times if the actuated TSC is applied. Overall, the average cycle time increases from 57 seconds in the scenario with low VRU demand to 71 seconds in the scenario with high VRU demand, on average. The increased cycle times negatively affect bicycle waiting times (compare Figure 5.7c). On the other hand, larger VRU demand leads to lower bicycle waiting times in the OptIIC scenario, because bicycle green phase durations are extended while cycle times remain approximately 60 seconds. Figure 5.8b shows the green and red phase durations. It needs to be noted that red phase durations are only shown for those cycles with requested bicycle green phases. Especially in the scenario with low bicycle demand, the signal sometimes remains red for several cycles in the absence of bicyclists. The extended green phases lead to more bicyclists passing without stopping: from 64 % in the scenario with low VRU demand to 75 % in the scenario with high VRU demand (in comparison to approximately 49 % in the TSC scenario). All in all, the signal coordination (on all directions, not only the main road) leads to a LOS of A-B with significantly shorter green phases than in the TSC scenario. In the scenarios with high VRU demand, average bicycle delays in the OptIIC scenario are below 10 seconds and approximately in the same range like vehicle delays.

Pedestrian waiting times show a similar tendency, but the impact of VRU demand is not as strong as for bicyclists (compare Figure 5.7d). Again, pedestrian waiting times are negatively affected by increasing VRU demand in the TSC scenario because of the increased cycle times as explained above. In the OptIIC scenario, pedestrian green phase durations are fixed, and the improvements with increasing VRU demand result from the increased weighting factors of VRU green phases, from waiting pedestrians already having requested a green phase as explained in Section 4.7, and from longer bicycle green phases that block the way for vehicles. In the future, pedestrian green phase durations in the OptIIC scenarios could be adjusted dynamically such that pedestrians further benefit from the adjacent bike signal being green for a longer period of time. All in all, pedestrian LOS is similar for both control scenarios presented in Figure 5.7d.

As explained in Chapter 4, pedestrian and bicycle LOS can be influenced by changing green phase durations, maximum waiting times, and weighting factors. Given the simulation results and depending on policy considerations, a more VRU-friendly setup is conceivable for the presented demand scenario. Such a detailed prioritization is not easily possible in the TSC scenario. However, pedestrians do have an inherent disadvantage in the implemented OptIIC policy: in contrast to vehicles and bicyclists, their green phase is only requested when they are already at the intersection. In order to reduce pedestrian delays to very low values, if desired, the overall control setup hence needs to be challenged: pedestrians might have to be integrated into the scheduling policy ahead of time or be provided with a strict priority (comparable to a zebra crossing) that will always overrule other reservations.

5.5.2 Energy Consumption

EVs have the potential to significantly reduce both local and global carbon dioxide (CO_2) emissions as compared to internal combustion engine vehicles (ICEVs) – especially if energy

generation will be more sustainable in the future [Rostami-Shahrbabaki, Fehn, et al., 2021]. In order to achieve sustainability goals and reduce the dependence on fossil fuels, Germany, among other countries, is promoting a higher share of EVs via financial incentives and infrastructure measures [ADAC, 2022]. Additionally, several countries are discussing measures to ban the sales of ICEVs in the near future [Harloff et al., 2021]. Regarding the futuristic traffic scenario evaluated in this thesis, it is assumed here that all motorized vehicles at the intersection will be electric.

The significantly reduced vehicle delays in the OptIIC scenario lead to more vehicles passing the intersection zone without significant acceleration and deceleration. Additionally, even if vehicles are delayed, they smoothly adjust their speed in such a way that the sum of squared accelerations is minimized as described in Section 5.3. These circumstances are expected to lead to a decrease in energy consumption that will be evaluated in the following. In the following, the modeling of energy consumption will be explained, and the evaluation at the considered intersection will be presented.

Energy Consumption Modeling

The main difference of energy consumption modeling to fuel consumption modeling is that EVs do not consume energy while idling, and that they can regenerate energy during deceleration phases. There exist many approaches for modeling EV energy consumption that differ regarding their levels of detail and their intended purposes. A good introduction is given, for example, by Fiori et al. [2016], Luin et al. [2019], and Rostami-Shahrbabaki, Fehn, et al. [2021]. Most importantly, energy consumption models can be categorized as either being "forward models" or "backward models". Forward models are more detailed and complex. Starting from the engine, they model individual vehicle components and can be used in the industry to evaluate the impact of different vehicle configurations on energy consumption. However, their complexity makes them computationally intensive and it is difficult to combine them with surrounding frameworks such as a traffic simulation framework [Fiori et al., 2016]. Backward models work backwards in the sense that they first compute the tractive contribution required at the wheels and, based on this power, compute the energy needed at the motor. Along with vehicle characteristics, they use data that can be retrieved from microscopic traffic simulations [Luin et al., 2019]. In particular, the power at the wheels can be calculated in every time step depending on the current acceleration $acc(t)\left[\frac{m}{sec^2}\right]$ and the current speed $v(t)\left[\frac{m}{sec}\right]$, which makes the evaluation of energy consumption based on the presented simulation setup straightforward. In the following, the energy consumption at the intersection will be evaluated based on the backward model presented by Fiori et al. [2016] and Luin et al. [2019]. First of all, the model will be explained in several steps.

Step 1: In the first step, the instantaneous power at the wheels $P_W(acc(t), v(t))$ at time t is calculated using the formula

$$P_W(acc(t), v(t)) = p_1 \cdot acc(t) \cdot v(t) + p_2 \cdot v(t) + p_3 \cdot v^2(t) + p_4 \cdot v^3(t) \quad \left[\frac{J}{sec}\right], \qquad (5.13)$$

Calculation	Explanation and calibrated values according to [FIORI et al., 2016]	Parameter value
$p_1 = m$	m $= 1521\,\mathrm{kg}$ is the vehicle mass.	$p_1 = 1521.00$
$p_2 = m \cdot g \cdot (cos(\theta) \cdot \frac{C_r \cdot c_2}{1000} + sin(\theta))$	g $= 9.8066\,\mathrm{m/sec^2}$ is the gravitational acceleration. θ $= 0$ is the road grade (no road grade is assumed here). C_r $= 1.75$ and c_2 $= 4.575$ are rolling resistance parameters.	$p_2 \approx 119.42$
$p_3 = m \cdot g \cdot cos(\theta) \cdot \frac{C_r \cdot c_1}{1000}$	m, g, θ, and C_r are explained above. c_1 $= 0.0328$ is a rolling resistance parameter.	$p_3 \approx 0.86$
$p_4 = \frac{1}{2} \cdot \rho_{Air} \cdot A_f \cdot C_D$	$\rho_{Air} = 1.2256\,\frac{\mathrm{kg}}{\mathrm{m^3}}$ is the air mass density A_f $= 2.3316\,m^2$ is the frontal area of the vehicle. C_D $= 0.28$ is the aerodynamic drag coefficient of the vehicle.	$p_4 \approx 0.40$

Table 5.5: Explanation of parameter calculations.

that returns the power in Joule per second (1 Joule per second corresponds to 1 Watt). The parameters p_1, p_2, p_3, and p_4 depend on numerous factors including vehicle mass, aerodynamic coefficients, and rolling resistance parameters. Table 5.5 shows the definitions of the parameters and lists the values that were obtained for a Nissan Leaf by FIORI et al. [2016]. These values are going to be used in the evaluation presented here as well. As can be seen in the table, parameter p_1 is significantly larger than the other parameter values, which leads to $p_1 \cdot acc(t) \cdot v(t)$ being the dominant term in Equation 5.13. Therefore, if a vehicle is decelerating ($acc(t) < 0$), the power at the wheels $P_W(acc(t), v(t))$ will be negative as well (except for very small values of $|acc(t)|$).

Step 2: Having calculated the power at the wheels, the model now moves backwards to the vehicle battery using a simplified energy flow model as illustrated in Figure 5.9. If the vehicle is in traction mode, i.e., if $P_W(acc(t), v(t)) > 0$, the energy flows from the battery to the wheels. It is evident that, depending on electric losses in the battery, conversion losses in the motor, and mechanical losses in the gearbox, some power is lost. In order to simplify the model, the efficiencies of all involved components are combined to one single efficiency value η_p (called propulsion efficiency) by LUIN et al. [2019]. As shown in Figure 5.9, the required power can then be calculated as follows

$$P(acc(t), v(t)) = \frac{P_W(acc(t), v(t))}{\eta_p} \quad \left[\frac{J}{sec}\right], \text{ if } P_W(acc(t), v(t)) \geq 0. \tag{5.14}$$

If the vehicle is breaking, the power at the wheels $P_W(acc(t), v(t))$ is negative and the electric motor works as a generator that converts the kinetic energy into electric energy that recharges the vehicle battery. In this case, the portion of energy that reaches the battery depends on

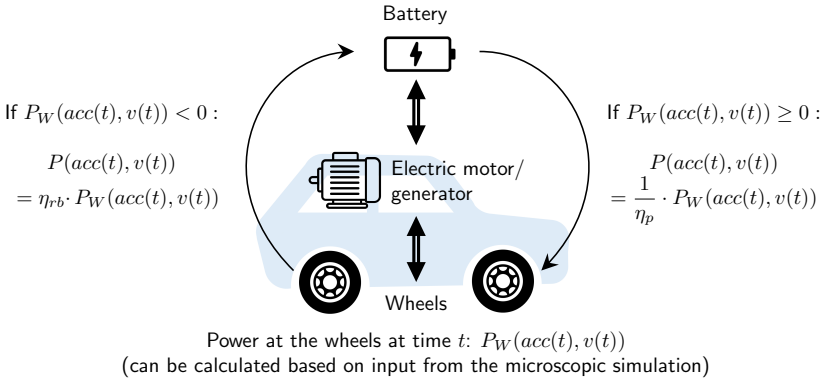

Figure 5.9: Explanation of energy flow

the regenerative breaking efficiency η_{rb} as also shown in Figure 5.9. In this case, the power can be calculated as follows:

$$P(acc(t), v(t)) = \eta_{rb} \cdot P_W(acc(t), v(t)) \quad \left[\frac{J}{sec}\right], \text{ if } P_W(acc(t), v(t)) < 0. \tag{5.15}$$

The values for η_p and η_{rb} provided by Luin et al. [2019] are used in the presented evaluation. For simplicity reasons, the easiest of their presented approaches is used, where both parameters are independent of the current vehicle and battery state. The authors assume the propulsion efficiency η_p to be 89.5 % and the regenerative breaking efficiency η_{rb} to be 87.5 % in their study. Clearly, these values may vary significantly depending on the vehicle components and the battery temperature, among other impacting factors.

Step 3: Based on the power required in every time step, the energy consumption of a vehicle over the entire trajectory is calculated. This is schematically displayed in Figure 5.10. Let k be the simulation step that starts at time t^k and ends at time t^{k+1}. Vehicle states can be obtained (and manipulated) via the API in between two simulation steps, i.e., at times t^k and t^{k+1}. For the evaluation of the energy consumption, it is assumed that both acceleration and speed remain constant during one simulation step, and the power in each simulation step is calculated based on these values. As shown in Figure 5.10, the acceleration in simulation step k can be calculated as $acc(k) = \frac{1}{\tau}\left(v(t^{k+1}) - v(t^k)\right)$, where τ is the simulation step size. The average speed during simulation step k is defined as $v(k) = \frac{1}{2}\left(v\left(t^k\right) + v\left(t^{k+1}\right)\right)$ and is illustrated by the step function in Figure 5.10. The power $P(acc(k), v(k))$ in simulation step k is then calculated applying Equations 5.13 to 5.15. While the equations return the instantaneous power in Joule per second, one simulation step does not exactly last one second. Therefore, the power needs to be multiplied by the step size τ. The energy consumption of the entire trajectory is then given as

$$P_{veh} = \sum_{k \in K_{veh}} P\left(acc_{veh}(k), v_{veh}(k)\right) \cdot \tau, \tag{5.16}$$

where K_{veh} is the set of all simulation steps that are relevant for the calculation of the energy consumption of the considered vehicle veh. In order to make the energy consumption of different trajectories comparable, all vehicles will cover the exact same distances.

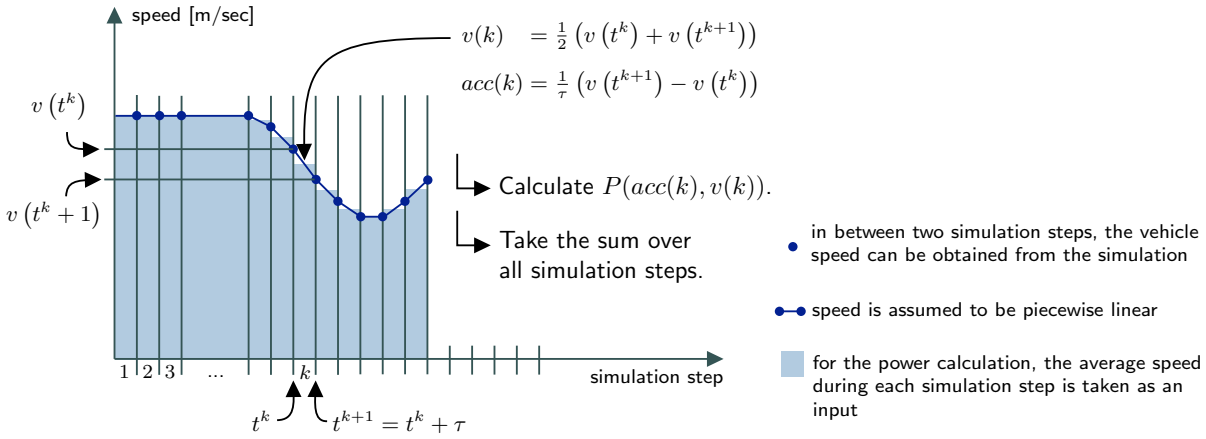

Figure 5.10: Piecewise constant trajectory obtained from the microscopic traffic simulation.

Evaluation

In the given intersection scenario, all vehicle trajectories are evaluated for a distance of 500 meters with the intersection in the middle of the path. This makes sure that vehicles have crossed the intersection and returned to driving at the maximum allowed speed. Additionally, since no spill-back effects occur in the considered scenarios, all vehicles enter the communication range of the intersection with a speed of 30 kilometers per hour. Figure 5.11 shows three different example trajectories. Each trajectory representation features diagrams with position, speed, acceleration, and energy consumption over time. The first one, shown in Figure 5.11a, shows the trajectory of a vehicle that has passed the intersection without experiencing delay. Figure 5.11b shows the trajectory of a vehicle that stopped at the traffic signal. Figure 5.11c shows the trajectory of a vehicle in the OptIIC scenario that experiences the same delay as the vehicle in Figure 5.11b (approximately 10 seconds). It can be seen that the vehicle in Figure 5.11c does not stop at the intersection but decelerates in order to meet the assigned arrival time and accelerates again before entering the intersection zone.

Since both efficiency factors applied in Step 2 of the modeling approach (η_p and η_{rb}) are between zero and one, the regenerative breaking will not regenerate the entire energy used during the acceleration phase. It is hence most beneficial overall to remain at a constant speed. This is reflected in the overall energy consumption of the three presented trajectories. The overall energy consumption of the trajectory shown in Figure 5.11a is 23.91 Wh. With the additional breaking and accelerating, the energy consumption rises to 26.94 Wh (Figure 5.11b) and 26.60 Wh (Figure 5.11c). Interestingly, the energy consumption of those two trajectories is almost the same, even though stronger accelerations are applied in the TSC trajectory. As can be seen from the depicted power curves, this mainly results from the efficient energy regeneration. Additionally, $acc(t) \cdot v(t)$ is the dominant term when calculating the instantaneous power at the wheels, and the stronger acceleration values in the TSC example trajectory are applied at lower speeds. This leads to a lower peak consumption of approximately 16,000 J/sec (as compared to almost 21,000 J/sec in Figure 5.11c).

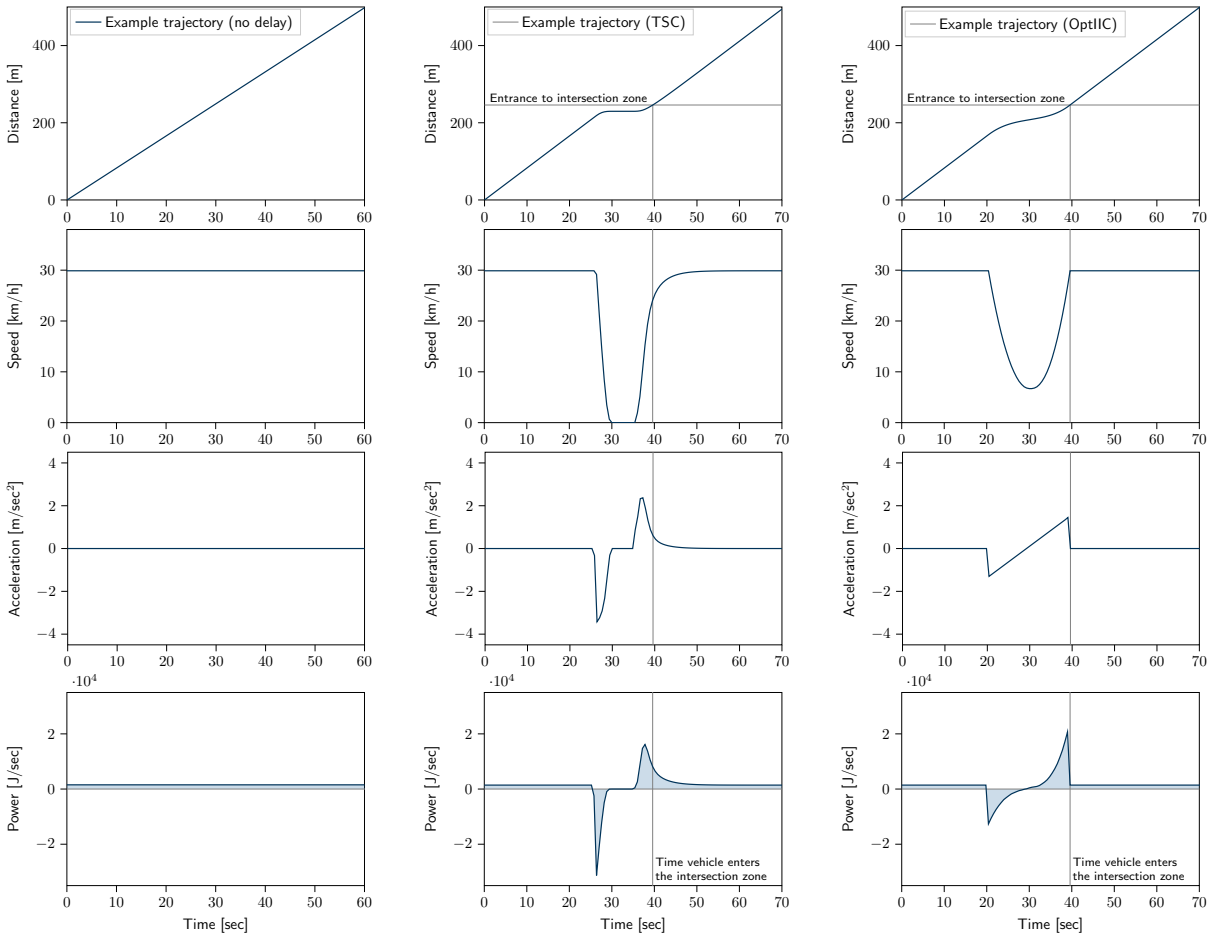

(a) Baseline trajectory (no delay caused by the intersection).

(b) Trajectory of a vehicle in the TSC scenario with a delay of 10 seconds.

(c) Trajectory of a vehicle in the OptIIC scenario with a delay of (10 seconds).

Figure 5.11: Three different example trajectories considered for the energy evaluation.

Regenerative breaking is not considered in most of the current analyses (compare, e.g., Hu et al. [2021]). However, it has a significant influence on the overall energy consumption as visible in Figure 5.11. Without regenerative breaking capabilities, the energy consumption of the trajectory shown in Figure 5.11b is 39.11 Wh and of the trajectory shown in Figure 5.11c is 37.44 Wh. For entire driving cycles, Fiori et al. [2016] report that regenerative breaking can increase the driving range by up to 40 %.

In the following, results will be evaluated for the scenarios with medium pedestrian and medium bicycle demand. Energy consumption is evaluated for passenger vehicles only, because the model is not calibrated for buses and trucks. Nevertheless, similar relative effects can be expected for buses and trucks as well. As described above, vehicles traveling at a constant speed and without delay have an energy consumption of 23.91 Wh on the considered distance of 500 meters. In fact, the energy consumption of the trajectory shown in Figure 5.11a can be considered as a baseline consumption, and the additional energy consumption due to

	Avg. consumption per vehicle [Wh]			*In addition to "base consumption" [Wh]*		
	TSC	OptIIC	Diff. (%)	TSC	OptIIC	Diff. (%)
Morning Peak	26.97	25.34	−6.0 %	3.06	1.43	−53 %
Evening Peak	26.98	25.32	−6.2 %	3.07	1.41	−54 %
	Total consumption during peak hour [Wh]			*In addition to "base consumption" [Wh]*		
	TSC	OptIIC	Diff. (%)	TSC	OptIIC	Diff. (%)
Morning Peak	42,073.20	39,530.40	−6.0 %	4,773.60	2,230.80	−53 %
Evening Peak	44,786.80	42,031.20	−6.2 %	5,096.20	2,340.60	−54 %

Table 5.6: Comparison of average energy consumption for the different considered scenarios.

the "disturbance" caused by the intersection can be compared. As shown in Table 5.6, the intersection with the TSC scenario adds an average of 3.06 Wh per vehicle in the morning and 3.07 Wh in the evening peak hour. The intersection with OptIIC adds 1.56 Wh per vehicle in the morning and 1.41 Wh in the evening peak hour. This is a significant reduction of approximately 50 %. Altogether, more than 2 kWh are saved during the peak hours. By adjusting the objective function, the trajectory optimization in the OptIIC scenario could be redesigned in such a way that the energy consumption is further reduced. However, it can be seen that the overall reduction potential is limited, because the largest part of the energy consumption is the base consumption which cannot be decreased by a different control strategy or trajectory planning setup. Additionally, the energy needs of auxiliary devices, such as heating unit, air conditioning, and radio, are not considered yet and are expected to add an additional 700-2,500 Joule per second [Luin et al., 2019]. This further reduces the relative potential for reduction. When optimizing the trajectories, it is thus debatable whether focus should be put on energy consumption, or on driving comfort and perceived safety. In order to get a first estimate of trajectory smoothness, the maximum applied acceleration and deceleration values are presented in the following.

5.5.3 Maximum Acceleration and Deceleration

According to Bae et al. [2019], acceleration and deceleration values of vehicles significantly impact safety and passenger comfort. Additionally, strong acceleration and deceleration increase polluting tire wear [Stein, 2021]. This evaluation is hence concluded with a comparison of maximum acceleration and deceleration values applied in the simulation. The morning peak scenario with medium VRU demand is presented here by way of example. In order to be consistent with the above evaluation of energy consumption, only passenger vehicles are taken into account. Figure 5.12 shows the distribution of maximum applied acceleration and deceleration values for both the TSC and the OptIIC setup in steps of 0.5 m/sec^2. In both figures, the values are categorized as 'comfortable', 'normal', and 'aggressive'. These categories are defined according to Bae et al. [2019] (with rounded values), who surveyed several studies on driving behavior. The authors assume that maximum acceleration and (absolute) deceleration values should remain below 1.5 and 2 m/sec^2, respectively, for a comfortable driving experience. For automated shuttles carrying both seated and standing passengers, both values should remain below 0.9 m/sec^2.

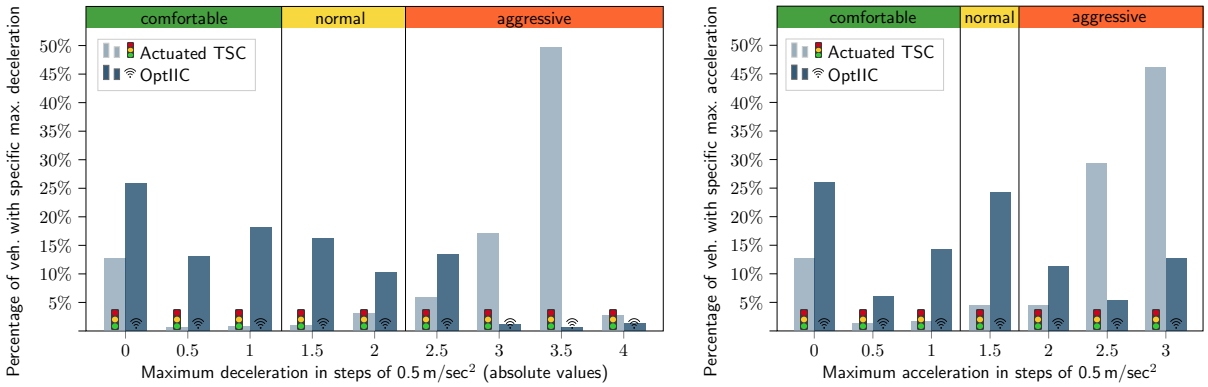

(a) Maximum deceleration values.

(b) Maximum acceleration values.

Figure 5.12: Maximum applied deceleration and acceleration values. Aggressive/normal/comfortable deceleration and acceleration are defined according to Bae et al. [2019].

First of all, Figure 5.12 shows that the percentage of vehicles with no delay (maximum acceleration and deceleration value of 0 m/sec^2) is doubled from approximately 13 % in the TSC scenario to approximately 26 % in the OptIIC scenario. Furthermore, delayed vehicles show relatively high acceleration and deceleration values in the TSC scenarios with peak percentages at the assumed acceleration and deceleration limits. Approximately 75 % of all vehicles in the TSC scenario experience absolute deceleration values above 2.0 m/sec^2, and approximately 80 % experience acceleration values above 1.5 m/sec^2. By contrast, in the OptIIC scenarios, only 16 % of vehicles experience deceleration and 29 % experience acceleration values in the 'aggressive' range. The peak value for maximum acceleration between 1 and 1.5 m/sec^2 apparent in Figure 5.12b results from turning vehicles accelerating after having crossed the intersection. To summarize, approximately 13 % of vehicles in the TSC scenario and 45 % in the OptIIC scenario stay within the stricter 'comfortable' range. On average, maximum applied deceleration (absolute value) is reduced from 2.89 to 0.98 m/sec^2 (a reduction of 66 %), and maximum applied acceleration is reduced from 2.15 to 1.13 m/sec^2 (a reduction of 47 %).

In order to further evaluate and improve upon passenger comfort and safety, jerk needs to be taken into account in future analyses [Bae et al., 2019]. In the OptIIC scenario, jerk can be integrated into the objective function of the optimal control problem as done by Ntousakis et al. [2016]. Additionally, for further analyses of the OptIIC scenario, the impacts of changing communication and assignment distances on trajectory smoothness could be investigated. An earlier assignment of the vehicle arrival time could lead to smoother trajectories, but at the same time limits the flexibility of the scheduling algorithm. In the TSC scenario, acceleration and deceleration (and jerk) could be bounded more strictly. Clearly, as has been discussed with the state of the art of TSC in Section 2.1, this will have a direct impact on the saturation flow rate and, consequently, on the capacity. In a connected vehicle environment, the optimal control problem for smooth trajectory planning could be applied at signalized intersections as well. However, at small intersections, such as the one simulated in this chapter, there are many permitted movements. In particular, all vehicle turning movements need to give way to VRUs, and left-turning movements additionally need to wait for oncoming traffic. Therefore,

vehicles might need to stop within the intersection and it is thus not always recommendable to make them arrive at the intersection with a high speed. Additionally, due to the stochastic VRU behavior, it is not clear when exactly a vehicle queue will be dissolved. Therefore, the potential for planning smooth vehicle trajectories is limited in the TSC scenario as compared to the OptIIC that strictly separates conflicting movements.

5.6 Summary

This chapter described the implementation of the previously presented strategies in detail. The explanations show that each of the road user groups is modeled individually, and a focus is put on representing the heterogeneity that can be found in reality. Additionally, model input parameters and their assumed values are established based on literature findings. Overall, it can be concluded that the level of detail is in fact sufficient for a simulation-based comparison of the presented strategies with an existing TSC. To this end, a real intersection in Munich was replicated in aimsun.next, the OptIIC strategy was implemented, and a simulation-based evaluation was conducted using demand measured at the site. The chapter thus provides and answer to Research Question 3: *"What effects could automated intersection control have when applied to a realistic multimodal intersection?"*. In addition to comparing road user delays, the energy consumption and applied acceleration and deceleration values of vehicles were compared. In the OptIIC scenarios, the trajectory planning of vehicles on the approach to the intersection was improved by solving an optimal control problem with the objective of minimizing the sum of squared accelerations. The following results can be summarized:

- ✓ Applying the OptIIC scheme, average vehicle delays can be reduced by up to 72 % and average bus delays by up to 86 %, while at the same time keeping VRU delays on approximately the same level as with the TSC.
- ✓ Energy consumption caused by the "disturbance" of the intersection control can be reduced by up to 54 %. These results could be improved even further by adjusting the objective function of the trajectory planning approach to minimize energy consumption. However, the total energy consumption consists of a large base consumption that cannot be decreased, and potential for further reduction is thus limited.
- ✓ Maximum applied acceleration and deceleration values are significantly decreased in the OptIIC scenario (by 47 % and 66 % on average, respectively). To further increase driving comfort and trajectory smoothness, the objective function of the trajectory optimization problem could include both acceleration and jerk in the future.

It needs to be noted that the presented results were measured applying the control strategies to a single intersection. The comparison hence doesn't take the interdependencies with surrounding intersections and the existing TSC coordination with the intersections on the one-way main road into account. However, the evaluation gives a first impression of the potential that the presented strategy has for urban traffic. Additionally, the very promising OptIIC results can be obtained where coordination is not possible or it is decided to apply a coordination for bicycle traffic (as was done in the presented scenarios). Further analyses of a corridor of intersections or even a small network will be left for future work.

Chapter 6

Conclusions and Future Research

This chapter concludes the thesis by highlighting the main contributions and key results in Section 6.1 and providing an outlook on possible future research topics in Section 6.2.

6.1 Summary and Conclusions

This thesis presented and evaluated new integrated intersection control strategies for future urban traffic scenarios with CAVs, pedestrians, and bicyclists. They are unique in the sense that pedestrians and bicyclists are fully integrated into AIM strategies in a demand-responsive way. In order to ensure accessibility of public space, the integration is made possible without pedestrians and bicyclists having to be equipped with connected devices. The developed control schemes are assigned to two broader categories: the *slot-based* control (SlotIIC) strategies work with a discretization of space and time. Discrete zones of the intersection are reserved for specific vehicle or VRU movements during discrete time slots. They are assigned on an FCFS basis that is appended by a set of rules to integrate pedestrians and bicyclists in such a way that defined maximum waiting times are not exceeded. The *optimization-based* (OptIIC) strategies work with a scheduling optimization problem that resolves conflicts and assigns vehicle arrival times and VRU signal green phases by applying a rolling-horizon scheme. The objective function minimizes the sum of weighted delays and, via the weighting factors and suitable constraints, offers the possibility to balance delays and prioritize individual or groups of road users to achieve policy objectives. All presented control strategies were implemented and tested using the microsimulation platform aimsun.next in combination with Python and the Gurobi solver (for the optimization-based scenarios). The most promising control setup was additionally implemented within a simulation framework of a realistic intersection in Munich with measured heterogeneous demand. In this final evaluation, vehicle trajectories on the approach to the intersection were optimized by repeatedly solving an optimal control problem, and resulting energy consumption and maximum applied acceleration were evaluated.

First of all, the evaluation of both strategy types considering the key requirements defined in Chapter 1 is summarized in the following. Both schemes integrate all considered road users and can thus be considered to be **multimodal**. The control strategies ensure **safety** by detecting conflicting movements and temporally shifting vehicle arrival times and signal green phases such that sufficient time gaps are ensured. In contrast to conventional TSC, vehicle and VRU movements within the intersection are strictly separated in order to eliminate accidents with turning vehicles hitting pedestrians or bicyclists. In terms of **efficiency**, both strategy types outperform conventional TSC in several scenarios. However, in scenarios with large vehicle

demand, the alternating right-of-way assigned by the FCFS-based SlotIIC scheme can be inefficient. Due to the optimized allocation of space-time and implicit vehicle platoon formation, the OptIIC strategies lead to additional significant improvements considering both intersection capacity and road user delays. Both strategy types allow for limiting VRU waiting times and are able to **balance** the delays of the different road user groups by implementing suitable upper bounds. With the weighting factors considered in the objective function, the OptIIC strategies offer further dials to balance road user delays and additionally allow for the prioritization of user groups. The presented OptIIC scheme can hence be implemented as a **policy instrument** by prioritizing certain road users depending on the environment of the intersection, the current demand situation, and societal interests. The impacts of parameter settings are complex and hence need to be tuned for specific situations. While the SlotIIC strategies could also possibly be extended with more rules to overwrite existing reservations, the integration of policies is not straight-forward. Both control strategies allow for the **demand-responsive** integration of all road users with vehicles directly signing up with the controller and VRUs being recognized by the infrastructure. At the same time, VRUs are not required to wear connected devices and the VRU signalization principally works as it does today. The strategies can hence be considered to be **low-tech**. However, the implemented OptIIC strategies require VRU detection and are thus more technically demanding. The fixed time slots and conflict regions of the SlotIIC strategies make it difficult to integrate **heterogeneous road users**, e.g., vehicles with different dimensions like buses or trucks. The consideration of continuous time and the dynamic calculation of conflict regions applied in the OptIIC scheme significantly improves the real-world applicability with regard to this aspect. Additionally, the **transferability** to other, possibly non-symmetric, intersections is improved. Nevertheless, it needs to be noted that both control schemes require intersection designs with separate vehicle and bicycle lanes.

From the above evaluation, it becomes clear that the SlotIIC scheme cannot fulfill all defined requirements and its drawbacks make it difficult to be implemented at a realistic intersection. With the OptIIC strategy, the consideration of heterogeneous vehicle dimensions and different turning radii is instead straight-forward. Therefore, the OptIIC strategy was implemented in the simulation-based evaluation considering a realistic intersection and compared to the fully actuated TSC that is currently implemented on site. The OptIIC scheme was able to reduce average vehicle and bus delays by up to 72 % and 86 %, respectively, while keeping VRU delays on approximately the same level as with the TSC. The bus prioritization via increased weighting factors has proven to be successful. Furthermore, vehicle energy consumption caused by accelerating and decelerating at the intersection as well as maximum applied acceleration and deceleration values (as a measure of comfort) could be significantly reduced.

Overall, the main contributions of the thesis are (i) the integration of pedestrians and bicyclists into AIM strategies, (ii) the balanced consideration of all road users and the integration of policy objectives, and (iii) the simulation-based evaluation assuming a real intersection with measured demand. This final evaluation demonstrates the substantial improvements compared to the currently applied TSC. The presented control approaches and evaluations contribute to answering the research questions as shown in Figure 6.1. The lower part of the figure summarizes the most promising open issues of each question, which leads us to the next section.

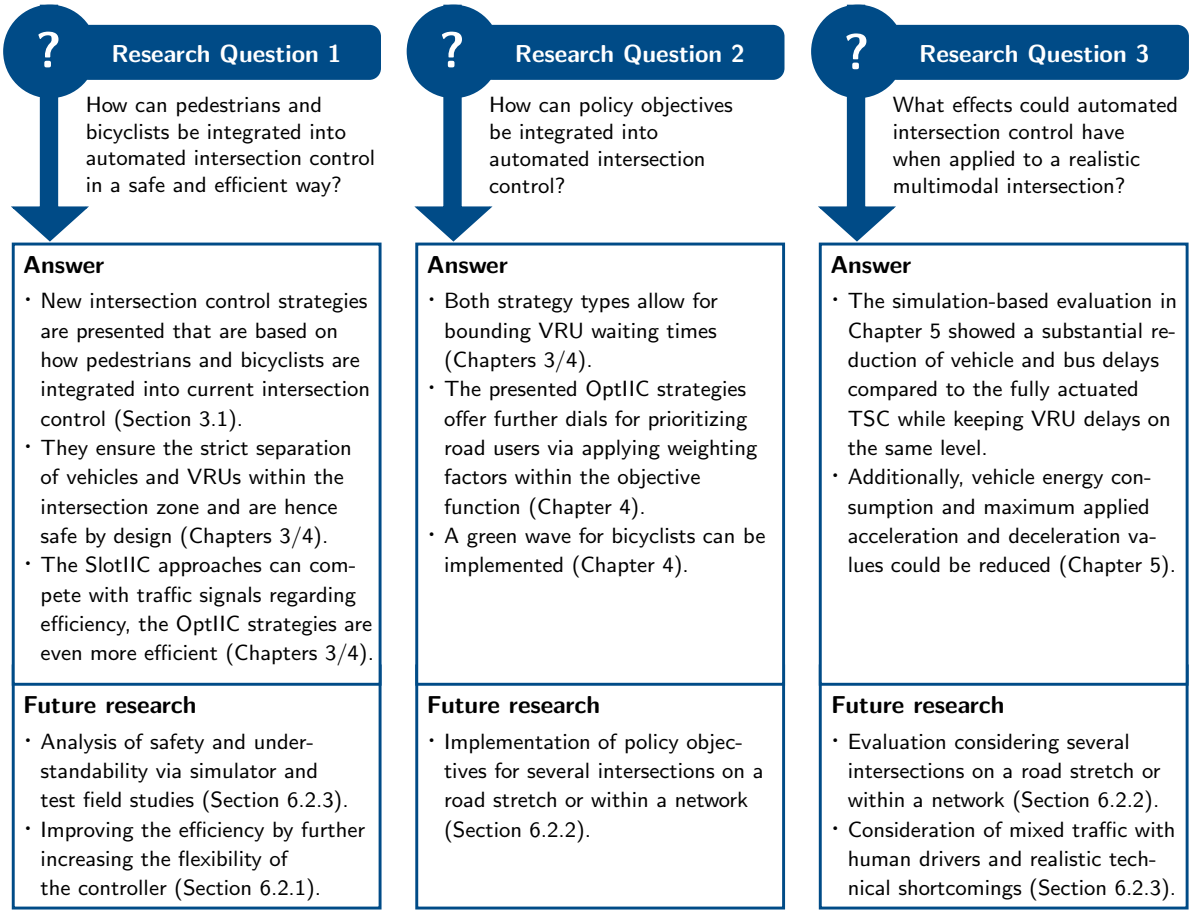

Figure 6.1: Answers to the research questions defined in Chapter 1.

6.2 Future Research

Following the research questions defined in Chapter 1, the control strategies and evaluation criteria in this thesis were developed on the edge between the optimization of a futuristic control setup and the applicability in a livable, multimodal urban environment. The presented intersection control framework can be extended into several directions to address a variety of further research questions. They can broadly be categorized into three areas that will be described in the following sections: Possible extensions to achieve further efficiency improvements at future intersections are described in Section 6.2.1. Section 6.2.2 presents ideas on how to extend the control for networks of several intersections. Finally, Section 6.2.3 addresses challenges that arise if applying the control in practice, such as possible technical shortcomings and public acceptance.

6.2.1 Efficiency Improvements

The control strategies presented in this thesis showed convincing results considering road user delays and intersection capacities. This especially holds true for the OptIIC scheme. The efficiency of the intersection control could be further improved by increasing the flexibility of the controller or including more information into the decision-making process. First of all, some

simplifying constraints have been made in this thesis that could be relaxed in order to improve the overall efficiency. One simplification is that vehicles cross the intersection at a pre-defined and constant speed. Instead, vehicle speeds could be limited by some lower and upper bound and be decided on within the optimization. It is also possible that vehicles accelerate or decelerate while crossing the intersection, i.e., they are not only assigned with an arrival time and a specified speed, but a sophisticated trajectory. Furthermore, in a multi-lane intersection, incoming and outgoing lanes could be assigned within the optimization procedure, or lanes could be assigned for alternate directions [Mitrovic et al., 2020]. In a revolutionary vision of the future, even road spaces without lanes are conceivable, such that the entire two-dimensional space can be freely allocated (compare, e.g., [Papageorgiou, Mountakis, et al., 2021; B. Li et al., 2018]).

Additionally, signal infrastructure for pedestrians and bicyclists is assumed to be similar to today's infrastructure in this thesis. In particular, signal heads are assumed to look and function like today. Some efficiency improvements are possible even if VRUs do not significantly change their behavior or need to be equipped with technological devices. For example, pedestrian signals could be directional and block space-time only for the requested direction of pedestrian movement. Additionally, green phase durations and clearance times could be dynamically shortened or extended based on input from the VRU detection. This could lead to a more efficient use of the available space and thus reduce delays. Further improvements can be expected, if (at least some) pedestrians and bicyclists use connected applications that sign up with the infrastructure ahead of time and reserve specific time slots similarly to vehicles. Such information could additionally be used within a possible network extension, where routing advice could be included.

6.2.2 Network Extension

The idea of providing a green wave for bicyclists that was integrated into the control design in Chapter 4 already shows the importance of considering a road stretch with several intersection zones in the future. Additionally, it is clear that the analyses at a single intersection zone cannot account for network effects. For a more realistic evaluation, spillback effects from downstream intersections can be considered as proposed by M. I.-C. Wang et al. [2021]. Additionally, as briefly described in Section 4.7, R. Chen et al. [2020] were able to stabilize queues in a network with 7×7 identical intersections by combining the optimization-based control strategy with a max pressure control. Such an approach could further be appended with considering multimodal traffic or applying strategies for optimally distributing the traffic within the network. Ultimately, more realistic networks with multimodal traffic and different types of roads and intersections could be considered, where some areas are suitable for heavy vehicle traffic and some areas prioritize VRU movement more strictly.

6.2.3 Real-World Applicability and Acceptance

The presented results show a great potential for future traffic scenarios where all vehicles are connected and automated, and no human drivers are present on the road. However, a penetration rate of 100% CAVs will not come overnight. As mentioned in Chapter 1, it is conceivable that manually driven vehicles will be banned from at least parts of the street network once

CAVs have been proven to be significantly safer than human drivers [J. F. Müller and Gogoll, 2020]. Nevertheless, large parts of the traffic network will have to cope with mixed traffic of CAVs and human-driven vehicles in the near future. It has been shown in this thesis that the centralized intersection controller along with human-machine interfaces that can be as simple as signal heads is able to efficiently control an intersection zone with CAVs and VRUs. Human-driven vehicles could similarly be integrated into the control via signal phases. First such ideas have been proposed by Dresner and Stone [2006], but they have not yet been analyzed in combination with optimization techniques and for multimodal traffic. It is open for further assessment if such a mixed layout with signal phases and individual trajectories is superior to state of the art TSC and how different penetration rates affect the performance.

Even in a fully connected traffic environment, information and resulting vehicle actions might be imperfect. Communication latency, package drop rates, positioning inaccuracies, and other potential flaws are not considered in this thesis. The scenarios could be made more realistic by integrating stochastically occurring disturbances, and the robustness of the approach could be analyzed and improved. Improving the real-world applicability also includes the vehicle trajectory optimization that is currently simplified by assuming piecewise-constant acceleration as described in Section 5.3. The feasibility of recommended trajectories could be tested in a vehicle-in-the-loop environment similar to the experiment described by Fayazi, Vahidi, and Luckow [2019]. This would also allow for actually measuring resulting fuel or energy consumption, and passenger comfort – and ultimately further improving on these aspects. This leads to the last, and arguably most important, aspect. Thorough simulator studies and experiments in closed field tests (possibly including augmented reality features) are necessary to analyze whether the designed control architecture with a mixture of individual vehicle trajectories and phase-based VRU consideration is understandable and desirable from the road users' point of view. It is especially important to evaluate whether the traffic situation is comprehensible from the VRU perspective, and if pedestrians and bicyclists feel safe crossing the intersection. These analyses could also challenge the assumed VRU behavior models, the simultaneous right of way for pedestrians and bicyclists, and the focus on delays and waiting times as the primary evaluation criteria. In fact, it is conceivable that the perceived safety and level of traffic stress, which are increasingly investigated in literature (compare, e.g., [Ferenchak and Marshall, 2020]) are considered more relevant.

Finally, CAVs are not common on our roads yet, but their advent provides the opportunity to re-think the way our streets and intersections are organized. In this process, it is important to develop a vision for future urban traffic, to consider all road users, and to understand the impacts that technological implementations will have both microscopically and network-wide. This thesis contributes to these challenges by proposing possible new intersection control algorithms, assessing their local effects, and evaluating how different control parameter settings could support the implementation of policies. For example, prioritizing PT vehicles or providing a green wave for bicyclists leads to a better LOS for environmentally friendly traffic modes and can ultimately support their usage. Clearly, intersection control alone will not change the overall traffic situation in a city. Therefore, such policies need to be integrated into an overall concept defined by society and politics and combined with appropriate infrastructure development, attractive PT, and financial incentives, for example.

List of Figures

List of Tables

List of Terms and Abbreviations

3GPP 3rd Generation Partnership Project 4

ACC adaptive cruise control 4, 157
ADAS advanced driving assistance systems 4
AIM autonomous intersection management 20–23, 26, 33, 34, 36–38, 40–45, 47, 53, 55, 71, 89, 108, 162, 183, 184, 189, 193, 219–225
API application programming interface 73, 88, 128, 153, 156, 177
AV automated vehicle 1, 5, 7

B&B branch and bound 106, 107
BSM basic safety message 3

C-ITS Cooperative ITS 3
C-V2X Cellular V2X 4
CAM cooperative awareness message 3
CAV connected automated vehicle 1, 3, 6, 7, 9–11, 19, 20, 38, 41–45, 153, 157, 158, 172, 183, 186, 187, 193, 199
CO_2 carbon dioxide 174

DSRC Dedicated short-range communications 3, 4, 158

ETSI European Telecommunications Standards Institute 3
EU European Union 1, 3, 4, 6
EV electric vehicle 171, 174, 175

FCFS first come, first served 27, 29–34, 40–43, 55, 60, 62, 63, 65, 74, 75, 87–90, 105, 109, 128–131, 137, 138, 150, 183, 184, 191, 220–225
FIFO first in, first out 27

GIS geographic information system 154
GLOSA green light optimal speed advisory 19, 51, 85, 122, 149
GPS Global Positioning System 16, 157, 220

HBS Handbuch zur Bemessung von Straßenverkehrsanlagen 15, 16, 49, 70, 77, 78, 193

HCM Highway Capacity Manual 14–16, 49, 70, 77, 78, 161, 193
HMI human machine interface 52, 94

ICEV internal combustion engine vehicle 174, 175
IEEE Institute of Electrical and Electronics Engineers 3
ITS intelligent transportation systems 3, 6, 50, 51
ITSA initial time slot auction 30

LED light-emitting diode 51
LOS level of service 15, 16, 18, 38, 40, 43, 48–51, 64–66, 70, 77–79, 81, 82, 84, 86, 88, 90, 107, 120, 123, 136, 138, 139, 143, 150, 152, 173, 174, 187, 193, 239
LTE long term evolution 4

MILP mixed-integer linear program 31–33, 37, 43, 44, 105, 111, 221–225

NEMA National Electrical Manufacturers Association 171
NHTSA National Highway Transportation Safety Administration 6

OBU On-Board Unit 4
OD origin-destination 58, 59, 62, 81, 82, 84, 117, 154, 161, 170
OptIIC optimization-based integrated intersection control 93, 105, 127–132, 137, 138, 140–142, 145, 150–154, 156, 163, 164, 168, 170–175, 178–185, 191, 193
OSM Open Street Map 44

PDR packet drop rate 3, 158
PT public transport 7, 16–18, 44, 137, 150–152, 159, 171, 187, 191, 240, 241

RiLSA "Richtlinien für Lichtsignalanlagen" 11, 76, 83, 102, 161, 162
RSU Road Side Unit 4
RToR Right-Turn-on-Red 48, 68, 70, 83, 147

SlotIIC slot-based integrated intersection control 47, 74–82, 86, 88–90, 93, 102, 121, 128–130, 138, 141, 142, 147, 149, 150, 153, 154, 163, 183, 184, 190, 193
SPaT signal phase and timing 4
STM Signal Timing Manual 11, 17, 43

TRB Transportation Research Board 16
TSC traffic signal control 3, 8–11, 16, 18, 19, 25, 40–42, 75, 77–83, 85, 88, 89, 112, 151–153, 168, 171–174, 178–184, 187, 190, 192, 221–225, 229, 239–242

TSE time slot exchange 29
TUM Technical University of Munich 168

U.S. United States 3–6

V2I Vehicle-to-Infrastructure 3, 16, 19, 73
V2V Vehicle-to-Vehicle 3, 16
V2X Vehicle-to-Everything 3
VDA Verband der Automobilindustrie 5
VIL vehicle-in-the-loop 39
VRU vulnerable road user 6, 7, 9, 15, 16, 48–54, 56, 57, 60, 68, 70, 73–75, 81, 89–91, 93, 96, 97, 100, 107, 117, 118, 122–125, 127, 128, 130, 136, 150–152, 154, 156, 162, 169, 172–174, 180–184, 186, 187, 189, 193, 240

WLAN wireless local area network 3, 4, 157

Publications

The content of the following peer reviewed papers is entirely or partly described in this dissertation. For each paper, the addressing sections are indicated. The publications are ordered by year.

- Niels, Erciyas, et al. [2018]
  - Section 5.2: Parameter settings in car-following models for CAVs.
- Niels, Mitrovic, Bogenberger, et al. [2019]
  - Section 3.1: Consideration of pedestrians at signalized intersections.
  - Section 3.5: Integration of pedestrians into slot-based intersection control.
  - Section 3.7: Results for scenarios with vehicles and pedestrians.
- Niels, Mitrovic, Dobrota, et al. [2020]
  - Section 3.8: Extension of the slot-based intersection control to an intersection with several lanes on each approach.
- Niels, Bogenberger, et al. [2020]
  - Section 3.1: Consideration of bicyclists at signalized intersections.
  - Section 3.6: Integration of bicyclists into slot-based intersection control.
  - Section 3.7: Results for scenarios with vehicles and bicyclists.
  - Section 5.2: Bicycle behavior modeling.

Bibliography

Ackermann, Claudia; Matthias Beggiato; Luka-Franziska Bluhm; Alexandra Löw; Josef F Krems (2019). "Deceleration parameters and their applicability as informal communication signal between pedestrians and automated vehicles". In: *Transportation Research Part F: Traffic Psychology and Behaviour* 62, pp. 757–768. doi: 10.1016/j.trf.2019.03.006.

ADAC (2020). *Welche Hersteller bieten bereits C2X an? ADAC-Umfrage 6/2020*. Last accessed: Nobember 14, 2021. url: https://assets.adac.de/image/upload/v1594712609/ADAC-eV/KOR/Text/PDF/Umfrage_Hersteller_Car2X_dl45xm.pdf.

ADAC (2022). *Förderung für Elektroautos: Hier gibt es Geld*. Last accessed: April 23, 2022. url: https://www.adac.de/rund-ums-fahrzeug/elektromobilitaet/kaufen/foerderung-elektroautos/.

Aimsun (2020). *Aimsun Next 20 User's Manual*. In software. Last accessed: April 3, 2022. url: www.aimsun.com.

Alrutz, Dankmar; Carola Bachmann; Juliane Rudert; Wilhelm Angenendt; Arne Blase; Fabian Fohlmeister; Peter Häckelmann (2012). "Verbesserung der Bedingungen für Fußgänger an Lichtsignalanlagen". In: *Berichte der Bundesanstalt für Straßenwesen* Heft V 217. issn: 0943-9331.

Andert, Edward; Mohammad Khayatian; Aviral Shrivastava (2017). "Crossroads: Time-sensitive autonomous intersection management technique". In: *Proceedings of the 54th Annual Design Automation Conference 2017*, pp. 1–6. doi: 10.1145/3061639.3062221.

Aoki, Shunsuke; Ragunathan Rajkumar (2018). "Dynamic intersections and self-driving vehicles". In: *2018 ACM/IEEE 9th International Conference on Cyber-Physical Systems (ICCPS)*. IEEE, pp. 320–330. doi: 10.1109/iccps.2018.00038.

Automotive News (2021). *How Honda's Level 3 self-driving technology works*. Last accessed: November 11, 2021. url: https://europe.autonews.com/automakers/how-hondas-level-3-self-driving-technology-works.

Ayoubi, Ayda (2017). *The Future of Pedestrian Crossing*. The Journal of the American Institute of Architects. Last accessed: March 26, 2021. Photos by Direct Line. url: https://www.architectmagazine.com/technology/the-future-of-pedestrian-crossing_o.

Azimi, Reza; Gaurav Bhatia; Ragunathan Rajkumar; Priyantha Mudalige (2014). "STIP: Spatio-temporal intersection protocols for autonomous vehicles". In: *2014 ACM/IEEE International Conference on Cyber-Physical Systems (ICCPS)*. IEEE, pp. 1–12. doi: 10.1109/iccps.2014.6843706.

Azimi, Reza; Gaurav Bhatia; Ragunathan Rajkumar; Priyantha Mudalige (2015). "Ballroom intersection protocol: Synchronous autonomous driving at intersections".

In: *2015 IEEE 21st International Conference on Embedded and Real-Time Computing Systems and Applications*. IEEE, pp. 167–175. DOI: 10.1109/rtcsa.2015.20.

Bae, Il; Jaeyoung Moon; Jeongseok Seo (2019). "Toward a comfortable driving experience for a self-driving shuttle bus". In: *Electronics* 8.943, pp. 1–13. DOI: 10.3390/electronics8090943.

Bansal, Prateek; Kara M. Kockelman (2017). "Forecasting Americans' long-term adoption of connected and autonomous vehicle technologies". In: *Transportation Research Part A: Policy and Practice* 95, pp. 49–63. DOI: 10.1016/j.tra.2016.10.013.

Bark, Sam (2014). *Red Traffic Lights, NYC*. Last accessed: June 21, 2022. URL: https://www.flickr.com/photos/122671098@N08/14088153615.

Bashiri, Masoud; Cody H. Fleming (2017). "A platoon-based intersection management system for autonomous vehicles". In: *2017 IEEE Intelligent Vehicles Symposium (IV)*. IEEE, pp. 667–672. DOI: 10.1109/ivs.2017.7995794.

Bashiri, Masoud; Hasan Jafarzadeh; Cody H. Fleming (2018). "PAIM: Platoon-based Autonomous Intersection Management". In: *2018 21st International Conference on Intelligent Transportation Systems (ITSC)*. IEEE, pp. 374–380. DOI: 10.1109/itsc.2018.8569782.

Belkhouche, Fethi (2018). "Collaboration and optimal conflict resolution at an unsignalized intersection". In: *IEEE Transactions on Intelligent Transportation Systems* 20.6, pp. 2301–2312. DOI: 10.1109/tits.2018.2867256.

Bellan, Rebecca (2021). *Cruise launches driverless robotaxi service in San Francisco*. TechCrunch. Last accessed: November 23, 2021. URL: https://techcrunch.com/2021/11/03/cruise-launches-driverless-robotaxi-service-for-employees-in-san-francisco/.

Beyer, Felix (2009). "Koordinierung von Lichtsignalanlagen auf innerstädtischen Radrouten in Wien anhand der Bedürfnisse der Radfahrer." Diploma Thesis. TU Dresden, Fakultät Verkehrswissenschaften.

Bian, Yougang; Shengbo Eben Li; Wei Ren; Jianqiang Wang; Keqiang Li; Henry Liu (2019). "Cooperation of Multiple Connected Vehicles at Unsignalized Intersections: Distributed Observation, Optimization, and Control". In: *IEEE Transactions on Industrial Electronics* 67.12, pp. 10744–10754. DOI: 10.1109/tie.2019.2960757.

Bichiou, Youssef; Hesham A Rakha (2018). "Developing an optimal intersection control system for automated connected vehicles". In: *IEEE Transactions on Intelligent Transportation Systems* 20.5, pp. 1908–1916. DOI: 10.1109/tits.2018.2850335.

Bonneson, James; Srinivasa R Sunkari; Michael Pratt; Praprut et al. Songchitruksa (2011). *Traffic signal operations handbook*. Tech. rep. FHWA/TX-11/0-6402-P1. The Texas A&M University for the Federal Highway Administration and the Texas Department of Transportation.

Botello, Bryan; Ralph Buehler; Steve Hankey; Andrew Mondschein; Zhiqiu Jiang (2019). "Planning for walking and cycling in an autonomous-vehicle future". In: *Transportation Research Interdisciplinary Perspectives* 1, p. 100012. DOI: 10.1016/j.trip.2019.100012.

Brosseau, Marilyne; Sohail Zangenehpour; Nicolas Saunier; Luis Miranda-Moreno (2013). "The impact of waiting time and other factors on dangerous pedes-

trian crossings and violations at signalized intersections: A case study in Montreal". In: *Transportation Research Part F: Traffic Psychology and Behaviour* 21, pp. 159–172. DOI: 10.1016/j.trf.2013.09.010.

Buehler, Ralph; John Pucher; Adrian Bauman (2020). "Physical activity from walking and cycling for daily travel in the United States, 2001–2017: Demographic, socioeconomic, and geographic variation". In: *Journal of Transport & Health* 16, p. 100811. DOI: 10.1016/j.jth.2019.100811.

Business Insider (2016). *Forscher basteln an einer Zukunft ohne Ampeln*. Last accessed: June 14, 2022. URL: https://www.businessinsider.de/wissenschaft/forscher-basteln-an-einer-zukunft-ohne-ampeln-2016-3/.

Calvert, Simeon; Isabel WIlmink; Haneen Farah (2017). *Next steps in describing possible effects of automated driving on traffic flow*. Tech. rep. TrafficQuest Centre for Expertise on Traffic Management. DOI: 10.13140/RG.2.2.25387.44328.

Cardwell, Diane (2014). *Copenhagen Lighting the Way to Greener, More Efficient Cities*. The New York Times. Last accessed: March 27, 2021. URL: https://www.nytimes.com/2014/12/09/business/energy-environment/copenhagen-lighting-the-way-to-greener-more-efficient-cities.html.

Carlino, Dustin; Stephen D. Boyles; Peter Stone (2013). "Auction-based autonomous intersection management". In: *Proceedings of the 16th IEEE Intelligent Transportation Systems Conference, The Hague, Netherlands, October 2013*. IEEE. DOI: 10.1109/itsc.2013.6728285.

Chand, Suresh; Vernon Ning Hsu; Suresh Sethi (2002). "Forecast, solution, and rolling horizons in operations management problems: A classified bibliography". In: *Manufacturing & Service Operations Management* 4.1, pp. 25–43. DOI: 10.1287/msom.4.1.25.287.

Chen, Lei; Cristofer Englund (2016). "Cooperative Intersection Management: A Survey". In: *IEEE Transactions on Intelligent Transportation Systems* 17.2, pp. 570–586. DOI: 10.1109/tits.2015.2471812.

Chen, Rongsheng; Jeffrey Hu; Michael W Levin; David Rey (2020). "Stability-based analysis of autonomous intersection management with pedestrians". In: *Transportation Research Part C: Emerging Technologies* 114, pp. 463–483. DOI: 10.1016/j.trc.2020.01.016.

Choi, Myungwhan; Areeya Rubenecia; Hyo Hyun Choi (2019). "Reservation-based traffic management for autonomous intersection crossing". In: *International Journal of Distributed Sensor Networks* 15.12, pp. 1–15. DOI: 10.1177/1550147719895956.

Day, Christopher M; Susan Langdon; Aleksandar Stevanovic; Alison Tanaka; Kevin Lee; Edward J Smaglik; Larry Overn; Nithin Agarwal; Lucy Richardson; Stacie Phillips (2019). "Traffic signal systems research: Past, present, and future trends". In: *Transportation Research Board Centennial Papers*.

De Angelis, Marco; Arjan Stuiver; Federico Fraboni; Gabriele Prati; Víctor Marín Puchades; Filippo Fassina; Dick de Waard; Luca Pietrantoni (2019). "Green wave for cyclists: Users' perception and preferences". In: *Applied Ergonomics* 76, pp. 113–121. DOI: 10.1016/j.apergo.2018.12.008.

De Hartog, Jeroen Johan; Hanna Boogaard; Hans Nijland; Gerard Hoek (2010). "Do the health benefits of cycling outweigh the risks?" In: *Environmental Health Perspectives* 118.8, pp. 1109–1116. DOI: 10.1289/ehp.0901747.

Dorrier, Jason (2014). *IHS Automotive Report Says 'Not If, But When' for Self-Driving Cars*. SingularityHub. Last accessed: November 12, 2021. URL: https://singularityhub.com/2014/01/16/is-the-ihs-forecast-of-54-million-self-driving-cars-by-2035-too-conservative/.

Dresner, Kurt; Peter Stone (2004). "Multiagent traffic management: A reservation-based intersection control mechanism". In: *International Joint Conference on Autonomous Agents and Multiagent Systems*. Vol. 3. IEEE Computer Society, pp. 530–537.

Dresner, Kurt; Peter Stone (2006). "Human-Usable and Emergency Vehicle–Aware Control Policies for Autonomous Intersection Management". In: *The Fourth Workshop on Agents in Traffic and Transportation (ATT 06), Hakodate, Japan, May*.

Dresner, Kurt; Peter Stone (2008). "A Multiagent Approach to Autonomous Intersection Management". In: *Journal of Artificial Intelligence Research* 31, pp. 591–656. DOI: 10.1613/jair.2502.

EENews Europe (2019). *Platform uses AI and V2X to optimize traffic flow*. Last accessed: June 21, 2019. URL: https://www.eenewsembedded.com/en/platform-uses-ai-and-v2x-to-optimize-traffic-flow/.

Eisenkopf, Alexander; Hartmut Fricke; Regine Gerike; Markus Friedrich; Hans-Dietrich Haasis; Günter Knieps; Andreas Knorr; Kay Mitusch; Stefan Oeter; Franz Josef Radermacher; Gernot Sieg; Jürgen Siegmann; Bernhard Schlag; Wolfgang Stölzle; Dirk Vallée; Peter Vortisch; Hermann Winner (2017). *Automatisiertes Fahren im Straßenverkehr*. Gutachten des Wissenschaftlichen Beirats beim Bundesminister für Verkehr und digitale Infrastruktur.

El Hamdani, Sara; Nabil Benamar; Mohamed Younis (2020). "Pedestrian support in intelligent transportation systems: challenges, solutions and open issues". In: *Transportation Research Part C: Emerging Technologies* 121, p. 102856. DOI: 10.1016/j.trc.2020.102856.

Elhenawy, Mohammed; Ahmed A. Elbery; Abdallah A. Hassan; Hesham A. Rakha (2015). "An intersection game-theory-based traffic control algorithm in a connected vehicle environment". In: *2015 IEEE 18th International Conference on Intelligent Transportation Systems*. IEEE. IEEE, pp. 343–347. DOI: 10.1109/itsc.2015.65.

European Commission (2020). *2019 road safety statistics: what is behind the figures?* Last accessed: June 19, 2022. URL: https://ec.europa.eu/commission/presscorner/detail/en/qanda_20_1004.

European Union (2010). *Directive 2010/40/EU of the European Parliament and of the Council of 7 July 2010 on the framework for the deployment of Intelligent Transport Systems in the field of road transport and for interfaces with other modes of transport (Text with EEA relevance)*. Last accessed: June 19, 2022. URL: http://data.europa.eu/eli/dir/2010/40/2018-01-09.

Fairley, Peter (2017). "Self-Driving Cars Have a Bicycle Problem". In: *IEEE Spectrum* 54.3, pp. 12–13. DOI: 10.1109/MSPEC.2017.7864743.

Fajardo, David; Tsz-Chiu Au; S. Travis Waller; Peter Stone; C. Y. David Yang (2011). "Automated Intersection Control: Performance of a Future Innovation Versus Current Traffic Signal Control". In: *Transportation Research Record* 2259.1, pp. 223–232. doi: 10.3141/2259-21.

Fayazi, Seyed Alireza; Ardalan Vahidi (2018). "Mixed-integer linear programming for optimal scheduling of autonomous vehicle intersection crossing". In: *IEEE Transactions on Intelligent Vehicles* 3.3, pp. 287–299. doi: 10.1109/tiv.2018.2843163.

Fayazi, Seyed Alireza; Ardalan Vahidi; Andre Luckow (2019). "A Vehicle-in-the-Loop (VIL) verification of an all-autonomous intersection control scheme". In: *Transportation Research Part C: Emerging Technologies* 107, pp. 193–210. doi: 10.1016/j.trc.2019.07.027.

Ferenchak, Nicholas N; Wesley E Marshall (2020). "Validation of bicycle level of traffic stress and perceived safety for children". In: *Transportation Research Record* 2674.4, pp. 397–406. doi: 10.1177/0361198120909833.

Ferreira, Michel; Ricardo Fernandes; Hugo Conceição; Wantanee Viriyasitavat; Ozan K Tonguz (2010). "Self-organized traffic control". In: *VANET '10: Proceedings of the seventh ACM international workshop on VehiculAr InterNETworking*, pp. 85–90. doi: 10.1145/1860058.1860077.

Festag, Andreas (2015). "Standards for vehicular communication—from IEEE 802.11p to 5G". In: *e & i Elektrotechnik und Informationstechnik* 132.7, pp. 409–416. doi: 10.1007/s00502-015-0343-0.

FGSV - Forschungsgesellschaft für Strassen- und Verkehrswesen (2001). *Handbuch für die Bemessung von Straßenverkehrsanlagen (HBS)*. FGSV-Verlag. isbn: 978-3-94179-035-3.

FGSV - Forschungsgesellschaft für Strassen- und Verkehrswesen (2015a). *Handbuch für die Bemessung von Straßenverkehrsanlagen (HBS)*. FGSV-Verlag. isbn: 978-3-86446-103-3.

FGSV - Forschungsgesellschaft für Strassen- und Verkehrswesen (2015b). *Richtlinien für Lichtsignalanlagen (RiLSA), Lichtzeichenanlagen für den Straßenverkehr*. FGSV-Verlag.

FHWA - Federal Highway Administration (2012). *Manual on Uniform Traffic Control Devices. 2009 Edition Including Revision 1 dated May 2012 and Revision 2 dated May 2012*. Tech. rep. U.S. Department of Transportation.

FHWA - Federal Highway Administration (2017). *National Household Travel Survey*. Tech. rep. Washington, DC: U.S. Department of Transportation. url: https://nhts.ornl.gov.

Figliozzi, Miguel; Nikki Wheeler; Christopher M Monsere (2013). "Methodology for estimating bicyclist acceleration and speed distributions at intersections". In: *Transportation Research Record* 2387.1, pp. 66–75. doi: 10.3141/2387-08.

Fiori, Chiara; Kyoungho Ahn; Hesham A Rakha (2016). "Power-based electric vehicle energy consumption model: Model development and validation". In: *Applied Energy* 168, pp. 257–268. doi: 10.1016/j.apenergy.2016.01.097.

Freyer, Lola; Mark-Simon Krause; Jürgen Follmann (2019). "Freies Rechtsabbiegen für den Radverkehr an lichtsignalgeregelten Knotenpunkten". In: *Straßenverkehrstechnik* 5, 2019, pp. 325–331.

Friedrich, Bernhard (2016). "The effect of autonomous vehicles on traffic". In: *Autonomous Driving*. Springer, pp. 317–334. doi: 10.1007/978-3-662-48847-8_16.

Furth, Peter G; Peter J Koonce; Yu Miao; Fei Peng; Michael Littman (2014). "Mitigating Right-Turn Conflict with Protected Yet Concurrent Phasing for Cycle Track and Pedestrian Crossings". In: *Transportation Research Record* 2438.1, pp. 81–88. doi: 10.3141/2438-09.

Gartner, Nathan H; Farhad J Pooran; Christina M Andrews (2001). "Implementation of the OPAC adaptive control strategy in a traffic signal network". In: *ITSC 2001. 2001 IEEE Intelligent Transportation Systems. Proceedings (Cat. No. 01TH8585)*. IEEE, pp. 195–200. doi: 10.1109/ITSC.2001.948655.

Gipps, Peter (1981). "A behavioural car-following model for computer simulation". In: *Transportation Research Part B: Methodological* 15.2, pp. 105–111. doi: 10.1016/0191-2615(81)90037-0.

Gipps, Peter (1986). "Multsim: a model for simulating vehicular traffic on multi-lane arterial roads". In: *Mathematics and Computers in Simulation* 28.4, pp. 291–295. doi: 10.1016/0378-4754(86)90050-9.

Glomb, Lukas; Frauke Liers; Florian Rösel (2020). "A rolling-horizon approach for multi-period optimization". In: *European Journal of Operational Research* 300.1, pp. 189–206. doi: 10.1016/j.ejor.2021.07.043.

Grigoropoulos, Georgios; Seyed Abdollah Hosseini; Andreas Keler; Heather Kaths; Matthias Spangler; Fritz Busch; Klaus Bogenberger (2021). "Traffic Simulation Analysis of Bicycle Highways in Urban Areas". In: *Sustainability* 13.3, p. 1016. doi: 10.3390/su13031016.

Groningen Cycling City (2016). *Green light for all cyclists. How does it work?* Last accessed: November 29, 2021. url: https://groningenfietsstad.nl/en/green-light-for-all-cyclists-how-does-it-work/.

Guney, Mehmet Ali; Ioannis A Raptis (2020). "Scheduling-Based Optimization for Motion Coordination of Autonomous Vehicles at Multilane Intersections". In: *Journal of Robotics* 2020, pp. 1–22. doi: 10.1155/2020/6217409.

Guo, Qiangqiang; Li Li; Xuegang Jeff Ban (2019). "Urban traffic signal control with connected and automated vehicles: A survey". In: *Transportation Research Part C: Emerging Technologies* 101, pp. 313–334. doi: 10.1016/j.trc.2019.01.026.

Hainen, Alex; Bryan Mulligan; Johannes Deetlefs; Iain Mulligan; Peter Ashley (2019). "Co-deployment of DSRC radio and cellular connected vehicle technology in Tuscaloosa, AL and Northport, AL". In: *2019 ITS America Annual Meeting*. ITSWC.

Harloff, Thomas; Torsten Seibt; Uli Baumann; Gregor Hebermehl (2021). *Die Ausstiegs-Fahrpläne der EU und der Länder*. auto motor sport. Last accessed: April 23, 2022. url: https://www.auto-motor-und-sport.de/verkehr/verbrenner-aus-immer-mehr-verbote-zukunft-elektroauto/.

Hausknecht, Matthew; Tsz-Chiu Au; Peter Stone (2011). "Autonomous intersection management: Multi-intersection optimization". In: *2011 IEEE/RSJ International Con-*

ference on Intelligent Robots and Systems. IEEE, pp. 4581–4586. DOI: 10.1109/iros.2011.6094668.

He, Zhengbing; Liang Zheng; Lili Lu; Wei Guan (2018). "Erasing lane changes from roads: A design of future road intersections". In: *IEEE Transactions on Intelligent Vehicles* 3.2, pp. 173–184. DOI: 10.1109/tiv.2018.2804164.

Hoogendoorn, Serge P; Winnie Daamen (2006). "Free speed distributions for pedestrian traffic". In: *TRB 85th Annual Meeting Compendium of Papers*.

Hu, Yonghui; Yibing Wang; Xufeng Jin; Jingqiu Guo; Lihui Zhang; Jun Simon Hu (2021). "Urban Eco-driving of Connected and Automated Vehicles in Traffic-Mixed and Power-heterogeneous Conditions". In: *2021 IEEE International Intelligent Transportation Systems Conference (ITSC)*. IEEE, pp. 873–878. DOI: 10.1109/itsc48978.2021.9564612.

Hughes, Ronald G; Herman Huang; Charles V Zegeer; Michael J Cynecki, et al. (2001). *Evaluation of automated pedestrian detection at signalized intersections*. Tech. rep. United States. Federal Highway Administration.

Isaksson-Hellman, Irene (2012). "A study of bicycle and passenger car collisions based on insurance claims data". In: *Annals of Advances in Automotive Medicine. Annual Scientific Conference*. Vol. 56. Association for the Advancement of Automotive Medicine, pp. 3–12.

Jin, Qiu; Guoyuan Wu; Kanok Boriboonsomsin; Matthew Barth (2012). "Advanced intersection management for connected vehicles using a multi-agent systems approach". In: *2012 IEEE Intelligent Vehicles Symposium*. IEEE, pp. 932–937. DOI: 10.1109/ivs.2012.6232287.

Jin, Qiu; Guoyuan Wu; Kanok Boriboonsomsin; Matthew Barth (2013). "Platoon-based multi-agent intersection management for connected vehicle". In: *16th International IEEE Conference on Intelligent Transportation Systems (ITSC 2013)*. IEEE, pp. 1462–1467. DOI: 10.1109/itsc.2013.6728436.

Kaltenhäuser, Bernd; Karl Werdich; Florian Dandl; Klaus Bogenberger (2020). "Market development of autonomous driving in Germany". In: *Transportation Research Part A: Policy and Practice* 132, pp. 882–910. DOI: 10.1016/j.tra.2020.01.001.

Kamal, Md Abdus Samad; Jun-ichi Imura; Tomohisa Hayakawa; Akira Ohata; Kazuyuki Aihara (2015). "A vehicle-intersection coordination scheme for smooth flows of traffic without using traffic lights". In: *IEEE Transactions on Intelligent Transportation Systems* 16.3, pp. 1136–1147. DOI: 10.1109/tits.2014.2354380.

Karloff, Howard (1991). *Linear programming*. Birkhäuser Basel.

Kaths, Heather; Georgios Grigoropoulos; Klaus Krämer (2019). "Green signal countdown timers for bicycle traffic – Results from a field study". In: *Cycling Research Board 2019*.

Kaths, Heather; Andreas Keler; Klaus Bogenberger (2021). "Calibrating the Wiedemann 99 Car-Following Model for Bicycle Traffic". In: *Sustainability* 13.6, p. 3487. DOI: 10.3390/su13063487.

Kaths, Jakob; Eftychios Papapanagiotou; Fritz Busch (2015). "Traffic signals in connected vehicle environments: Chances, challenges and examples for future traffic signal control". In: *2015 IEEE 18th International Conference on Intelligent Transportation Systems*. IEEE, pp. 125–130. DOI: 10.1109/itsc.2015.29.

Kenney, John B (2011). "Dedicated short-range communications (DSRC) standards in the United States". In: *Proceedings of the IEEE* 99.7, pp. 1162–1182. doi: 10.1109/jproc.2011.2132790.

Khayatian, Mohammad; Mohammadreza Mehrabian; Edward Andert; Rachel Dedinsky; Sarthake Choudhary; Yingyan Lou; Aviral Shirvastava (2020). "A Survey on Intersection Management of Connected Autonomous Vehicles". In: *ACM Transactions on Cyber-Physical Systems* 4.4, pp. 1–27. doi: 10.1145/3407903.

Knight, P; J Bedingfeld; E Gould (2011). *Traffic Management Techniques for Cyclists: Final Report*. Tech. rep. Transport Research Laboratory.

Köllner, Christiane (2020). *Fahrzeugvernetzung per C-V2X oder pWLAN?* Springer-Professional. Last accessed: November 14, 2021. url: https://www.springerprofessional.de/car-to-x/automatisiertes-fahren/fahrzeugvernetzung-per-c-v2x-oder-pwlan-/17822610.

Koonce, Peter; Lee Rodegerdts (2008). *Traffic signal timing manual.* Tech. rep. FHWA-HOP-08-024. U.S. Department of Transportation. Federal Highway Administration.

Kothuri, Sirisha; Krista Nordback; Andrew Schrope; Taylor Phillips; Miguel Figliozzi (2017). "Bicycle and pedestrian counts at signalized intersections using existing infrastructure: Opportunities and challenges". In: *Transportation Research Record* 2644.1, pp. 11–18. doi: 10.3141/2644-02.

Kothuri, Sirisha Murthy (2014). "Exploring Pedestrian Responsive Traffic Signal Timing Strategies in Urban Areas". PhD thesis. Portland State University.

Larson, Travis; Amy Wyman; David S Hurwitz; Matt Dorado; Shaun Quayle; Stacy Shetler (2020). "Evaluation of dynamic passive pedestrian detection". In: *Transportation Research Interdisciplinary Perspectives* 8, p. 100268. doi: 10.1016/j.trip.2020.100268.

LCT GesmbH (2018). *Smart City Technology Safety*. Last accessed: January 15, 2019. url: https://lct.co.at/bodenleuchte/smart-city-technology.

Lee, Joyoung; Byungkyu Park (2012). "Development and evaluation of a cooperative vehicle intersection control algorithm under the connected vehicles environment". In: *IEEE Transactions on Intelligent Transportation Systems* 13.1, pp. 81–90.

Levin, Michael W; Stephen D Boyles (2016). "A multiclass cell transmission model for shared human and autonomous vehicle roads". In: *Transportation Research Part C: Emerging Technologies* 62, pp. 103–116. doi: 10.1016/j.trc.2015.10.005.

Levin, Michael W; Stephen D Boyles; Rahul Patel (2016). "Paradoxes of reservation-based intersection controls in traffic networks". In: *Transportation Research Part A: Policy and Practice* 90, pp. 14–25. doi: 10.1016/j.tra.2016.05.013.

Levin, Michael W; Hagen Fritz; Stephen D Boyles (2016). "On optimizing reservation-based intersection controls". In: *IEEE Transactions on Intelligent Transportation Systems* 18.3, pp. 505–515. doi: 10.1109/tits.2016.2574948.

Levin, Michael W; David Rey (2017). "Conflict-point formulation of intersection control for autonomous vehicles". In: *Transportation Research Part C: Emerging Technologies* 85, pp. 528–547. doi: 10.1016/j.trc.2017.09.025.

Li, Bai; Youmin Zhang; Yue Zhang; Ning Jia; Yuming Ge (2018). "Near-optimal online motion planning of connected and automated vehicles at a signal-free and lane-free

intersection". In: *2018 IEEE Intelligent Vehicles Symposium (IV)*. IEEE, pp. 1432–1437. DOI: 10.1109/ivs.2018.8500528.

Li, Li; Fei-Yue Wang (2006). "Cooperative driving at blind crossings using intervehicle communication". In: *IEEE Transactions on Vehicular technology* 55.6, pp. 1712–1724. DOI: 10.1109/tvt.2006.878730.

Li, Zhixia; Madhav V Chitturi; Dongxi Zheng; Andrea R Bill; David A Noyce (2013). "Modeling reservation-based autonomous intersection control in VISSIM". In: *Transportation Research Record* 2381.1, pp. 81–90. DOI: 10.3141/2381-10.

Li, Zhuofei; Mahmoud Pourmehrab; Lily Elefteriadou; Sanjay Ranka (2018). "Intersection control optimization for automated vehicles using genetic algorithm". In: *Journal of Transportation Engineering, Part A: Systems* 144.12, p. 04018074.

Liang, Xiao; S Ilgin Guler; Vikash V Gayah (2020). "Traffic Signal Control Optimization in a Connected Vehicle Environment Considering Pedestrians". In: *Transportation Research Record* 2674.10, pp. 499–511. DOI: 10.1177/0361198120936268.

Lioris, Jennie; Ramtin Pedarsani; Fatma Yildiz Tascikaraoglu; Pravin Varaiya (2016). "Doubling throughput in urban roads by platooning". In: *IFAC-PapersOnLine* 49.3, pp. 49–54. DOI: 10.1016/j.ifacol.2016.07.009.

Liu, S.; W. Xiang; M. X. Punithan (2018). "An Empirical Study on Performance of DSRC and LTE-4G for Vehicular Communications". In: *2018 IEEE 88th Vehicular Technology Conference (VTC-Fall)*. IEEE, pp. 1–5. DOI: 10.1109/vtcfall.2018.8690979.

Lord, Dominique; Alison Smiley; Antoine Haroun (1998). "Pedestrian accidents with left-turning traffic at signalized intersections: Characteristics, human factors, and unconsidered issues". In: *77th Annual Transportation Research Board Meeting, Washington, DC*.

Luin, Blaž; Stojan Petelin; Fouad Al-Mansour (2019). "Microsimulation of electric vehicle energy consumption". In: *Energy* 174, pp. 24–32. DOI: 10.1016/j.energy.2019.02.034.

Lutz, Christiane (2018). *Ein Hoch auf die rote Ampel!* Sueddeutsche Zeitung. URL: https://www.sueddeutsche.de/muenchen/150-jahre-ampel-1.4243910.

MacArthur, John; Michael Harpool; Daniel Scheppke (2019). *How Technology Can Affect the Demand for Bicycle Transportation: The State of Technology and Projected Applications of Connected Bicycles*. Tech. rep. ITC-RR-759. Transportation Research and Education Center (TREC).

Mannion, Patrick (2017). *V2V and V2X automobiles and infrastructure roll out*. u-blox.com. Last accessed: June 21, 2022. URL: https://www.u-blox.com/en/v2v-and-v2x-automobiles-and-infrastructure-roll-out.

Marnell, Patrick; Halston Tuss; David Hurwitz; Kirk Paulsen; Chris Monsere (2013). "Permissive left-turn behavior at the flashing yellow arrow in the presence of pedestrians". In: *Proceedings of the 7th International Driving Symposium on Human Factors in Driver Assessment, Training, and Vehicle Design*. University of Iowa. DOI: 10.17077/drivingassessment.1531.

Mattke, Sascha (2016). *Autonom und ohne Ampeln*. heise online. Last accessed: June 21, 2022. URL: https://www.heise.de/hintergrund/Autonom-und-ohne-Ampeln-3175720.html.

Mavromatis, Ioannis; Andrea Tassi; Robert J Piechocki; Mahesh Sooriyabandara (2020). "On Urban Traffic Flow Benefits of Connected and Automated Vehicles". In: *2020 IEEE 91st Vehicular Technology Conference (VTC2020-Spring)*. IEEE, pp. 1–7.

McLeod, Ken (2014). *Survey: Bicyclists unsure of connected and automated car technology*. Tech. rep. The League of American Bicyclists.

Meeder, Mark; Ernst Bosina; Ulrich Weidmann (2017). "Autonomous vehicles: Pedestrian heaven or pedestrian hell". In: *17th Swiss Transport Research Conference*.

Milakis, Dimitris; Maaike Snelder; Bart van Arem; Bert van Wee; Gonçalo Homem de Almeida Correia (2017). "Development and transport implications of automated vehicles in the Netherlands: scenarios for 2030 and 2050". In: *European Journal of Transport and Infrastructure Research* 17.1. doi: 10.18757/EJTIR.2017.17.1.3180.

Mitrovic, Nikola; Igor Dakic; Aleksandar Stevanovic (2020). "Combined Alternate-Direction Lane Assignment and Reservation-Based Intersection Control". In: *IEEE Transactions on Intelligent Transportation Systems* 21.4, pp. 1779–1789. doi: 10.1109/TITS.2019.2943521.

Modigliani, Franco; Franz E Hohn (1955). "Production Planning Over Time and the Nature of the Expectation and Planning Horizon". In: *Econometrica, Journal of the Econometric Society* 23.1, pp. 46–66. doi: 10.2307/1905580.

Morrison, David R; Sheldon H Jacobson; Jason J Sauppe; Edward C Sewell (2016). "Branch-and-bound algorithms: A survey of recent advances in searching, branching, and pruning". In: *Discrete Optimization* 19, pp. 79–102. doi: 10.1016/j.disopt.2016.01.005.

Mueller, Edward A (1970). "Aspects of the history of traffic signals". In: *IEEE Transactions on Vehicular Technology* 19.1, pp. 6–17.

Müller, Eduardo Rauh; Rodrigo Castelan Carlson; Werner Kraus Junior (2016a). "Intersection control for automated vehicles with MILP". In: vol. 49. 3. Elsevier, pp. 37–42. doi: 10.1016/j.ifacol.2016.07.007.

Müller, Eduardo Rauh; Rodrigo Castelan Carlson; Werner Kraus Junior (2016b). "Time optimal scheduling of automated vehicle arrivals at urban intersections". In: *2016 IEEE 19th International Conference on Intelligent Transportation Systems (ITSC)*. IEEE, pp. 1174–1179. doi: 10.1109/itsc.2016.7795705.

Müller, Julian F; Jan Gogoll (2020). "Should manual driving be (eventually) outlawed?" In: *Science and engineering ethics* 26.3, pp. 1549–1567.

Namazi, Elnaz; Jingyue Li; Chaoru Lu (2019). "Intelligent intersection management systems considering autonomous vehicles: a systematic literature review". In: *IEEE Access* 7, pp. 91946–91965. doi: 10.1109/access.2019.2927412.

National Association of City Transportation Officials (2014). *Urban bikeway design guide*. Island Press.

National Highway Traffic Safety Administration (2018). *Traffic Safety Facts: Critical Reasons for Crashes Investigated in theNational Motor Vehicle Crash Causation Survey*. online. url: https://crashstats.nhtsa.dot.gov/Api/Public/Publication/812506.

National Highway Traffic Safety Administration (NHTSA) (2020). *SAE Automation Levels*. Last accessed: Sept 30, 2020. URL: https://www.nhtsa.gov/technology-innovation/automated-vehicles.

Naumann, Rolf; Rainer Rasche; Jürgen Tacken (1998). "Managing autonomous vehicles at intersections". In: *IEEE Intelligent Systems and their Applications* 13.3, pp. 82–86. DOI: 10.1109/5254.683216.

NEMA - National Electrical Manufacturers Association (2003). *NEMA Standards Publication TS 2-2003 v02. 06–Traffic Controller Assemblies with NTCIP Requirements*.

Niels, Tanja; Klaus Bogenberger; Nikola Mitrovic; Aleksandar Stevanovic (2020). "Integrated Intersection Management for Connected, Automated Vehicles, and Bicyclists". In: *2020 IEEE 23rd International Conference on Intelligent Transportation Systems (ITSC)*. IEEE, pp. 1–8. DOI: 10.1109/itsc45102.2020.9294600.

Niels, Tanja; Mustafa Erciyas; Klaus Bogenberger (2018). "Impact of connected and autonomous vehicles on the capacity of signalized intersections – Microsimulation of an intersection in Munich". In: *Proceedings of 7th Transport Research Arena TRA 2018, April 16-19, 2018, Vienna, Austria*. Zenodo. DOI: 10.5281/zenodo.1491430.

Niels, Tanja; Nikola Mitrovic; Klaus Bogenberger; Aleksandar Stevanovic; Robert L. Bertini (2019). "Smart Intersection Management for Connected and Automated Vehicles and Pedestrians". In: *6th International Conference on Models and Technologies for Intelligent Transportation Systems*. DOI: 10.1109/mtits.2019.8883362.

Niels, Tanja; Nikola Mitrovic; Nemanja Dobrota; Klaus Bogenberger; Aleksandar Stevanovic; Robert L. Bertini (2019). *Demo Video of the Integrated Intersection Control for Connected, Automated Vehicles and Pedestrians*. URL: https://vimeo.com/351534462.

Niels, Tanja; Nikola Mitrovic; Nemanja Dobrota; Klaus Bogenberger; Aleksandar Stevanovic; Robert L. Bertini (2020). "Simulation-based evaluation of a new integrated intersection control scheme for connected automated vehicles and pedestrians". In: *Transportation Research Record* 2674.11, pp. 779–793. DOI: 10.1177/0361198120949531.

Nobis, Claudia; Tobias Kuhnimhof (2018). *Mobilität in Deutschland – MiD Ergebnisbericht*. Studie im Auftrag des Bundesministers für Verkehr und digitale Infrastruktur. infas, DLR, IVT, infas 360. URL: www.mobilitaet-in-deutschland.de.

Ntousakis, Ioannis A; Ioannis K Nikolos; Markos Papageorgiou (2016). "Optimal vehicle trajectory planning in the context of cooperative merging on highways". In: *Transportation Research Part C: Emerging Technologies* 71, pp. 464–488. DOI: 10.1016/j.trc.2016.08.007.

Nygårdhs, Sara (2021). "Cyclists' adaptation to a countdown timer to green traffic light: A before-after field study". In: *Applied Ergonomics* 90, p. 103278. DOI: 10.1016/j.apergo.2020.103278.

Olsson, Jack; Michael W Levin (2020). "Integration of Microsimulation and Optimized Autonomous Intersection Management". In: *Journal of Transportation Engineering, Part A: Systems* 146.9, p. 04020087. DOI: 10.1061/jtepbs.0000407.

Olstam, Johan; Fredrik Johansson; Adriano Alessandrini; Peter Sukennik; Jochen Lohmiller; Markus Friedrich (2020). "An approach for handling uncertainties related to behaviour and vehicle mixes in traffic simulation experiments with automated vehicles". In: *Journal of Advanced Transportation* 2020, pp. 1–17. DOI: 10.1155/2020/8850591.

Paniati, Jeffrey F; Marilena Amoni (2006). *Traffic signal preemption for emergency vehicle: a cross-cutting study*. Tech. rep. FHWA-JPO-05-010. Federal Highway Administration.

Papageorgiou, Markos; Marion Leibold; Martin Buss (2015). *Optimierung*. Vol. 4. Springer. DOI: 10.1007/978-3-662-46936-1.

Papageorgiou, Markos; Kyriakos-Simon Mountakis; Iasson Karafyllis; Ioannis Papamichail; Yibing Wang (2021). "Lane-Free Artificial-Fluid Concept for Vehicular Traffic". In: *Proceedings of the IEEE* 109.2, pp. 114–121. DOI: 10.1109/JPROC.2020.3042681.

Papathanasopoulou, Vasileia; Ioulia Markou; Constantinos Antoniou (2016). "Online calibration for microscopic traffic simulation and dynamic multi-step prediction of traffic speed". In: *Transportation research part C: emerging technologies* 68, pp. 144–159. DOI: 10.1016/j.trc.2016.04.006.

Papathanassiou, Apostolos; Alexey Khoryaev (2017). "Cellular V2X as the Essential Enabler of Superior Global Connected Transportation Services". In: *IEEE 5G Tech Focus* 1.2. URL: https://futurenetworks.ieee.org/tech-focus/june-2017/cellular-v2x.

Pechinger, Mathias; Guido Schröer; Klaus Bogenberger; Carsten Markgraf (2021). "Benefit of Smart Infrastructure on Urban Automated Driving - Using an AV Testing Framework". In: *2021 IEEE Intelligent Vehicles Symposium (IV)*. IEEE. IEEE, pp. 1174–1179. DOI: 10.1109/iv48863.2021.9575651.

Pelosi, C; GP Padilla; MCF Donkers (2020). "Energy Optimal Coordination of Fully Autonomous Vehicles in Urban Intersections". In: *IFAC-PapersOnLine* 53.2, pp. 15090–15095. DOI: 10.1016/j.ifacol.2020.12.2031.

Penmetsa, Praveena; Emmanuel Kofi Adanu; Dustin Wood; Teng Wang; Steven L Jones (2019). "Perceptions and expectations of autonomous vehicles – A snapshot of vulnerable road user opinion". In: *Technological Forecasting and Social Change* 143, pp. 9–13. DOI: 10.1016/j.techfore.2019.02.010.

Ploeg, Jeroen; Bart TM Scheepers; Ellen Van Nunen; Nathan Van de Wouw; Henk Nijmeijer (2011). "Design and experimental evaluation of cooperative adaptive cruise control". In: *2011 14th International IEEE Conference on Intelligent Transportation Systems (ITSC)*. IEEE, pp. 260–265. DOI: 10.1109/itsc.2011.6082981.

Priemer, Christian; Bernhard Friedrich (2009). "A decentralized adaptive traffic signal control using V2I communication data". In: *2009 12th International IEEE Conference on Intelligent Transportation Systems*, pp. 1–6. DOI: 10.1109/ITSC.2009.5309870.

Pucher, John; Ralph Buehler (2008). "Making Cycling Irresistible: Lessons from The Netherlands, Denmark and Germany". In: *Transport Reviews* 28.4, pp. 495–528. DOI: 10.1080/01441640701806612.

Qian, Xiangjun; Florent Altché; Jean Grégoire; Arnaud de La Fortelle (2017). "Autonomous Intersection Management systems: criteria, implementation and evaluation". In: *IET Intelligent Transport Systems* 11.3, pp. 182–189. DOI: 10.1049/iet-its.2016.0043.

Ralphs, Ted; Yuji Shinano; Timo Berthold; Thorsten Koch (2018). "Parallel solvers for mixed integer linear optimization". In: *Handbook of parallel constraint reasoning*. Springer, pp. 283–336. DOI: 10.1007/978-3-319-63516-3_8.

Rasouli, Amir; John K Tsotsos (2020). "Autonomous vehicles that interact with pedestrians: A survey of theory and practice". In: *IEEE Transactions on Intelligent Transportation Systems* 21.3, pp. 900–918. DOI: 10.1109/TITS.2019.2901817.

Retting, Richard A; Janella F Chapline; Allan F Williams (2002). "Changes in crash risk following re-timing of traffic signal change intervals". In: *Accident Analysis & Prevention* 34.2, pp. 215–220. DOI: 10.1016/s0001-4575(01)00016-1.

Rios-Torres, Jackeline; Andreas Malikopoulos; Pierluigi Pisu (2015). "Online optimal control of connected vehicles for efficient traffic flow at merging roads". In: *2015 IEEE 18th International Conference on Intelligent Transportation Systems*. IEEE, pp. 2432–2437. DOI: 10.1109/itsc.2015.392.

Robertson, Douglas; Everett C. Carter (1984). "The Safety, Operational, and Cost Impacts of Pedestrian Indications at Signalized Intersections". In: *Transportation Research Record* 959, pp. 1–7.

Rostami-Shahrbabaki, Majid; Fabian Fehn; Gysele Lima Ricci; Klaus Bogenberger (2021). "Effects of Different Shares of Electric Vehicles in Cities on Global CO2 Emissions: A Microsimulation-Based Analysis". In: *2021 IEEE International Intelligent Transportation Systems Conference (ITSC)*. IEEE, pp. 3190–3197. DOI: 10.1109/itsc48978.2021.9565128.

Rostami-Shahrbabaki, Majid; Tanja Niels; Sascha Hamzehi; Klaus Bogenberger (2020). "An Independent Trajectory Advisory System in a Mixed-Traffic Condition: A Reinforcement Learning-Based Approach". In: *IFAC-PapersOnLine* 53.2, pp. 15667–15673. DOI: 10.1016/j.ifacol.2020.12.2550.

SAE International (2014). *Taxonomy and Definitions for Terms Related to Driving Automation Systems for On-Road Motor Vehicles*. DOI: https://doi.org/10.4271/J3016_201806.

Sayin, Muhammed O; Chung-Wei Lin; Shinichi Shiraishi; Jiajun Shen; Tamer Başar (2018). "Information-driven autonomous intersection control via incentive compatible mechanisms". In: *IEEE Transactions on Intelligent Transportation Systems* 20.3, pp. 912–924. DOI: 10.1109/tits.2018.2838049.

Schaar, K; K Bogenberger; S Breitenberger (2013). "Modellbasierte Schaetzung der Gesamtzahl deutscher Lichtsignalanlagen/Model based estimation of the total amount of German traffic lights". In: *Straßenverkehrstechnik* 57.8.

Schepperle, Heiko; Klemens Böhm (2007). "Agent-based traffic control using auctions". In: *International Workshop on Cooperative Information Agents*. Springer, pp. 119–133.

Schepperle, Heiko; Klemens Böhm; Simone Forster (2007). "Towards valuation-aware agent-based traffic control". In: *Proceedings of the 6th international joint conference*

on Autonomous agents and multiagent systems - AAMAS '07. 185. ACM Press, pp. 1–3. DOI: 10.1145/1329125.1329349.

SCHIMMELPFENNIG, KARL-HEINZ; UDO NACKENHORST (1985). "Bedeutung der Querbeschleunigung in der Verkehrsunfallrekonstruktion-Sicherheitsgrenze des Normalfahrers". In: *Verkehrsunfall und Fahrzeugtechnik* 23.4.

SCHLEINITZ, K; T PETZOLDT; L FRANKE-BARTHOLDT; J KREMS; T GEHLERT (2017). "The German Naturalistic Cycling Study–Comparing cycling speed of riders of different e-bikes and conventional bicycles". In: *Safety Science* 92, pp. 290–297. DOI: 10.1016/j.ssci.2015.07.027.

SCHMIDT, HERBIE (2021). *Autonomes Fahren: "Wir haben keine Zuverlässigkeitsprobleme"*. Neue Zürcher Zeitung. Last accessed: November 15, 2021. URL: https://www.nzz.ch/mobilitaet/autonomes-fahren-mobileye-vizepraesident-jungwirth-im-interview-ld.1654385?mktcid=nled&mktcval=162&kid=nl162_2021-11-12&ga=1&trco=.

SCHMÖCKER, JAN-DIRK; SONAL AHUJA; MICHAEL GH BELL (2008). "Multi-objective signal control of urban junctions–Framework and a London case study". In: *Transportation Research Part C: Emerging Technologies* 16.4, pp. 454–470. DOI: 10.1016/j.trc.2007.09.004.

SETHI, SURESH; GERHARD SORGER (1991). "A theory of rolling horizon decision making". In: *Annals of Operations Research* 29.1, pp. 387–415. DOI: 10.1007/bf02283607.

SEWALKAR, PARAG; JOCHEN SEITZ (2019). "Vehicle-to-pedestrian communication for vulnerable road users: Survey, design considerations, and challenges". In: *Sensors* 19.2, p. 358. DOI: 10.3390/s19020358.

SHAH, RONAK (2018). *A world without traffic signals: It's not as chaotic as it sounds*. Financial Express. Last accessed: March 26, 2021. URL: https://www.financialexpress.com/auto/car-news/a-world-without-traffic-signals-its-not-as-chaotic-as-it-sounds/1347725/.

SHANKER, RAVI; ADAM JONAS; SCOTT DEVITT; KATY HUBERTY; SIMON FLANNERY; WILLIAM GREENE; BENJAMIN SWINBURNE; GREGORY LOCRAFT; ADAM WOOD; KEITH WEISS; JOSEPH MOORE; ANDREW SCHENKER; PARESH JAIN; YEJAY YING; SHINJI KAKIUCHI; RYOSUKE HOSHINO; ANDREW HUMPHREY (2013). *Autonomous Cars: Self-Driving the New Auto Industry Paradigm*.

SIEMENS MOBILITY GMBH (2017). *100 Jahre Ampel*. Last accessed: June 21, 2022. URL: https://press.siemens.com/global/de/feature/100-jahre-ampel.

SMITH, HARRIET R; BRENDON HEMILY; MIOMIR IVANOVIC (2005). *Transit signal priority (TSP): A planning and implementation handbook*. Tech. rep. funded by the United States Department of Transportation.

STEBBINS, SIMON; MARK HICKMAN; JIWON KIM; HAI L VU (2017). "Characterising green light optimal speed advisory trajectories for platoon-based optimisation". In: *Transportation Research Part C: Emerging Technologies* 82, pp. 43–62. DOI: 10.1016/j.trc.2017.06.014.

STEIN, ULF (2021). "Reifenabrieb hat den größten Anteil am Mikroplastikeintrag in die Umwelt". In: *Spektrum.de*. Last accessed: June 24, 2022. URL: https://scilogs.

spektrum . de / plastik - in - der - umwelt / warum - autofahren - so - viel - mikroplastik-in-die-umwelt-traegt/.

Stevanovic, Aleksandar (2010). *Adaptive traffic control systems: domestic and foreign state of practice*. Project 20-5 (Topic 40-03).

Stevanovic, Aleksandar; Nikola Mitrovic (2018). "Combined Alternate-Direction Lane Assignment and Reservation-based Intersection Control". In: *2018 21st International Conference on Intelligent Transportation Systems (ITSC)*. IEEE, pp. 14–19. doi: 10.1109/itsc.2018.8569755.

Stevanovic, Aleksandar; Jelka Stevanovic; Cameron Kergaye (2013). "Green light optimized speed advisory systems: Impact of signal phasing information accuracy". In: *Transportation Research Record* 2390.1, pp. 53–59. doi: 10.3141/2390-06.

Tachet, Remi; Paolo Santi; Stanislav Sobolevsky; Luis Ignacio Reyes-Castro; Emilio Frazzoli; Dirk Helbing; Carlo Ratti (2016). "Revisiting Street Intersections Using Slot-Based Systems". In: *PLOS ONE* 11.3, e0149607. doi: 10.1371/journal.pone.0149607.

TAVF: Teststrecke für automatisiertes und vernetztes Fahren Hamburg (2020). *Traffic Light Forecast (TLF) 2.0*. Last accessed: March 26, 2021. url: https://tavf.hamburg/en/neues-von-tavf/news/35-experts-discussed-the-data-model-of-the-tlf-specific-interface.

Taylor, Dean B; Hani S Mahmassani (2000). "Coordinating Traffic Signals for Bicycle Progression". In: *Transportation Research Record* 1705.1, pp. 85–92. doi: 10.3141/1705-13.

TomTom International BV (2019). *TomTom Traffic Index*. Last accessed: June 9, 2020. url: www.tomtom.com/traffic-index.

Tonguz, Ozan K. (2018). *How Vehicle-to-Vehicle Communication Could Replace Traffic Lights and Shorten Commutes*. IEEE Spectrum. url: https://spectrum.ieee.org/transportation/infrastructure/how-vehicletovehicle-communication-could-replace-traffic-lights-and-shorten-commutes.

Transportation Research Board (TRB) (2000). *Highway Capacity Manual*. Tech. rep. Transportation Research Board.

Twaddle, Heather; Georgios Grigoropoulos (2016). "Modeling the speed, acceleration, and deceleration of bicyclists for microscopic traffic simulation". In: *Transportation Research Record* 2587.1, pp. 8–16. doi: 10.3141/2587-02.

Typaldos, Panagiotis; Ioannis Papamichail; Markos Papageorgiou (2020). "Minimization of fuel consumption for vehicle trajectories". In: *IEEE Transactions on Intelligent Transportation Systems* 21.4, pp. 1716–1727. doi: 10.1109/tits.2020.2972770.

United Nations (2019). *World Urbanization Prospects: The 2018 Revision (ST/ESA/SER.A/420)*. United Nations - Department of Economic and Social Affairs, Population Division.

Urbanik, Thomas; Alison Tanaka; Bailey Lozner; Eric Lindstrom; Kevin Lee; Shaun Quayle; Scott Beaird; Shing Tsoi; Paul Ryus; Doug Gettman, et al. (2015). *Signal timing manual*. Vol. 1. Transportation Research Board Washington, DC.

Van der Zee, Renate; Marco Te Brömmelstroet (2018). "In Groningen the Car plays a Cameo Role". In: *Ride a Bike! Reclaim the City*. Birkhäuser, pp. 56–59.

Van Houten, Ron; Ralph Ellis; Jin-Lee Kim (2007). "Effects of various minimum green times on percentage of pedestrians waiting for midblock "walk" signal". In: *Transportation Research Record* 2002.1, pp. 78–83. DOI: 10.3141/2002-10.

VanMiddlesworth, Mark; Kurt Dresner; Peter Stone (2008). "Replacing the stop sign: Unmanaged intersection control for autonomous vehicles". In: *Proceedings of the 7th international joint conference on Autonomous agents and multiagent systems-Volume 3*. International Foundation for Autonomous Agents and Multiagent Systems, pp. 1413–1416.

Varaiya, Pravin (2013). "Max pressure control of a network of signalized intersections". In: *Transportation Research Part C: Emerging Technologies* 36, pp. 177–195. DOI: 10.1016/j.trc.2013.08.014.

Vasirani, Matteo; Sascha Ossowski (2012). "A market-inspired approach for intersection management in urban road traffic networks". In: *Journal of Artificial Intelligence Research* 43, pp. 621–659. DOI: 10.1613/jair.3560.

VDA: Verband der Automobilindustrie (2015). *Automatisierung. Von Fahrerassistenzsystemen zum automatisierten Fahren.* Last accessed: Nov 23, 2021. URL: https://www.google.com/url?sa=t&rct=j&q=&esrc=s&source=web&cd=&cad=rja&uact=8&ved=2ahUKEwiQ7__G8a70AhWMKewKHbrQAGQQFnoECBkQAQ&url=https%3A%2F%2Fen.vda.de%2Fdam%2Fvda%2Fpublications%2F2015%2Fautomatisierung.pdf&usg=AOvVaw0EEqgiOv45ird0vVCAeFoh.

Wagner, Peter (2016). "Traffic control and traffic management in a transportation system with autonomous vehicles". In: *Autonomous Driving*. Springer, pp. 301–316. DOI: 10.1007/978-3-662-48847-8_15.

Wang, Michael I-C; Charles H-P Wen; H Jonathan Chao (2021). "Roadrunner+: An Autonomous Intersection Management Cooperating with Connected Autonomous Vehicles and Pedestrians with Spillback Considered". In: *ACM Transactions on Cyber-Physical Systems (TCPS)* 6.1, pp. 1–29. DOI: 10.1145/3488246.

Wang, Yunpeng; Pinlong Cai; Guangquan Lu (2020). "Cooperative autonomous traffic organization method for connected automated vehicles in multi-intersection road networks". In: *Transportation Tesearch Part C: Emerging Technologies* 111, pp. 458–476. DOI: 10.1016/j.trc.2019.12.018.

Wevers, Kees; Meng Lu (2017). "V2X Communication for ITS - from IEEE 802.11p Towards 5G". In: *IEEE 5G Tech Focus* 1.2. URL: https://futurenetworks.ieee.org/tech-focus/march-2017/v2x-communication-for-its.

Williams, H Paul (2013). *Model building in mathematical programming*. John Wiley & Sons.

Wu, Jia; Abdeljalil Abbas-Turki; Abdellah El Moudni (2012). "Cooperative driving: an ant colony system for autonomous intersection management". In: *Applied Intelligence* 37.2, pp. 207–222. DOI: 10.1007/s10489-011-0322-z.

Wu, Wei; Yang Liu; Wei Hao; George A Giannopoulos; Young-Ji Byon (2022). "Autonomous intersection management with pedestrians crossing". In: *Transportation Research Part C: Emerging Technologies* 135, p. 103521. DOI: 10.1016/j.trc.2021.103521.

Wu, Xinkai; Xiaozheng He; Guizhen Yu; Arek Harmandayan; Yunpeng Wang (2015). "Energy-optimal speed control for electric vehicles on signalized arterials". In: *IEEE*

Transactions on Intelligent Transportation Systems 16.5, pp. 2786–2796. DOI: 10.1109/tits.2015.2422778.

Wu, Yuanyuan; Haipeng Chen; Feng Zhu (2019). "DCL-AIM: Decentralized coordination learning of autonomous intersection management for connected and automated vehicles". In: *Transportation Research Part C: Emerging Technologies* 103, pp. 246–260. DOI: 10.1016/j.trc.2019.04.012.

Yao, Zhihong; Haoran Jiang; Yang Cheng; Yangsheng Jiang; Bin Ran (2020). "Integrated schedule and trajectory optimization for connected automated vehicles in a conflict zone". In: *IEEE Transactions on Intelligent Transportation Systems* 23.3, pp. 1841–1851. DOI: 10.1109/tits.2020.3027731.

Yu, Chunhui; Weili Sun; Henry X Liu; Xiaoguang Yang (2019). "Managing connected and automated vehicles at isolated intersections: From reservation-to optimization-based methods". In: *Transportation Research Part B: Methodological* 122, pp. 416–435. DOI: 10.1016/j.trb.2019.03.002.

Zenfting, Joe Gilpin; Tobin Bonnell; Matt Fralick; Kirk Paulson; Lindsay (2021). *Bicycle Detection*. Tech. rep. Alta Planning + Design.

Zhang, Yaohua; Sha A Mamun; John N Ivan; Nalini Ravishanker; Khademul Haque (2015). "Safety effects of exclusive and concurrent signal phasing for pedestrian crossing". In: *Accident Analysis & Prevention* 83, pp. 26–36. DOI: 10.1016/j.aap.2015.06.010.

Zhong, Zijia; Mark Nejad; Earl E Lee (2021). "Autonomous and Semiautonomous Intersection Management: A Survey". In: *IEEE Intelligent Transportation Systems Magazine* 13.2, pp. 53–70. DOI: 10.1109/mits.2020.3014074.

Zhu, Feng; Satish V Ukkusuri (2015). "A linear programming formulation for autonomous intersection control within a dynamic traffic assignment and connected vehicle environment". In: *Transportation Research Part C: Emerging Technologies* 55, pp. 363–378. DOI: 10.1016/j.trc.2015.01.006.

Zohdy, Ismail H; Raj Kishore Kamalanathsharma; Hesham Rakha (2012). "Intersection management for autonomous vehicles using iCACC". In: *2012 15th International IEEE Conference on Intelligent Transportation Systems*. IEEE, pp. 1109–1114. DOI: 10.1109/itsc.2012.6338827.

Appendix

A Literature Review

On the following pages, an overview on reviewed AIM studies and their characteristics is provided.

Table A.1: Overview of reviewed AIM studies – Part I.

Paper	Intersection Modeling	Traffic Coordination	Scheduling Policy	Trajectory Planning	Evaluation Method	Benchmark	Further comments
Andert et al. [2017]	Conflict points/regions	Centralized	FCFS	Simplified	Matlab & Test using radio controlled cars	FCFS-method by [Dresner and Stone, 2008]	Focus: account for communication delay and positioning errors
Aoki and Rajkumar [2018]	Safe pattern	Decentralized	Existing traffic rules	Not considered	Customized simulation software AutoSim	Traffic signal, stop sign	Consideration of dynamic bottlenecks (construction zones etc.)
Azimi et al. [2014]	Space discretization	Decentralized	FCFS	Simplified	Customized simulation software AutoSim	Traffic signal	Considers GPS accuracies
Azimi et al. [2015]	Space discretization	Centralized	FCFS	Not specified	Customized simulation software AutoSim	Traffic signal	
Bashiri and Fleming [2017]	Space discretization	Centralized	FCFS for platoons; optimization-based	Not specified	Simulation not specified	Stop sign	Only platoon leaders communicate with the intersection controller.
Bashiri, Jafarzadeh, et al. [2018]	Space discretization	Centralized	Optimization-based for platoons	Not specified	Simulation not specified	Traffic signal	
Belkhouche [2018]	Conflict points/regions	Decentralized	Trajectory-based	Integrated with scheduling	Customized simulation	None (proof of concept)	
Bian et al. [2019]	Safe pattern	Decentralized	FCFS	Integrated with scheduling	Numerical simulation	FCFS-method by [Dresner and Stone, 2008]	FCFS policy determines sequence of vehicles, exact arrival times are determined with trajectory planning
Bichiou and Rakha [2018]	Space discretization	Centralized	FCFS	Optimized	Simulation software 'INTEGRATION'	Traffic signal, stop sign	

Table A.2: Overview of reviewed AIM studies – Part II.

Paper	Intersection Modeling	Traffic Coordination	Scheduling Policy	Trajectory Planning	Evaluation Method	Benchmark	Further Remarks
Carlino et al. [2013]	Safe pattern	Centralized	Auction-based	Not considered	Customized simulation software 'AORTA'	FCFS	
R. Chen et al. [2020]	Conflict points/regions	Centralized	Optimization-based (MILP)	Not considered	Numerical simulation	None	Focus: Integrate pedestrians, consider network of intersections
Choi et al. [2019]	Space discretization	Centralized	Genetic algorithm	Not specified	Simulation type not specified	FCFS	
Dresner and Stone [2004]	Space discretization	Centralized	FCFS	Integrated with scheduling	Custom simulation software (Java-based)	TSC (pre-timed)	First notable work on AIM
Dresner and Stone [2006]	Space discretization	Centralized	FCFS	Not specified	Custom simulation software (Java-based)	TSC (pre-timed)	Consideration of mixed traffic, pedestrians, and bicyclists via traffic signals.
Dresner and Stone [2008]	Space discretization	Centralized	FCFS	Simplified	TSC, stop sign	Customized simulation software	
Elhenawy et al. [2015]	Safe pattern	Centralized	Game theory	Not considered	Monte Carlo simulation	Four-way stop sign	
Fajardo et al. [2011]	Space discretization	Centralized	FCFS	Simplified	Custom micr. traffic simulation (AIM4)	TSC (pre-timed)	Refine existing approach and test for several scenarios.
Fayazi and Vahidi [2018]	Safe pattern	Centralized	Optimization-based (MILP)	Simplified	Custom micr. traffic simulation	TSC (pre-timed)	Present new scheduling policy.
Fayazi, Vahidi, and Luckow [2019]	Safe pattern	Centralized	Optimization-based (MILP)	Simplified	Vehicle-in-the-Loop	TSC	Evaluates fuel consumption with real vehicle.
Ferreira et al. [2010]	Safe pattern	Decentralized	Rule-based, imitates actuated TSC	Not specified	Simulation software DIVERT	TSC installed in Porto, PT	

Table A.3: Overview of reviewed AIM studies – Part III.

Paper	Intersection Modeling	Traffic Coordination	Scheduling Policy	Trajectory Planning	Evaluation Method	Benchmark	Further Remarks
Guney and Raptis [2020]	Space discretization	Centralized	Particle swarm optimization	Simplified	Numerical simulations (MATLAB)	TSC	
Hausknecht et al. [2011]	Space discretization	Centralized	FCFS	Not described	Simulation (not specified)	Different navigation policies	Simulates a network of intersections, tests navigation policies.
He et al. [2018]	Conflict points/regions	Centralized	FCFS	Simplified	Custom micr. traffic simulation (Java-based)	FCFS with fixed lane-assignment, TSC (pre-timed)	Turning and through movements are allowed from any lane.
Jin et al. [2012]	Space discretization	Partially centralized	FCFS and priority-based	Simplified	Micr. traffic simulation (SUMO)	TSC	
Jin et al. [2013]	Space discretization	Partially centralized	FCFS for platoons	Simplified	Micr. traffic simulation (SUMO)	TSC (pre-timed)	Only platoon leaders communicate with the intersection controller.
Kamal et al. [2015]	Conflict points/regions	Centralized	Trajectory-based	Integrated with scheduling	Numerical simulation	TSC	
J. Lee and Park [2012]	Safe pattern	Centralized	Non-linear optimization	Integrated into scheduling	Micr. traffic simulation (VISSIM)	TSC (actuated)	
Levin, Boyles, and Patel [2016]	Space discretization	Centralized	FCFS	Not described	Simulation (not specified)	TSC	Shows several scenarios in which TSC outperforms FCFS.
Levin, Fritz, et al. [2016]	Conflict points/regions	Centralized	Optimization-based	Not described	Simulation (not specified)	FCFS	
Levin and Rey [2017]	Conflict points/regions	Centralized	Optimization-based (MILP)	Not considered	Numerical simulation	FCFS	

Table A.4: Overview of reviewed AIM studies – Part IV.

Paper	Intersection Modeling	Traffic Coordination	Scheduling Policy	Trajectory Planning	Evaluation Method	Benchmark	Further Remarks
B. Li et al. [2018]	Vehicle-based	Centralized	Optimization-based	Integrated into scheduling	Numerical simulation	None	Considers a lane-free intersection
L. Li and F.-Y. Wang [2006]	Safe pattern	Decentralized	Optimization-based (tree search)	Integrated into scheduling	Simulation (not specified)	None	
Zhixia Li et al. [2013]	Space discretization	Centralized	FCFS with adaptions	Integrated into scheduling	Micr. traffic simulation (Vissim)	TSC (pre-timed)	Turning movements are allowed from any lane.
Zhuofei Li et al. [2018]	Safe pattern	Centralized	Genetic Algorithm	Optimized	Custom simulation (Java)	TSC (actuated)	
Mitrovic et al. [2020]	Space discretization	Centralized	FCFS with alternate lanes	Not specified	Custom simulation FAUSim	TSC (pre-timed), FCFS	Assigns alternate lanes to resolve some conflicts on the approach to the intersection.
E. R. Müller et al. [2016a]	Space discretization (single zone)	Centralized	Optimization-based (MILP)	Reactive	Micr. traffic simulation (aimsun)	TSC (pre-timed)	
E. R. Müller et al. [2016b]	Conflict points/regions	Centralized	Optimization-based (MILP)	Reactive	Micr. traffic simulation (aimsun)	TSC (pre-timed)	
Naumann et al. [1998]	Conflict points/regions	Decentralized	Rule-based	Simplified	Custom simulation	None	
Olsson and Levin [2020]	Conflict points/regions	Centralized	Optimization-based (MILP)	Simplified	Micr. traffic simulation (aimsun)	TSC (semi-actuated)	
Rios-Torres et al. [2015]	Space discretization (single zone)	Centralized	FCFS	Optimized	Simulation (Matlab/Simulink)	Right of way on main road	Merging roads are considered instead of a "classic" intersection.

Table A.5: Overview of reviewed AIM studies – Part V.

Paper	Intersection Modeling	Traffic Coordination	Scheduling Policy	Trajectory Planning	Evaluation Method	Benchmark	Further Remarks
Sayin et al. [2018]	Space discretization	Centralized	Optimization-based	Not described	Micr. traffic simulation (SUMO)	FCFS	Driver agents' utilities are considered in the objective function.
Schepperle, Böhm, and Forster [2007]	Space discretization (single zone)	Centralized	Auction-based	Not considered	Custom simulation (Java)	FCFS	
Schepperle and Böhm [2007]	Conflict points/regions	Centralized	Auction-based	Not described	Custom simulation (Java)	FCFS	
Tachet et al. [2016]	Space discretization (1 zone)	Centralized	FCFS; *BATCH*	Not considered	Queuing theory	FCFS	
VanMiddlesworth et al. [2008]	Safe pattern	Decentralized	Rule-based (similar to stop signs)	Not described	Customized simulation software	Four-way stop sign, TSC	
Vasirani and Ossowski [2012]	Space discretization	Decentralized	Auction-based	Simplified	Customized simulation software	FCFS	
M. I.-C. Wang et al. [2021]	Conflict points/regions	Centralized	Optimization-based (MILP)	Simplified	Micr. traffic simulation (SUMO)	FCFS, TSC (pre-timed)	Integrates pedestrians and considers spill-back effects from downstream intersections.
Y. Wang et al. [2020]	Conflict points/regions	Centralized	FCFS	Optimized	Matlab simulation	TSC (pre-timed and actuated)	Considers a network of intersections and includes routing advice.

Table A.6: Overview of reviewed AIM studies – Part VI.

Paper	Intersection Modeling	Traffic Coordination	Scheduling Policy	Trajectory Planning	Evaluation Method	Benchmark	Further Remarks
J. Wu et al. [2012]	Safe pattern	Centralized	Ant colony optimization	Not described	Simulation software not specified	FCFS, TSC (pre-timed and adaptive)	
W. Wu et al. [2022]	Space discretization	Centralized	Optimization-based	Not described	Numerical simulation	None	Proposes an "autonomous pedestrian shuttle" to transport pedestrians across the intersection.
Y. Wu et al. [2019]	Space Discretization	Decentralized	Machine learning	Not described	Customized simulation (Python-based)	FCFS, TSC (pre-timed)	
Yao et al. [2020]	Safe pattern	Centralized	Optimization-based (MILP)	Optimized	Simulation (Matlab)	FCFS	Evaluates fuel consumption.
Yu et al. [2019]	Space discretization	Centralized	FCFS, *BATCH*, optimization-based	Not considered	Numerical simulation	TSC (pre-timed)	Compares different scheduling approaches.
Zhu and Ukkusuri [2015]	Conflict points/regions	Centralized	Optimization-based	Not considered	Numerical simulation	TSC (actuated)	Considers dynamic traffic assignment within a grid of intersections.
Zohdy et al. [2012]	Conflict points/regions	Centralized	Optimization-based	Simplified	Matlab and simulation software 'INTEGRATION'	TSC (pre-timed)	Evaluates fuel consumption.

B Solvability of the Scheduling Optimization Problem and Validity of Resulting Schedules

As described in Section 4.3.1, an optimization problem is solvable, if it is *feasible* and *bounded*. Both characteristics are fulfilled for Problem I. Additionally, it is proven that resulting schedules are in fact valid from a practical point of view.

Feasibility of the Optimization Problem

Levin and Rey [2017] prove that their formulation of the optimization problem has at least one feasible solution. Their proof can easily be applied here as well. The idea is that vehicles are sorted in increasing order by their earliest possible arrival times. Then, the first vehicle veh_1 is assigned to cross the intersection at its earliest possible arrival time, i.e., $\hat{t}_1 = t_1^{min}$. The second vehicle is assigned to arrive at the intersection after the first vehicle has left the intersection. Let Δ be an upper bound on the time needed by one vehicle to cross the intersection, given by the longest vehicle path through the intersection and a minimum assumed speed. Then $\hat{t}_2 = \max\{t_2^{min}, \hat{t}_1 + \Delta\}$. The third vehicle is assigned after the second vehicle has left the intersection, and so on. It is easy to see that all formal constraints except for Constraints (4.27) are fulfilled. Since delays can grow virtually boundlessly and the delays of vehicles are constrained by Θ_{veh}, this can be problematic. However, in practical problems with a finite number of vehicles, this does not happen. Assume that n vehicles are considered in the optimization, i.e., $|\mathcal{V}| = n$. Then, following the construction of a feasible solution explained above, delays can be derived as follows: $delay_1 = 0$, $delay_2 \leq \Delta, \ldots, delay_n \leq (n-1) \times \Delta$. Therefore, choosing $\mathcal{M} > \Theta_{veh} > n \times \Delta$ is a safe option. As explained before, Θ_{veh} needs to be carefully chosen large enough to not infringe on feasibility.

Boundedness of the Optimization Problem

The presented minimization problem needs to be bounded below in order to have a finite optimal solution. It can be seen from Constraints (4.25) and (4.26), that $delay_i \geq 0$ for all vehicles veh_i in $\mathcal{V}$. Since $\gamma_i \geq 0$ for all vehicles veh_i in $\mathcal{V}$, the objective function is bounded as well: $\sum_{veh_i \in \mathcal{V}} \gamma_i \cdot delay_i \geq 0$. Together with the feasibility shown above, the problem is hence solvable.

Validity of Resulting Schedules

Since the constraints allow for multiple vehicles with conflicting movements to be within the intersection zone at the same time, it is theoretically conceivable that gridlocks could occur. However, this is not the case, as will be proven in the following. The key is that the scheduling algorithm *only* assigns the exact time $\hat{t}_{veh}$ for each vehicle veh to enter the intersection. The time that veh arrives at any potential conflict point p within the intersection zone then only depends on $\hat{t}_{veh}$ and the pre-defined distances between the entrance to the intersection o_{veh} and p, and on the also pre-defined vehicle speed $\hat{v}_{veh}$.

Remark. *The schedule resulting from the optimization does not lead to gridlocks.*

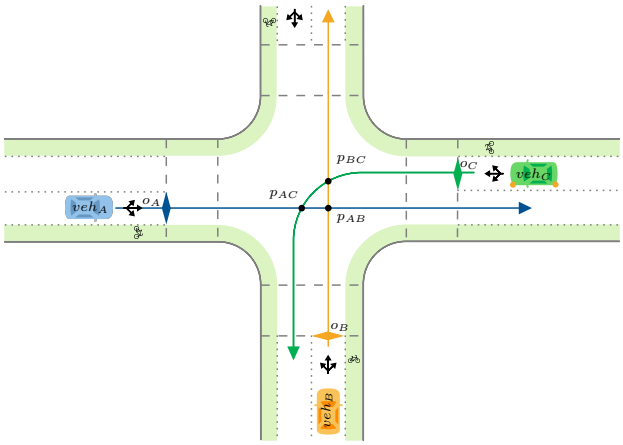

Figure B.1: An example situation of three vehicles with different origins and destinations crossing the intersection zone.

Proof. The remark is proven by contradiction. Let veh_A, veh_B and veh_C be three vehicles that cross the intersection zone and let p_{AB}, p_{AC} and p_{BC} denote the conflict points of their respective paths through the intersection zone as illustrated in Figure B.1.

Assume that a gridlock has been created by the intersection control, i.e., a situation comparable to the following: veh_A is supposed to cross p_{AB} before veh_B and p_{AC} after veh_C, veh_B is scheduled to cross p_{BC} before veh_C. This would lead to the following:

$$\hat{t}_{veh_A,p_{AB}} < \hat{t}_{veh_B,p_{AB}} \tag{1}$$
$$\hat{t}_{veh_B,p_{BC}} < \hat{t}_{veh_C,p_{BC}} \tag{2}$$
$$\hat{t}_{veh_C,p_{AC}} < \hat{t}_{veh_A,p_{AC}}. \tag{3}$$

Recall that the scheduling algorithm assigns only the arrival times of vehicles at the respective entrance to the intersection zone. The time needed by each vehicle veh from entering the intersection zone to reaching a certain conflict point is defined by the distance between these two positions and the assigned speed of veh. In particular, the following holds:

$$\hat{t}_{veh_i,p_{ij}} = \hat{t}_{veh_i} + \frac{dist_{o_i,p_{ij}}}{\hat{v}_i} \qquad \text{for } i,j \in \{A,B,C\}. \tag{4}$$

Combining all of these expressions leads to:

$$\begin{aligned} \hat{t}_{veh_A,p_{AB}} &\overset{(1)}{<} \hat{t}_{veh_B,p_{AB}} \\ &= \hat{t}_{veh_B} + \frac{dist_{o_B,p_{AB}}}{\hat{v}_B} \\ &\overset{dist_{o_B,p_{AB}} < dist_{o_B,p_{BC}}}{<} \hat{t}_{veh_B} + \frac{dist_{o_B,p_{BC}}}{\hat{v}_B} \end{aligned}$$

$$
\begin{aligned}
&= \hat{t}_{veh_B,p_{BC}} \\
&\overset{(2)}{\downarrow} \\
&< \hat{t}_{veh_C,p_{BC}} \\
&= \hat{t}_{veh_C} + \frac{dist_{o_C,p_{BC}}}{\hat{v}_C} \\
&\overset{dist_{o_C,p_{BC}} < dist_{o_C,p_{AC}}}{\downarrow} \\
&< \hat{t}_{veh_C} + \frac{dist_{o_C,p_{AC}}}{\hat{v}_C} \\
&= \hat{t}_{veh_C,p_{AC}} \\
&\overset{(3)}{\downarrow} \\
&< \hat{t}_{veh_A,p_{AC}} \\
\Rightarrow \hat{t}_{veh_A,p_{AB}} &< t_{veh_A,p_{AC}} \; \lightning
\end{aligned}
$$

This is not possible, since the intersection geometry and the location of conflict points displayed in Figure B.1 show that vehicle veh_A first passes p_{AC} before arriving at p_{AB}, i.e., $dist_{o_A,p_{AB}} > dist_{o_A,p_{AC}}$.

From Equation (4) it can be obtained that $\hat{t}_{veh_A,p_{AB}} = \hat{t}(veh_A) + \frac{dist_{o_A,p_{AB}}}{\hat{v}_A}$ and $\hat{t}_{veh_A,p_{AC}} = \hat{t}(veh_A) + \frac{dist_{o_A,p_{AC}}}{\hat{v}_A}$, which consequently leads to

$$
\hat{t}_{veh_A,p_{AB}} = \hat{t}_{veh_A} + \frac{dist_{o_A,p_{AB}}}{\hat{v}_A} \overset{dist_{o_A,p_{AB}} > dist_{o_A,p_{AC}}}{\downarrow} > \hat{t}_{veh_A} + \frac{dist_{o_A,p_{AC}}}{\hat{v}_A} = \hat{t}_{veh_A,p_{AC}},
$$

where $\hat{t}_{veh_A}$ is the only value that is assigned by the scheduling algorithm and the other measures are input values derived from the physical context. □

C Bicycle Trajectories

The following figures show example trajectories of bicyclists who stopped at the traffic signal (taken from the TSC scenario at the realistic intersection). Figure C.1 shows how the bicycle queue dissolves after the signal turns green. It can be seen that trajectories sometimes overlap as there are two parallel bicycle lanes for through movement. Figure C.2 shows the corresponding speed curves. Some bicyclists seem to suddenly travel at a higher speed after crossing the signal (displayed by the dark blue and brown trajectories, for example). This is because they were not riding at free-flow speed when approaching the stop bar.

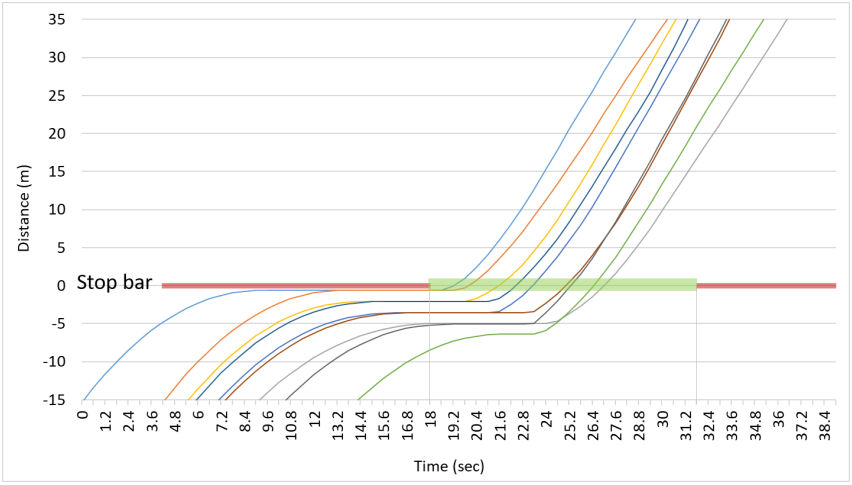

Figure C.1: Example trajectories of bicyclists that stopped at the traffic signal.

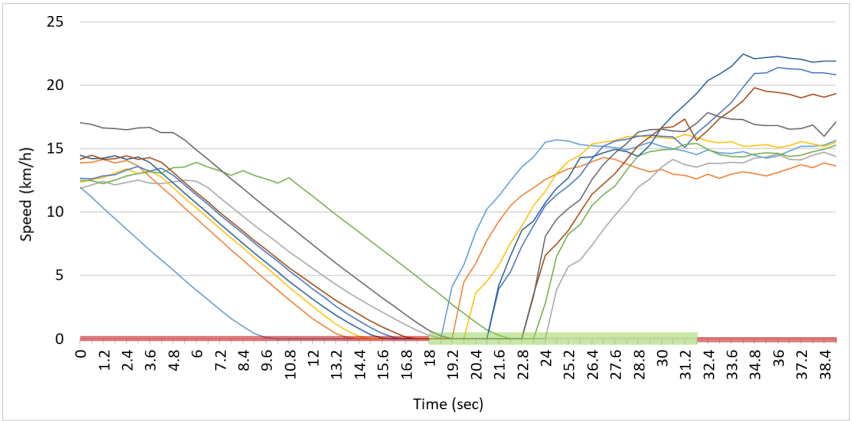

Figure C.2: Example speed curves of bicyclists that stopped at the traffic signal.

D Trajectory Planning: Simplified Version

This section briefly describes the rule-based trajectory adjustment procedure that can be applied if the trajectory doesn't need to be optimized. In each time step, the speed for each considered vehicle for the next time step is calculated in several steps that are described in the flowcharts shown in Figures D.1a and D.2 and are partly illustrated in Figure D.1b. The overall idea is that the minimum speed of a vehicle on the approach should be as large as possible, i.e., vehicles should maintain a speed close to the average required speed that results from their distance to the intersection and the time until the scheduled arrival time. The procedure is only applied to vehicles on the approach to the intersection with a fixed time slot for crossing the intersection. Figures D.1a and D.1b explain how the speed is calculated for a single vehicle veh without taking surrounding vehicles into account. The resulting velocity, which is "ideal" from the ego-perspective, is then used as an input to the procedure displayed in Figure D.2, where leader vehicle, speed limit, and kinematic limitations are considered. Only the speed resulting from applying the overall procedure is finally returned to the microscopic simulation.

Similarly to with the optimization-based approach presented in Chapter 5, the state information used in the trajectory adjustment procedure in Figure D.1a for vehicle veh at time t^k consists of the vector $[dist, v, \hat{t}, \hat{v}]$ where $dist_{veh}(t^k)$ is the distance of vehicle veh to the entrance of the intersection at time t^k (corresponding to the position of the front bumper of veh), $v_{veh}(t^k)$ describes the velocity of veh at time t, $\hat{t}_{veh}$ is the assigned arrival time at the intersection and $\hat{v}_{veh}$ is the predefined speed for crossing the intersection. In Step 1 of Figure D.1a, the required average speed on the approach to the intersection given the currently remaining distance and time is calculated:

$$\bar{v}_{veh}(t^k) = \frac{dist_{veh}(t^k)}{\hat{t}_{veh} - t^k}.$$

As illustrated in the top left part of Figure D.1b, this average speed does not take into account that vehicle veh should arrive at the intersection with a pre-defined speed $\hat{v}_{veh}$. In fact, if $\bar{v}_{veh}(t^k)$ differs from $\hat{v}_{veh}$, then veh will have to accelerate or decelerate before entering the intersection, which affects the average required speed until starting the speed adjustment. Therefore, a loop is implemented. In Step 2.1 of Figure D.1, the time $t^{adj}(\bar{v}, \hat{v})$ and distance $dist^{adj}(\bar{v}, \hat{v})$ needed to accelerate or decelerate, i.e. to ***adj**ust* the speed from $\bar{v} = \bar{v}_{veh}(t)$ to $\hat{v} = \hat{v}_{veh}$ are calculated, assuming the minimum and maximum acceleration that applies for veh:

$$t^{adj}(\bar{v}, \hat{v}) = \begin{cases} \frac{\hat{v}-\bar{v}}{acc^{max}_{veh}} & \text{if } \hat{v} \geq \bar{v} \\ \frac{\hat{v}-\bar{v}}{acc^{min}_{veh}} & \text{otherwise.} \end{cases} \tag{5}$$

$$dist^{adj}(\bar{v}, \hat{v}) = t^{adj}(\bar{v}, \hat{v}) \times \frac{\hat{v} + \bar{v}}{2}. \tag{6}$$

Now, the required average speed is calculated for the approach until the position and time

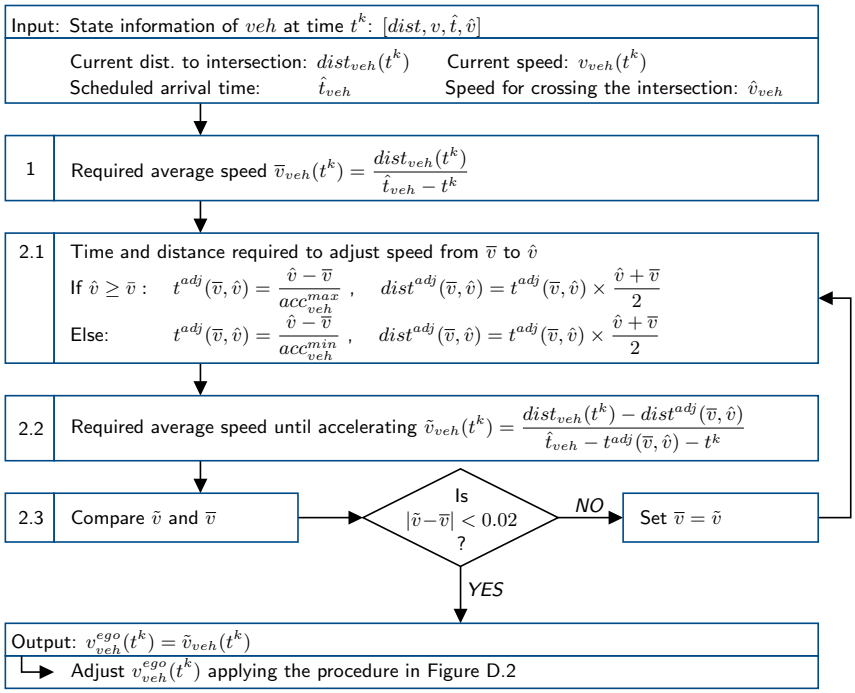

(a) Flowchart of calculating the new speed of vehicle veh at time t^k from the ego perspective.

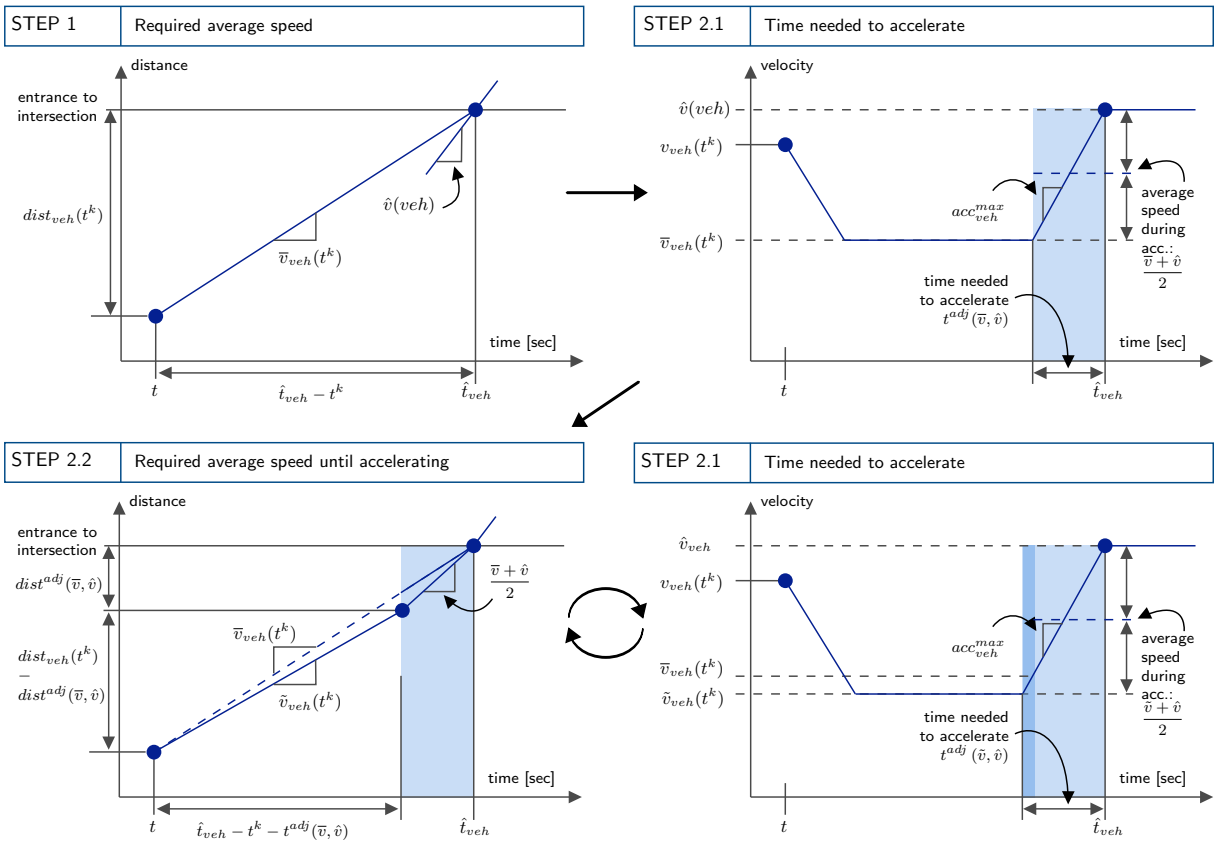

(b) Visualization of Steps 1, 2.1, and 2.2 of Figure D.1a.

Figure D.1: Flowchart and visualization of calculating the new speed of vehicle veh at time t^k from the ego perspective.

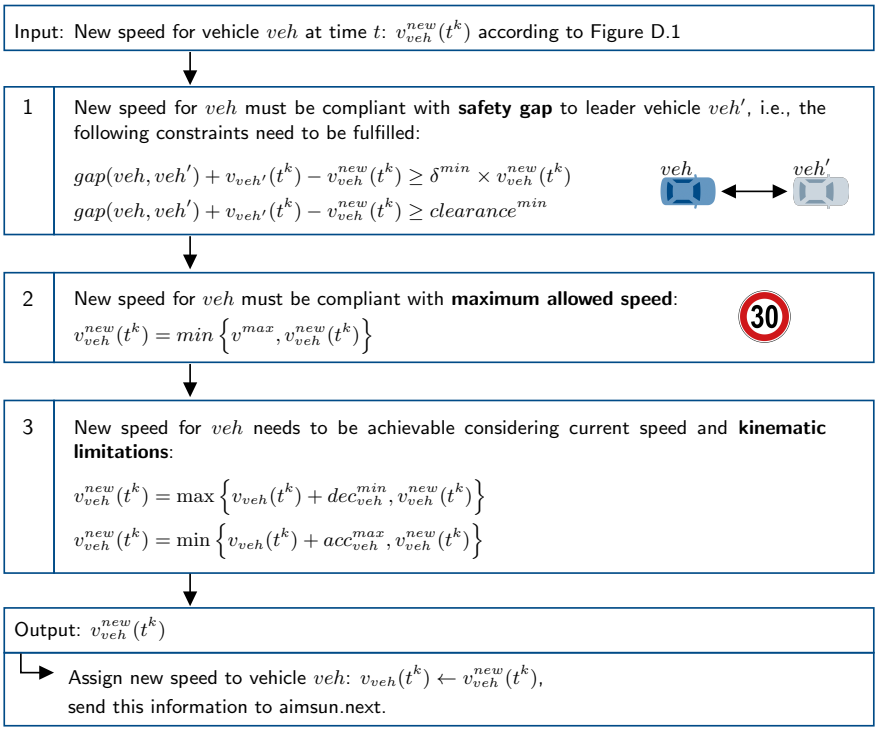

Figure D.2: Flowchart of calculating the optimal speed of vehicle veh at time t^k (after an arrival time $\hat{t}$ has been assigned for veh).

where the speed adjustment will start, compare Step 2.2:

$$\tilde{v}_{veh}(t) = \frac{dist_{veh}(t) - dist^{adj}(\bar{v}, \hat{v})}{\hat{t}_{veh}(t) - t^{adj}(\bar{v}, \hat{v})}. \tag{7}$$

Of course, $\tilde{v}_{veh}(t^k)$ might differ significantly from $\bar{v}_{veh}(t^k)$, see Figure D.1b. In that case, the time and distance needed to adjust the speed from $\tilde{v}_{veh}(t^k)$ to $\hat{v}_{veh}$ will also differ and thus need to be calculated again. This is done in the loop containing Steps 2.1-2.3, which means that Equations (5)-(7) are run iteratively. Usually, after very few iterations, $\tilde{v}$ does not change any more. Now, it needs to be checked whether the speed of veh can safely be adjusted such that $v_{veh}^{new}(t) = \tilde{v}_{veh}(t)$. This depends on the feasibility of $\tilde{v}$ with respect to the distance to the leader vehicle, the speed limits, and kinematic limitations. Therefore, before sending $\tilde{v}$ to aimsun.next, it is adjusted applying the procedure displayed in Figure D.2.

Analogously to the setup described in Chapter 5, the procedure is run sequentially for vehicles in upstream direction to account for the relatively large simulation steps. Let the vehicles be sorted by proximity to the intersection. When the feasible acceleration for vehicle veh is calculated, the applied acceleration of veh' is already known. The necessary gap can thus already be calculated taking the new speed of veh' into account. It needs to be noted that this approach has only been tested in scenarios with a homogeneous vehicle fleet and might lead to problems if acceleration capabilities differ.

E Intersection Layouts

This section presents screenshots of the simulated intersections with distances, lane widths, etc. to make the simulation studies more transparent.

E.1 Intersections in Chapter 3 and Chapter 4

Figure E.1 shows the intersection that is simulated for the evaluation of vehicle-only scenarios and the scenarios with vehicles and pedestrians in Chapter 3.

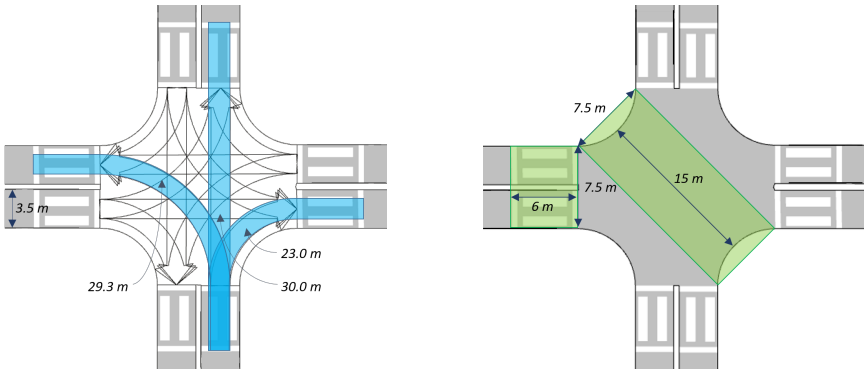

Figure E.1: Intersection layout used for the analyses of vehicle-only scenarios and scenarios with vehicles and pedestrians in Chapter 3.

Figure E.2 shows the intersection that is simulated for the evaluation of scenarios with vehicles and bicyclists in Chapter 3 and for all scenarios in Chapter 4.

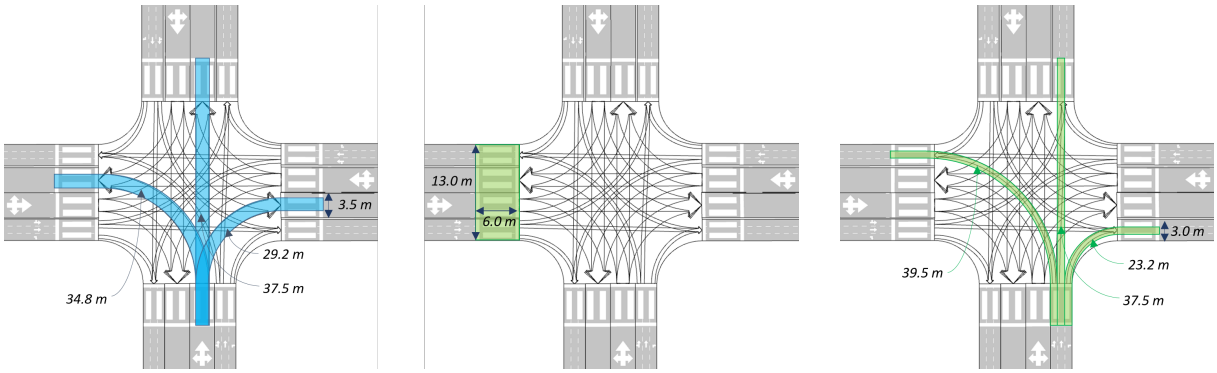

Figure E.2: Intersection layout used for the analyses of scenarios with vehicles and bicyclists in Chapter 3 and for all analyses in Chapter 4.

E.2 Realistic Intersection

This subsection explains the modeling of the considered real intersection zone in Munich, Germany.

Overall Intersection Layout

Figure E.3 shows all allowed vehicle movements within the considered intersection. Vehicle lane widths on the southern approach are 3.25 meters, all other vehicle lanes have a width of 3.5 meters. Figure E.4 shows bicycle movements. Bicycle lane width is 1.0 meters, and there are two parallel lanes for each through movement. Figure E.5 shows the pedestrian crosswalks at the considered intersection.

Figure E.3: Layout of the considered intersection showing all allowed vehicle movements.

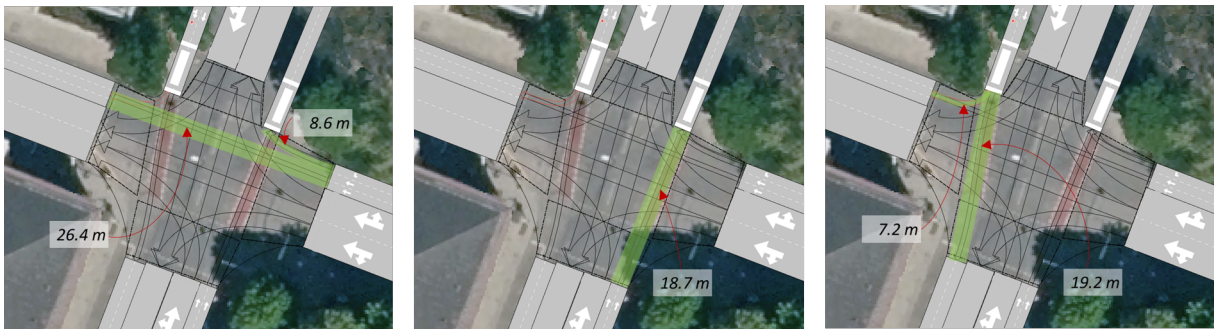

Figure E.4: Layout of the considered intersection showing all allowed bicycle movements.

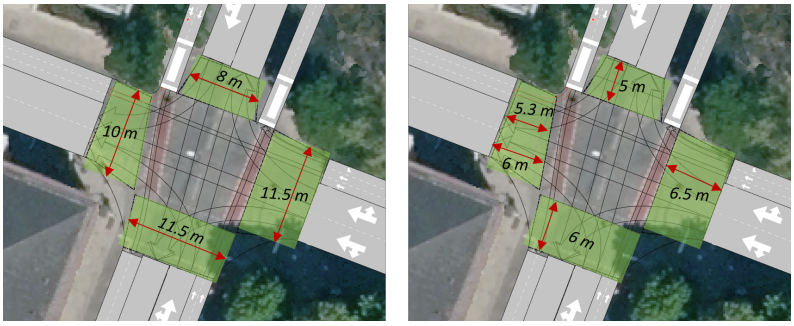

Figure E.5: Layout of the considered intersection showing the pedestrian crosswalks.

Turning Radii and Speeds

Turning radii at the considered realistic intersection are shown in Figure E.6. Table E.1 lists how these radii impact the assumed speed for crossing movements. As described in Section 5.2, a maximum lateral acceleration of $3\,\mathrm{m/sec^2}$ is assumed.

Figure E.6: Turning radii at considered intersection zone.

Radius R $[m]$	**Lateral acceleration** $acc\ [m/sec^2]$	**Velocity** $v = \sqrt{a * R}$ $v[m/sec]$	**Velocity** $[km/h]$
9.0	3.0	5.2	18.7
10	3.0	5.5	19.8
10.5	3.0	5.6	20.2

Table E.1: Turning velocity depending on curve radius and comfortable lateral acceleration.

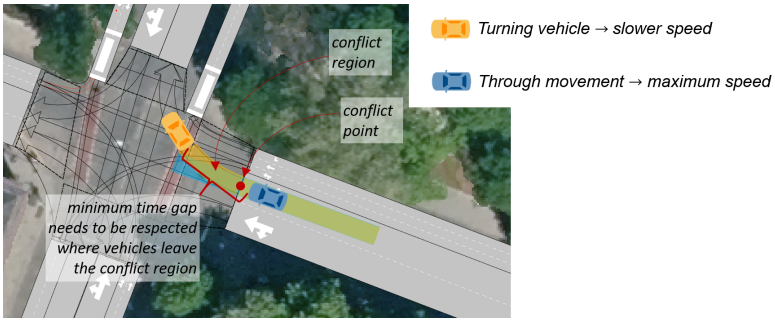

Figure E.7: Diverging movements with slow vehicle in front.

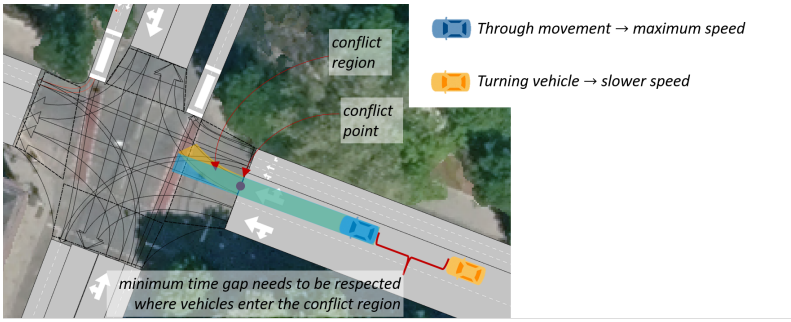

Figure E.8: Diverging movements with fast vehicle in front.

Conflict Regions

In principle, conflict regions within the intersection are spanned as described in Chapter 4 and will not be described here in detail. This section will specifically focus on merging and diverging vehicle movements (i.e., with the same origin or destination), because the slower speeds of turning vehicles impose a special challenge on resolving these conflicts.

Diverging movements As described in Chapter 4, vehicle movements with the same origin are separated at the entrance to the intersection. This is ensured by Constraint (4.16), i.e.,

$$t_i \geq t_j + \Delta_{ji}^{min} \quad \forall\, veh_i, veh_j \in \mathcal{V} \mid o_i = o_j \;\&\; dist_i > dist_j,$$

where $dist_i$ and $dist_j$ denote the distances of two vehicles veh_i and veh_j to the intersection at the time the scheduling program is solved. The minimum headway Δ_{ji}^{min} includes the time that is needed for the front vehicle veh_j to cross the stop bar and a minimum time gap δ_{ji}^{min} as explained in Section 4.2.1. In this particular more realistic situation, the minimum headway needs to be further adapted depending on whether the slower turning vehicle or the faster through movement vehicle enters the intersection first.

If the slower vehicle enters first, separating the movements at the entrance to the intersection with the headway described above would lead to problems. The faster vehicle would "catch up" within the intersection and thus fall short of the minimum headway or be enforced to slow down. Instead, the minimum time gap δ needs to be respected where

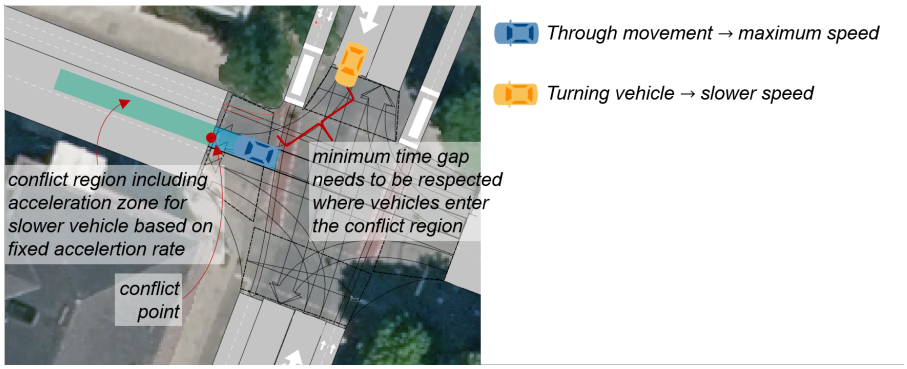

Figure E.9: Merging movements with fast vehicle passing the conflict point first.

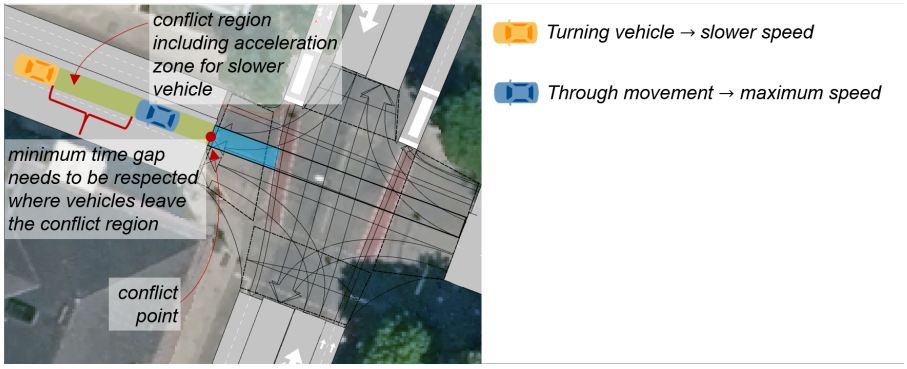

Figure E.10: Merging movements with slow vehicle passing the conflict point first.

vehicles leave their conflict region as shown in Figure E.7. This is considered with adapted headways Δ that take the time needed for crossing the conflict regions into account.

If the faster vehicle enters the intersection first (as shown in Figure E.8), no changes need to be made from the safety point of view. However, the headway at the entrance to the intersection needs to be increased to allow the vehicles to adjust their speeds before entering the intersection. To make this a bit more clear, let us assume that the orange vehicle in Figure E.8 follows the blue vehicle at a constant speed of 8.3 meters per second and with the minimum allowed time gap of 0.7 seconds (i.e., with a headway of approximately 1.2 seconds if we assume that the blue vehicle is 4 meters long). The orange vehicle needs to slow down *before* entering the intersection. It will hence increase its headway to the blue vehicle and would not be able to reach the intersection on time if scheduled to enter 1.2 seconds after the blue vehicle. Therefore, a speed adjustment zone is considered that is defined by the difference in crossing speeds and an assumed fixed deceleration rate of 1.2 $\mathrm{m/s^2}$ (which can be achieved by all vehicles). Clearly, the lost time due to the deceleration also needs to be considered when calculating the earliest possible arrival time of a turning vehicle without a leader.

Merging movements A similar situation arises, when vehicles enter the intersection from different origins, but have the same destination. In this situation, the conflict point lies at the

exit from the intersection.

If the faster vehicle exits first, then the conflict needs to be resolved at the beginning of the conflict regions as shown in Figure E.9. If the slow vehicle exits the intersection first, then the conflict needs to be resolved at the end of the conflict region. As shown in Figure E.10, the conflict region does not end at the exit from the intersection, but after the slower vehicle has accelerated to maximum speed.

Similarly to the explanations in Section 4.2, all of these spatial and speed-wise considerations will be transformed into adapted headways and the conflict will then be resolved at the common conflict point.

F Setup of Benchmark Traffic Signal Control Schemes

This section describes the setup of TSC that is used as a benchmark in different evaluations. The descriptions are enhanced by screenshots from the simulation.

F.1 Pre-timed Traffic Signal Control Applied in Chapter 3

The implemented TSC is pre-timed and two-phase with the two phases as shown in Figure F.1. The first phase includes all vehicle movements coming from the east and west, the second phase includes vehicle movements coming form the south and north. In each of the phases, left-turning movements are permitted and need to give way to oncoming traffic. Green phase durations for both phases are shown in Figure F.2. In the presented analyses, pedestrian movements are not simulated, but pedestrian LOS is calculated analytically.

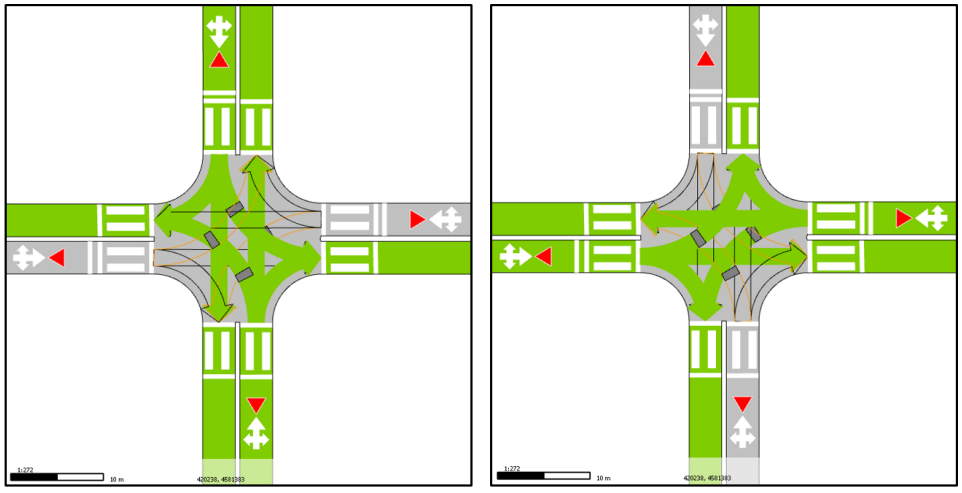

Figure F.1: Two phases of the implemented TSC.

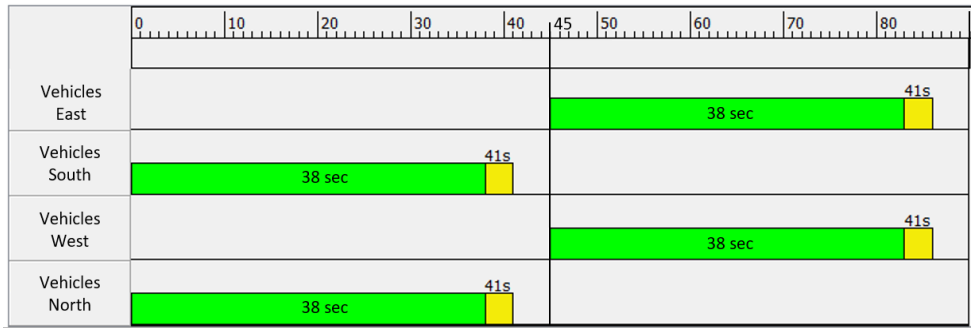

Figure F.2: Green phase durations of the pre-timed TSC.

F.2 Fully Actuated Traffic Signal Control Applied in Chapter 3

Similarly to the pre-timed TSC described above, the fully actuated TSC applied in Chapter 3 is a two-phase signal with permitted left-turning movements. The two phases shown in Figure F.1 are now not pre-timed, but are actuated by detectors placed at a distance of 25 meters from the intersection on each of the four approaches, see Figure F.3. Detectors on the northern and southern approaches actuate phase I, detectors on the eastern and western approaches actuate phase II. Both phases will be activated at least for the minimum green phase duration of 15 seconds, even in the absence of detector actuations. This allows pedestrians and bicyclists to cross the street or intersection in every cycle without specific VRU actuation. The green phase duration is extended in the presence of detector actuations. Maximum gap is set to 3 seconds, i.e., the green phase ends if neither of their assigned detectors has been actuated within the last three seconds. Additionally, a maximum green time of 38 seconds is implemented, such that the cycle time 90 seconds is not exceeded.

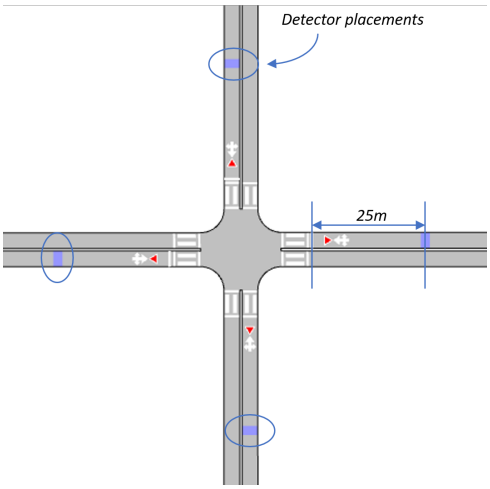

Figure F.3: Detector placement for the fully actuated TSC.

F.3 Fully Actuated Traffic Signal Control at the Realistic Intersection Zone

The signal plan of the implemented fully actuated TSC is shown in Figure F.4. Phases I, III, V, VII, and the all-red phases each have a fixed duration. The dynamic phases II and VI are always implemented with their minimum green phase duration and extended if their assigned detectors are actuated. As shown in the figure, they also allow pedestrians and bicyclists to cross. Phases IV and VIII are only activated based on actuation and skipped otherwise. The necessary vehicle detectors are placed on each approach as shown in Figure F.5. Again, they are at a distance of 25 meters from the entrance to the intersection. Similarly to the actuated TSC described in Appendix F.2, a maximum gap of 3 seconds is implemented.

Additionally, PT prioritization is implemented in the presented study. The PT vehicle signs up at a distance of approximately 130 meters to the entrance of the intersection (see Figure F.5)

and requests phase II to be served. If the phase is currently active, it will remain green for a maximum duration of 60 seconds. If a different phase is active at the moment the PT prioritization is requested, the controller will run all mandatory phases until reaching phase II with minimum green time. The prioritization request ends with the maximum dwell time of 60 seconds or with the bus leaving the intersection.

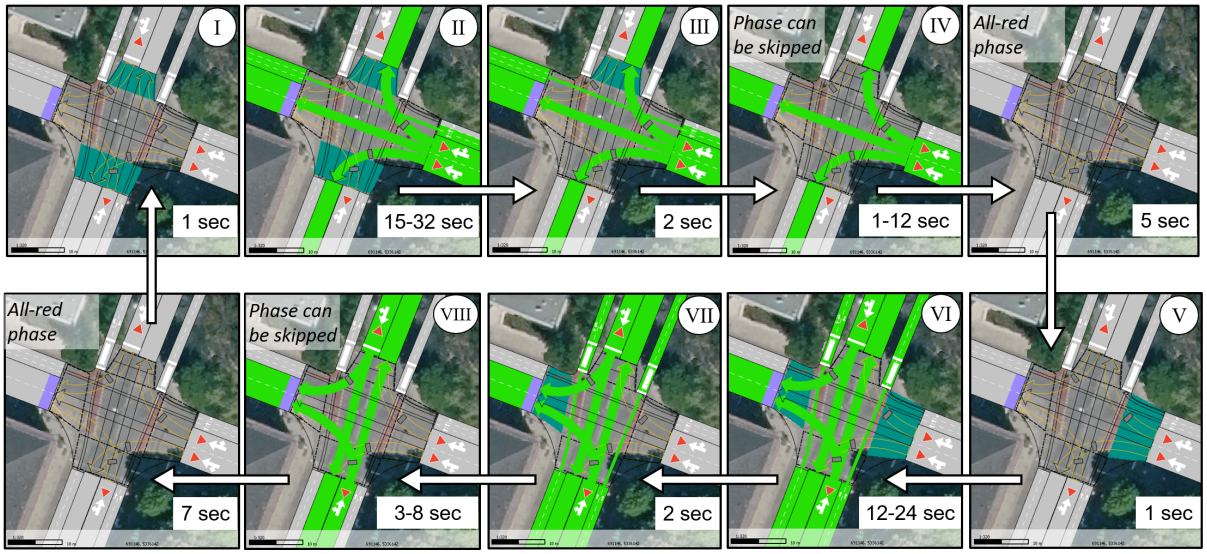

Figure F.4: Fully actuated TSC at the considered intersection.

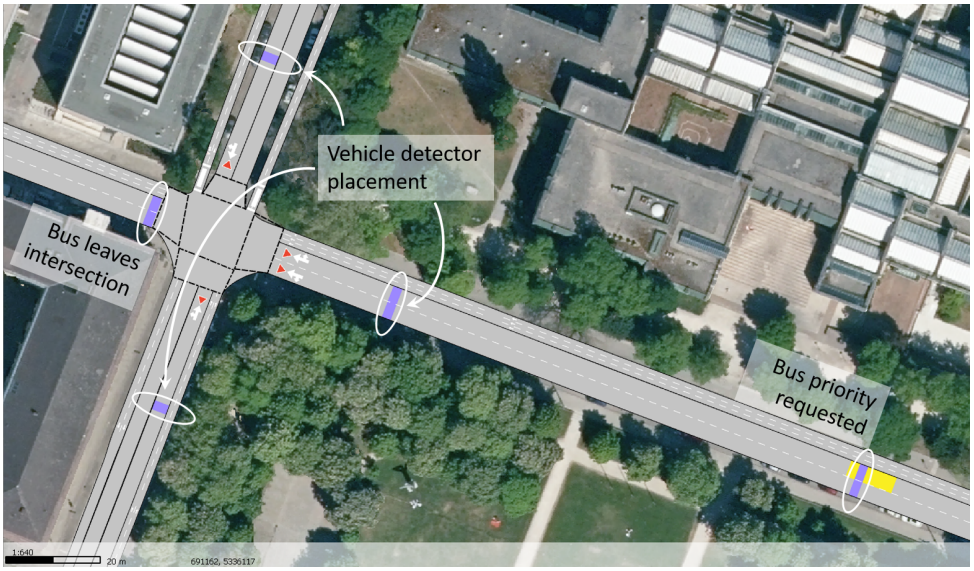

Figure F.5: Detector placement at the considered intersection.

F.4 Calculation of Average Pedestrian Waiting Times for Fixed-time Two-phase Traffic Signals

In the fixed-time two-phase TSC scenario with a cycle time of T seconds and a pedestrian green phase duration (for each of the two phases) of G seconds, pedestrians wanting to cross diagonally need to cross two legs of the intersection. The maximum and average waiting times of pedestrians thus consist of two components. First of all, it is assumed that pedestrians will decide upon the arrival at the intersection, whether they will first cross the eastern leg or the southern leg of the intersection. This decision depends on which signal head currently shows green light or will turn green first. The waiting times of the pedestrian before and after crossing the first leg will then be added.

Let us assume that the cycle time T can be divided as follows: $G + R + G + R$, where G are the green phase durations of the two phases and R are the clearance times that are needed by pedestrians to cross the intersection.

Step 1: Calculation of waiting times before crossing the first leg. The probability that one of the legs shows green light upon the arrival of pedestrian ped is $\frac{2G}{T}$ and the probability that both legs currently show red light is $\frac{T-2G}{T}$. The maximum waiting time for pedestrian ped before crossing the first leg is $\frac{1}{2} \cdot (T - 2G)$ and the mean waiting time can be calculated as $\frac{T-2G}{T} \cdot \frac{1}{4}(T - 2G) = \frac{(T-2G)^2}{4T}$.

Step 2: Calculation of waiting times after crossing the first leg. It is assumed that pedestrian ped will need R seconds to cross the first leg of the intersection. If pedestrian ped arrived during the red phase of the intersection (both legs show a red signal), then pedestrian ped will start crossing at the beginning of the green phase and thus wait for the rest of the green phase plus clearance time until the next green phase starts, i.e., the waiting time after crossing the first leg will be $G + R - R = G$. If the pedestrian ped arrived during the green phase of the first leg, then a part of this green phase has already passed and the maximum waiting time will equally be G, but the mean waiting time will be $\frac{1}{2} \cdot G$. Combined with the previously explained probabilities, the mean waiting time after crossing the first leg will be $\frac{2G}{T} \cdot \frac{1}{2} \cdot G + \frac{T-2G}{T} \cdot G = G(\frac{2G}{2T} + \frac{T-2G}{T}) = G \cdot (\frac{G+T-2G}{T}) = G \cdot \frac{T-G}{T}$.

Step 3: Sum of the two Components. Finally, the two waiting times add up. The maximum waiting time applies when the pedestrian arrives after the signal of one of the phases just turned red. The total waiting time will then be $\frac{1}{2}(T - 2G) + G = \frac{1}{2} \cdot T$. The average total waiting time is $\frac{(T-2G)^2}{4T} + G \cdot \frac{T-G}{T}$.

Example Calculation

Example with $T = 90\,\text{seconds}$ and $G = 35\,\text{seconds}$:

- Maximum waiting time diagonal: $\frac{1}{2} \cdot T = 45$
- Mean waiting time diagonal: $\frac{20^2}{360} + 35 \cdot \frac{55}{90} = 1.1 + 21.4 = 22.5$.